DEVELOPMENT OF DRIVING CYCLES AND A MATHEMATICAL MODEL FOR FUEL ECONOMY CHARACTERIZATION OF LIGHT DUTY VEHICLES IN SRI LANKA

Surath Gajanayake

198099f

Degree of Doctor of Philosophy

Department of Mechanical Engineering

University of Moratuwa
Sri Lanka

June 2024

DECLARATION

"I declare that this is my own work, and this thesis/dissertation does not incorporate without acknowledgement any material previously submitted for a Degree or Diploma in any other University or institute of higher learning and to the best of my knowledge and belief it does not contain any material previously published or written by another person except where the acknowledgement is made in the text.

Also, I hereby grant to the University of Moratuwa the non-exclusive right to reproduce and distribute my thesis/dissertation, in whole or in part in print, electronic or other medium. I retain the right to use this content in whole or part in future works (such as articles or books).

Name of the Candidate: S.P. Gajanayake

Signature:

Date: 09/06/2024

The supervisor/s should certify the thesis/dissertation with the following declaration.

The above candidate has carried out research for the Masters/MPhil/PhD thesis/ Dissertation under my supervision.

Name of the main supervisor: Dr A.G.T. Sugathapala

Signature of the supervisor: Date : 12/08/2024

Name of the main co-supervisor: Prof. J.M.S.J. Bandara

Signature of the supervisor: Date : 12.08.2024

ABSTRACT

Estimating the fuel consumption of vehicles under varying driving patterns is challenging and lacks a clear theoretical base. The study aims to provide a scientific basis for a better understanding of driving patterns and their influence on the fuel economy performance of in-use light duty vehicles in Sri Lanka. The study encompasses two specific objectives: the development of driving cycles to represent the local driving conditions of selected vehicle types and the development of a mathematical model capable of estimating fuel economy values of different light duty vehicle types under varying driving patterns. The methodology adopted during the study comprises the theoretical development of two local driving cycles: one specifying both 2W and 3W and the other specifying the characteristics of 4W and the development of a mathematical model that can estimate fuel economy values under varying driving conditions. The main findings of the study portray the characteristics of the two driving cycles developed for the Colombo Metropolitan Area: one cycle spans a period of 1499s which is developed to mimic the driving behavior of 4W whereas the other cycle spans a period of 1215s which is dedicated for 2W and 3W. When developing the said two cycles, data has been acquired from 19 major routes comprising 72 route links within the Colombo Metropolitan region. The micro-trip-based method is opted when developing driving cycles. Krigging spatial interpolation has been utilized as the classification technique for micro-trip generation. The mathematical model developed for the fuel economy characterization is undergone two-way validation, i.e., simulation-based validation and the validation based on manufacturer's data. When validated, the estimation accuracy of the model gets converged to a band between 89.61% to 92.78%. Conclusively, it can be stated that the developed and validated theoretical model can be utilized as a tool to estimate the fuel consumption of different vehicle types under varying driving conditions. Furthermore, it is recommended to refer to the local driving cycles developed to mimic the local driving behavior when using the theoretical model for localized fuel consumption estimations.

DEDICATION

To my beloved parents, Dr. Damayantha Gajanayake and Dr. (Mrs.) Geethani Gajanayake and to my beloved brother, Dr. Sarith Gajanayake.

ACKNOWLEDGEMENT

First and foremost, I am deeply grateful to my supervisors Dr Thusitha Sugathapala and Senior Prof. Saman Bandara for providing me with this opportunity, and for introducing me to this fascinating field of sustainable mobility. I would like to thank both of my mentors for their excellent supervision, supportiveness, encouragement, endless dedication, and guidance throughout my PhD. I have greatly benefited from their keen research insight and scientific rigour, and the work provided in this thesis would not have been possible without their support.

Secondly, I would like to thank Dr, Rasika Perera, the Chairman of my PhD progress review committee, who did provide extremely significant constructive reviews on my work which helped me to mold the research accordingly.

Thirdly, I wish to extend my gratitude to Dr Dimantha De Silva for providing me with accessibility to the necessary data acquisition tools for route selection.

Fourthly, I would like to thank the research coordinator of the Department of Mechanical Engineering, Dr Nalaka Samaraweera for guiding me in the administerial work of the PhD.

Last, but not least, I would like to thank my beloved wife and my beloved parents for encouraging me to pursue postgraduate studies and for supporting me throughout my journey.

CONTENTS

LIST OF FIGURES

LIST OF TABLES

LIST OF ABBREVIATIONS

Abbreviations	Definition
2W	Two-wheelers
3W	Three-wheelers
4W	Four-wheelers
AADT	Average Annual Daily Traffic
A/C	Air Conditioning
ADR	Australian Design Rules
ADT	Annual Daily Traffic
ADVISOR	ADvanced VehIcle SimulatOR
AFR	Air-Fuel Ratio
AMT	Automated Manual Transmission
AP	Afternoon Peak
API	Application Programming Interface
ARTEMIS	Assessment and Reliability of Transport Emission Models and Inventory Systems
ASHRAE	American Society of Heating Refrigerating and Air-conditioning Engineers
AT	Automatic Transmission
BEV	Battery Electric Vehicle
BS	Bharat Standards
BSFC	Brake Specific Fuel Consumption
CADC	Common Artemis Driving Cycle
CAI	Controlled Autoignition
CC	Cylinder Capacity
CDA	Cylinder Deactivation
CDC	Colombo Driving Cycle
CI	Compression-Ignition
CMA	Colombo Metropolitan Area
CMDC	Colombo Metropolitan Driving Cycle

CP	Characteristic Parameter
CR	Compression Ratio
CSI	Cumulative Similarity Index
CUEDC	Composite Urban Emission Driving Cycle
CVT	Continuously Variable Transmission
DC	Driving Cycle
DSD	Divisional Secretariat Division
EOP	Evening Off Peak
EP	Evening Peak
EPA	Environmental Protection Agency
EPAS	Electronic Power Assisted Steering
EU	European Union
EV	Electric Vehicles
FC	Fuel Consumption
FT	Fixed Transmission
FTP	Federal Test Procedure
FWD	Front Wheel Drive
GFEI	Global Fuel Economy Initiative
GHG	Green House Gas
GIS	Geographic Information Software
GPS	Global Positioning System
GVWR	Gross Vehicle Weight Rating
HEV	Hybrid Electric Vehicle
HPAS	Hydraulic Power Assisted Steering
HWFET	High Way Fuel Economy Test
IC	Internal Combustion
ICE	Internal Combustion Engine
IEA	International Energy Agency
IMDC	Indian Motorcycle Driving Cycle
IMMA	International Motorcycle Manufacturers' Association
ISFC	Indicative Specific Fuel Consumption

ISO	International Standardization Organization
JP	Japanese Driving Cycle
LA01	Los Angeles 01 driving cycle
LA92	Los Angeles 92 driving cycle
LDV	Light Duty Vehicle
LoS	Level of Service
METI	Ministry of Economics, Trade and Industry
MOP	Morning Off Peak
MT	Manual Transmission
NEDC	New European Driving Cycle
NREL	National Renewable Energy Laboratory
OBD	On Board Diagnostic
PKE	Positive Kinetic Energy
PV	Performance Value
RH	Relative Humidity
RMS	Root Mean Square
RPM	Revolutions Per Minute
RWD	Rear Wheel Drive
SAE	Society of Automobile Engineers
SAFD	Speed Acceleration Frequency Distribution
SAPD	Speed Acceleration Probability Distribution
SC03	Supplemental Federal Test Procedure with A/C system turned on.
SDG	Sustainable Development Goals
SFC	Specific Fuel Consumption
SFTP	Supplemental Federal Test Procedure
SI	Spark Ignition
SL	Sri Lanka
SSD	Sum Square Difference
TPES	Total Primary Energy Supply
UNEP	United Nations Environmental Program
US	United States

US06	The United States Supplemental Federal Test Procedure
USCAFE	The United States Corporate Average Fuel Economy
USFTP	The United States Federal Test Procedure
WLTC	World Harmonized Light Vehicle Test Cycle
WLTP	World Harmonized Light Vehicle Test Procedure
WMTC	World Motorcycle Test Cycle

1. INTRODUCTION

1.1 Motivation

Despite the technological advancements in the sector of automobile engineering and transportation, energy consumption and the emission of mass pollutants and greenhouse gases have become major challenges in the global context. The fact that fossil fuels which cater to over 80% of the global Total Primary Energy Supply in 2022, is being a depleting energy resource, paves the way for the said challenges to reach an alarming state. Moreover, the transportation sector is accountable for approximately 29% of the global final energy demand, whereas 70% of the said energy is consumed by the road transport sector [1].

United Nations Environment Programme (UNEP) which has foreseen these challenges in the global domain, has defined certain policy framework which needs to be carried out in national and regional context. Emphasizing the significance of improving energy efficiency, UNEP has defined a specific target to double the improvement in the energy efficiency of newly manufactured Light Duty Vehicles (LDVs) by 2030, under the 7th Sustainable Development Goal (SDG7) concerning the affordable and clean energy [2].

Fuel economy programmes and emission reduction targets have proven to be the most effective policy tools in obtaining control over the mentioned issues. Global Fuel Economy Initiative (GFEI) is one such international organization which undertakes research, provides necessary advocacy, and assists countries to tailor-make policy tools to increase the fuel economy and reduce emission inventories [3]. To achieve that, several instruments have been introduced by GFEI that countries can utilize viz., standards, taxes or labelling schemes [4]. Sri Lanka is also among the initial 25 countries of the global rollout of the GFEI programme and several policies related alignments have been proposed [3]. Aligning with the said standards, there are several

initiatives in Sri Lanka to develop a fuel economy labelling programme for vehicles. Hence, there is a national-level necessity for developing a benchmark for rating the performance of vehicles in terms of fuel economy values. Nevertheless, the real performance of vehicles, especially LDVs, in local traffic and driving conditions is not fully established. Furthermore, prior to the initiation of the fuel economy labelling programme, a strong scientific basis should be developed in order to reflect the performance of LDVs in localized driving conditions. However, in depth research studies that are required to develop a sound scientific base of the energy labelling scheme including, the development of local driving cycles (DC) to mimic the local traffic and driving behaviour have not been carryout so far.

1.2 Aim and Objectives

The research study aims to provide a scientific basis for a better understanding of driving patterns and their influence on the fuel economy performances of in-use LDVs in Sri Lanka. To obtain the research aim throughout the study, two specific objectives have been defined. The first specific objective encompasses the development of driving cycles to represent local driving conditions of selected vehicle categories whereas the second specific objective encompasses the development of a mathematical model capable of estimating fuel economy values of different LDV categories under varying driving patterns.

1.3 Scope of the Study

During the research study, the fuel economy characteristics of LDVs in Sri Lanka's active fleet are analyzed. The LDVs are defined as road vehicles with a tare weight not exceeding 3,500 kgs. Within Sri Lanka's active fleet, several engine and propulsion technologies exist. The proposed study is specifically limited to LDVs equipped with Internal Combustion (IC) engines with Spark Ignition (SI) technology, which is employed with gasoline engines and with Compression Ignition (CI) technology,

which is employed with diesel engines. Furthermore, when LDVs are considered, only the two-wheeled, three-wheeled and four-wheeled motorized LDVs are taken into account. Moreover, when developing local driving cycles, the geographical scope is converged to Colombo Metropolitan Area, which is the main region of transportation and vehicle usage.

1.4 Methodology

To achieve the said specific objectives, a methodology is developed, which comprises eight main elements viz., (i) the literature survey on the performance of LDVs and characterization of driving cycles, (ii) theoretical formulation of local driving cycles and the validation of the developed driving cycles against the population data, (iii) identification of governing parameters (both technical and operational) and related governing equations and conditions of fuel economy characteristics of vehicles, (iv) establishment of functional relationships among governing parameters identified, (v) data acquisition from selected categories of LDVs, namely two-wheelers (2W), three-wheelers (3W) and four-wheelers (4W) in real driving conditions and validation of the established functional relationships, (vi) formulation of relationships between fuel economy and identified parameters, (vii) development of a theoretical model for the relationship between fuel economy and driving pattern, and (viii) the validation of the model through laboratory testing (both physical validation and simulation-based validation).

1.5 Significance of the Research Study

This research study is highly significant as it aims to develop an improved scientific basis for understanding real-world driving patterns and how they impact fuel economy of light duty vehicles (LDVs) in Sri Lanka. Currently, there is a lack of data on the actual on-road performance and fuel efficiency of the nation's vehicle fleet under local traffic conditions. By formulating representative driving cycles and mathematical

models, the study will help establish accurate fuel economy benchmarks tailored to Sri Lankan driving habits. Moreover, the research has national importance in supporting initiatives around fuel economy labeling schemes and vehicle emissions regulation for the country. The study methodology to gather real-world vehicle data could even be extended to analyze broader sustainability issues around transportation. Overall, the expected outcomes of localized driving cycles and fuel consumption models can promote evidence-based policymaking to address issues like energy efficiency in transport, energy security and urban air pollution from the expanding vehicle fleet.

2. LITERATURE REVIEW

Fuel economy is an essential parameter in assessing the performance of any mode of transport, including light duty vehicles. With the increasing number of vehicles manufactured and used on the roads, their fuel consumption has become a vital factor [5]. There is a direct relationship between fuel economy and Green House Gas (GHG) emissions, while it relates to air pollution as well [6]. Therefore, the authorities, regulatory bodies and manufacturers have paid more attention to making the vehicles more fuel efficient and environmentally sustainable. Hence various test procedures have been introduced to measure fuel economy and emissions. Various driving cycle test procedures have been introduced regionally viz. New European Driving Cycle (NEDC) for the European region, United States Corporate Average Fuel Economy (USCAFE) Driving Cycle, United States Federal Test Procedure (USFTP) and Highway Fuel Economy Test (HWFET) for United States region, JC08 Driving Cycle for the Japanese region and Worldwide Harmonized Light duty Test Cycle (WLTC) to represent the entire global domain [7]. There is no clear definition for driving patterns. Yet most of the researchers/authors try to define a driving pattern using Characteristic Parameters (CPs) [8]. Characteristic Parameters also known as Performance Values (PVs), describe the time series illustration of a vehicle's speed and CPs make it possible to explicitly distinguish one driving pattern from another [8]. CPs can be introduced viz. Mean Speed, Positive Kinetic Energy (PKE), Percentage of Idling Time, Average Positive Acceleration, etc. [8]. A Driving Cycle means a generalized (normalized) representation of various driving patterns in a speed-time analysis. A DC is formulated in a way such that the values of CPs of a DC are approximately equal to the respective average values of the CPs of driving patterns [8]. DCs are very important to assess the environmental impact of traffic, i.e., the mass emission of air pollutants and fuel consumption. To control the impact, several engine control strategies and optimizing vehicles' powertrain configurations are suggested by DC analysis.

2.1 Literature review on vehicle categorization

According to the United States Environment Protection Agency's (EPA) definition, an LDV is defined as a road vehicle with a Gross Vehicle Weight Rating (GVWR) not exceeding 8,500 lbs. [9]. GVWR is defined as the weight specified by the respective manufacturer as the loaded weight of a single vehicle [10]. When determining GVWR, it includes the weight of a vehicle as specified by the manufacturer including the vehicle's chassis, body, engine fluids, fuel, accessories, driver, passengers and cargo but specifically excluding that of any trailers [11],[12]. In Sri Lankan context, the analogous vehicle categories to LDVs are defined as vehicles with a weight classification of GVWR not exceeding 3,500 kg [13]. Similarly, according to Bharat Stage (BS) VI standard which is in practice in India [14], the Australian Design Rules (ADR) 79/03 standard, which is defined for the Australian region [15], China 5 Standard which is effective to entire Chinese Mainland region [16], the standards which are defined by Ministry of Economics, Trade and Industry (METI), Japan for the entire Japanese region [17] and Euro VI standard which is defined for the entire European Union [18], the LDVs are classified as road vehicles with a GVWR not exceeding 3,500 kg.

According to the Motor Traffic Act, 2009 of Sri Lanka, there are specific vehicle classes which include into LDV category viz. Light motorcycles, Motorcycles, Motor Tricycles and Dual-Purpose Motor Vehicles [13]. The registered vehicle population of Sri Lanka reached 8.3 million by mid of the year 2022 out of which over 7 million can be classified as LDVs [19]. This depicts that LDVs account for approximately 84.34% of the entire registered vehicle fleet in Sri Lanka.

Considering the active fleet in Sri Lanka, which surpassed 5.6 million vehicles by the year 2022, the approximate survival percentage of vehicles is around 68% to 69% [20]. The LDVs account for the majority share of the in-use fleet with more than 4.8 million vehicles, claiming a share of 86% of the in-use fleet [19], [20]. It is conspicuous that, the LDVs are accountable for the majority share of national energy/fuel demand. Consequently, LDVs are contributing to the major share of emissions in the national

context. This highlights the significance of studying the fuel economy characteristics of LDVs to ensure sustainability in the transportation sector, in relation to energy and environmental performances.

During the study, the focus is given to motorcycles and 4W which fall under light duty vehicles having a gross vehicle weight rating of less than 3.5 tons. Colloquially, the motorcycles are referred to as two-wheeled motor vehicles. Yet, different classification norms have been adopted throughout the world for motorcycles, viz. mopeds, motor bicycles, motor tricycles, quadricycles, etc.. When considering the general categorization of all types of road vehicles concerning European Union (EU) standards, the types from Category L to Category O can be cited. During the present study, an emphasis was placed on category L-type vehicles. When focusing on the said categorization it is clear that all types of 2W and 3W are included within 'Category L'. In addition to 2W and 3W, quadricycles too have been included in Category L. When considering Light Duty Vehicles (LDVs), all the vehicles falling under Category L and a subset of Category M and Category N are included. When considering the portions which get included within LDVs from Category M and Category N are the sub-classes of motor vehicles having at least four wheels and the Gross Vehicle Weight Rating (GVWR) not exceeding 3.5 tons. Despite the development of the latest versions of the Worldwide Harmonized Light Vehicle Test Procedure (WLTP), which is the benchmark driving cycle across the globe for all types of LDVs, a separate driving cycle has been developed for the Category L vehicles, i.e., Worldwide Harmonized Motorcycle Test Cycle (WMTC) [172]. Due to its inherent limitations concerning power output (engine/motor) and the weight ratings (being significantly lighter than that of Category M and Category N vehicles), the speed responses (quantified as top speed) have major discrepancies comparatively to that of other categories of LDVs. Therefore, when analyzing the driving patterns w.r.t. shortlisted Characteristic Parameters (CPs), viz., average speed, average acceleration, average deceleration, etc., significant mismatches can be anticipated between Category L and other types of LDVs.

Table 1: Type ‘L’ Vehicle Categorization as per WMTC.

Vehicle Class	Vehicle Class Name
L1e	Moped
L2e	Three-wheel Moped
L3e	Motorcycle
L4e	Motorcycle and sidecar
L5e	Tricycle
L6e	Light Quadricycle
L7e	Heavy Quadricycle

As stated in Table 1 a much broader classification is performed on the WMTC vehicle classification [172]. When referring to the classification stated in Table 1, the following key characteristics can be highlighted as portrayed in Table 2 [173].

Table 2: Key Characteristics of Motorcycle Classes

Vehicle Class	Top Speed (km/h)	Engine Capacity (CC)
L1e	<45	<50
L2e	<45	<50
L3e	>45	>50
L4e	>45	>50
L5e	>45	>50
L6e	<45	<50
L7e	>45	>50

The same categorization criteria are referred to by the International Motorcycle Manufacturers Association (IMMA) as well [174]. Since the objective of the study is to develop driving cycles to suit the local conditions, it is important to investigate Sri Lankan regulatory landscape w.r.t. vehicle classifications. The regulatory landscape is

explained as mentioned below. The classification of active LDV fleet in Sri Lanka as per Section 122 of the Motor Traffic Act amended by Act no.08 of 2009 is depicted in Table 3 [175].

Table 3: Classification of Light Duty Vehicles in Sri Lanka

Class	Description
A1	Light motorcycles of which Engine Capacity does not exceed 100CC.
A	Motorcycles whose Engine Capacity exceeds 100CC.
B1	Motor Tricycles or vans of which tare does not exceed 500kg and Gross vehicle weight does not exceed 1000 kg; Motor vehicles in this class include an invalid carriage.
B	Dual-purpose Motor vehicles of which Gross Vehicle Weight does not exceed 3500 kg and the seating capacity does not exceed 9 seats inclusive of the driver's seat.

As per the classification stated in Table 3, there are two motorcycle classes (A1 and A), one tricycle class (B1) and another class for dual-purpose motor vehicles (B). Although there are various sub-classes for motorcycles, motorcycles (L3e) and motor tricycles (L5e) are two of the major fleet categories in the Sri Lankan context. By 2020. Over 1.1 million registered 3W were claiming a portion of over 14% of the total registered vehicle fleet in Sri Lanka.[178]. Though the quadricycles are a new introduction to the vehicle fleet in Sri Lanka, they can be considered as negligible since the number of quadricycles is just over two thousand and around 0.03% of the entire road vehicle population. Thus, the study can be narrowed down to two types of vehicle categories, i.e., two-wheeled motorcycles and motor tricycles.

When considering the DCs developed pertaining to Figure 76, with a focus on motorcycles, USA Federal Test Procedure (FTP) is the test cycle that has been used for the emission measurements and type approval procedures of motorcycles in the USA since the mid-1960s, representing home-to-work commuting in Los Angeles, California. The FTP includes a series of accelerations, decelerations, and idling (such as at stoplights). It also includes starting the vehicle after it has been parked for an

extended period (called a “cold start”), as well as a start on a warmed-up engine (called a “hot start”). The total distance covered by the FTP is about 11 miles and the average speed is about 21 mph, with a maximum speed of about 56 mph. The maximum acceleration rate is a relatively mild 3.3 mph/sec, which is due to the limitations of the dynamometer technology at the time the test was developed. As per FTP, a motorcycle is defined as “any motor vehicle with a headlight, taillight, and stoplight and having two wheels, or three wheels and a curb mass less than or equal to 793 kilograms (1749 pounds)”. Thus, referring to the said definition for a motorcycle under FTP, it also includes both 2W and 3W under the same class.

In most of the regions, the revised WMTC has been adopted as their emission regulatory driving cycle, especially in the EU, Japan, South Korea and the USA which are among the leading vehicle manufacturers. When considering the utility of motorcycles (2W and 3W in general), South and South-East Asian regions claim a major portion and Indonesia, Thailand and Vietnam are among them. In these three countries, Euro 3 standard is adopted for motorcycles, which is equivalent to ECE-R40 and ECE-R47 DCs [177], [178], [179], [180], [181]. When analysing the regional utilization of driving cycles to measure emissions of motorcycles, it is clear that a common driving cycle for a particular region/country of interest has been used to benchmark the emission performance of 2W, 3W and 4W quadricycles. Since Sri Lankan driving context can closely be related to South and South-East Asian driving conditions (Indian/Indonesian/Vietnamese etc.), it is advisable and recommended to adhere to a similar procedure in developing driving cycles, especially for motorcycles; that means developing driving cycles for 2W, 3W and four-wheeled quadricycles in general, rather than developing specific driving cycles for each category.

When analyzing the characteristic parameters of the regionally developed DCs, the necessity for the development of a specific driving cycle for the Colombo Metropolitan area could be emphasized. When comparing the top speeds of the developed Colombo Metropolitan DC (CMDC) versus Indian Motorcycle Driving Cycle (IMDC), there is a lucid discrepancy between the values since CMDC claims for a top speed of around 36 km/h whereas IMDC claims for a top speed of around 55 km/h [182]. Moreover,

the discrepancy between the acceleration values could be highlighted. The average acceleration and deceleration values of IMDC could be cited as 1.26 m/s^2 and -1.33 m/s^2 whereas those of CMDC could be cited as 0.33 m/s^2 and -0.36 m/s^2 [182]. This depicts that the average acceleration and deceleration values portray major discrepancies between the proposed CMDC and the compared IMDC. This further highlights the necessity of the development of a dedicated DC to suit Colombo Metropolitan traffic conditions.

2.2 Literature review on the factors affecting the fuel consumption of LDVs.

Various studies have been carried out by researchers worldwide to identify the factors affecting the fuel consumption of LDVs. The fundamental factors affecting the fuel economy of any type of road vehicle can be listed viz. vehicle type, vehicle size, vehicle age and accumulated distance travelled, fuel type, tyre type and maintenance, maintenance condition of the vehicle, road conditions, ambient weather conditions and traffic conditions (or driving cycle) and how the vehicle is driven [5]. In particular, the traffic conditions and how the vehicle is driven could critically affect the fuel economy of a vehicle [5]. According to Badran et al., the fuel economy of a vehicle significantly depends on the altitude at which the vehicle are driven, the load conditions of the vehicle, aerodynamic drag and the use of air-conditioning units [23]. According to Slavin et al., the vehicular fuel economy depends upon factors viz. vehicle weight, vehicle aerodynamic characteristics, engine/powertrain type, transmission type, RWD/FWD drivetrain type, tyre pressure, control and calibration, road type, traffic and driving style [24]. An empirical formula for fuel economy has been derived by Gautam et al. [25], based on the variables: vehicle type, fuel price, government policies, the weight of the vehicle and power of the vehicle engine for US passenger vehicles. The said empirical formula is shown in Equation (1).

$$FE = \beta_0 e^{\beta_1 (VT)} (FP)^{\beta_2} (CAFE)^{\beta_3} (Wt)^{\beta_4} (HP)^{\beta_5} e^{u} \quad (1)$$

where,

FE – Fuel Economy;

VT – Vehicle Type;

FP – Real Petroleum Price per gallon;

$CAFE$ – Corporate Average Fuel Economy;

Wt– Weight of the automobiles and

HP – Horsepower of the engine.

Moreover, $\beta_0, \beta_1, \beta_2, \beta_3, \beta_4, \beta_5$ and u are hypothesized coefficients that need to be determined empirically.

The relationship in Equation (1) is hypothesized using a more economic-biased perspective. Hilliard et al. have stratified the fundamental factors affecting the fuel economy of road vehicles into five main types viz. engine factors, drivetrain factors, vehicle factors, operating factors and test cycles [25]. Engine factors can be considered to affect at a higher degree on the fuel consumption of a road vehicle which is powered by an IC engine. All IC engines are governed by the first and second laws of thermodynamics, and operate on thermodynamic cycles consisting of a sequence of processes which include compression, heat addition, expansion and heat rejection [25]. Commonly, there is a tendency to refer to any heat that an engine system transfers to the atmosphere as a heat loss. However, there is a fundamental requirement that some of the heat supplied to the system must be rejected to a colder region, adhering to the second law of thermodynamics. The thermal efficiency of an engine is strongly a function of the Air-Fuel Ratio (AFR) and Compression Ratio (CR) in addition to the nature of the operating cycle [25]. Ament et al. have set up an experimental study to analyze the effects of engine factors on fuel economy using a 1975 Chevrolet, 5.7-litre gasoline engine with an 8.2 to 1 compression ratio and a 0.9 Air-Fuel Equivalence Ratio (Lambda Value) [26]. An ideal engine with the aforementioned AFR and CR values should have a maximum thermal efficiency of 44% with a heat rejection of 56% based on the fuel-air cycle [25]. But the real engine produced only about half this efficiency with a heat rejection of 80%. The potentially recoverable engine losses cause the real engine to perform 24% less than the ideal engine in this scenario. The

potentially recoverable engine losses can be listed viz. cycle losses, pumping losses and mechanical friction losses. Hilliard et al. have calculated the energy balance of an IC engine of the aforementioned test vehicle in terms of the percentage of total fuel supplied and the results are shown in Table 4 [25].

Table 4**:** Energy Balance in terms of the percentage of fuel supplied [25].

Attribute	Percentage of total fuel supplied
Net shaft power	20.4%
The second law of heat rejection	56.0%
Potentially Recoverable Losses	
Heat Loss	5.2%
Time Loss	2.6%
Exhaust Blowdown Loss	0.8%
Pumping Loss	7.2%
Friction Loss	7.2%
Leakage, incomplete combustion, errors of approximations	0.6%
Total fuel supplied	100.0%

When analyzing the test results shown in Table 4, it's conspicuous that nearly 23% of the fuel supplied is consumed to overcome the potentially recoverable losses. Certain improvements in engine technology can potentially decrease engine losses and consequently increase the fuel economy of a vehicle.

Typically, IC engines can be categorized into two types i.e., Spark Ignition (SI) engines and Compression Ignition (CI) engines. Generally, SI engines are powered by gasoline whereas CI engines are powered by Diesel. Giles [28] has illustrated the fuel economy characteristics of a gasoline engine which is shown in Figure 1.

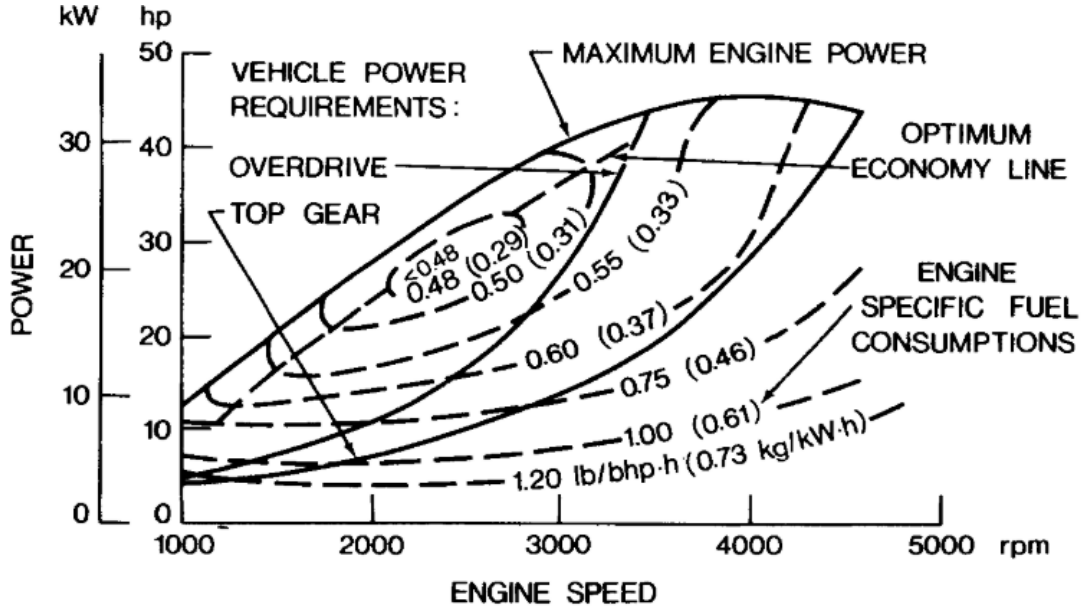

Figure 1: Fuel economy characteristics of a gasoline engine – Adopted from Reference [28].

Specific fuel consumption (SFC) of an engine can be defined as the mass of fuel required to generate a unit measurement of power within a unit measurement of time. There are 2 types of SFC viz, Indicative Specific Fuel Consumption (ISFC) and Brake Specific Fuel Consumption (BSFC). ISFC can be defined as the mass of fuel required to generate a unit measurement of power on the piston surface of the engine within a unit measurement of time whereas BSFC can be defined as the mass of fuel required to generate a unit measurement of power which is available on the crankshaft of the engine within a unit measurement of time. During the analysis, Giles [28] used BSFC to quantify the fuel economy characteristics. By connecting the engine operating points with the lowest BSFC for each power setting, an optimum fuel economy line which denotes the maximum efficiency of the engine can be produced as shown in Figure 1.

The effect of auxiliary loads on the engine is another significant aspect that affects the overall operating fuel economy of a vehicle. The engine performance diagrams provided by manufacturers usually represent the gross engine performance which is the performance of the engine with only the built-in equipment required for self-sustained operation, and all other installations and accessories not essential to the operation are stripped off [27]. The auxiliary equipment viz. the alternator, air

conditioning (A/C) unit, power-assisted steering and braking, water pump and cooling fan demand for engine power [30], [39], [40], [41], [42].

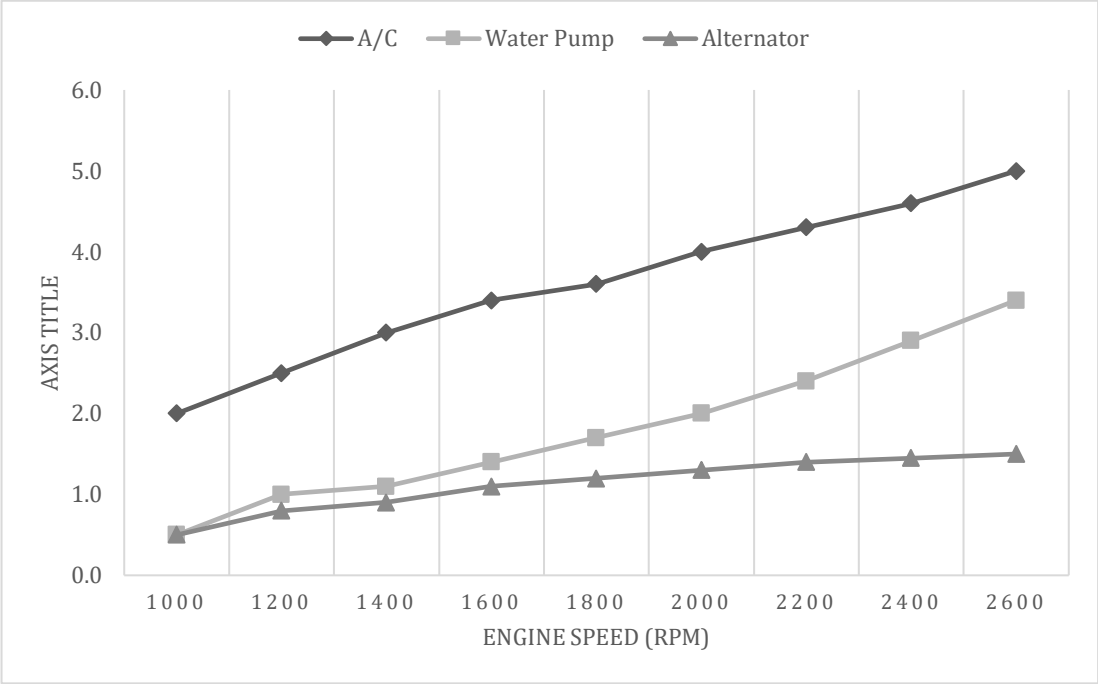

Figure 2: Accessory power requirements of a full-size passenger car - Adopted from Reference [31].

Figure 2 clearly shows that different auxiliaries have different power requirements which make a considerable demand on the engine power. Also, it's conspicuous that all the auxiliary loads which are belt-driven units depict a closely proportional relationship with the engine speed where the auxiliaries appeal for higher power demand during higher engine speeds [32], [33].

Gasser et al. have analyzed the effect of auxiliary vehicle equipment on the overall operating fuel economy of an intermediate car with automatic transmission [30]. They have tested the fuel economy w.r.t. the EPA Urban Cycle and the test results are shown in Table 5.

Table 5: Effect of engine accessories on the fuel economy of an intermediate car with automatic transmission [30].

Type of accessory	Urban cycle (mpg equivalent)
A/C System	1.5
Alternator	0.9
Fan	0.1
Power steering	0.1

When comparing the results in Table 5 with the power demand patterns in Figure 3, it's clear that the A/C system affects the most as an auxiliary load and consequently affects the fuel economy. Also the A/C system appeals for a higher driving torque than any other auxiliary equipment [33], [34]. A common characteristic of the belt-driven engine auxiliary units is that their input power for operation is proportional to the engine speed, whereas the output power is not relevant to the engine speed [35], [36], [37]. To reduce the auxiliary power demand of the A/C system on the engine, several alternative techniques have been suggested viz. charging the batteries by running the engine in the optimal efficiency region, using the stored battery power and the electric motor to run the compressor or using the thermal mass storage of the vehicle [43], [44]. Lee et al. have set up an experimental study to quantify the efficiency of an A/C system of a vehicle through an analysis of the effects of each component's contribution to the deterioration in the fuel economy [34].

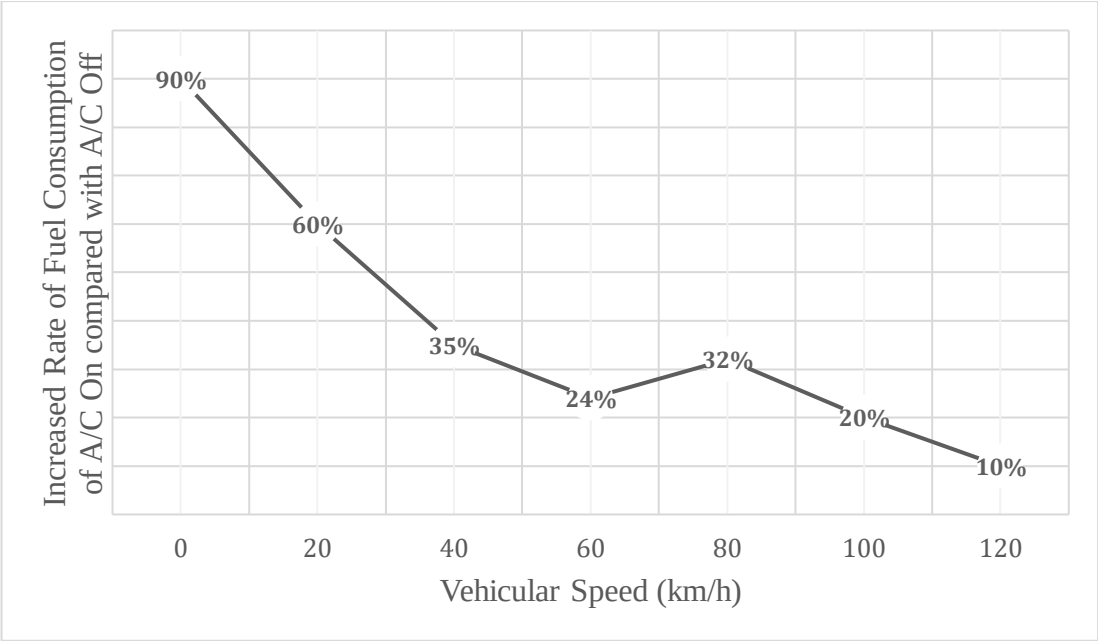

Figure 3: Comparison of the increased rates of the fuel consumption with the A/C on and with the A/C off at different vehicle speeds - Adopted from reference [34]

Figure 3 shows the results of the experimental study concerning the variation in fuel consumption at different vehicle speeds in the A/C-on and the A/C-off conditions. A second peak value was noted at the vehicle speed of 75km/h when a gear shift occurred as the vehicle speed increased [34]. The total generated engine power needed to be increased as the vehicle speed increased. However, the engine speed did not increase proportionally to the vehicle speed increment from 50km/h to 70km/h owing to the gear shift. Therefore, additional engine torque, which comes from the additional fuel consumption, was required to compensate for the increased power requirement [36]. During the idling condition, the BSFC has the highest value with a 90% increased rate of fuel consumption w.r.t. the A/C off condition. Among the A/C system components, the most significant component affecting fuel consumption is the compressor which caused a fuel consumption increase of 77-89% [44]. The other components' impact can be listed as: from the blower: 6-12%; from the cooling fan: 4-10%; from the clutch 0.7-2% [45], [46].

The transmission system or the drivetrain of a vehicle is another key factor which determines the fuel economy [26]. Drive-train elements in a modern vehicle can be

listed viz. the transmission including the clutch or torque converter, the driveshaft including universal joints, the differential and the final drive assembly and axle shafts [26], [48]. Primarily, there are two main types of transmission for road vehicles i.e., manual transmission (MT) and automatic transmission (AT) with a torque converter. Other types of transmission viz. hydrostatic transmission and continuously variable transmission (CVT) are also in use. When there exists a finite number of gear ratios, it's impossible to perfectly match the engine and the vehicle across the operating range of the engine. Due to this imperfect match, the engine generally operates at less than optimum efficiency at a given speed and load. On par with the developments in CVT technology which has an infinite number of gear ratios would yield a 10% fuel economy improvement [26].

During a simulation analysis performed by Chen et al. [49], a comparison between the fuel economy performance of a CVT and a fixed transmission (FT) is evaluated. According to the comparison, CVT outperforms FT in terms of overall fuel efficiency by 3.53% for a series Hybrid Electric Vehicle (HEV) [49]. The torque converter and the torque converter clutch are critical devices governing overall power transfer efficiency in automatic transmission powertrains [50]. In a study conducted by Eckert et al. [51], a multi-objective optimization using fuzzy control of a vehicle equipped with an automated manual transmission (AMT) was simulated. According to the simulation results, a maximum level of fuel saving of 19.72% was obtained using the fuzzy-controlled gear shifting mechanism whereas hydrocarbon, carbon monoxide and nitrogen oxides were reduced by 12.90%, 29.20%, and 17.02% respectively [51].

The axle ratio is another significant factor which determines the fuel efficiency on the drive train [52]. The overall drive-train ratio or the axle ratio is often spoken of as the N/V ratio where N refers to engine RPM and V, vehicle velocity in mph, with the transmission in its highest gear [25]. In general, a decrease in axle ratio will result in reduced fuel consumption.

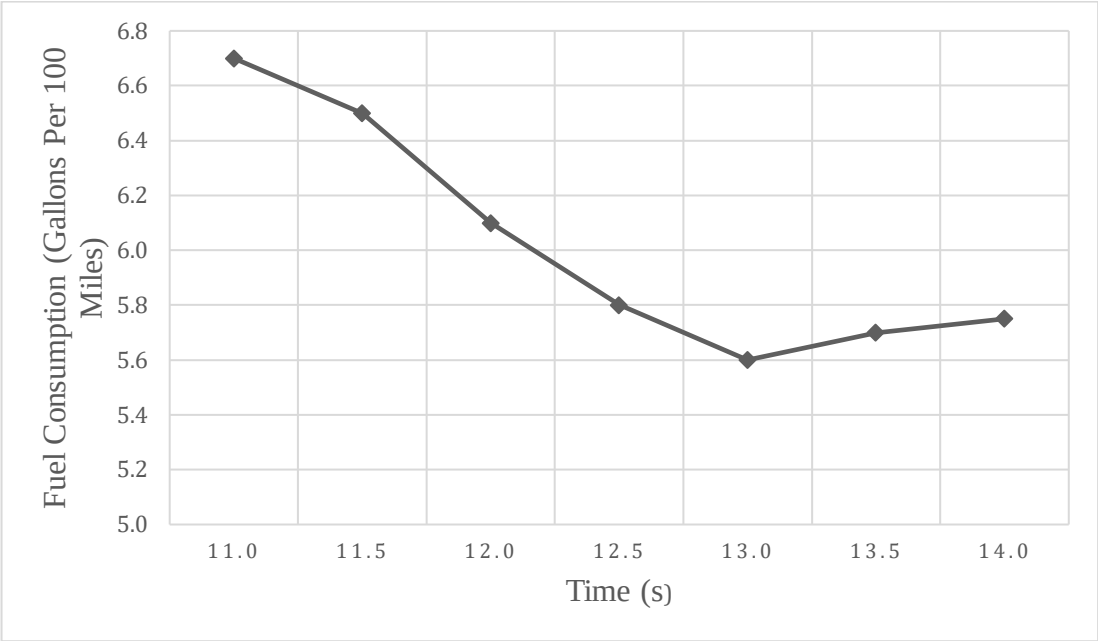

Figure 4: The effect of vehicle axle ratio on fuel consumption and performance - Adopted from reference [51].

The impact of the axle ratio in the drivetrain on the fuel economy of a vehicle is shown graphically in Figure 4. It's clearly shown that the axle ratio has an inversely proportional behaviour w.r.t. fuel economy.

The reduction of vehicle weight is also one of the significant measures for obtaining improved fuel economy [27]. This is because the propelling force, and hence the power, required to accelerate a vehicle is proportional to its weight [27]. In "stop and go" driving conditions in the city or an urban environment, frequent acceleration leads to higher fuel consumption for a heavier vehicle than a lighter vehicle [27]. To reduce the vehicle weight, the unibody construction has been largely replaced by the separate body-frame construction. The lightweight materials viz. composites, high-strength low-alloy steel, plastics, Aluminium and metal-plastic laminates are being used for vehicle manufacturing [54]. The usage of lightweight materials for vehicle manufacturing can improve fuel economy by 6-8% for each 10% in weight reduction [55]. Cheah [56] has experimentally analyzed the impact of vehicular weight on fuel

consumption where the results depict that a 10% reduction in vehicular weight has reduced the fuel consumption of a car by 5.6% and of a light truck by 6.3% [56]. Not only the vehicles equipped with IC engines but also the electric vehicles (EVs) of which a 10% reduction in weight can improve electric range by 13.7% [57]. Also, the reconfiguration of the vehicle from the front engine, rear-wheel drive to the front engine, and front-wheel drive would lead to a considerable reduction in vehicular weight, which consequently increases fuel economy [58].

Aerodynamic drag is always a significant factor affecting the operating fuel economy of road vehicles. It's important to note that the aerodynamic drag or wind resistance is not just related to fuel economy but also to emission performance, stability, noise, surface dirt control and component and interior cooling [25]. According to several simulations and wind tunnel tests carried out by Priyadarshini et al. [59], it was found that, for every 10% increase in drag, the fuel consumption was approximately increased 1 L/100 km. The aerodynamic drag of a road vehicle is accountable for a major portion of a vehicle's fuel consumption and contributes up to 50% of total vehicle fuel consumption at highway speeds [60]. Reducing aerodynamic drag offers an inexpensive solution to improve fuel economy and hence shape optimization has become an essential part of the vehicle design process [61]. It has been found that, 40% of the drag force is concentrated at the rear of the geometry [62]. The main cause of vehicular aerodynamic drag is due to pressure drag or form drag [63]. Pressure drag on vehicles due to flow separation constitutes more than 80% of the total aerodynamic drag, whereas the remaining 20% is contributed by frictional drag [64]. Moreover, 53% of the usable energy from the engine is consumed to overcome the aerodynamic drag at highway speeds [62]. A reduction of 15% in aerodynamic drag at a highway speed of 55mph can result in about 5-7% in fuel saving [65].

Following equations from (2) to (4) represent the tractive dynamics of a vehicle pertaining to aerodynamic drag resistance. Equation (2) represents the determination of aerodynamic drag force whereas (3) and (4) denote the determination of the reuiqred power to overcome aerodynamic drag.

$$F_d = C_d.\frac{1}{2}.A.\rho.v^2 \quad (2)$$

$$P = F.v \quad (3)$$

$$P_d = k_1 v^3 \quad (4)$$

In Equations (2), (3) and (4), the terminologies are identified as the following: F_d: Drag Force (N) ; C_d: Drag Coefficient; ρ:density of fluid (kg/m^3); v : flow velocity (m/s); A : The frontal area (m^2), P: Tractive-Power (W); F: Tractive-Force (N); and P_d: Tractive power required to overcome the drag (W), k_1: proportionality constant. When a vehicle is moving at a constant speed, $P_d = F_d.v$; which means that the tractive power to overcome drag is equal to the product of Drag Force (F_d) and vehicle speed (v) [66]. Hence as given in Equation (4), the power required to overcome the drag is proportional to the cube of the relative velocity of the flow (v^3) [67]. This critically emphasizes the impact of vehicular speed on the power required to overcome the aerodynamic drag. Thus it emphasizes a higher degree of increase in fuel consumption.

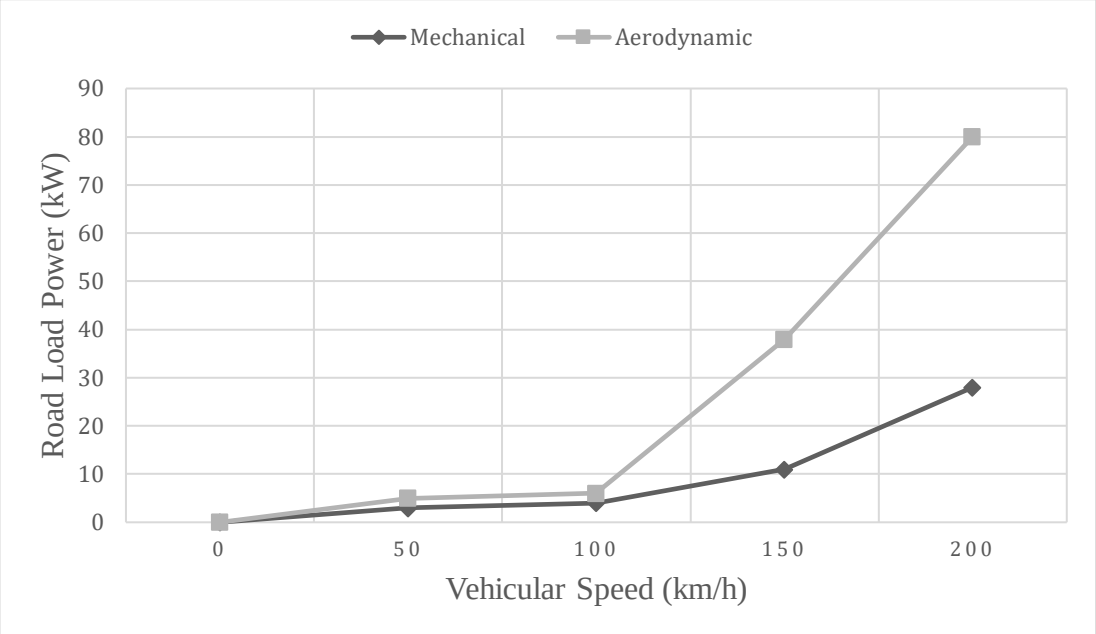

Figure 5: Tractive-power requirement to overcome the aerodynamic resistance and mechanical resistance versus the vehicular speed - Adopted from reference [69].

Kelly et al. have experimentally studied the power requirements of a typical passenger car cruising at a speed greater than 80 km/h and consequently found out that the power required to overcome the aerodynamic resistance is greater than that of rolling resistance of tyres and the resistance in the transmission [68]. In Figure 5, it is clearly shown that the power required to overcome the aerodynamic drag is exponentially increasing with the vehicular speed and with a higher gradient than the mechanical resistance.

Table 6: Components of aerodynamic resistance coefficient [69].

Components of Aerodynamic Resistance Coefficient	Typical Value
Forebody	0.06
Afterbody	0.14
Underbody	0.06
Skin friction	0.03
Total body drag	0.28
Wheel and wheel wells	0.09
Drip-rails	0.01
Window recesses	0.01
External mirror (one)	0.01
Total protuberance drag	0.12
Cooling system	0.04
Total internal drag	0.04
Overall total drag	0.44

Table 6 shows the compilation of the aerodynamic drag coefficient. The aerodynamic drag coefficient is determined using the coast-down test where the test vehicle is run up to its top speed and then the driveline is disconnected from the engine and then the vehicle starts decelerating. With the effects of the rolling resistance of the tyres and driveline resistance separated from the total resisting force, the aerodynamic resistance and consequently the aerodynamic resistance coefficient can be determined [70], [71]. According to the said data, the aerodynamic drag can be sectioned into 3 main types

of viz. total body drag affecting 64.4%, total protuberance drags affecting 27.6% and total internal drag affecting 8% for the total drag [72], [73].

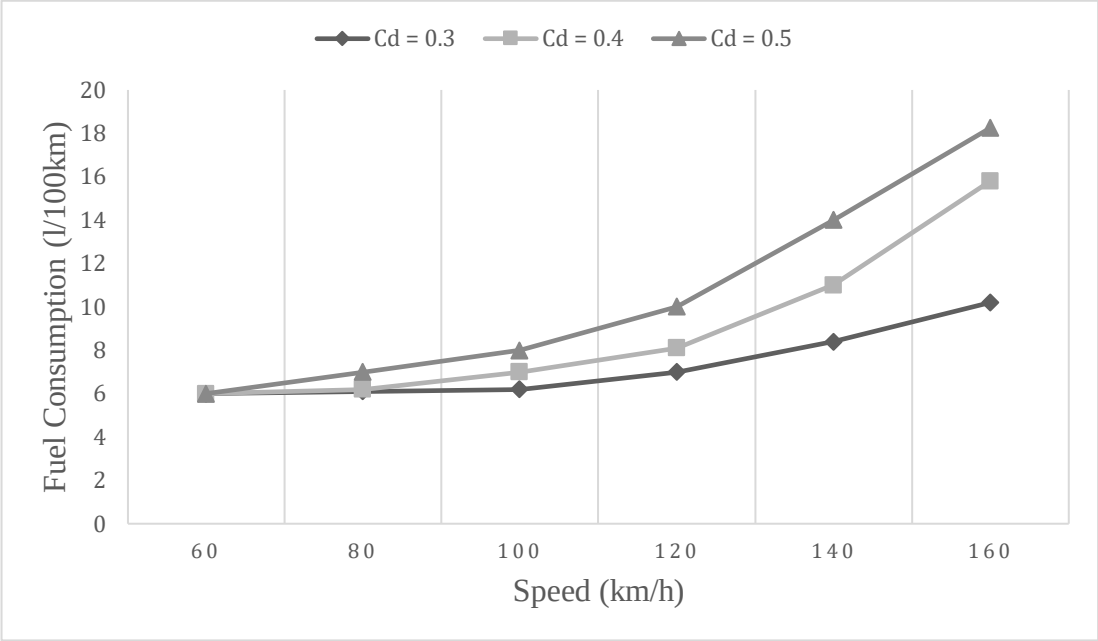

Figure 6 : Effect of the reduction in aerodynamic resistance coefficient on the fuel economy at different speeds for a mid-sized passenger car - Adopted from reference [74].

Hucho et al. [74] have experimentally analyzed the effect of the reduction in aerodynamic resistance coefficient on the fuel economy at different speeds for a mid-sized passenger car, as shown in Figure 6. It can be claimed the fact that with the reduction of the aerodynamic resistance coefficient, a significant gain in fuel economy can be obtained. Various design techniques have adhered to in consideration of the reduction of the aerodynamic resistance coefficient [75]. Even smaller considerations such as a lip or midget spoiler on the rear trunk of a passenger car can have a profound impact in reducing the overall drag of the vehicle and also influence the other factors viz. wind stability [76].

Pneumatic tyres, flexible toroid structures filled with compressed air [77], are a key component affecting vehicle fuel efficiency through rolling resistance. A tyre's reinforcing carcass contains high elastic modulus cord plies encased in lower modulus rubber [78]. Tyres are classified into bias-ply and radial-ply designs based on cord

arrangement [78]. Bias-ply tyres have crisscrossed plies flexing in multiple directions [78], [79]. This internal motion creates friction and road wipe, increasing resistance [79]. In contrast, radial-ply tyres have circumferential cord layers aided by a tread belt [79], [80]. Lacking wipe losses, radial tyres can have 60% lower rolling resistance [81], [82].

Tyre construction and cord orientation fundamentally impact surface interaction and energy dissipation. Bias-ply tyres see higher losses from multi-axis deformation. Radial tyres move more vertically, keeping more cords in tension, reducing wasted energy. Optimizing tyre design and materials can therefore improve vehicle efficiency.

$$R_f = R - \frac{1}{2}.c_x.\rho.A.V_a^k \quad (5)$$

The terminology in Equation (5) can be described as: R_f: Rolling Resistance; R: Overall vehicle resistance; c_x: Aerodynamic drag coefficient; ρ: Mass density of air; A: Frontal area of the vehicle;V_a: Relative air streaming speed w.r.t.. the vehicle; k : speed exponent (for speeds up to 1 m/s: k=1 and for speeds over 1 m/s: k=2).

Equation (5) provides the method of calculating the rolling resistance in consideration with the following assumptions: if the vehicle is cruising at a constant speed on a flat road and the vertical component of the air resistance is neglected [84]. Rolling resistance contributes to 10-13% of the overall fuel consumption of a vehicle [85]. The increase in fuel economy for a 10% decrease in rolling resistance is approximately 1.1% [86], [87]. Djordjevic et al. [96] experimentally tested the relationship between tyre inflation pressure and the corresponding fuel consumption of a vehicle.

Table 7: Corresponding fuel consumption and rolling resistance force for variable tyre inflation pressure values [96].

Tyre inflation pressure [bar]	3.0	2.5	2.0	1.5	1.0	0.5
Rolling resistance force [N]	117	122	125	143	175	235
Fuel Consumption [l/100km]	6.00	5.99	5.97	6.11	6.21	7.22

The data in Table 7 shows that the rolling resistance force gradually increases on par with the decrease of tyre inflation pressure at a constant speed of 32.1 km/h. When a tire is properly inflated, the contact patch (the portion of the tire that touches the road surface) is evenly distributed, and the center of the contact patch is located near the center of the tire. However, when the level of inflation is lower, the tire deforms more, and the center of the contact patch moves forward. This shift in the contact patch center results in a larger portion of the tire deforming and compressing against the road surface, leading to increased rolling resistance.

The increased rolling resistance due to lower tire pressure has a direct impact on fuel economy. As the rolling resistance increases, the engine needs to work harder to overcome this resistance, consuming more fuel in the process. Conversely, properly inflated tires minimize the rolling resistance, resulting in better fuel economy.

It is important to note that the level of tire inflation is not taken into account in the current study. The rolling resistance calculations and analyses assume properly inflated tires and do not consider variations in tire pressure. This assumption is made to simplify the model and focus on other factors affecting fuel consumption.

However, it's worth acknowledging that tire pressure is a crucial factor in real-world driving conditions. Regularly monitoring and maintaining proper tire pressure can

contribute to improved fuel economy and overall vehicle performance. Future studies could incorporate the effect of tire pressure variations on rolling resistance and fuel consumption to provide a more comprehensive analysis.

Despite not explicitly considering tire pressure variations, the current study still provides valuable insights into the impact of rolling resistance on fuel economy. The developed model and analyses offer a foundation for understanding the relationship between rolling resistance and fuel consumption, while acknowledging the potential influence of tire pressure as an additional factor.

There have been many emergent technologies to reduce the BSFC of a road vehicle viz. downsizing of powertrain systems, improved output power-to-weight ratio, turbocharging, cylinder deactivation and stop-start in congested urban driving [89]. Fraser et al. [90] carried out driving-cycle simulations with a vehicle to investigate the fuel consumption benefits that can be accrued through downsizing. The original vehicle engine was a 2.0 L gasoline direct-injection engine, and it was tested against a 1.2 L turbocharged gasoline direct-injection engine. The simulations reported by Fraser et al. [90] showed a fuel saving of almost 15% through downsizing and turbocharging the engine. Douglas et al. [91] investigated the effects of cylinder deactivation (CDA) and air-controlled autoignition (CAI) on fuel consumption and emissions. The driving-cycle simulation results have depicted that the engines using both CDA and CAI have shown a fuel consumption saving of 10% and a reduction of 28% in NOx emissions during the tests carried out on NEDC [92]. Three different hybrid systems with stored energy in a battery or a flywheel or as high-pressure fluid in a hydraulic system were analyzed by Dingel et al. [94]. The simulation results have shown a decrease in fuel consumption during three instances of approximately 31%, 33% and 27.5% respectively when they were tested on NEDC [94]. Gear shift indicators are also another approach to improving the fuel economy of vehicles [95]. They are devices which are designed to indicate to the driver when a gear shift should be made and the onboard computer calculates the fuel consumption when in any gear and suggests a shift the lowest attainable fuel consumption [95]. Vagg et al. have shown through simulations that fuel consumption can be reduced by 4.3% by adhering to the gear shift-indicating mechanism [95]. Also, Norris et al. [96] have shown that

the fuel consumption of a Mini Cooper and a Ford Transit van could be reduced by 4% and 7% respectively by adhering to a gear shift indicating mechanism.

Driver behaviour pattern or personal driving style is another significant factor affecting the overall fuel economy of a vehicle [98]. Therefore, eco-driving techniques have been introduced in order to improve fuel economy which can potentially reduce 10-15% of fuel consumption [99]. Technological advancements aimed at reducing fuel consumption and emission of vehicles take a considerable time to be adopted by the manufacturers, thus their impact and the payback time to the consumer will be close to a decade [100]. Concentrating on driver's behaviour helps to reduce the fuel consumption of vehicles in the short run [101]. An added advantage of driver behaviour improvement is that, on the development of new technology, most of the improvement made through driver behaviour changes would be preserved [102]. The awareness of good driving habits among drivers could potentially affect overall fuel consumption [103]. Beusen et al. [103] have conducted experiments on a sample of 10 drivers for 5 months before and after the awareness course and have observed fact that the overall fuel consumption of the fleet was reduced by 5.8%. De Vlieger [104] has conducted tests on a total of 10 cars to evaluate the impact of aggressive driving on fuel consumption and has found out that it could potentially increase fuel consumption by 40% and also the emission by four-fold in comparison with the normal driving behaviour. The usage of the throttle pedal is also a behavioural factor affecting fuel consumption [105]. According to a study conducted by Alessandrini et al. [105], it was noted the fact that the drivers use the throttle pedal independently of the driving cycle, where different drivers were shown different throttle positions in the same traffic conditions. Another important aspect of eco-driving is early gear shifting [102]. It was observed that shifting earlier into a higher gear, during the tests carried out on NEDC had shown a reduction of 3.6% in fuel consumption [106]. The applied accelerations and speeds during a trip, determine emissions and fuel consumption [109]. Lie et al. [107] have analyzed different characteristics of drivers and have identified four types of drivers using 23 personal characteristics, viz. aggressive, conservative, professional and experienced drivers. According to Brundell-Freij et al. [108], there are 9 dominant

driver behaviour factors exist, out of which the stopped time, speed changes and the time driven with high accelerations and high engine speeds are predominant.

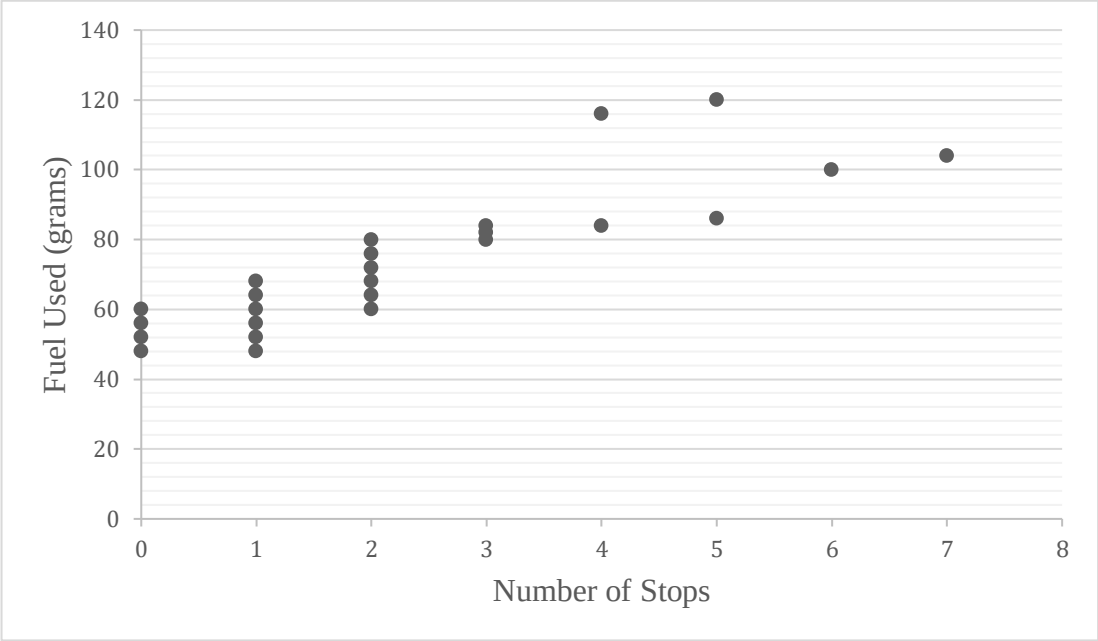

Figure 7: Relationship between the number of stops and fuel consumption - Adopted from reference [110].

The relationship between the number of stops and fuel consumption is determined using test data by Zheng et al. [110] is shown in Figure 7. It's depicted that the fuel consumption is increased on par with the increment in the number of stops. The aggressiveness of driving will be increased on par with the frequency of the stops since it incorporates an increased number of acceleration and deceleration phases. Smoother acceleration and deceleration profiles on driver behaviour will pave the way for better fuel economy [111], [112], [113], [114].

Two primary methods of influencing driver behaviour for improved fuel economy are analyzed by Wijayasekara et al. [115]. Those methods can be identified viz. driver education, driver feedback. Driver education entails training the drivers on fuel-efficient driving styles [103], [112]. It has been observed that over time, some drivers tend to depart from fuel-efficient behaviour even though they are being trained to adhere to eco-driving [115], [116]. On the other hand, the driver feedback mechanism entails real-time or non-real-time feedback on the fuel economy and how to change

the behaviour to obtain an improved fuel economy. Real-time driver feedback devices known as passive driving assistance tools have been observed to be extremely effective [117], [118]. The primary focus of real-time feedback devices is safety [119]. Audio, visual and haptic feedback mechanisms were investigated in the prior literature and among them, it can be argued that the visual feedback devices are the optimal [120], [121]. Hughes et al. [122] have experimentally shown that drivers may have up to 50% spare attention capacity in regular driving conditions. Furthermore, the studies conducted by Birrell et al. have shown that the glancing behaviour at an in-vehicle information system may lead to neither visual distraction nor increased mental workload [123]. Therefore, the introduction of passive driving assistance devices can be recommended as one of the most feasible solutions to align driving styles with eco-driving behaviour. It is shown that these types of passive devices can potentially decrease fuel consumption by 9-20% [115].

2.3 Literature review on the driving cycle development.

A driving cycle is another significant factor affecting the fuel economy of vehicles [58]. A driving cycle can be defined as a series of data points representing speed versus time, speed and gear selection as a function of time, speed versus distance or time versus gradient in a specific region or a part of a road segment [92], [124], [125], [126]. Driving cycles are primarily used for three main purposes viz. traffic engineering purposes, estimation of emission inventories and estimation of fuel consumption [92], [127], [128], [129]. To obtain emission inventories and fuel consumption values, the vehicles are tested on a chassis dynamometer using a given driving cycle [130], [131], [132], [133]. Driving cycles can primarily be stratified into 2 types of viz. transient cycles and modal cycles [124]. Transient cycles are developed using on-road data whereas modal cycles are developed by composing the collected data using a selected mechanism [124]. In general, it can be identified that there are four main steps of driving cycle development viz. route selection, data collection, cycle construction and cycle assessment [134], [135]. Even though there's a general methodology for developing a driving cycle, different approaches have been adopted by different

countries/regions based on time constraints, resource availability and information availability [136].

The first step in developing a driving cycle is to select suitable routes. If the routes selected are not representative of the actual road network of the area to capture the traffic behaviour, then the data collected would be biased [136]. When opting for the routes in a particular region, the selected routes should best represent the actual network and the typical traffic flow affected by spatial or temporal conditions viz. land use, road type, topography, availability of signalized intersections and population density in the respective region [124], [137], [138]. Also, the vertical alignment of the road surface of the selected routes is important since the gradient of the road surface has an impact on fuel consumption and consequently on emissions as well [136]. Other than the said criteria, the micro-texture of the road surface, altitude, temperature and the weather conditions of the selected routes are also contributory factors [139], [140], [141], [142].

Several route selection procedures have been adopted by various parts of the world. In Pune, India, a predefined set of origin/destination pairs were combined with the highest overall Average Annual Daily Traffic (AADT) and the routes have been opted based on the frequency of utility by the traffic [143]. In Hong Kong (China), route selection is performed mainly based on the experience and knowledge of experts on the local traffic [136]. Similarly in Colombo, Sri Lanka, a version of local driving cycles was developed mainly based on the knowledge and experience of the professionals and experts in the transportation domain [136]. The approach based on know-how and experience is associated with lower cost factors, hence enabling developing countries to adopt their local driving cycles. In Bangkok, Thailand, the route selection process in the development of the local driving cycles is mainly based on traffic flow data and travel speed [144]. When developing the ARTHEMIS driving cycle for the European region, a quite different approach has been adopted, since the drivers of the test fleet were given the freedom to follow the traffic flow [136]. This approach can be recommended ahead of other techniques since it increases the representativeness of the sample and reduces the biassing effect. The drawback of this approach is that to

increase the representativeness, the size of the sample should be increased. Consequently, the said approach might involve higher cost factors. The route selection approach adopted in Melbourne, Sydney and Perth, Australia, has shown a better scientific basis than the other suggested approaches. In the said approach, multiple criteria have been used to determine the routes viz. land use, road type, driving condition and the availability of public transportation [145], [146], [147], [148].

The second step in the development procedure of driving cycles is data collection which is a vital phase since it directly impacts the overall quality of the research output. To elevate the quality of research deliverables, the collected data set should be reliable, representative, homogeneous and consistent [136]. There exist two techniques in data collection viz. the chase-car technique and the instrumented private-car technique [149]. In the chase-car technique, an equipped vehicle which can measure instantaneous speed data is used to chase a target vehicle in predetermined routes within a particular area of interest [150]. When developing LA01 and LA92 driving cycles, the method of data acquisition that has been adopted was the chase-car technique [151]. Also, when developing both the Pune driving cycle and the Manila driving cycle, the chase-car technique has been used [143], [152]. There are pros and cons to this approach. The main advantage of this approach is that it's very cost-effective and few resources are required compared to the instrumented-car technique. Yet the major disadvantages are that it's quite difficult to obtain the exact driving data of the testcar which is being chased and also, this technique is vulnerable to road accidents [150]. In the instrumented-car technique, which is also named as on-board measurement method, a data logging device is installed in selected vehicles and the instantaneous speed data is recorded [136]. Several instruments have been adopted by the researchers to acquire and log the data viz. on-board diagnostic (OBD) data logging devices, GPS-based devices, optical sensor-based speed data logging devices etc. [127]. ARTEMIS driving cycle in the European Union region and Composite Urban Emission Driving Cycle (CUEDC) in Australia were developed using the instrumented-car technique [148], [153]. The instrumented-car technique can be associated with higher cost factors in comparison with the chase-car technique since the data acquisition devices would be costly and to obtain an unbiased sample, it's

recommended to obtain data from a larger sample set. Also unlike in the chase-car technique, in the instrumented-car technique, the route selection process is critical since, if the routes are not selected accurately, the results can depict dramatic variations from the actual behaviour of the region of interest [148]. The said method is suitable for countries or regions with aggressive and irregular driving behaviour. Also, for countries which have mixed traffic conditions viz. aggressive/congested and non-congested roads, a hybrid method of combining both the chase-car and the instrumented-car techniques can be recommended [136].

The third phase in driving cycle development is cycle construction where the driving cycle is modelled using the acquired data from the selected routes. There exist four major driving cycle construction methods viz. micro-trip-based cycle construction, segment-based cycle construction, pattern classification cycle construction and modal cycle construction [154]. Micro-trip-based cycle construction techniques can be defined as driving activity between adjacent stops, including a leading idle period [154]. In this technique, micro-trips are assigned in a way such that the target population parameters are met [136]. When opting for micro-trips, two main methods are used viz. random selection method and the best incremental method [154]. In some cases, a hybrid method of both the random selection method and the best incremental method is used in instances such as when developing the primary driving cycle for Colombo, Sri Lanka [136]. The major limitation of the said method is that it is not possible to differentiate micro-trips on the Level of Service (LoS) [154]. On the other hand, the segment-based cycle construction method adheres to a similar procedure as the micro-trip-based method, yet instead of adjacent stops being opted as the selection criteria, LoS is considered when segmenting the trips [154]. This method is suitable for traffic engineering purposes but not for emission or fuel consumption measurement purposes since trip segments are divided on the traffic condition and physical characteristics of the road and therefore, it can lead the way to speed and acceleration mismatches [154]. The segment-based method has been opted for the development of driving cycles for the expressways since the durations of the adjacent stops are presumably longer [136]. The third method of driving cycle construction is pattern classification. In this approach, the whole trip is divided into heterogeneous classes

using the statistical method and when dividing the trip, the kinematic sequence is used [154]. One of the major drawbacks of this approach is that it requires more information to divide collected data into kinematic sequences and to classify the routes. In the fourth method, i.e., modal cycle construction, real-world driving patterns are divided into acceleration, deceleration, cruising and idling components [136]. In this method, Markov Chain Theory is used assuming that the likelihood of a particular modal event depends only upon the previous modal event [155]. There exist four basic steps when developing a driving cycle using the modal cycle construction method viz.

- Using the Maximum Likelihood clustering method, collected data is divided into snippets based on acceleration.
- Snippets are assigned into modal bins using the Maximum Likelihood clustering method according to average, maximum and minimum speeds and acceleration rates.
- Define modes based on acceleration rates and average speed and then develop a transition matrix which contains succession probabilities among different modes.
- Using Markov Chain theory, the snippets are chained into one cycle, considering the transition probability matrix.

After constructing the driving cycle, it's necessary to validate the cycle. This activity is performed during the cycle assessment phase. By doing so, it'll assure that the developed driving cycle truly represents the actual driving pattern in the respective area or region [136]. Performance Values (PVs) or Characteristic Parameters (CPs) are used to assess the driving cycles [136], [156]. The PVs are determined for both the population and the candidate cycles. Then the percentage deviation of each PV is calculated w.r.t. the population and the candidate cycle. Finally, the summation of the percentage deviation values of PVs is determined. When determining the summation, a weightage is introduced, and the absolute deviation values are multiplied by the weightage [136]. The respective weights are defined by the relevance of each parameter with the purpose of the driving cycle development [136].

Table 8: Commonly used Performance Values for cycle assessment [136].

Subcategory	Performance Values (Target Parameters)
Maxima and minima	Speed, acceleration, deceleration and acceleration rate.
Percentages	Idle time, acceleration time, deceleration time, cruise time and creeping time.
Means and averages	Average speed, average running speed, average acceleration and average deceleration, mean length of a driving period, and average number of acceleration/deceleration changes within one driving period.
Standard deviations and percentiles.	Speed and acceleration standard deviation, the speed at the 95th percentile, acceleration, and deceleration rate at the 95th percentile.
Other emission-related parameters.	Root mean square (RMS) acceleration, Positive-acceleration kinetic energy (PKE), Speed Acceleration Probability Distribution (SAPD), and Speed Acceleration Frequency Distribution (SAFD).

Table 8 shows the assessment criteria for driving cycle validation as listed by Galgamuwa et al. To elevate the representativeness of the candidate cycle, the mentioned performance values in Table 8 should be with a minimum deviation of those of the population. After determining the PVs, one driving cycle is opted from the candidate cycles set. If there exists more than one candidate cycle with approximately similar PVs, then SAPD or SAFD is used for further assessment. Usually, when generating SAPD and SAFD, speed vs acceleration vs probability or frequency is plotted in a three-dimensional space. In some cases, SAPD/SAFD ratio is used as the assessment criterion. The smallest sum square difference (SSD) technique is used to determine the most representative candidate cycle by determining the SSD of SAPD/SAFD between the candidate cycle and the population [136].

Various driving cycles have been developed in different parts/regions of the world, to represent the local traffic behaviour of the respective regions. Barlow et al. have listed 256 driving cycles which have been developed in different parts of the world. Driving cycles can be characterized using more than 30 parameters which are defined as art-kinema parameters. These parameters can be stratified into six categories viz. distance related; time-related; speed-related; acceleration related; stop related and dynamics-related parameters. Barlow et al. have classified all 256 driving cycles into 28 driving cycle development programs as listed in Annex 1 [158].

When analyzing Annex 2, it can conspicuously be cited the fact that there are 42 performance values to assess a candidate's driving cycle. Also using these PVs, each driving/test cycle can be characterized.

Several attempts by researchers in Sri Lanka could be seen in developing a local driving cycle to suit the local conditions. A study carried out by Gamalath et al, [159] provides a representative driving cycle for the traffic corridor from Katubedda junction to Fort, Colombo along the Galle Road. The said study was carried out only for the LDVs.

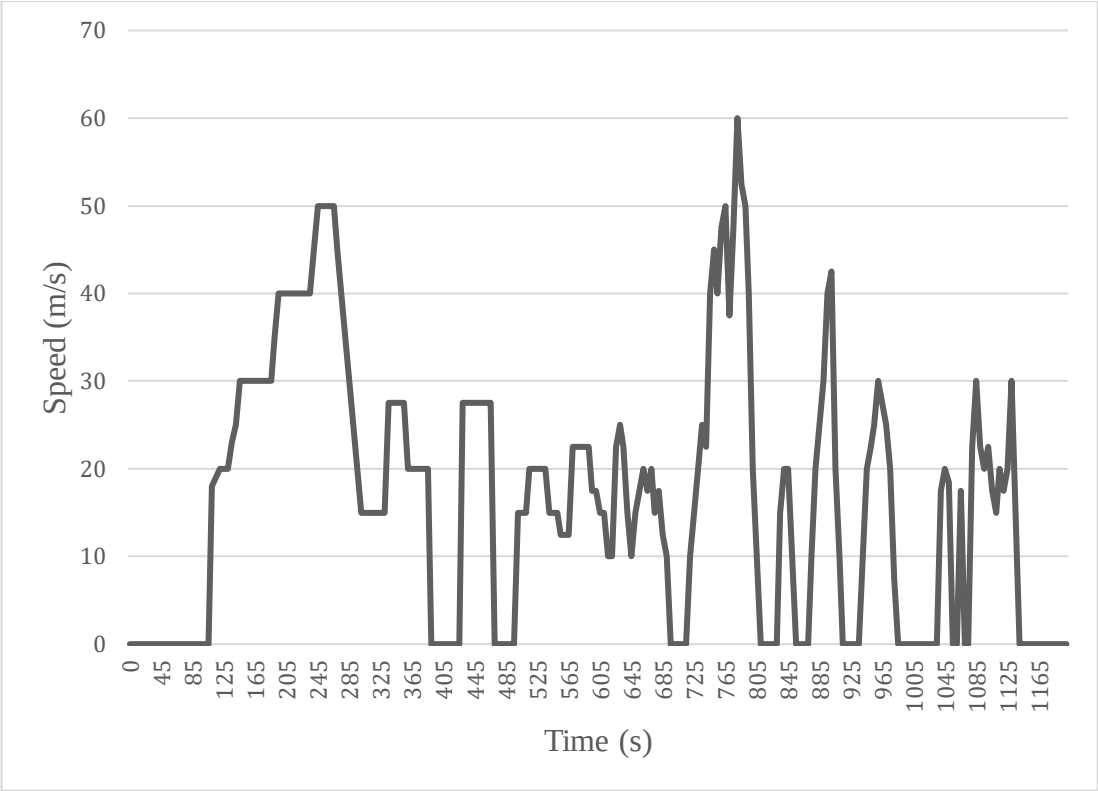

Figure 8: The representative driving cycle for the traffic corridor from Katubedda – Fort along the Galle Road for LDVs - Adopted from reference [159].

Figure 8 depicts the consequent driving cycle of the said study. The developed driving cycle shows an average speed of 21.37 km/h average running speed of 25.78km/h, an average acceleration of 2.03km/h/s and an average deceleration of 2.02km/h/s with acceleration, deceleration, cruising and idling proportions of 27.37%, 23.70%, 31.43% and 17.49% respectively [160]. The methodology for the cycle construction adopted when developing the said driving cycle was micro-trip-based cycle construction and the data acquisition was performed using the instrumented-car technique.

Another attempt in developing a representative driving cycle for the Southern Expressway can be cited in a study conducted by Galgamuwa et al. [161]. The said study has covered a road section from the Kottawa interchange to the Pinnaduwa interchange with a road length of 108 km. The segment-based cycle construction method was adopted with the instrumented-car technique as the method of data acquisition. The PVs can be cited as average speed, average acceleration and average

deceleration bearing the values of 80.6 km/h, 0.45 m/s^2 and 0.25 m/s^2 respectively [162].

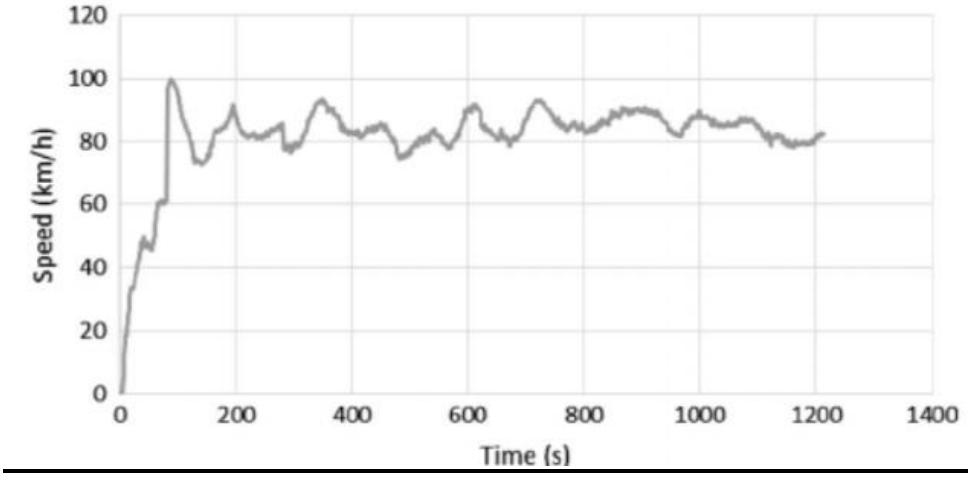

Figure 9: The representative driving cycle for Southern Expressway, Sri Lanka – Adopted from reference [162].

Another attempt in developing a driving cycle for Galle via the routes of B128 and B130 can be cited in the study conducted by Rupasinghe et al. [163]. The segment-based cycle construction technique was adopted while adhering to the instrumented-car technique for data acquisition. The said driving cycle for Galle has recorded an average speed of 27.53 km/h with a travel time of 892 seconds.

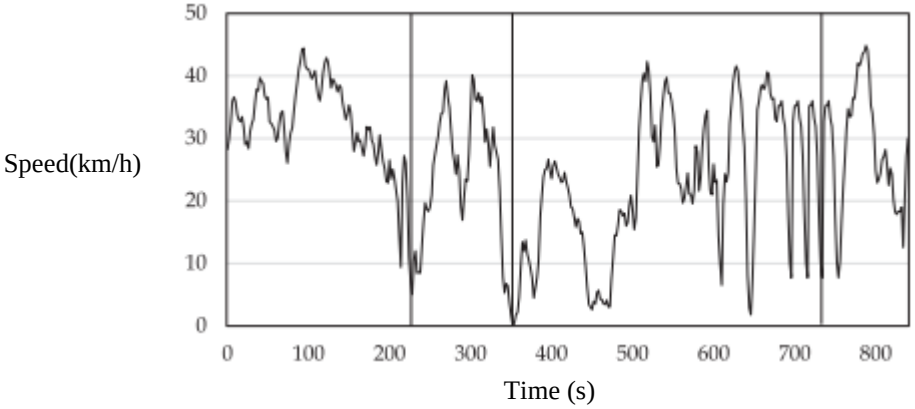

Figure 10: Driving cycle during morning peak hours at B130 route – Adopted from reference [163].

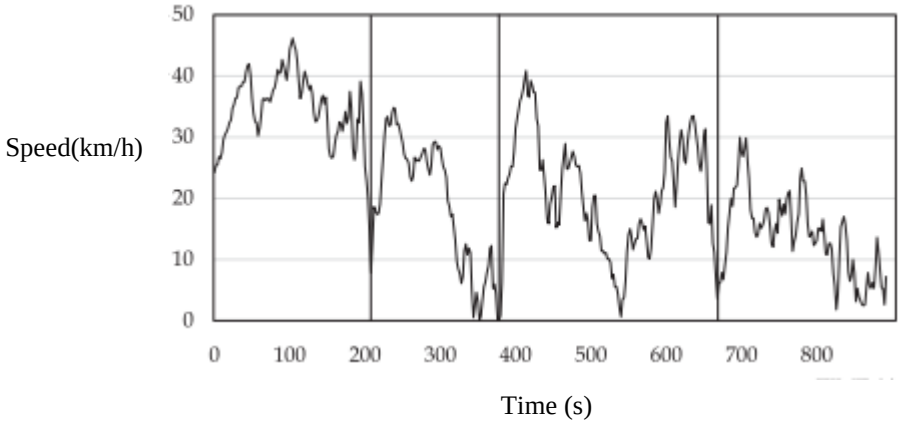

Figure 11: Driving cycle during noon peak hours at B130 route – Adopted from reference [163].

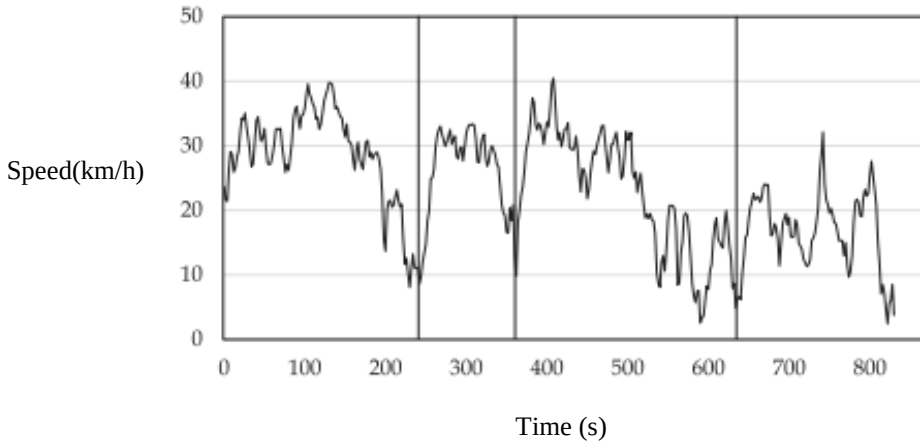

Figure 12: Driving cycle during evening peak hours at B130 route – Adopted from reference [163].

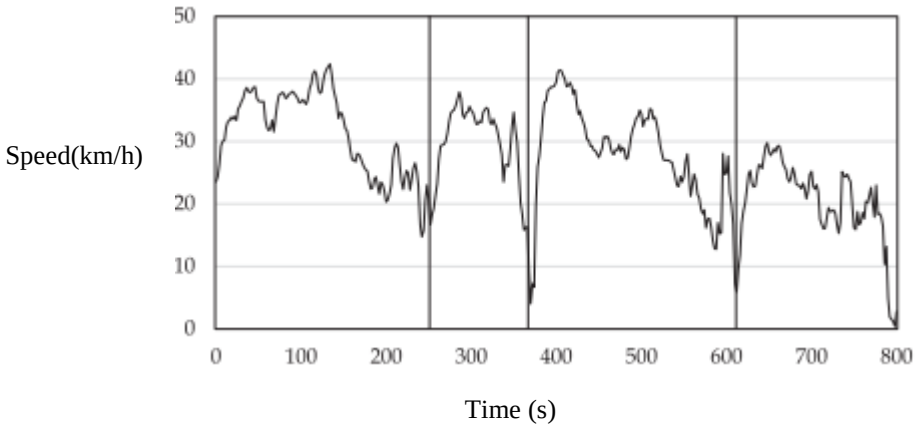

Figure 13: Driving cycle during peak hours at B128 route – Adopted from reference [163].

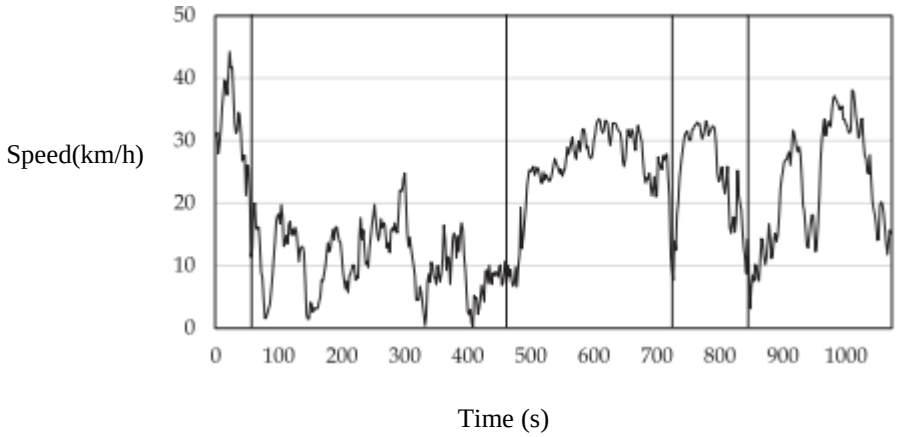

Figure 14 Driving cycle during off-peak hours at B128 route – Adopted from reference [163].

Driving cycles have been developed to represent different traffic congestion scenarios depending on morning peak, noon peak, evening peak and off-peak hours [162]. These representative driving cycles are shown in Figure 10 – Figure 14.

The studies which have been conducted locally within Sri Lanka, have shown several limitations on the technology that has been adopted for data collection, sample size, route selection methodology, data acquisition techniques, cycle construction methodology and cycle validation techniques. In the development of the Galle driving

cycle, the limitation of a smaller sample size can be seen since they have used only four LDVs to acquire data. Also, they had fixed the GPS data logging device to the vehicles selected from the university and hence it reflects an issue related to the representativeness of the local traffic. In the respective study, the researchers used the intersection-based cycle construction method which was less accurate. During the study carried out by Gamalath et al. to develop a local driving cycle for the road stretch from Katubedda to Fort along the Galle Road, certain limitations can be cited viz. the number of vehicles used for the data collection is not lucidly mentioned; the method of data acquisition, i.e., the type of data logging device that has been used and its level of accuracy and precision are not lucidly mentioned; Also the cycle validation criteria are limited only to five PVs [159]. The study which was conducted by Galgamuwa et al. to develop a representative driving cycle for Southern Expressway has shown improvements in both the approach and the technology that has been utilized in the data acquisition phase [161].

Apart from the regional or national contextual attempts in the development of local driving cycles, the necessity of a worldwide driving cycle to represent the driving and traffic patterns in the global domain was highlighted by the United Nations Economic Commission for Europe (UN-ECE), under a program launched by the World Forum for the Harmonization of Vehicle Regulations in 2013 [163]. The main intention of the development of the Worldwide harmonized Light duty driving Test Cycle (WLTC) is to represent typical driving characteristics around the world and to have a legislative worldwide harmonized type-approval procedure from 2017 onwards [163].

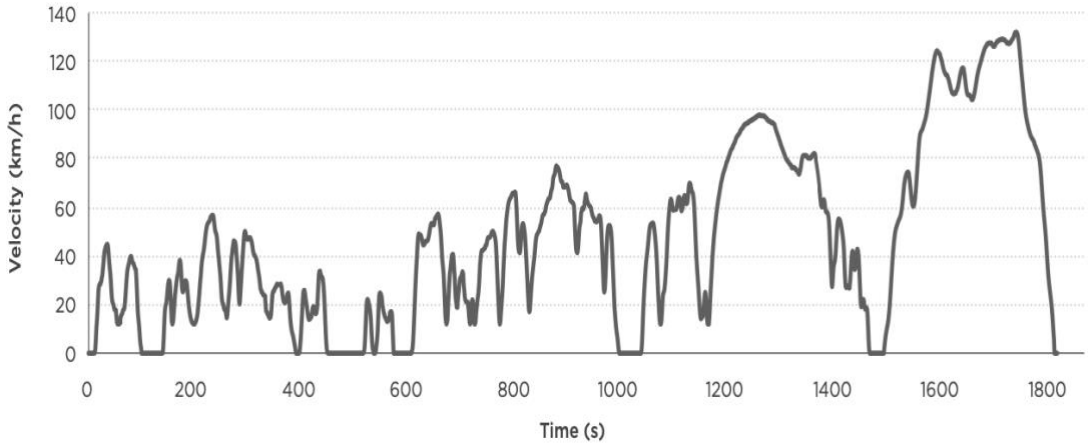

Figure 15: Worldwide harmonized Light duty vehicle Test Procedure (WLTP) - Adopted from reference [164].

Figure 15 depicts the WLTP driving cycle which is developed to represent worldwide driving and traffic patterns. The PVs of the WLTP driving cycle can be listed as mentioned in Table 9.

Table 9: Performance Values of WLTP driving cycle [164].

Performance Values	WLTP
Start Condition	Cold
Duration (s)	1800
Distance (km)	23.27
Mean Velocity (km/h)	46.5
Maximum Velocity (km/h)	131.3
Stop phases	9
Duration: (s)	

Stop	226
Constant Driving	66
Acceleration	789
Deceleration	719
Shares:	
Stop	12.6%
Constant Driving	3.7%
Acceleration	43.8%
Deceleration	39.9%
Mean positive acceleration (m/s^2)	0.41
Maximum positive acceleration ((m/s^2)	1.67
Mean positive acceleration*velocity (m^2/s^3) (acceleration phases only)	4.54
Mean positive acceleration*velocity (m^2/s^3) (whole cycle)	1.99
Maximum positive velocity*acceleration (m^2/s^3)	21.01
Mean deceleration (m/s^2)	-0.45
Minimum deceleration (m/s^2)	-1.50

When analyzing the PVs on par with the PVs of NEDC, it can lucidly be seen that the WLTP driving cycle depicts more extensive shares in acceleration and deceleration phases which could reflect the urban driving conditions. The cycle duration also gets increased up to 30 minutes and the distance is almost doubled hence, it depicts the extensiveness of the test cycle. Therefore, the obtained test data could potentially be

of higher accuracy and with a higher degree of representativeness with the respective data of the population.

The driving cycle which has been developed for Colombo, Sri Lanka has not been updated for the past five years, thus the upgrading of the said driving cycle and expansion of its scope to the Colombo Metropolitan Area is one of the deliverables of this proposed study. It's necessary to develop a harmonized driving cycle for the entire country, to set a benchmark standard for local emissions and fuel consumption estimations. The development of a mathematical model to estimate the fuel economy of LDVs on both the technical and operational characteristics will be determined during the proposed study. Also, the effect of driving patterns on the operating fuel economy of LDVs will be analyzed and a theoretical model will be developed in terms of numerical and analytical forms during the study.

2.3.1 The rationale for the development of unique driving cycles for 2W, 3W, and 4W

The driving cycle development methodology comprises four phases viz., route selection, data collection, cycle construction and cycle validation.
Firstly, different schemes of vehicle classifications that have been adopted throughout different regions of the world will be discussed. When considering the general categorization of all types of road vehicles w.r.t. European Union (EU) standards, the following types stated in Table 12 can be shown.

Table 10: General Vehicle Categorization in the European Union [171]

Vehicle Category	Characteristics
Category L	Mopeds, Motorcycles, Motor Tricycles and Quadricycles.
Category M	Motor vehicles have at least four wheels are for the carriage of passengers.
Category N	Power-driven vehicles have at least four wheels for the carriage of goods.
Category O	Trailers (including semitrailers).

When focusing on the categorization stated in Table 10, it's conspicuous that all types of 2W and 3W are included within 'Category L'. In addition to 2W and 3W, the quadricycles too have been included in Category L. When considering Light Duty Vehicles (LDVs), all the vehicles falling under Category L and a subset of Category M and Category N are included. When considering the portions which get included within LDVs from Category M and Category N are the sub-classes of motor vehicles having at least four wheels and the Gross Vehicle Weight Rating (GVWR) not exceeding 3.5 tons. Despite the development of the latest versions of the Worldwide Harmonized Light Vehicle Test Procedure (WLTP), which is the benchmark driving cycle across the globe for all types of LDVs, a separate driving cycle has been developed for the Category L vehicles, i.e., World Motorcycle Test Cycle (WMTC). Due to its inherent limitations w.r.t. power output (engine/motor) and the weight ratings (being significantly lighter than Category M and Category N vehicles), the speed responses (quantified as top speed) have major discrepancies comparatively to that of other categories of LDVs. Therefore, when analyzing the driving patterns w.r.t. shortlisted Characteristic Parameters (CPs) viz. average speed, average acceleration and deceleration, etc., significant mismatches can be anticipated between Category L and other types of LDVs. When considering 2W, 3W and 4W, all these three types of vehicles fall under the categorization of Light Duty Vehicles (LDVs) which are defined as road vehicles having GVWR of no more than 3.5 tons.

Even though WMTC is called a "motorcycle test cycle", it includes 2W, 3W and quadricycles (four-wheeled motorcycles) under its umbrella. Colloquially motorcycles are referred to the motorized 2W, yet when it's categorized with a scientific basis, there are seven vehicle classes under the motorcycles category. Any four-wheeled road vehicle having a gross vehicle weight rating (GVWR) of no more than 3.5 tons will be falling under the class of "motorcar". The same categorization criteria are referred to by International Motorcycle Manufacturers' Association (IMMA) as well. Since the objective of the study is to develop driving cycles to suit the local conditions, it's important to investigate Sri Lankan regulatory landscape w.r.t. vehicle classifications. The 2W categorization adopted in Sri Lanka is shown in Table 11.

Table 11: 2W categorization adopted by the government of Sri Lanka (SL) for vehicle importation [184].

Category	Classification of category
Category 1	50 cc < Engine capacity < 150 cc and Vmax < 50km/h or Engine capacity < 150 cc and 50 km/h < Vmax < 100 km/h.
Category 2	Engine capacity < 150 ccs and 100 km/h < Vmax < 115 km/h or Engine capacity > 150 ccs and Vmax < 115 km/h.
Category 3	2W having 115 km/h < Vmax < 130 km/h.
Category 4	2W having 130 km/h < Vmax < 140 km/h.
Category 5	2W having Vmax > 140 km/h.

As per Table 11, only 2W is included in that categorization whereas, in the WMTC categorization, 2W, 3W and 4W have been included. When comparing the local categorization in Sri Lanka and global categorization in WMTC, minor discrepancies can be noted in terms of defining the criteria for engine capacity (for ICE vehicles) and top speed.

When developing motorcycle classes, WMTC has adopted a methodology comprising three vehicle classes viz. Class 1, Class 2 and Class 3 as stated in Table 12.

Table 12: Motorcycle classification as per WMTC [185].

Classification	Characteristics
Class 1	Vehicles that fulfil the following specifications belong to class 1: Engine capacity <= 50 cm^3 and 50 km/h < Vmax < 60 km/h or 50 cm^3 < Engine capacity < 150 cm^3 and Vmax <= 50 km/h or Vehicles with engine capacity < 150 cm^3 and Vmax < 100 km/h. Vmax is the maximum vehicle speed.
Class 2	Vehicles that fulfil the following specifications belong to class 2: Engine capacity < 150 cm^3 and Vmax >= 100 km/h or Engine capacity >= 150 cm^3 and Vmax < 130 km/h. Vmax is the maximum vehicle speed

Class 3	Vehicles with engine capacity >= 150 cm^3 and Vmax >= 130 km/h belong to class 3.

When referring to WMTC's classification on motorcycles, it's conspicuous that the classification has taken both 2W and 3W into account. This too reflects that the inclusion of all types of 2W and 3W within Class 1 to Class 3 of motorcycle classification as per WMTC, the design characteristics and performance characteristics too could be evaluated under a common criterion.

As per the prevailing regulatory standards to define the vehicular classifications, they suggest that it's acceptable to develop a general driving cycle for powered 2W and powered 3W in common including quadricycles as well, whereas the remaining LDV types (except the ones falling under the motorcycle category as per WMTC categorization) should be analyzed with a separate driving cycle.

As per the directive of the United Nations Economic Commission for Europe (UN-ECE), the European Union (EU) has developed its regulatory standards for exhaust emissions and commonly called 'Euro Standards' spanning from Euro 1 to Euro 6. Euro 1 was first introduced in 1992 which was followed by Euro 2 in 1996, Euro 3 in 2000, Euro 4 in 2005, Euro 5 in 2009 and the latest revision of Euro 6 in 2014 and effective today (2021). The next probable revision to the Euro standards is estimated by 2025 [186],[187].

The adoption of different driving cycles throughout different regions of the world, for fuel consumption and emission estimation, is depicted in Table 13.

Table 13: Comparison of driving cycle tests to estimate emissions for various regions/countries. (Pre-Stage 2 -WMTC Period) [186], [187], [188], [189].

Class of Motorcycle	China	EU	India	Japan	South Korea	USA
L1e – Moped	ECE-R47					
L2e – Three-wheel Moped						

L3e – Motorcycle	ECE-R40	ECE-R40	Indian Driving Cycle (IDC)	TRIAS/LA4	ECE-R40	FTP
L4e – Motorcycle sidecar						
L5e – Tricycle						
L6e – Light quadricycle						
L7e – Heavy quadricycle						

Table 13 depicts the region-wide utility of driving cycle tests to estimate emissions before the introduction of WMTC Stage-2. During the pre-WMTC Stage-2 period, only the motorcycles equipped with Spark Ignition (SI) and Compression Ignition (CI) engines were tested. After the introduction of WMTC Stage-2, i.e., in 2005, on par with the Euro 4 standard, the adoption of driving cycles for emission estimations in different regions is shown in Table 14.

Table 14: Comparison of driving cycle tests to estimate emissions for various regions/countries. (Stage 2 -WMTC Period) [188], [189], [190], [191], [192].

Class of Motorcycle	China	EU	India	Japan	South Korea	USA
L1e – Moped	ECE-R47					
L2e – Three-wheel Moped						
L3e – Motorcycle	ECE-R40	WMTC, Stage 2	Indian Driving	TRIAS/LA4	ECE-R40	

L4e – Motorcycle sidecar			Cycle (IDC)			FTP
L5e – Tricycle						
L7e – Heavy quadricycle						
L6e – Light quadricycle						

The utility of driving cycles to test different motorcycle classes throughout different regions from 2005 until the introduction of the revised WMTC in 2014 is shown in Table 15. When comparing Table 13 with Table 14, both look quite similar besides the replacement of ECE-R40 by WMTC Stage-2 in the EU, which can be cited as a major improvement.

Table 15: Comparison of driving cycle tests to estimate emissions for various regions/countries. (Post-Stage 2 -WMTC Period) [186], [187], [188], [189], [190], [191].

Class of Motorcycle	China	EU	India	Japan	South Korea	USA
L1e – Moped	ECE-R40 / ECE-R47	Revised-WMTC	Revised-WMTC (weighted to suit Indian conditions)	ISDO 6460 Cycle	Revised-WMTC	FTP/Revised-WMTC (FTP mainly for type approval)
L2e – Three-wheel Moped				Revised-WMTC		
L3e – Motorcycle						

L4e – Motorcycle sidecar						
L5e – Tricycle						
L7e – Heavy quadricycle						
L6e – Light quadricycle						

Table 15 depicts the adoption of DCs for emission testing procedures during the Euro 5 and Euro 6 standards period. In most of the regions, the revised WMTC has been adopted as their emission regulatory DC, especially in the EU, Japan, South Korea and the USA which are among the leading vehicle manufacturers. Therefore, using the facts depicted in Tables 13, 14 and 15, it can be seen the fact that the adoption of a gradual harmonization in emission testing procedures throughout the world. When considering the utility of motorcycles (2W and 3W in general), South and South-East Asian regions claim a majority portion and Indonesia, Thailand and Vietnam are among them. In all these three countries, Euro 3 standard is adopted for motorcycles, which is equivalent to ECE-R40 and ECE-R47 DCs.

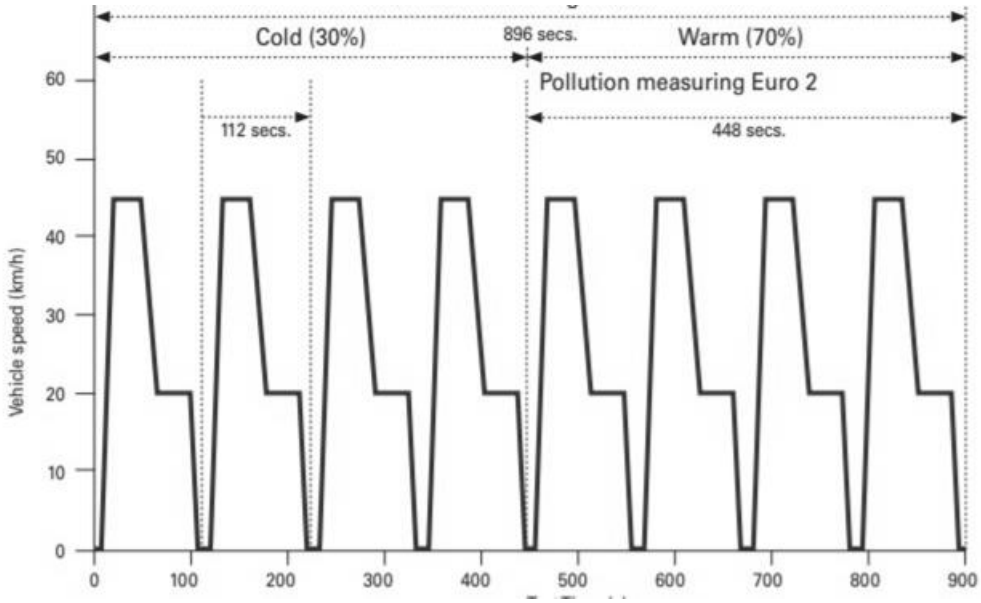

Figure 16: ECE-R47 Driving Cycle - Adopted from reference [192].

Figure 16 depicts the vastly used ECE-R47 DCs which were used during the pre-WMTC era. This DC is equivalent to Euro 3 standard and was used specifically for motorcycle testing.

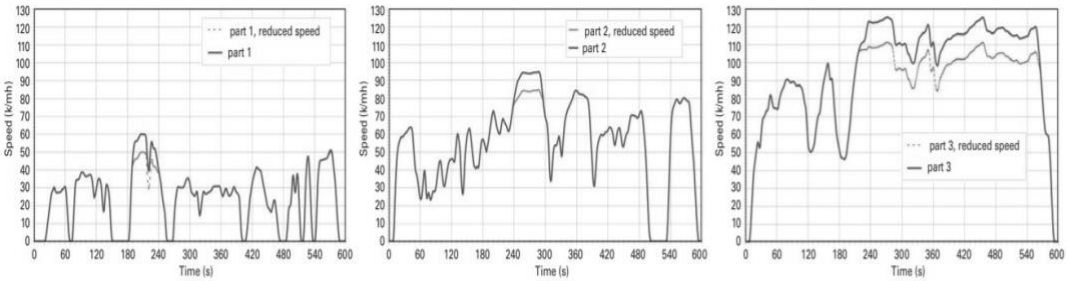

Figure 17: a) Part 1 of WMTC b) Part 2 of WMTC c) Part 3 of WMTC - Adopted from reference [193].

Figure 17 depicts the 3 phases of WMTC. Part 1 of WMTC represents the urban driving condition whereas Part 2 and Part 3 of WMTC represent the extra-urban and Highway driving conditions respectively. The total WMTC cycle spans 1800 s. WMTC is used under Euro 4,5 and 6 standards. When comparing the ECE-R47 DC and WMTC, the main improvement that can be cited in WMTC is that it reflects real-world driving better than ECE-R47 which is graphically depicted in Figure 16. Technically, ECE-R47 is a modal driving cycle whereas WMTC is a transient driving

cycle where it has more apparent acceleration and deceleration phases than ECE-R47. Moreover, WMTC has been developed by extracting data from real-world driving.

When analyzing the regional utilization of driving cycles to measure emissions of motorcycles, it's conspicuous that a common driving cycle for a particular region/country of interest has been used to benchmark the emission performance of 2W, 3W and 4W quadricycles. Since Sri Lankan driving context can closely be related to South and South-East Asian driving conditions (Indian/Indonesian/Vietnamese etc.), it's advisable and recommended to adhere to a similar procedure in developing driving cycles, especially for motorcycles, which means developing driving cycles for 2W, 3W and 4W quadricycles in general, rather than developing specific driving cycles for each category, i.e., 2W, 3W and 4W quadricycles.

The scope of the main study i.e., to develop driving cycle(s) to estimate the performance (fuel economy) of LDVs. When considering the LDVs, 2W, 3W and 4W quadricycles (motorcycles by definition), they are a subset of LDVs. Besides the said motorcycle classes, the rest of the LDV classes are composed of other 4W road vehicles comprising a gross vehicle weight rating (GVWR) not exceeding 3.5 tons. Conclusively, as per the analysis done in this chapter, two driving cycles will be developed at the end of the study: a common driving cycle will be developed to reflect the driving characteristics of motorcycle classes and a separate driving cycle will be developed to mimic the driving characteristics of other classes of 4W LDVs.

Driving cycles have been developed regionally to assess the performance of LDVs, in terms of fuel economy and emissions. An LDV which is tested the performance under a particular regional DC portrays quite different test results when it's being tested under a different regional DC. The major reasons for these discrepancies can be listed viz. the strong regional variations in driving patterns, ambient temperatures, start conditions, vehicle preconditioning, determination of vehicles' road loads and masses and others [196]. Another major challenge when formulating DC conversion factors is that the stringencies of the different regional standards and values measured under different boundary conditions are not directly comparable [197]. Especially, the test-

driving cycles applied on the chassis dynamometers reflecting local driving conditions cause large discrepancies w.r.t. engine loads and emission behaviour.

2.4 Literature review on auxiliary engine loads.

To align with the sustainable development targets, fuel economy and emissions-related regulations and targets have been imposed both at the national and international levels. When developing policies related to sustainable road transportation and energy consumption related to transportation, it's of paramount importance to identify the factors contributing towards the energy consumption of road transportation and to develop a baseline model using both theoretical and empirical approaches. The major contributors of the power demand of a light duty vehicle (LDV) are the power demanded to overcome the aerodynamic drag resistance, rolling resistance, grade resistance and inertial resistance. Besides the said major factors, the auxiliary power demand is also assumed to be a considerable contributor and during the study, the impact of the auxiliary engine equipment is studied and quantified. The study's scope encompasses the auxiliary devices such as air-conditioning units, alternators, water-pump and the power steering-pump.

Several previous studies have been carried out by researchers to evaluate the impact of auxiliary engine loads on the overall power demand of vehicles and the respective impact on the operating fuel consumption of a given vehicle. During this section, the prior art is discussed and appraised to earmark the possible gaps in the previous work. Welstand et. al. in their study has revealed that the auxiliary loads which are belt-driven units depict a closely proportional relationship with the engine speed, where the auxiliaries appeal for higher power demand during higher engine speeds [201].

The study conducted by Welstand et. al. portrays that during normal idling engine speed range from 800 – 1000 RPM, the auxiliary power appeal can be noted at around 1.75 kW with air-conditioning (A/C) turned-off and 3.25 kW with A/C turned-on [201]. Moreover, at a higher operating region of around 3000 RPM, the increased auxiliary power demand can be noted at around 9 – 9.5 kW with A/C turned on. Moreover, an (A/C) system appeals for a higher driving torque than any other auxiliary

equipment. A common characteristic of the belt-driven engine auxiliary units is that their input power for operation is proportional to the engine speed, whereas the output power may not be relevant to the engine speed. When looking into the prior art related to the energy demand of automotive A/C systems, the study conducted by Nadamoto et al. depicts the fact that the compressor is the most significant component affecting the power demand since it causes a 77-89% increase in energy consumption [202]. The impact of subordinate components can be listed viz., 6-12% contribution from the blower, 4-10% contribution from the cooling fan and 0.7-2% contribution from the clutch [202]. A/C system plays a crucial role when it comes to electric vehicles (EVs), including both hybrid electric vehicles (HEVs) and battery electric vehicles (BEVs). EVs have inadequate waste heat to warm up the cabin and the climate control system has a very significant effect on the energy consumption efficiency and operating range. The mobile climate control systems based on the magnetocaloric effect and thermoelectric effect could be utilized to optimize the range efficiency [203]. The vapour compression refrigeration-dedicated heater AC systems, reversible vapour compression heat pump AC systems, and non-vapour compression AC systems have been critically appraised by Zhang et. al. as the latest developments in air-conditioning and heat pump systems on the EVs [204].

There exist various types of water pumps viz. Mechanical pumps, electric pumps, etc. The major drawback of mechanical pumps is that they pump in proportion to engine speed and not in proportion to the heat rejection requirements [205]. Hence, it's significant to study the operating characteristics of the water pump and its impact on fuel consumption. In general, 1-2 kW of power is transferred from the crankshaft to the water pump [206]. The efficiency of a water pump lies in a very low range due to its losses. According to the said facts, the mechanical efficiency of a water pump typically lies between 37.5% - 55.0% within an RPM range of 2,000 – 5,000 respectively [207]. The losses incorporated with the water pump can be stratified into 3 main types of viz. Mechanical losses, hydraulic losses and volumetric losses [205]. Furthermore, the mechanical losses are the frictional losses associated with the dynamic parts of the pump, hydraulic losses are the internal losses in the impeller

whereas volumetric losses are due to the leakage of liquid from the discharge side to the suction side of the centrifugal pump [205].

There has been an increasing demand for electric power since electrical and electronic devices have replaced many of the automotive mechanical devices on par with the technology advancement. Two major evolutions of auto-electrical systems can be stated viz. change from 6-volt to 12-volt system and switching from DC generators to AC alternators [208]. AC alternator can be considered one of the most significant pieces of equipment in the auto-electric system. The electrical power in a vehicle is generated as a direct result of consuming fuel within the engine to drive the alternator [209]. With a nominal efficiency level of 40% in the engine, 98% in the belt train and 55% in the alternator, the electricity generation has an overall efficiency of around 21% [209]. When concentrating on the losses in the alternator, can be stratified into 3 types viz. electrical, magnetic and mechanical losses [209]. When appraising the literature, it can be noted the fact that, in general, the output power losses are increased on par with the increase in the engine speed. Consequently, the increase in alternator losses can be identified as proportional to the increase in operating fuel consumption.

Nowadays, most of the previously belt-driven engine auxiliaries are driven by electricity. For example, the water/coolant pump and the power-steering pump are more often driven by electricity. Furthermore, with the increased market utilization of electric vehicles (EVs), including hybrid-electric vehicles and battery-electric vehicles, the necessity of electrically powered auxiliaries has increased. Estimating the power demand of the auxiliary loads is of greater importance than ever since it directly affects the range of EVs and could enhance the range anxiety of the users [210], [211]. The approach proposed by the study could eventually result in the development of a range prediction algorithm for EVs. Accurate range prediction is the key to minimizing range anxiety and helping drivers make the best use of their available energy [212], [213]. Thus, an accurate theoretical model is required to determine the major contributors of auxiliary loads which is the novelty that the study brings forth.

In most of the cited prior art, the auxiliary load determination has been performed using experimental evaluations whereas, in the proposed study, each sub-auxiliary

system is analytically appraised using the governing equations which can be highlighted as a novelty of the research study. Against the empirical approach adopted in referred literature, the study delves into a theoretical approach, especially on the determination of A/C load. In the next sections, the power demand on A/C, alternator, mechanical water pump and power-steering pump are discussed and analyzed.

2.5 Literature review on converting performance values (fuel consumption/emissions) from one driving cycle to another.

The main aim of developing DC conversion factors is to evaluate the performance, i.e., fuel economy and emissions of LDVs under different local conditions. For example, when converting the performance values of an LDV which is tested under the New European Driving Cycle (NEDC) to the Worldwide Harmonized Light Vehicle Test Cycle (WLTC), there will be an enhanced fuel consumption (l/100km) and emissions (CO_2 g/km) in WLTC in comparison to that of NEDC, since one of the deciding characteristic parameters of engine load, i.e., time proportion (percentage of total cycle time) of acceleration is 43.8% under WLTC which is more than double the value of 20.9% obtained under NEDC [202]. Thus, there will be significant discrepancies when converting the performance of an LDV from NEDC to WLTC. Especially, there will be major differences when converting performance values from modal driving cycles to transient and vice-versa. NEDC is considered to be a modal driving cycle (artificially constructed) which is not quite reflect real-world driving behaviour, whereas WLTC on the other hand is considered to be a transient driving cycle which depicts the characteristics of real-world driving.

When considering the emissions of LDVs, there are two main types viz. exhaust emissions and evaporative emissions. During the study, only exhaust emissions are analyzed. Furthermore, when considering exhaust emissions, there are also many different types of exhaust gases viz. Carbon Dioxide (CO_2), Carbon Monoxide (CO), Sulphur Dioxide (SO_2), Nitrogen Dioxide (NO_2) etc. When defining the scope of the study, the analysis is converged on studying the exhaust CO_2 emissions specifically. Typically, the DC conversion factors that have been developed during previous studies focus on converting CO_2 emission values between DCs. Once the CO_2 values are

obtained, using the Carbon balance equation for the combustion of Gasoline and Diesel, the CO_2 values can be converted into fuel consumption values. As per the Carbon balance method, 1 litre of Gasoline is equivalent to 2.392 kg of CO_2 whereas 1 litre of Diesel emits 2.640 kg of CO_2 [203]. Due to the utility of the Carbon balance method, the conversion of fuel consumption to CO_2 emission values is quite straightforward. When looking at the specific objectives of the study, one of them includes developing a mathematical model capable of estimating fuel economy values of different LDV categories under varying driving patterns. Since the study converges the performance assessment towards fuel economy, the aforementioned Carbon balance method can be used to determine the same using the CO_2 emissions.

When analyzing the prior studies, most of them have utilized regression techniques to develop DC conversion factors. The regression techniques that have been adopted differ by the mathematical nature (linear vs. nonlinear approaches), the inclusion or exclusion of the y-intercept, the differentiation into different vehicle technologies and the inclusion of additional independent variables (multiple regression analyses). Hence, the level of complexity and the achievable quality of the regression results vary among the different techniques. The major types of regression analyses used during past studies can be listed viz. logarithmic approach, single regression with zero intercept, single regression with calculated intercept and multiple regression method [202]. The listed approaches that have been used during past studies are elaborated on below.

$$\frac{C_2}{C_1} = a * \ln C_1 + d \tag{6}$$

Equation (6) depicts the logarithmic regression approach used to model conversion factors in a study conducted by International Council on Clean Transportation (ICCT) in 2007 [200]. In Equation (6), C_1 and C_2 denote the CO_2 emission values of the driving cycle which is being converted and the target driving cycle respectively. It is assumed that the quotient of CO_2, often denoted as the multiplier from both cycles, correlates with CO_2 from Cycle 1. The stated logarithmic method was proposed as the standard method of converting DCs during the 2007–2014-time span until this was replaced by

linear regression methods. When developing conversion factors using regression techniques, the fundamental technology differentiation of internal combustion engine (ICE) vehicles has been taken into account, i.e., Gasoline versus Diesel engine technology.

The other linear regression methods that have been adopted during past studies are portrayed in Equations (7) and (8).

$$C_2 = a * C_1 \tag{7}$$

The easiest way of exploring a correlation is implemented by a simple linear regression without a y-intercept. The resulting regression coefficient represents a constant factor for converting the CO_2 emissions of Cycle 1 into CO_2 emissions of Cycle 2. Though this method provides the lowest degree of accuracy when compared to the other regression approaches, this tends to provide comparatively higher useability due to its simplicity of adoption [201].

$$C_2 = a * C_1 + d \tag{8}$$

The other way of modelling the conversion factors using linear regression which is depicted in Equation (8), adds a y-intercept to the simple linear regression method used in Equation (7). The inclusion of the y-intercept into the simple linear regression analyses increases the degrees of freedom and hence reduces statistical uncertainties [201].

The other regression technique that has been utilized during the previous studies encompasses multiple regression methods taking the technological differences into account.

$$C_2 = a * C_1 + b * (TP) + d \tag{9}$$

In this model stated in Equation (9) with multiple regression, a second independent variable has been introduced i.e., TP – Technological Parameter. The parameter TP will include the effect of the technical parameters viz. aerodynamic drag, vehicle

weight, tyre rolling resistance, final drive ratio, peak torque, peak power and engine displacement. The inclusion of additional technical parameters (TP) might further improve the quality of the regression functions. In the study conducted by ICCT in 2014, it's been determined that the impact of the technical parameters viz. final drive-ratio, peak torque, peak power and engine displacement is negligible [202]. Thus, the aerodynamic drag, vehicle weight and tyre rolling resistance have been included in the regression study.

It can be seen that the simple linear regression approach provides the same data quality which was obtained in the logarithmic approach with a standard deviation of 7.5g CO_2/km. Excluding the y-intercept from the linear regression worsens data quality by approximately 30-35%. In the opposite direction, separating the fleet by technologies leads to improvements of 40%. Another 20% improvement can be achieved when including the aerodynamic drag in the regression analyses. At this final multiple regression level, average standard deviation remains around 2.5 g CO_2 /km [201], [202].

When analyzing the error function of each regression method, it can be cited that the maximum deviation between the real CO_2 emissions of cycle C_2 (target cycle) and the calculated one (using the regression analyses), lies around a probability of 68.3% which is significantly higher [202]. Furthermore, almost all the techniques that have been adopted in past studies include regression analyses in different levels to curve-fit the acquired data from the different pairs of driving cycles, in which the emission/fuel consumption values need to be converted between each other. A clear gap in prior studies can be identified in developing the DC conversion factors with a theoretical and scientific basis. Since a DC can be characterized using performance values viz. time proportions for acceleration, deceleration, idling, cruising, positive kinetic energy etc., it's advisable to develop a theoretical conversion model utilizing the said DC Performance values as base parameters. As one of the specific objectives of the research study, a theoretical model to estimate fuel economy values of different LDV classes under varying driving patterns is developed. The basic ideology behind the proposed theoretical model is to provide the said model with speed sequential data on a particular DC and the model will provide the output in terms of the fuel economy of

a given LDV. Therefore, the varying driving cycles can be analyzed by changing the speed sequential data with the speed data from an intended DC.

Overall, when considering the referred literature, a conspicuous research gap could be highlighted. This research study fills an important gap in understanding real-world driving patterns and fuel economy characterization of light duty vehicles in the Sri Lankan context. While previous attempts have been made to develop representative driving cycles and fuel consumption models locally, they have lacked robust scientific rigor and validation. Specifically, there is a lack of accurate, measurement-based data on actual on-road vehicle performance reflecting local traffic conditions. Furthermore, prior modeling efforts have predominantly relied on empirical approaches without a strong theoretical foundation. To address these deficiencies, the current study adopts a comprehensive methodology encompassing extensive field data gathering, spatial analytics to formulate driving cycles, and physics-based analytical modeling of fuel consumption. The model is then rigorously validated against physical testing and simulations. Such a first-principles approach backed by local experimental data is novel and highly significant to enable evidence-based transportation policymaking around issues like vehicle emissions and energy efficiency. Overall, the research methodology and outcomes presented help bridge a critical knowledge gap in this domain.

2.6 Summary

The literature review conducted in this chapter has provided insights into the factors affecting fuel consumption of light duty vehicles, the development of driving cycles, the impact of auxiliary engine loads, and the methods for converting fuel consumption values between different driving cycles.

Several key research gaps have been identified:

- Limited studies on the development of localized driving cycles in Sri Lanka that accurately represent the unique driving patterns and traffic conditions in the country.

- Lack of a comprehensive theoretical model that can estimate fuel consumption of different vehicle types under varying driving conditions, considering both technical and operational parameters.
- Insufficient analysis of the impact of auxiliary engine loads, particularly the A/C system, on the fuel consumption of vehicles in the Sri Lankan context.
- Need for a more robust methodology to convert fuel consumption values between different driving cycles, taking into account the specific characteristics of the cycles and vehicle technologies.

Based on these research gaps, the following research questions have been formulated:

- How can representative driving cycles be developed for different vehicle categories in Sri Lanka, considering the local driving patterns, traffic conditions, and road infrastructure?
- What are the key technical and operational parameters influencing fuel consumption in light duty vehicles, and how can they be integrated into a comprehensive theoretical model for fuel consumption estimation?
- How significant is the impact of auxiliary engine loads, particularly the A/C system, on the fuel consumption of vehicles in Sri Lanka, and how can this be accurately quantified and incorporated into the fuel consumption model?
- What is an appropriate methodology for converting fuel consumption values between different driving cycles, considering the specific characteristics of the cycles and vehicle technologies, to enable more accurate comparisons and estimations?

3. METHODOLOGY

The overall methodology of the study encompasses the development of two main components viz., the development of the local driving cycles and the development of the theoretical model to characterize the fuel economy values for LDVs. Though these two components are developed in separation, both are integral components of the main study. The following flow chart reflects the overall methodology that has been adopted during the study.

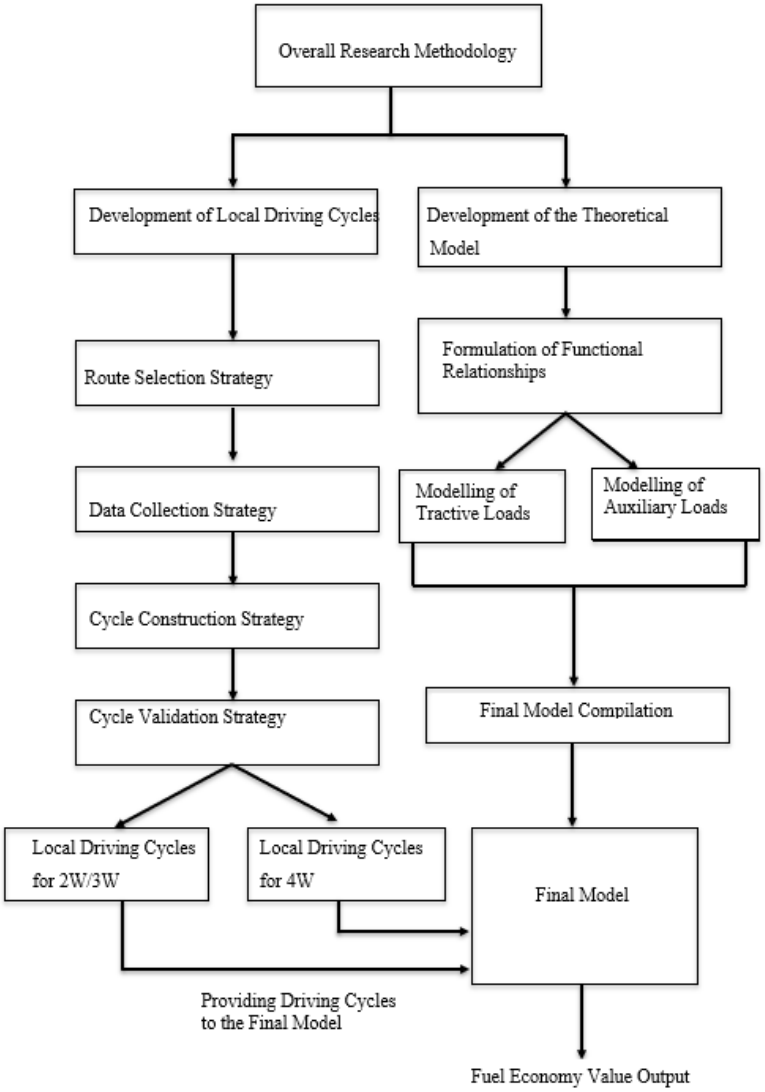

Figure 18: Flowchart reflecting the overall research methodology.

3.1 Route selection strategy

The first step of DC development is route selection. When selecting routes, the actual situations that happen along each route should be identified and ascertained. Since DCs represent the behaviour of traffic in a particular route network, the selection of proper route(s) is of greater importance. Several methodologies have been followed to select the best representative route network for DC development. Several factors should be looked upon when opting for a route network and they can be listed, viz., land use, road type, topography, availability of signalized intersections, population density, and vertical alignment of the road. When referring to the literature, two main methods can be identified for route selection which have been in practice for DC development throughout the world. They can be listed, viz., based on traffic-related parameters and based on knowledge and experience. Various traffic-related parameters have been utilized as selection criteria for routes. A few such parameters can be listed, viz., Average Annual Daily Traffic (AADT), Level of Service (LoS), kinematics-related parameters such as average speed, acceleration, the utility of intercity and intracity traffic flow data and a holistic approach with the consideration of land-use, road-type, topography and population density [180]. It is always better to use traffic-related parameters as a reference when opting for routes. This approach can commonly be seen in countries in European, American, Australian and Japanese regions, where there exists a proper traffic database to track the said parameters. Unlike in these countries, most of the third world developing countries lack documented traffic data. Thus, knowledge or experience-based methods are commonly used as route selection criteria in these parts of the world. Here the experience or knowledge is referred to as that of the researchers or the domain experts. This method is highly dependent on the know-how capacity of the particular researcher; but since this does not incorporate a formal database with data acquisition techniques, this method can be cost-effective and hence is viable for developing countries.

During the study, a dedicated application called ‘Mtrada’ has been utilized. When opting for the routes through the said application, the distance matrix application programming interface (API) powered by Google™ has been used. Since there is a

lack of information on average daily traffic (ADT), the aforesaid method is used to determine the routes for driving cycle development. The geographical scope of the study is selected as the Colombo Metropolitan Area (CMA) encompassing 20 divisional secretariat divisions (DSDs) of the Western Province of Sri Lanka. It also comprises the following 3 districts: Colombo, Gampaha and Kalutara. Furthermore, the CMA comprises 995 km^2 and consists of a population of over 3.6 million. The boundary of the CMA is defined as the area demarcating both night-time and day-time population densities having more than 20 people/hectare. Out of the 20 DSDs, 11 DSDs are located within the Colombo district. Therefore, priority is given to the Colombo district when opting for routes for data collection. When selecting the routes, attention is given to both intracity and intercity traffic. Intracity routes are selected within the DSDs whereas intercity routes have opted between two respective DSDs.

Data is collected from 19 major routes comprising 72 route links as depicted in Table 16.

Table 16: Opted Routes for Data Collection in Colombo Metropolitan Area

Route Index	Route	Origin (Latitude, Longitude)	Destination (Latitude, Longitude)
1	Gamsabha Junction – Galle Face	6.86535, 79.89683	6.92862, 79.84452
2	Grandpass – Galle Face	6.94351, 79.86856	6.92862, 79.84452
3	Mattakkuliya – Galle Face (via Canal Road)	6.97173, 79.87850	6.92862, 79.84452
4	Rajagiriya – Galle Face (via Sri J'pura Road)	6.90914, 79.89572	6.92862, 79.84452
5	Gampaha – Kandy Road	7.09168, 79.99484	7.08051, 80.02729
6	Gampaha – Yakkala	7.09168, 79.99484	7.08608, 80.03349

7	Gampaha – Kadawatha	7.09168, 79.99484	7.00316, 79.96286
8	Kaduwela – Ambathale	6.93474, 79.97135	6.93219, 79.94513
9	Ambathale – Modara	6.93219, 79.94513	6.96505, 79.86853
10	Modara – Galle Face	6.96505, 79.86853	6.92862, 79.84452
11	Homagama – Maharagama	6.84554, 80.00774	6.84722, 79.92655
12	Maharagama – Nugegoda	6.84722, 79.92655	6.87014, 79.88817
13	Piliyandala – Boralesgamuwa	6.80158, 79.92298	6.84155, 79.90122
14	Kalutara – Panadura	6.58721, 79.96013	6.71262, 79.90757
15	Panadura – Moratuwa	6.71262, 79.90757	6.79763, 79.88840
16	Moratuwa – Dehiwala	6.79763, 79.88840	6.85156, 79.86606
17	Kesbewa – Piliyandala	6.78017, 79.94327	6.80158, 79.92298
18	Bandaragama – Horana	6.78017, 79.94327	6.79241, 79.94885
19	Kelaniya – Kiribathgoda	6.95212, 79.91850	6.97836, 79.92736

The number of samples to be collected from each route link is determined using the average speed of the vehicles traversing through each route link and the number of lanes of each route link.

$$N = \left(\frac{v_i^{-1}}{v_{max}^{-1}}\right)n \tag{10}$$

Equation (10) is used to determine the number of samples to be acquired from each route link. In Equation (10), N denotes the number of samples, v_i^{-1} denotes the inverse of the speed of the i^{th} route link segment, v_{max}^{-1} denotes the inverse of the speed of the route link having the maximum speed and n denotes the number of lanes. The formula in Equation (10) has been developed to determine the exact sizes of samples that need to be collected from each identified route link segment. Therefore, the number of samples has been determined as 185 from 72 route links.

3.2 Data collection strategy

Once the number of samples to be collected has been determined, then the sample collection times should be determined. Since the study contains 35 two-laned route link segments, two-laned roads are selected for sample collection period determination. Two route links are chosen randomly from the two-laned route link population set and the recorded average speed per each opted route link segment per 10-minute time interval on a random weekday has been plotted in the same graph as portrayed in Figure 19.

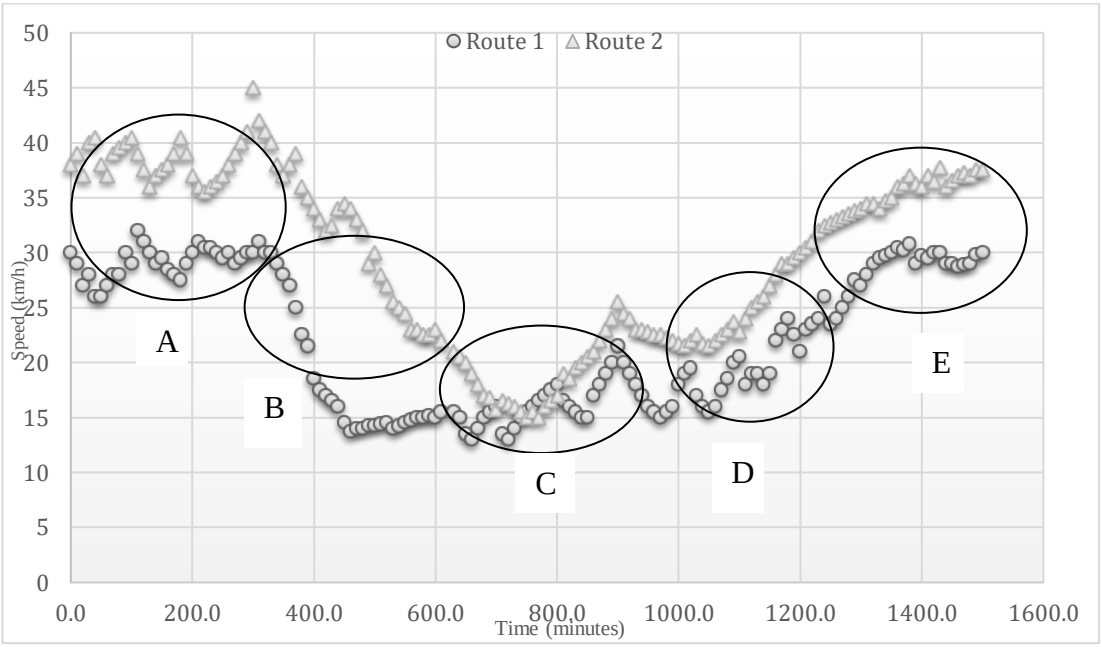

Figure 19: Annotated Speed Comparison Graph of Two-laned Route Link Segments.

The annotated graphs depict five-time segments for data collection from the selected route links. The regions of A, B, C, D and E denote the morning off-peak (MOP), morning peak (MP), afternoon peak (AP), evening peak (EP) and evening off-peak (EOP) time segments. The orange and blue data streams depict the speed data recorded in five-minute time intervals in two routes during a weekday. When analyzing the two plots shown in Figure 19, it can be stated the fact that both the plots show a similar kind of trend with an approximate symmetry at mid-day around noon where the highest level of congestion can be seen. Therefore, the data collection is performed under these five-time segments. It is recommended to collect a greater number of samples during peak time segments to reflect the level of congestion in the representative driving cycle.

As the secondary step of DC construction, data collection should be performed. Regardless of the approach adopted, the acquired data should be reliable, representative, consistent and homogeneous. The three main approaches that are in practice throughout the world can be listed, viz., chase-car method, instrumented-car method and hybrid method. Since local driving behaviour incorporates irregular kinematic patterns integrated with aggressive driving behaviour, the instrumented-car method has opted over the chase-car method. Moreover, the operational complexity associated with the latter approach is higher than that of the opted method.

Even though on-board diagnostics protocol (OBD– II) is available on almost all 4W after 1996, the said methodology is not feasible to acquire data from motorcycles since the majority of them do not accommodate an OBD port. Therefore, a mobile application-based method is suggested and recommended for data collection from motorcycles. The application is named ‘Geo-Updater’ and is custom developed for the said research purpose. The said methodology transfers and stores real-time data in a database. The proposed application is developed ergonomically in a way such that a driver can use it with less education on the functionality of the application. Visual aids have been added to the application to make it more user-friendly.

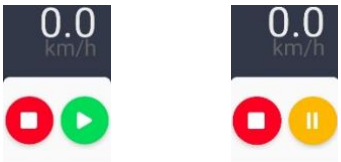

Figure 20: User Interface of the Geo-updater Application (when data collection frozen phase is shown on left and the active phase is shown on right).

Figure 20 portrays the user interfaces of the Geo-updater application when the data collection is on hold and when data collection is active. As shown in Figure 20, visual aids have been incorporated using colours and symbols for the functional buttons. The user interface is designed in a way such that it can easily be understood by a driver since there will be drivers of various educational backgrounds involved in the data collection phase to mitigate the sample bias. When developing the application, one of the most significant aspects to be decided is the average sampling interval of the application. It has been experimentally decided during the study. As per the Nyquist Sampling Criterion, the sampling frequency should be greater than or equal to two times that of the maximum spectral component of a given data set. Nyquist Criterion is shown in Equation (11).

$$f_s > 2f_i \tag{11}$$

In Equation (11), f_s denotes sampling frequency and f_i denotes the frequency of the spectral component with the highest frequency. It is important to adhere to Nyquist Criterion to mitigate aliasing and loss of data due to under-sampling. With the baseline idea of applying the Nyquist Sampling Criterion, an initial set of data is collected from the Geo-updater application from a randomly chosen vehicle.

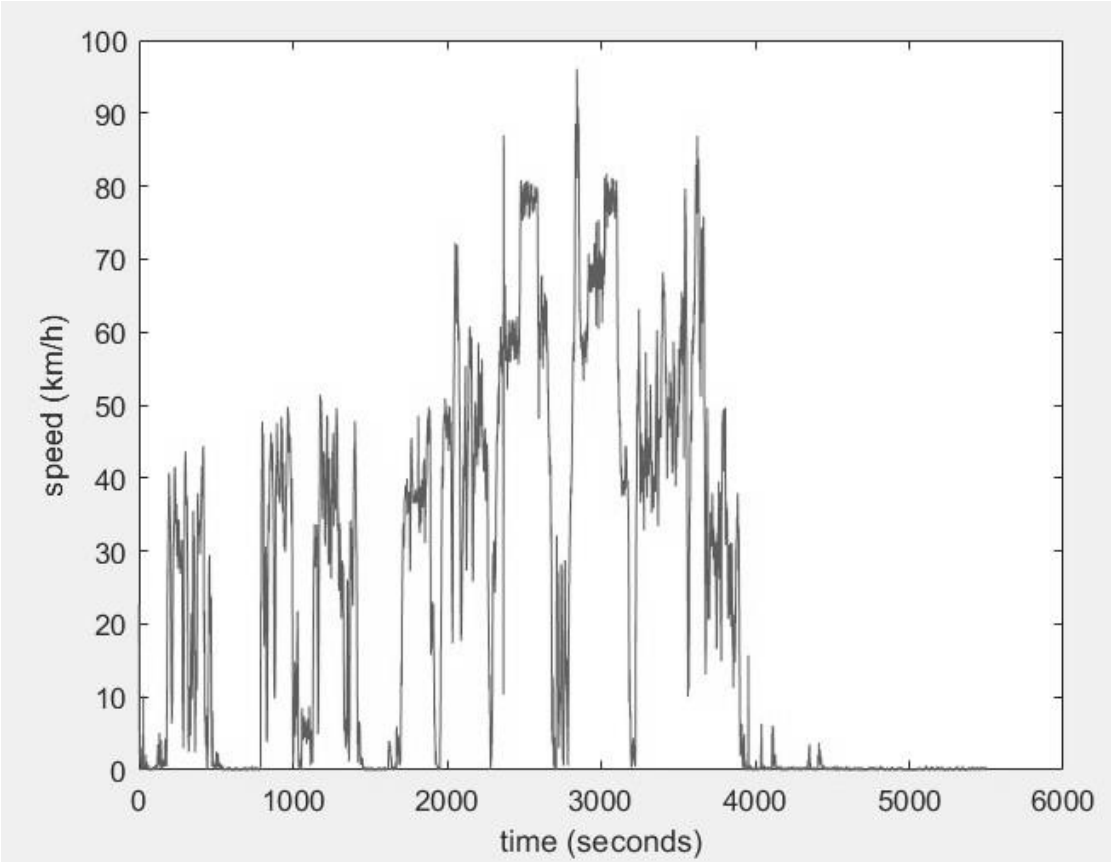

Figure 21: Speed versus time plot for the collected set of data.

Approximately 5000 data points have been acquired using the application and have been plotted as depicted in Figure 21. To determine the highest frequency spectral component, Fast Fourier Transform (FFT) has been utilized. When FFT is applied to the data set in Figure 21, the data points are transformed from the time domain to the frequency domain.

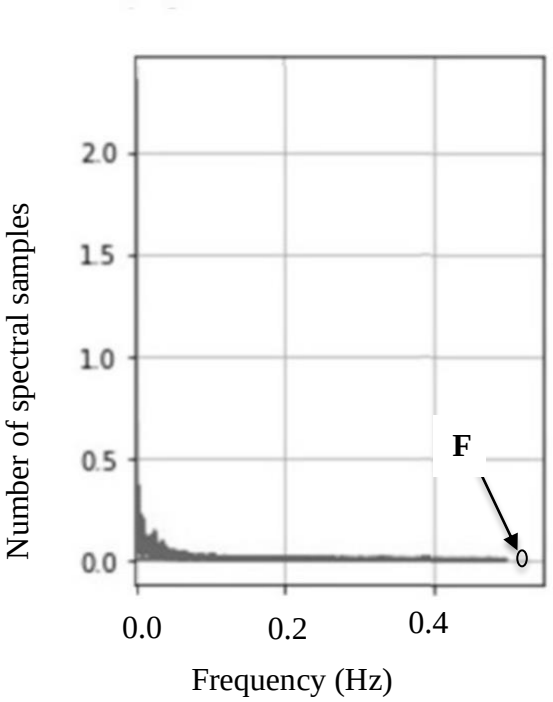

Figure 22 : Frequency plot showing the highest spectral component.

Figure 22 depicts the frequency domain data point distribution once FFT is applied. The distribution is symmetric around the origin. Since the frequency can not be negative, only the positive side of the plot is taken into consideration. Point F in Figure 22 denotes the highest spectral component of the data stream. Since the exact point is implicit in Figure 22, the region encompassed by F is zoomed in and transferred into another separate plot as in Figure 23.

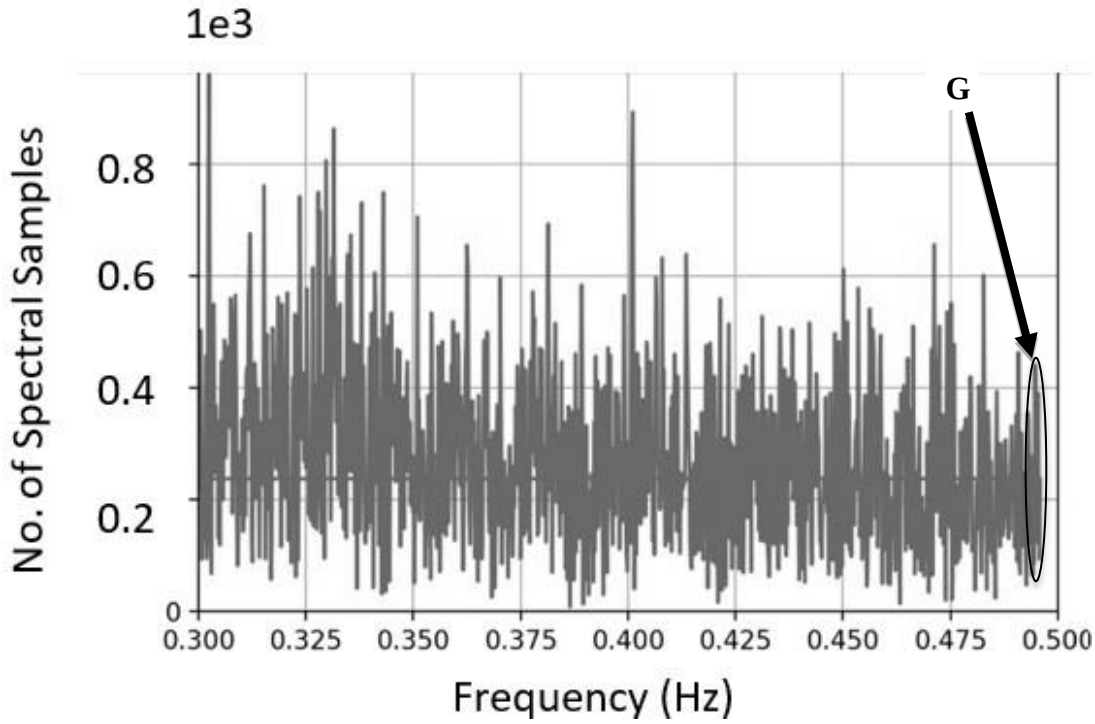

Figure 23: FFT transformed speed data sequence (Zoomed in).

In Figure 23, the local region G shows the highest spectral component which is lying around 0.490 Hz. Thus, when Nyquist Sampling Criterion is applied, the sampling frequency should be greater than or equal to twice the frequency of the maximum spectral component, i.e., 0.980 Hz. Hence, 1 Hz has opted as the average sampling interval for the study to minimize any potential data losses. In the developed application, the following data fields have been collected viz. user identification, time stamp, speed, longitude, latitude, altitude and bearing angle. Here, the time stamp is generated in Epoch time and that should be translated into standard time. The application is tested before the data collection using a test vehicle to observe the sample data and the respective plot is shown in Figure 24.

`

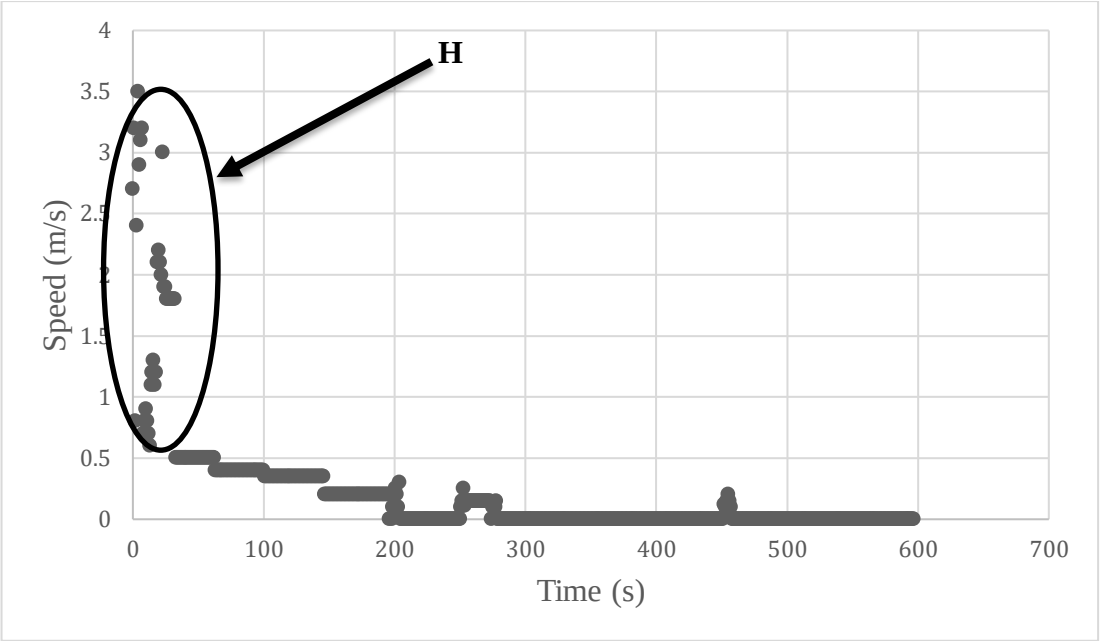

Figure 24: Speed vs. Time graph when the data collection device is at rest.

When analyzing Figure 24, it can be cited fact that even though the device is at rest, there are some speed values which are greater than 0 kmph. The transient behaviour of these speed points can be seen more often within the first 50-60 seconds after turning the app on and that is denoted by the local region H. Approximately after the first 60 seconds the speed curve reaches a steady-state behaviour which depicts the speed values which are less than 0.5 kmph. The reason behind the fluctuation of the speed points between 0 – 0.5 kmph can be concluded due to the fluctuation of the GPS signal streams (non-uniformity of GPS signal streams). Therefore to identify the stationary state of the device, the speed values which are less than 0.5 kmph, can be approximated to zero.

When collecting data, another critical aspect is the selection of the fleet sample. Ten vehicles comprising five motor tricycles and five motor 2W have been chosen for the study. When selecting the number of vehicles, the number has been decided by Motor Vehicle Emission Simulator's standard which states that five vehicles from each vehicle category should be selected for data collection. The selection of drivers is another aspect which should be paid attention to. When deciding on a driver pool, it should be variable in terms of age. Therefore, ten drivers have been selected from

different age groups and the mean age is around 37.4 years. Data is collected for two weeks covering both weekdays and weekend days. Per each data point, different data fields have been collected such as latitude, longitude, instantaneous speed, time stamp and device identification. The collected data points have been filtered per user by using the device identification which is a unique number given to each user.

The acquired data is then uploaded onto ArcGIS™ software to map the collected locations. The coordinates of the locations of the collected data points are mapped on a shape file containing the map of Sri Lanka. The corresponding map segment is portrayed in Figure 25.

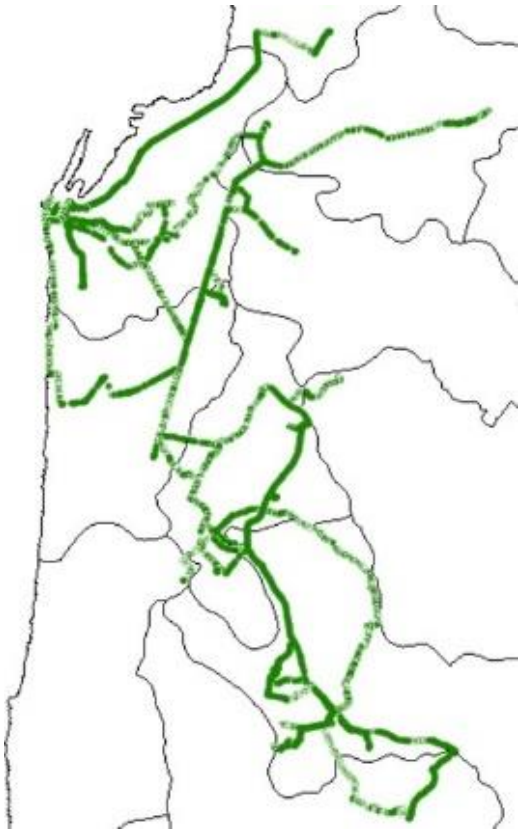

Figure 25: Collected latitude and longitude data visualized on ArcGIS map.

3.3 Cycle construction strategy

As per the four-stepped method in driving cycle construction, the third and the most critical step can be identified as the cycle construction step. Various approaches have

been adopted by researchers throughout the world in the development of driving cycles, viz., micro trip-based method, segment-based method, pattern classification method and modal cycle construction method. During the study, driving data is collected from arterial route links omitting the expressways. Therefore, the most prevalent traffic condition is the stop and go driving behaviour. The best method to model the stop-and-go traffic pattern is the micro trip-based method. In this method, the total collected data is segregated into multiple micro trips. A micro trip is defined as a trip having a leading idle period and a stop condition at the end which is depicted in Figure 26.

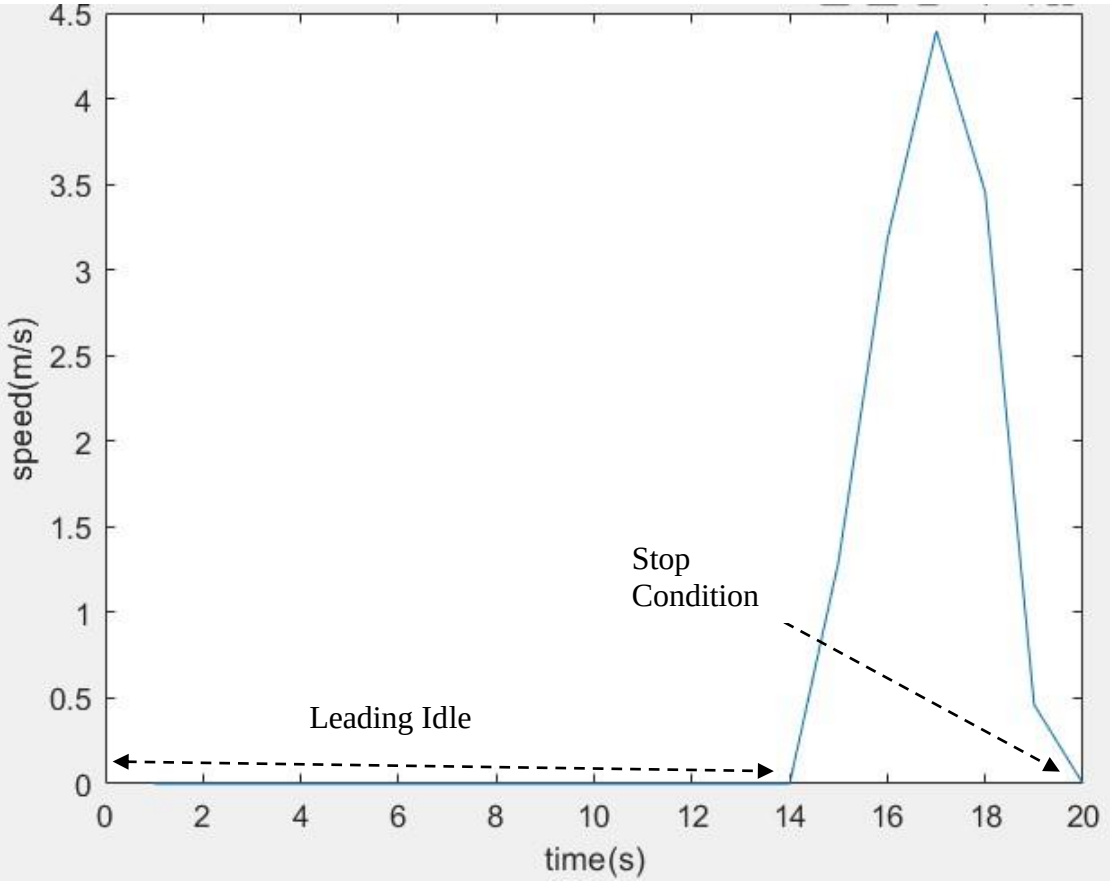

Figure 26 : Portrayal of a Micro Trip.

3.3.1 Cycle construction strategy for 2W and 3W.

Then the segregated micro trips should be clustered into classes depending on the average speed of each micro trip. There have been 2,556 micro trips in total and a MATLAB program is scripted to determine the average speed of each trip segment. There exist several methods for clustering micro trips. When referring to literature, the k-means clustering method can be found in most of the related research. Fotouhi et al. have used the k-means clustering method in developing the Tehran driving cycle [183]. When developing the Fuzhou driving cycle developed by Peng et al., again the k-means clustering method is utilized for the classification of micro trips [184]. Even though the said studies have used the k-means clustering method, there is an inconsistency on the spatial environment, i.e., two adjacent micro trips can be fallen into two different classes. For example, suppose the first micro trip is spanning for five seconds and the adjacent micro trip is spanning another five seconds. But, if the k-means clustering algorithm has a 'k' number of clusters, these two adjacent trips can fall into two different classes, let's say, urban traffic class and extra-urban traffic class. This kind of classification is inconsistent in terms of traffic behaviour. Therefore, spatial mapping is required to better reflect the spatial relationship of the classes and to mitigate the inconsistencies on the classification.

During the study, a novel approach is adopted in clustering the micro trips. Krigging spatial analysis is used to interpolate the speed data and to visualize it in the spatial domain. Using ArcGIS software, the ordinary Kriging interpolation is performed on the collated data set and the respective data is mapped on a Sri Lankan map as portrayed in Figure 27.

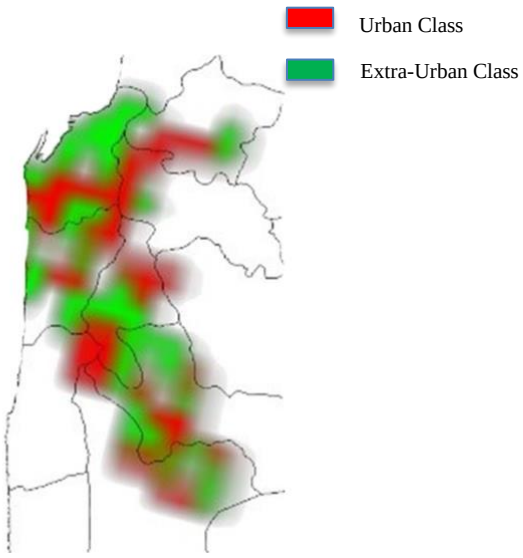

Figure 27 : Spatial Data Mapping for the Collected Data (2W and 3W).

As depicted in Figure 27, the speed data is classified into two classes which are spatially denoted using green and red. When classifying speed data of the micro trips into two classes, the Jenks Natural Breaks method has been utilized. Here, the two classes can be identified as shown in Table 17.

Table 17: Classification of Speed Classes Classification

Class Type	Average Speed (v) Range
Class 1 (Urban)	0 < v < 3.62 m/s
Class 2 (Extra – Urban)	3.62 m/s<= v < 8.16 m/s

As expected, the consistency of the classified data within their respective classes can be lucidly seen using the spatially interpolated speed data in Figure 36. The two classes have been named Urban class and Extra-Urban class, respectively. Once classified into

two classes, the next step is to determine the length of the representative driving cycle. When it comes to the length of the driving cycles, most of the driving cycles which have been used for regulatory purposes span between 900 – 1800 seconds. Therefore, the proposed driving cycle is also planned to have a duration of around 1200 seconds and comprise two phases, i.e., the urban phase and extra-urban phase. The time proportions of both phases are determined using the aggregated time duration of micro trips of each class. The urban class claims a time proportion of 52.75% whereas the extra-urban class claims for a time proportion of 47.25%. When developing the candidate cycles from the pool of micro trips, the said time length is paid attention to. The micro trips have been chosen randomly and connected to generate a lengthier micro trip to meet the said criteria of cycle length. Once such candidate cycles have been developed, the next step is to determine the characteristic parameters of the cycles. In the procedure, thirty candidate cycles have been developed. The number, thirty has opted since it adheres to the central limit theorem and the sample means of the characteristic parameters (CPs) would be converging towards the population means of the said CPs.

3.3.2 Cycle construction strategy for 4W.

There have been 5,112 micro trips in total on 4W. Similarly, as done in driving cycle development for 3W and 4W, the average speed is determined for each micro trip segment. As stated previously, Kriging interpolation is used to cluster the micro trips on 4W into two main snippets of urban and extra-urban traffic. Using ArcGIS software, the ordinary Kriging interpolation is performed on the collated data set and the respective data is mapped on a Sri Lankan map as portrayed in Figure 28.

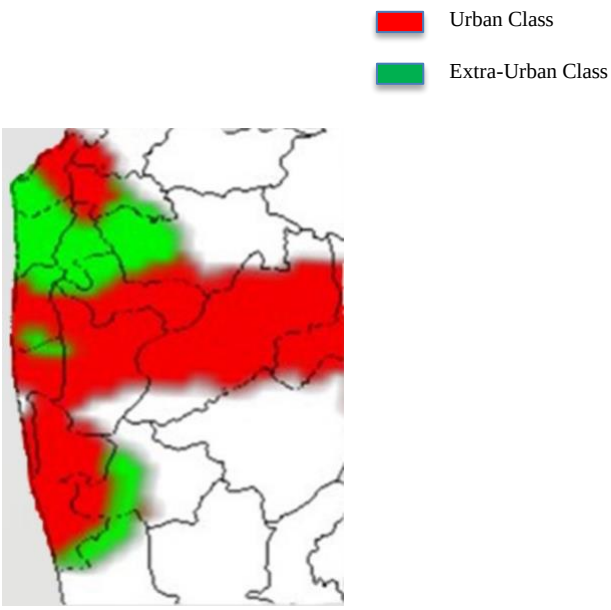

Figure 28: Spatial Data Mapping for the Collected Data (4W).

Similar to the 2W and 3W driving cycle construction method, Jenks Natural Breaks technique is used to determine the classes. Two classes have been defined using average speed as the main parameter. The said two classes are shown below in Table 18.

Table 18: Classification of Speed Classes. (4W)

Class Type	Average Speed (v) Range
Class 1 (Urban)	$0 < v < 5.77$ m/s
Class 2 (Extra – Urban)	$5.77 \text{ m/s} \leq v < 12.39$ m/s

The spatial consistency of the speed classes can be seen when Krigging analysis is used. When determining the cycle length, an approximate length of 1500 seconds has

been chosen since a usual test cycle spans between 900 – 1800 seconds. The selected representative extra-urban cycle spans for 495 seconds claiming a percentage time length of 33.02% whereas the urban cycle spans for 1004 seconds claiming a percentage time length of 66.98%. When deciding the contributions of urban and extra-urban phases to total time length, the average speed class proportions are taken into account. That means the average speed of each micro trip is determined and classified upon the determined average speed into two snippets as per the classification stated in Table 22. Subsequently, the total time of the micro trips on each snippet is determined and the same proportion is considered when assigning the time proportions of the representative driving cycle.

3.4 Cycle validation strategy

Five CPs have been chosen for the selection of the representative cycle from the pool of candidate cycles. This procedure is being performed iteratively for both the urban phase and extra-urban phase separately but in a similar manner. The selected set of CPs can be elaborated, viz., average speed, average running speed, average acceleration, average deceleration and the percentage of idle time. The similarity of each CP of the candidate cycle to that of the population is analysed and quantified using the formula stated in Equation (12).

$$CP_{SI} = \left\{1 - \left|\frac{CP_{\text{Population}} - CP_{Candidate}}{CP_{\text{Population}}}\right|\right\} \tag{12}$$

In Equation (12), CP_{SI} denotes the Similarity Index (SI) of the CPs, $CP_{\text{Population}}$ denotes the respective CP of the population data set whereas $CP_{Candidate}$ denotes the respective CP of the candidate cycle. For example, take the respective CP as average acceleration. Then, let's assume that the $CP_{Population}$ value is at 1.3587 m/s^2 and $CP_{Candidate}$ value is at 1.3713 m/s^2. Then, once the said values are substituted in Equation (12), an SI of 0.9908 has been obtained. Likewise, the same methodology is performed for other CPs as well.

$$CP_{CSI} = \sum_{i}^{5} \left\{ 1 - \left| \frac{CP_{i_{\text{Population}}} - CP_i}{CP_{i_{\text{Population}}}} \right| \right\} \quad (13)$$

As depicted in Equation (13), CP_{CSI} denotes the cumulative similarity index (CSI) which is the summation of each similarity index. During the study, five CPs have been opted and five similarity indices have been aggregated and a CSI has been determined. The candidate cycle with the highest CSI score has been opted as the representative driving cycle.

3.5 Methodology for estimating the power demand of engine auxiliaries

The auxiliary engine loads are one of the essential factors affecting a vehicle's performance on fuel economy. An auxiliary engine load can be defined as the energy utilized to operate auxiliary equipment which draws power from the respective engine. During the study, an analytical method is adopted to assess the impact of the engine auxiliary loads in terms of air-conditioning load, alternator load and water-pump load. The study portrays a novel approach for estimating and modelling the air-conditioning load which is the major contributor in terms of energy consumption. During the study, it is portrayed that an average car with 100 bhp (74.7 kW) of brake power, consumes approximately 5.4 kW of power for the functionality of engine auxiliary equipment at an operating engine speed of 3,000 RPM, which closely accounts for 7.2% of the total engine brake power output. It's conspicuous that the major contributors towards the engine power demand are air-conditioning unit and the alternator unit, accounting for a substantial portion of over 93% of the total auxiliary power requirement, whereas the water-pump and the power steering-pump are accountable for a power demand of 7% of the total auxiliary power demand. The novelty of the approach adopted during the study is that it theoretically determines the major contributor of the auxiliary power demand, i.e., air-conditioning load, whereas in the prior art, the approaches that can be referred to have used empirical method

3.5.1 Modelling and Estimating the Power Demand of an Automotive A/C System

A vehicle's (A/C) system is designed to regulate temperature and humidity levels, thereby ensuring passenger comfort. The main components of an automotive A/C system work together to provide cooling, including the compressor, belt, blower, cooling fan, condenser, receiver drier, filter, expansion valve, hose assembly, and evaporator core. In modeling the A/C system's load theoretically, the total load can be calculated by summing the contributions from various heat sources that must be cooled. These contributors may include heat from passengers, solar radiation, engine components, and ambient conditions outside the vehicle. By understanding the cumulative impact of these heat loads, the capacity and performance requirements for the A/C system can be better specified and designed.

$$Q_{\text{Total}} = Q_{\text{Met}} + Q_{\text{Rad}} + Q_{\text{Amb}} + Q_{\text{Exh}} + Q_{\text{Eng}} + Q_{\text{Ven}} \quad (14)$$

Equation (14) depicts the breakdown of the major contributors towards the automotive A/C load. Each of these load types will be discussed in the following sections and the total A/C load (Q_{Total}) will be modelled. In Equation (14), Q_{Total} denotes the total air-conditioning load, Q_{Met} denotes metabolic load, Q_{Rad} denotes radiation load, Q_{Amb} denotes ambient load, Q_{Exh} denotes exhaust load, Q_{Eng} denotes engine load and Q_{Ven} denotes ventilation load.

- **Modelling of Metabolic Load**

Passengers in a vehicle generate heat that must be removed by the A/C system, contributing to the total cooling load. This metabolic heat load consists of both sensible and latent heat components. Sensible heat is transferred from the human body through convective and radiative means, heating the air and surfaces around

passengers. Latent heat is associated with sweat evaporation from skin, which also imparts additional thermal energy to the cabin environment requiring removal.

Together, the dry sensible heat dissipation and evaporative latent heat loss comprise the total metabolic heat given off by vehicle occupants. As more passengers are present or activity levels increase, metabolic outputs typically rise. Therefore, analytical modeling of the A/C system capacity must account for expected variations in occupant heat generation. Factoring these sensible and latent metabolic loads into the overall cooling load calculations will lead to properly sized A/C components for maintaining passenger thermal comfort.

$$Q_{Met} = Q_{\text{Sensible}} + Q_{\text{Latent}} \tag{15}$$

Q_{Sensible} and Q_{Latent} can be determined using the formulas stated in (16) and (17).

$$Q_{\text{Sensible}} = \sum_{\text{Passengers}} M_{\text{Sensible}} A_{\text{Du}} \tag{16}$$

$$Q_{\text{Latent}} = \sum_{\text{Passengers}} M_{\text{Latent}} A_{\text{Du}} \tag{17}$$

In Equations (16) and (17), M_{Sensible} and M_{Latent} are the sensible metabolic heat production rate and the latent metabolic heat production rate respectively. It is found from the tabulated values in ISO 8986 [214]. When determining the metabolic load, an estimation of the body surface area A_{Du} as a function of height and weight and is determined using (18).

$$A_{\text{Du}} = 0.21 W^{0.425} H^{0.725} \tag{18}$$

In (18), W and H denote the mass and height of a human respectively. Since the study focuses mainly on the local context, an average height and weight of a person are determined about Sri Lankan context. The average height of a Sri Lankan regardless of gender lies around 162.0 cm whereas the average weight of a Sri Lankan (in 2015)

lies around 61.4 kg [215],[216]. Equations (16) and (17) require the number of passengers onboard to be estimated. Therefore, it's estimated as two occupants on average in a road vehicle travelling on Sri Lankan roads. It's assumed that the two occupants are comprised of one driver and one passenger. Moreover, the average metabolic load contribution by the passengers performing different activities is depicted in Table 19 [216].

Table 19: Metabolic load calculation of a passenger car. [216].

Occupant	Activity Level	Sensible Heat Production Rate (Wm^{-2})	Latent Heat Production Rate (Wm^{-2})
Driver	Moderate (arm work)	55	105
Passenger	Resting	50	50

The total sensible heat generation rate from two automobile occupants can be determined using Equation (19). This calculates the sum of the driver's sensible heat, accounting for moderate arm work from operating the vehicle, and the heat from the resting passenger. The total latent heat production rate is given by Equation (20), finding the sum of the driver's evaporative heat at their metabolic workload and the heat from the passenger.

Specifying distinct metabolic rates for the different occupants based on their in-vehicle activity allows for a more precise computation of the composite vehicle occupant heating. The derivations in Equations (19) and (20) quantify the overall dry and evaporative thermal loads that the A/C system must offset to maintain comfort. By separately summing the sensible and latent heat components from the driver and passenger, the complete metabolic heating burden imposed by inhabitants can be modeled.

.

$$M_{\text{Sensible}} = 105\ \text{Wm}^{-2} \tag{19}$$

$$M_{\text{Latent}} = 155\ \text{Wm}^{-2} \tag{20}$$

Hence, total metabolic load can be determined using (21) and (22).

$$Q_{\text{Sensible}} = \sum_{\text{passengers}}^{2} M_{\text{Sensible}} \bar{A}_{\text{DU}} \tag{21}$$

$$Q_{\text{Latent}} = \sum_{\text{passengers}}^{2} M_{\text{Latent}} \bar{A}_{\text{DU}} \tag{22}$$

In (21) and (22), $\bar{A}_{\text{DU}}$ denotes the mean human body surface area using the Du Bois method [218]. The estimated average body area of an average passenger is determined in the calculation performed below and the result is obtained as $\bar{A}_{\text{DU}}$ = 1.72 m^2, as stated in (23).

$$\begin{aligned} \bar{A}_{\text{DU}} &= 0.21(61.4^{0.425})(1.62^{0.725}) \\ &= 0.21(5.75)(1.42) \\ &= 1.72\ \text{m}^2 \end{aligned} \tag{23}$$

Then using the determined values for M_{Sensible}, M_{Latent} and $\bar{A}_{\text{DU}}$ substituted in (21) and (22), the sensible heat load Q_{Sensible} and the latent heat load Q_{Latent} of an A/C are determined as stated below:

$$\begin{aligned} Q_{\text{Sensible}} &= 105(1.72) \\ Q_{\text{Sensible}} &= 180.60\ \text{W} \end{aligned} \tag{24}$$

$$\begin{aligned} Q_{\text{Sensible}} &= 155(1.72) \\ Q_{\text{Sensible}} &= 266.66\ \text{W} \end{aligned} \tag{25}$$

Thus, the mean metabolic load of a 2-passengered car in the local context can be modelled as portrayed in this section. Therefore, the estimated metabolic heat load for a 2-passengered, average car can be determined as 447.26 W.

.

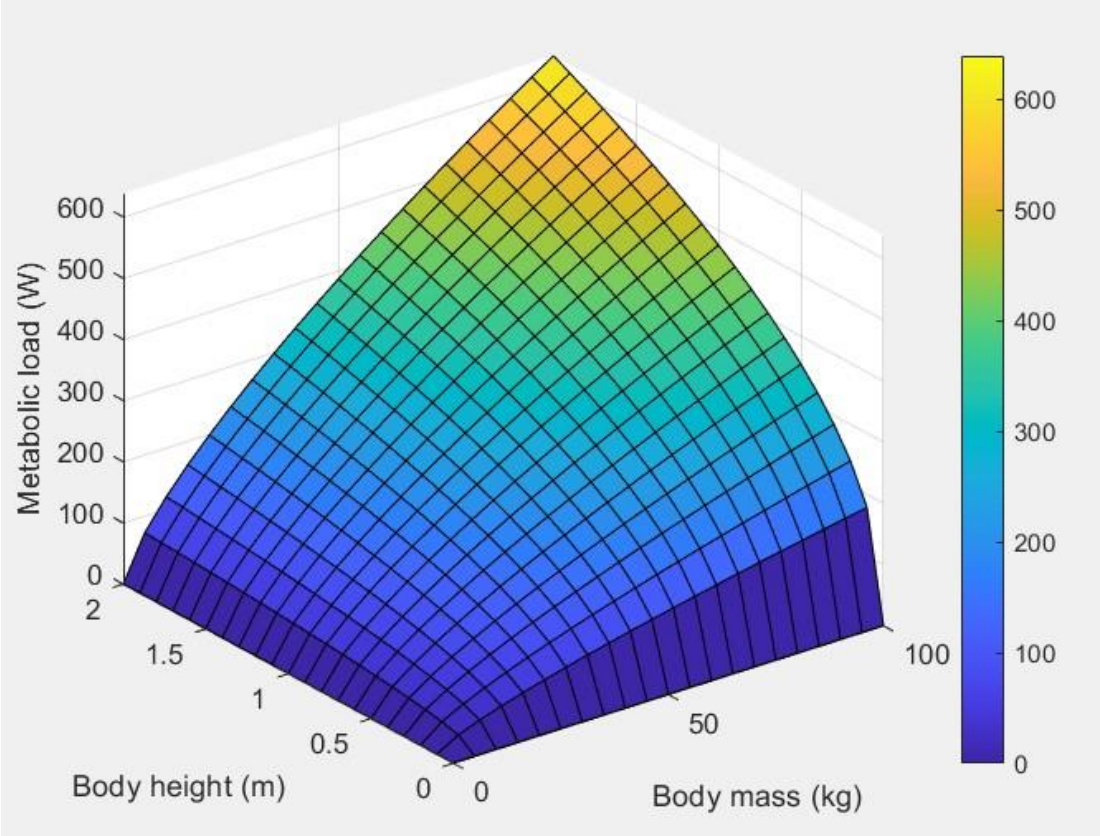

Figure 29 : Metabolic heat load distribution versus the body mass (kg) and the body height (m).

A three-dimensional representation of the metabolic heat generation within a two-occupant vehicle cabin is shown in Figure 29. This model visualizes the spatial distribution of thermal loads using the Du Bois body surface area correlations for subjects of different physical size. The graphical color scale denotes the local intensity of total heating from occupants, considering both sensible and latent components. As illustrated, increasing body mass and height leads to greater metabolic heat dissipation rates.

The driver heat generation incorporates arm motion representative of operating the vehicle, while the passenger is modeled at rest. The visualization demonstrates higher

heat fluxes from the driver as well as concentrated dissipation regions around the head and upper torso for both subjects. Integrating these localized distributions allows calculation of total occupant heating loads serving as inputs for A/C capacity requirements. This enables vehicle climate control systems to be sized appropriately based on expected variations in human anthropometrics.

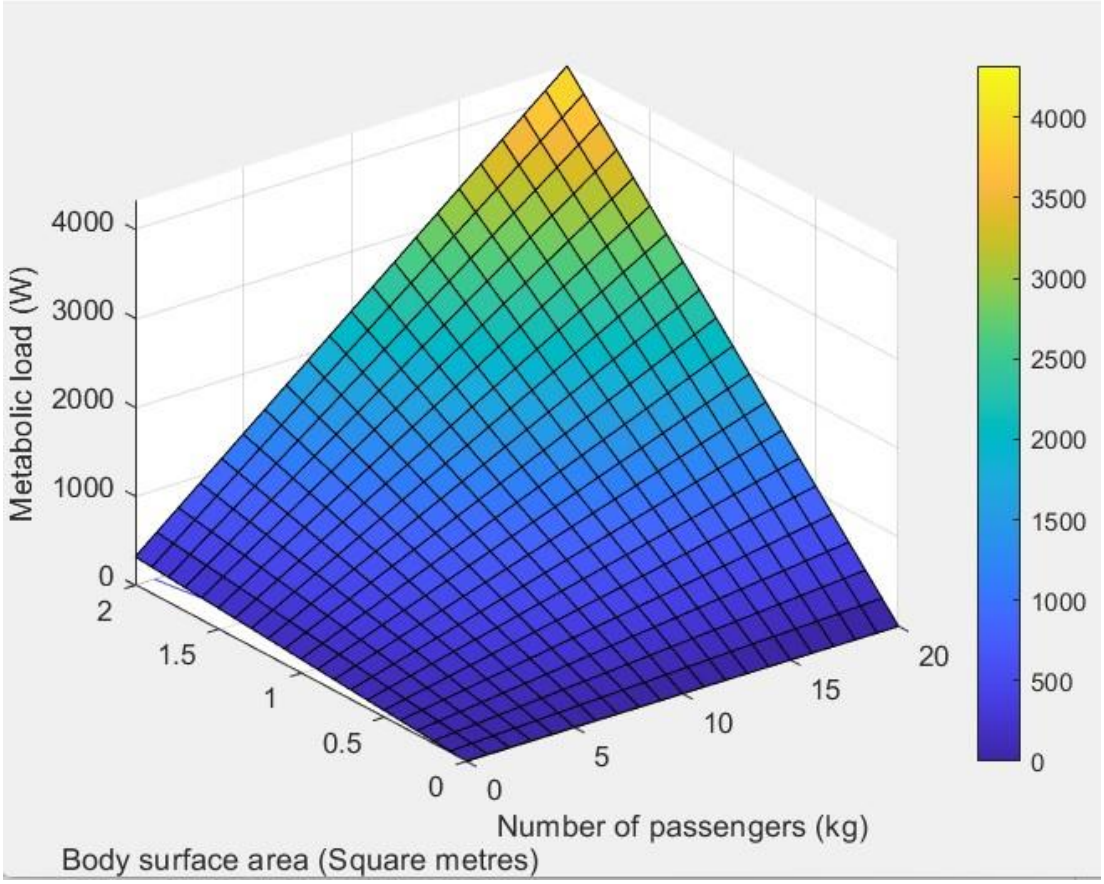

Figure 30: Metabolic heat load distribution versus body surface area (m^2) and the number of passengers. (Passenger units)

The relationship between total vehicle cabin metabolic heat load, number of occupants, and body surface area is shown in the surface plot of Figure 30. As illustrated, increasing either the quantity of passengers or their individual anthropometric size correlates with greater cumulative heat dissipation rates. This aligns with fundamental physiological expectations - more and larger bodies release more thermal energy that must be addressed by the A/C system.

The visualization can serve as a design tool for right-sizing climate control components and capacity. If an assumed average vehicle occupant condition underestimates likely body dimensions or occupant count, the modeled A/C loads may be lower than real-world needs. By incorporating potential variability in key anthropometric or seating capacity factors, vehicle HVAC systems can be specified to handle diverse passenger conditions while maintaining comfort. The trends highlighted in this metabolic heat distribution analysis are useful considerations during development of automotive climate control systems.

- **Modelling of Ambient Load**

The ambient temperature affects the calculation of external and internal cooling loads of an automotive A/C. The ambient load can be expressed as in (26).

$$Q_{Amb} = \sum_{i=1}^{n} S_{\mathrm{i}} U (T_{\mathrm{S}} - T_{\mathrm{i}}) \tag{26}$$

In (26), T_0 denotes average ambient temperature, T_{S} denotes average surface temperature, T_{i} denotes average cabin temperature, S_{i} denotes the surface area of the vehicular body (ith surface) and U denotes the overall heat transfer coefficient. When estimating the ambient load in the local context, the mean annual temperature in Sri Lanka is estimated at 27.50 C [219]. As in (26), T_{i} is determined by deducting 5.00 ^{0}C from the average ambient temperature whereas T_{S} is determined as stated in (28).

$$T_{\mathrm{i}} = T_0 - 5.00 \tag{27}$$

$$T_{\mathrm{S}} = T_0 + 5.00 \tag{28}$$

The term U can be determined using the formula in (29) in terms of R, i.e., net thermal resistance for a unit surface area. The overall heat transfer coefficient and the net thermal resistance for a unit surface area have an inversely proportional relationship as stated in (29).

$$U = 1/R \tag{29}$$

The R-value can be determined using the formula shown in (30).

$$R = {}^{1}/_{h} + {}^{ƛ}/_{k} \tag{30}$$

In Equation (30), h denotes the convection coefficient, k denotes the surface thermal conductivity and ƛ denotes the thickness of the surface element. The convection coefficient h depends on the orientation of the surface and the air velocity. Here, the following estimation is used to estimate the convection heat transfer coefficient as a function of vehicle speed and the relationship is shown in (31).

$$h = 0.6 + 6.64\sqrt{\bar{v}} \tag{31}$$

In (31), the terms can be elaborated as h denotes convection coefficient, $\bar{v}$ denotes the mean vehicular speed of the respective driving cycle and k denotes the surface thermal conductivity. Usually, thermal insulation is done using Polyethylene or Polyurethane foam sheets. Thus k value can be approximated as 0.04 W/K/m for Polyethylene foam. The ƛ value, which means the thickness of Polyethylene sheet typically ranges from 2mm to 10mm in LDV manufacturing. Thus, the average thickness of the sheet is taken as 6 mm for calculation purposes in the study.

Table 20: Kinematic parameters for different driving cycles.

Driving Cycle	Mean Speed (m/s)	$\sqrt{\bar{v}}$	h	$1/h$
NEDC	9.33	3.05	20.85	0.05
US06	21.64	4.65	31.48	0.03
JC08	6.77	2.60	17.86	0.06
WLTP	12.91	3.59	24.44	0.04

The ambient load varies w.r.t.. the air velocity along the vehicular surface. The air

velocity can be considered similar to the vehicular speed considering the relative motion between them. When considering different driving cycles as depicted in Table 20, the average speed varies among them. Therefore, the ambient load is varied respectively. Assuming the average speed of the Worldwide Harmonized Light Vehicle Test Procedure (WLTP) is 12.91 m/s, consequently, the h value can be determined as shown in Table 20. When the determined values are then substituted in (29) and (30), U, the overall heat transfer coefficient can be determined. Once the computed U value is substituted in (26), the ambient load can be determined as elaborated in the steps of (32) and (33) below:

$$R = 0.04 + \frac{6\text{x}10^{-3}}{0.04}$$
$$= 0.19\ W^{-1}m^2K \quad (32)$$

$$U = \frac{1}{\text{R}}$$
$$= \frac{1}{0.19}$$
$$= 5.26\ Wm^{-2}K^{-1} \quad (33)$$

When determining the ambient load, the surface areas of the vehicular exterior should be considered. During the study, the vehicular surface area is estimated using mean vehicular surface area, i.e., $\bar{S}$. The $\bar{S}$ is estimated to be around 102.50 square feet (9.52 m^2) which range between 87-118 square feet [221].

$$Q_{Amb} = \bar{S}U(T_S - T_i)$$
$$Q_{Amb} = (9.52)(5.26)(\ T_0 + 5.00 - \ [T_0 - 5.00])$$
$$Q_{Amb} = 500.75\ \text{W} \quad (34)$$

Therefore, the ambient load of an automotive air-conditioning of an average passenger car can be estimated at around 500.75W as stated in (34) and it can be considered a major contributor towards the air-conditioning load.

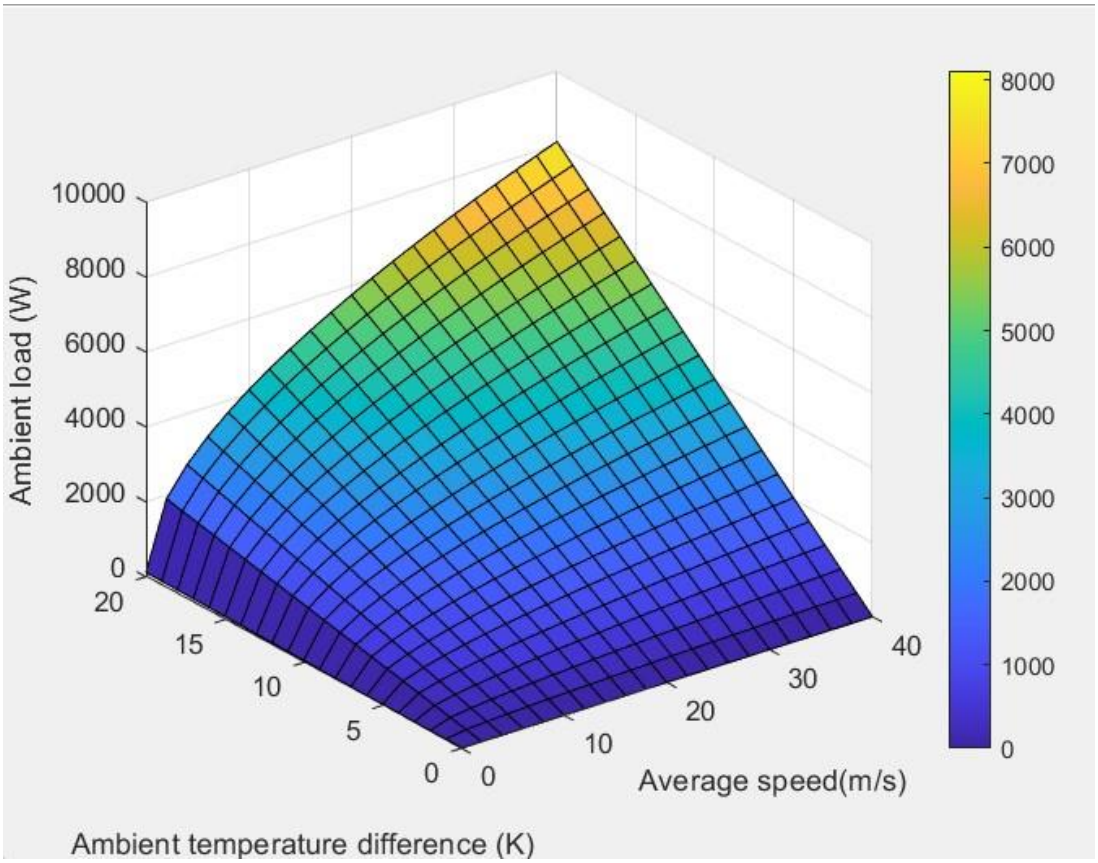

Figure 31 : Ambient heat load distribution versus average speed (m/s) and ambient temperature difference (K).

The distribution of ambient heat load is portrayed using the surface plot in Figure 31. The ambient heat load is increased on par with the increase in the temperature difference and the average speed of the vehicle. The ambient temperature difference signifies the temperature gap between the surface of the vehicular body and the cabin temperature.

- **Modelling of Radiation Load**

Radiation load is another key element in determining the total A/C load. The radiation load comprises three major components viz. direct radiation load, the diffuse radiation load and the reflected radiation load. The direct radiation load is caused by the radiation of direct sunlight whereas the diffuse radiation is part of solar radiation, which results from indirect radiation of daylight on a surface. The reflected load is caused by the reflected radiation from the surfaces [222]. The total radiation load can be modelled using the formula shown in (35) [218].

$$Q_{\text{Rad}} = \frac{1}{2} S\alpha (I_{\text{Dir}}\, Cos\theta + I_{\text{Dif}} + I_{\text{Ref}}) \quad (35)$$

In (35), Q_{Rad} denotes the total radiation load, S denotes the surface area, I_{Dir} denotes the direct radiation heat gain per unit area, θ denotes the angle between the surface normal and the position of the sun in the sky, α denotes the surface absorptivity, I_{Dif} denotes the diffuse radiation heat gain per unit area and I_{Ref} denotes reflected radiation heat gain per unit area. Considering the fact that solar radiation can affect only one particular half of the vehicle at a given time, the constant of ½ is added to (35). When determining the radiation load, it's important to obtain the position of the sun w.r.t. the earth.

The mean altitude angle of the sun, i.e., β w.r.t. the earth during the mid-year can be determined as -30^0. [223]

$$i_{\text{Dir}} = \frac{A}{e^{B/SinB}} \quad (36)$$

The direct radiation heat gain per unit area, i.e., i_{Dir} can be determined using (36). Assuming the mid of the year, the constants A and B can be approximated as; A = 1087.613 Wm^{-2} and B = 0.205 as per ASHRAE Handbook of Fundamentals [224]. When substituting the said A and B values in (36), the result shown in (37) is obtained.

$$i_{\text{Dir}} = 1087.613/e^{(0.205/Sin(-30)}$$

$= 1087.613/0.6636$

$i_{\text{Dir}} = 1{,}639$ W (37)

$$i_{\text{Dif}} = CI_{Dir}\,(1 + CosE)/2 \quad (38)$$

In (38), the constant C can be approximated to 0.134 [224]. Assuming that, E equals 45° then, i_{Dif} can be determined and the result is shown in (39).

$i_{\text{Dif}} = (0.13)(1639)(1+0.71)/2$

$i_{\text{Dif}} = 187.45$ W (39)

I_{Ref} can be determined using the direct and diffuse radiation heat gain per unit area as in (40).

$$i_{\text{Ref}} = (i_{\text{Dir}} + i_{\text{Dif}}) * \rho_{\text{g}}(1 - CosE)/2 \quad (40)$$

The term ρ_{g} denotes the ground reflectivity coefficient. It ranges from 0.20 – 0.35 for rough surfaces [225]. The mean ground reflectivity coefficient, i.e., $\overline{\rho_{\text{g}}}$ is assumed to be 0.30. The I_{Ref} value is then determined using (40) and the result is depicted below as stated in (41).

$$i_{\text{Ref}} = (1{,}639 + 187.45) * 0.30(1 - 0.71)/2$$

$$i_{\text{Ref}} = 80.27 \text{ W} \quad (41)$$

The value α, i.e., surface absorptivity is approximated as 0.4 [226]. Also, since θ is approximated to 45^0, $Cos\theta$ can be determined as 0.707.

$\dot{Q}_{s\,\text{Rad}} = 0.5\text{x}9.52\text{x}\ 0.4\ (1639\text{x}0.71 + 82.54 + 35.35)$

$$\dot{Q_{s\,\mathrm{Rad}}} = 2{,}430.80\ \mathrm{W} \tag{42}$$

Therefore, the total radiation load comprising of direct, diffuse and reflected radiation is determined as stated in (42) and it claims for one of the highest contributors of an automotive A/C with a power requirement of around 2.43 kW. Moreover, it accounts for a 24% contribution towards automotive A/C power demand. The automotive A/C energy efficiency can be improved by exploring the means of mitigating the impact of radiation heat load.

- **Modelling of Exhaust Load**

Since the study encompasses the scope of LDVs equipped with ICE, exhaust emission is generated and transmitted from the exhaust manifold of the engine through the exhaust lines underneath the cabin to the tailpipe. The higher temperature of the exhaust gas can contribute towards the thermal gain of the cabin through the cabin floor. The exhaust load can be modelled using the formula provided in (43).

$$\dot{Q}_{\mathrm{Exh}} = S_{\mathrm{Exh}} U (T_{\mathrm{Exh}} - T_{\mathrm{i}}) \tag{43}$$

In (43), the terms can be introduced viz. U denotes overall heat transfer coefficient, S_{Exh}denotes surface area exposed to exhaust gas temperature (area in contact with the exhaust line), T_{Exh} denotes exhaust gas temperature and T_{i} denotes cabin temperature.

In determining the average surface area exposed to exhaust heat, the following assumptions and calculations have been made. The length of an average car is assumed to be 15 feet (4.50 m) [227]. The length of an average exhaust line (L_{Exh}) is determined by multiplying the length of an average car by a factor of 0.75. Thus, L_{Exh} can be estimated as 3.38 m. The average diameter of the exhaust line (D) (Up to 2.5 litre IC engine/ 300 bhp vehicles) can be estimated as 2.5 inches (63.5 x 10^{-3} m). Assuming the area in contact with the exhaust line is the area of its projection on the bottom surface of the car, the relationship in (44) can be developed.

$$S_{\text{Exh}} = L_{\text{Exh}} \text{ x } D = 3.38 \text{ x } 63.5 \text{ x } 10^{-3}$$
$$= 214.6 \text{ x } 10^{-3} \text{ m}^2 \quad (44)$$

The average cabin temperature, T_{i} can be approximated ($T_0 - 5$) whereas the overall heat transfer coefficient, U can be approximated as 5.26 $\text{Wm}^{-2}\text{K}^{-1}$. In Equation (45), N denotes engine speed in RPM. The exhaust gas temperature (T_{Exh}) can be estimated using the linear function of RPM of the engine as stated in (45) [228].

$$T_{\text{Exh}} = 0.14N - 17 \quad (45)$$

Approximating the normal operating N of a 4-stroke ICE as 3000 then T_{Exh} can be determined as 403.0 ^{0}C when substituted in (45).

$$\dot{Q}_{\text{Exh}} = (214.60 * 10^{-3}) * 5.26 * (403.00 - 22.50)$$

$\dot{Q}_{\text{Exh}}$ = 429.51 W (46)

Consequently, as shown in (46), the average exhaust load of an automotive A/C can be determined as around 430 W under local conditions.

- **Modelling of Engine Load**

Engine load determines the amount of excess heat generated by the IC engine and the amount transmitted towards the cabin. The said engine load can be modelled using the formula stated in (47).

$$\dot{Q_{\text{Eng}}} = S_{\text{Eng}} U (T_{\text{Eng}} - T_{\text{i}}) \quad (47)$$

In (47), S_{Eng} denotes the surface area exposed to engine temperature, T_{Eng} denotes the engine temperature and T_{i} denotes the cabin temperature. The U value is estimated as 5.26 $\text{Wm}^{-2}\text{K}^{-1}$. Assuming that the area exposed to the engine temperature of an average

car is defined by (effective height = 0.5 x height), the value for S_{Eng} can then be determined as stated in (48).

$$\mathrm{S_{Eng}} = \text{Track length X Effective height} \quad (48)$$
$$= 0.65\ \mathrm{m^2}$$

The estimation of the engine temperature can be performed using the formula stated in (49) [229].

$$T_{\mathrm{Eng}} = -2 * 10^{-6} RPM^2 + 0.04 RPM + 77.5 \quad (49)$$
$$T_{\mathrm{Eng}} = -2 * 10^{-6} * 3000^2 + 0.04 * 3000 + 77.5$$
$$= 179.50^{\circ}\mathrm{C}\ \text{(the estimated engine temperature under given conditions)}$$

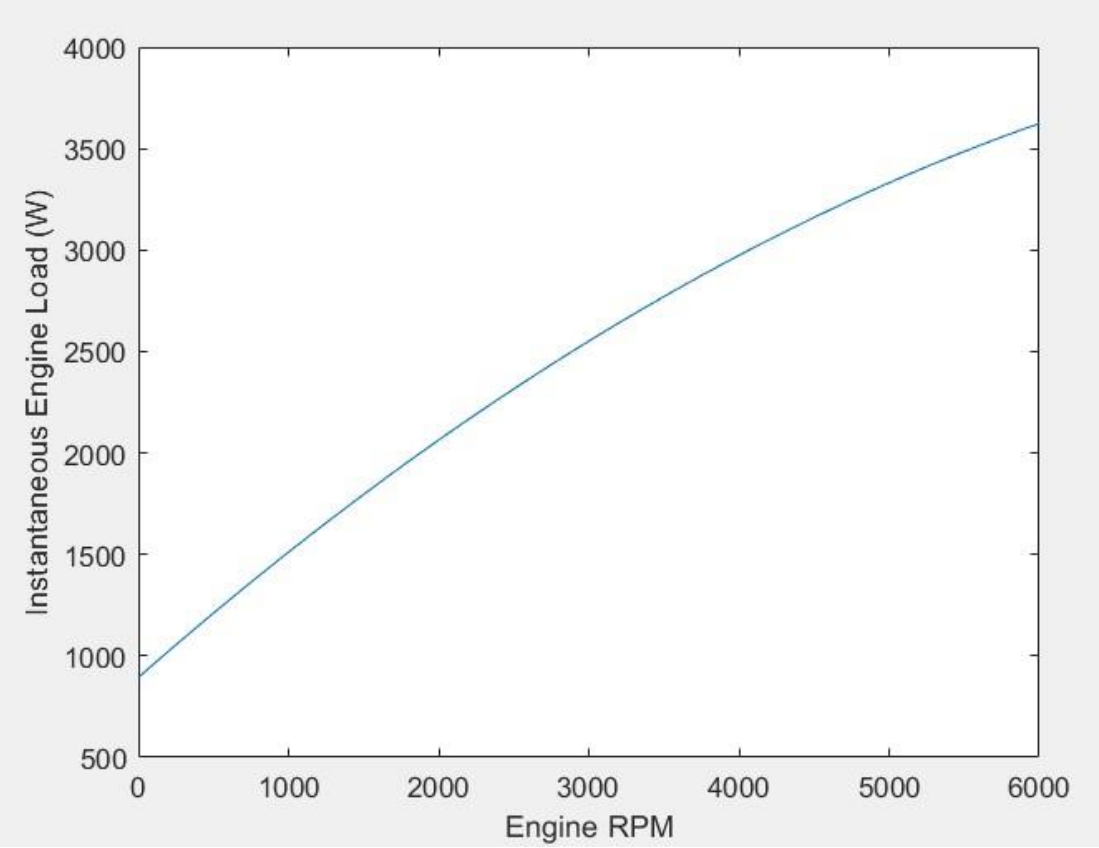

Figure 32 : Engine Load versus Engine RPM.

The variation of the engine load on par with the engine RPM can be portrayed in Figure 32. It can be clearly shown that the instantaneous engine heat load gets increased quadratically against the engine RPM.

$$\dot{Q_{\text{Eng}}} = S_{\text{Eng}} U\left(T_{\text{Eng}} - T_{\text{i}}\right)$$
$$= 0.65 * 5.26\ (179.50 - 22.50)$$
$$= 536.78\ \text{W} \quad (50)$$

Consequently, the engine load can be determined as stated in (50), using the steps stated above and the average engine load can be approximated as 540 W under given conditions.

- **Modelling of Ventilation Load**

Due to the leakage of air within the cabin to the atmosphere, ambient air is assumed to enter the cabin at the ambient temperature and with higher relative humidity. Typically, once reached the steady-state operation, the cabin air pressure is greater than the ambient air pressure. The said thermal load can be determined using the formula stated in (51) [222]:

$$\dot{Q_{\text{Ven}}} = \dot{m_{\text{ven}}}(e_o - e_{\text{i}}) \quad (51)$$

In (51), e_o denotes ambient enthalpy, e_{i} denotes cabin enthalpy and $\dot{m_{\text{ven}}}$ denotes ventilation mass flow rate. The formula which is used to determine the enthalpy (e) is stated in (52) [222].

$$e = 1006\bar{T} + (2.501 * 10^6 + 1770\bar{T})\bar{X} \quad (52)$$

In (52), $\bar{T}$ denotes the mean air temperature, $\bar{X}$ denotes the mean humidity ratio and $\bar{X}$ can be modelled using the formula stated in (53);

$$\bar{X} = 0.62 \frac{\emptyset P_s}{100P - \emptyset P_s} \quad (53)$$

In (53), $\emptyset$ is the relative humidity that is approximated as 74.0%, P_s is the ambient saturated vapour pressure which is estimated as 3693.03 Pa and P is the atmospheric pressure which is estimated as 1.01 bar = 1.01325 x 10^5 Pa about the local geography, i.e., Colombo, Sri Lanka.

Table 21: Relative Humidity (RH) and Saturated Vapor Pressures at given temperature values.

	Temperature (^{0}C)	Relative Humidity	Saturated Vapor Pressure
Ambient	27.50	74%	3,693.03 Pa
Cabin	22.50	50% (air-conditioned)	2,980.04 Pa

Once substituted the ambient values into (53), the value in (54) is obtained.

$\bar{X}_{\text{Amb}} = 0.62 \frac{0.74 * 3693.03}{100 * 1.001 * 10^5 - 0.74 * 3693.03}$

$\bar{X}_{\text{Amb}} = 0.62 \frac{2732.84}{1.01 * 10^7}$

$\bar{X}_{\text{Amb}} = 1.68 * 10^{-4}$ (54)

$\bar{X}_{\text{Amb}}$ denotes the ambient $\bar{X}$ value. Similarly, for cabin parameters, (55) is obtained.

$\bar{X}$

$\bar{X}_{\text{Cabin}} = 0.93 * 10^{-4}$ (55)

$\bar{X}_{\text{Cabin}}$ denotes the $\bar{X}$ value of the cabin. According to the local context, $\bar{X}$ = 74.0%; T = 27.5^{0}C and substituting the respective values into (52), the result in (56) can be obtained.

$$e_o = 1006(273.15 + 27.50) + (2.501 * 10^6 + 1770[273.15 + 27.50])(1.682 * 10^{-4})$$

$$e_o = 0.303 * 10^6 + 2.501 * 10^6$$

$$e_o = 0.304 * 10^6\ J \quad (56)$$

Assuming that the mean RH of an air-conditioned car lies around 50% (ranges between 30% - 65%, for temperatures between 20 – 25^{0}C)

$$e_{\mathrm{i}} = 1006(273.15 + 22.50) + (2.501 * 10^6 + 1770[273.15 + 22.50])(0.926 * 10^{-4})$$

$$e_{\mathrm{i}} = 0.299 * 10^6 + 2.501 * 10^6$$

$$e_{\mathrm{i}} = 0.298 * 10^6\ J \quad (57)$$

Similar to the method of obtaining (56), the result in (57) is achieved. Assuming a mean mass air flow rate of 0.02 m^3s^{-1}, the ventilation load can be determined as stated in (58).

$$\dot{Q_{\mathrm{Ven}}} = 0.02(0.304 - 0.298) * 10^6$$

$$\dot{Q_{\mathrm{Ven}}} = 0.02(0.304 - 0.298) * 10^6 \dot{Q_{\mathrm{Ven}}} = 120.00\ W$$

Consequently, the average ventilation load of an automobile is estimated under given local conditions as 120W, which lies comparatively lower than the other A/C loads.

Using the heat load demand, the A/C load can be determined using the co-efficient of performance (CoP) for the A/C compressor. Typically, the CoP can range between 2 to 4 under standard operating conditions for automotive A/C compressors. More modern A/C compressors can achieve CoP values in the range of 3 to 4. Three scenarios are mapped in Table 22 for the A/C load determination. Finally, a summary

of the determined values for each type of A/C load under local conditions is depicted as stated in Table 22.

Table 22: A/C load breakdown

A/C Load Type	Load (W)
Radiation Load	2430.80
Engine Load	536.78
Exhaust Load	429.51
Ambient Load	500.75
Metabolic Load	447.26
Ventilation Load	120.00
Cumulative Heat Load	4,465.10 W
A/C load for a CoP = 2	2,232.55 W
A/C load for a CoP = 3	1,488.37 W
A/C load for a CoP = 4	1,116.28 W

3.5.2 Estimating the power demand of an automotive alternator

Alternators are the primary source of electric energy within a vehicle. The electric power demand of contemporary automobiles has rapidly increased on par with the improvements in auto-electric appliances. The alternator provides the electric output as a consequence of the process of the energy conversion chain. Taking the average efficiency values into account, the ICE efficiency of 40%, the belt efficiency of 98% and the alternator efficiency of 55%, which leads to an overall energy efficiency of around 21% [230].

Simply stated, an alternator is a synchronous alternating current (AC) electric generator with direct current (DC) diode rectification and pulse width modulation voltage control [231]. It comprises the rotor, stator, diode rectifier and voltage regulator. It can be stated the fact that the peak efficiency of an automotive alternator lies around 55% at an operating RPM of around 1500. The loss in an alternator is

another important aspect to be analyzed since it can contribute towards increased fuel consumption. The losses can be lumped into three main types viz. electrical, magnetic, and mechanical.

Having considered the above-mentioned loss factors into account, the overall energy conversion efficiency of an alternator can be stated as:

$$\eta = \frac{P_{\text{Out}}}{P_{\text{In}}} \tag{59}$$

In (59), η denotes overall alternator efficiency, P_{In}_denotes input mechanical power and P_{Out} denotes output electrical power.

$$\eta = \frac{P_{\text{Out}}}{P_{\text{Out}}+P_{\text{Losses}}} \tag{60}$$

The η value can then be expressed as stated in (60).

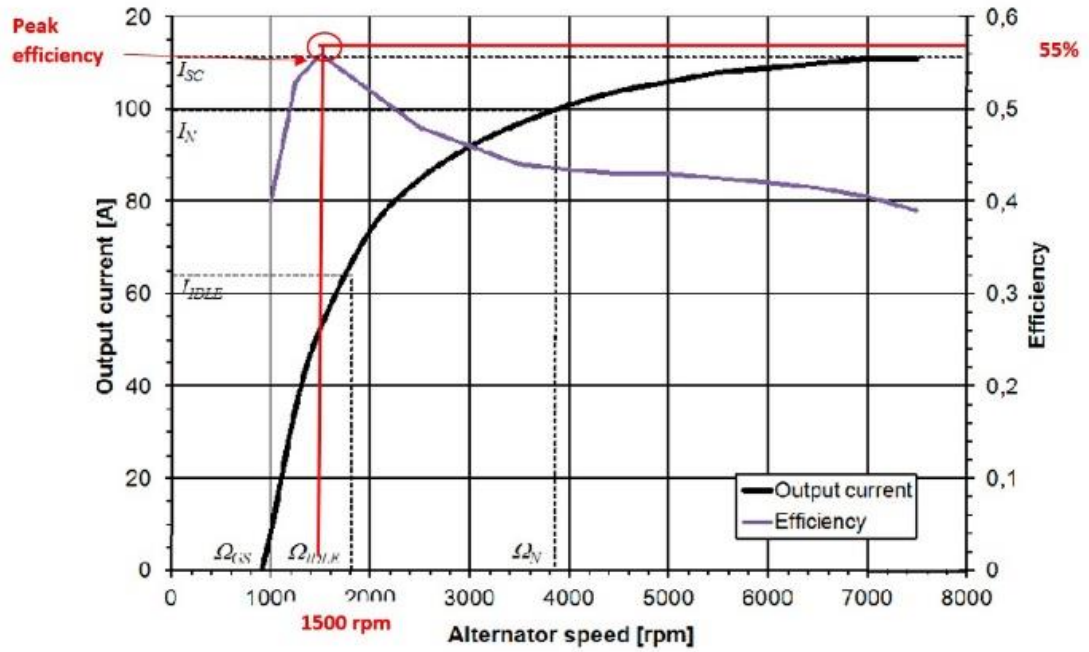

Figure 33: Operating regions of an alternator (Output Current, Efficiency vs Alternator RPM).

Referring to Figure 33, it can be stated that the peak efficiency of an automotive alternator lies around 55% at an operating RPM of around 1500. The term P_{Losses} in (60) denotes the aggregated power losses within the alternator. The typical voltage output of an automotive alternator lies in the range of 13.8 – 14.3 V. (for a 12V car-electric system). Assuming that the peak amperage of the alternator is 110.0 A with 14.0 V at 1,500 RPM, the input mechanical power demand of an alternator with 55% overall efficiency can be expressed as in (61):

$$P_{\text{Out}} = V_{out} * I_{Out} \tag{61}$$
$$P_{\text{Out}} = 14.0*110.0$$
$$P_{\text{Out}} = 1540.0 \text{ W}$$

Assuming the alternator efficiency, η is around 55%, then the average power demand of an alternator can be determined as stated in (62);

$$\eta = \frac{P_{\text{Out}}}{P_{\text{In}}}$$
$$P_{\text{In}} = \frac{1540}{0.55}$$

$$P_{\text{In}} = 2{,}800.0 \text{ W} \tag{62}$$

Therefore, the average input power demand of an automotive alternator can be determined as around 2.8 kW which is a significantly higher contributor.

3.5.3 Estimating the power demand of other engine auxiliaries

During the study, the mechanical water pump and the power steering pump have been identified and are studied as the other engine auxiliaries besides the A/C and the alternator. When estimating the power demand of the water pump and the power steering pump, previous literature has been critically appraised. Firstly, the power demand of a water pump is discussed and estimated. During driving cycle test schedules which span between 1200 – 1800 seconds, the cooling system's operation

of an ICE is of greater importance to ensure that the engine remains within the optimum operating temperature range. ICEs account for many types of heat losses. To maintain optimum operation within the engine, the operating temperature should be maintained using a cooling mechanism. The water pump is essential piece of equipment for pumping the coolant fluid within an engine block to maintain its optimum temperature. In every vehicle equipped with an ICE, the water pump can be seen in the form of either mechanical or electric. During the study, the mechanical version of the water pump will be discussed. It operates as an engine auxiliary load which is coupled to the engine crankshaft using a serpentine belt. The single-stage radial centrifugal pumps are used in the vast majority of motor vehicle cooling circuits. The speed of the pump and coolant flow rate is linked directly to the engine speed.

A typical mechanical water pump consists of an impeller located inside a spiral housing and sealed via an axial face seal. The spiral housing is mounted against the engine block with channels leading in and out of the coolant fluid channels within the engine block. The mechanical power arrives via the hub with a pulley. The channels on the pulley indicate the interface for the guides on the serpentine belt which transmits power from the crankshaft [232]. When referring to the relationship between the pressure generated within the water pump and the respective flow rate at different engine speeds, it can be seen the fact that on par with the increase in the engine speed, the pump pressure to gets increased [228]. Consequently, the amount of fluid power generation will also be increased. The mechanical efficiency of a water pump typically lies between 35% - 55% concerning the engine speed range from idle (1000 RPM) to 5000 RPM [230]. The input power required by the water pump varies from 185 W to 220 W w.r.t. the RPM range from 3000 – 5000 RPM. Considering the operating RPM of 3000, then the power demand of the water pump can be estimated at around 185 W.

As previously stated, the power steering pump is the other type of engine auxiliary that has been studied and the power demand of which has been discussed and estimated during the study. During driving cycle test schedules, the lateral motion of the vehicle steering is not considered. Hence, the power demand of the power steering pump during straight driving is discussed. When considering power steering mechanisms,

there exist two main technologies viz. hydraulic power-assisted steering (HPAS) and electronic power-assisted steering (EPAS). The power consumption during the course of the straight drive is having significant discrepancies between these two technologies. The studies of R. Herkommer, [233] had conspicuously shown the fact that fuel consumption gets reduced by up to 0.25 litres of fuel per 100 km when EPAS systems are introduced in LDVs. On the other hand, the conventional HPAS system consumes approximately 0.3 litres of fuel per 100 km [233], [234]. Power demand in the HPAS system is dependent upon the delivery of oil.

Usually, hydraulic pumps are fix-mounted on the engine; they are connected to the engine via the serpentine belt. Since the engine RPM of the vehicle gets varied during the drive, the flow delivered by the pump also gets varied proportionally. The pumps are designed to deliver full flow at engine idle speed. Therefore, it leads to the production of surplus oil when the engine runs at the operating RPM range. This aforesaid surplus oil is accountable for most of the losses, and power consumption, associated with HPAS. Furthermore, it's lucid the fact that the overall energy efficiency of the HPAS system, i.e., 60% is quite higher than that of the EPAS system, i.e., 22% [232], [233], [234]. Since the EPAS system is having a higher number of levels of power transmission than the HPAS system, it can lead to lowered efficiency values. Despite the lower efficiency, the overall power demand of the EPAS system is significantly less than that of the HPAS system. EPAS system is accountable for an overall power demand approximately of 38.5 W whereas the HPAS system claims an overall power demand of around 175 W. Therefore, the estimated power demand figures for straight driving in driving cycle schedules can be determined as 175W for LDVs equipped with HPAS systems whereas the power demand is around 38.5 W for LDVs equipped with EPAS systems.

- **Chapter Conclusion**

Auxiliary engine components play a significant role in contributing towards the engine power demand. The percentage contributions of each auxiliary load towards the engine power demand are portrayed in Table 23.

Table 23: Summary of the engine auxiliary power demand

Auxiliary Load Type	Estimated Power Demand (W)	Percentage of Total Auxiliary Power Demand
Air-conditioning unit (CoP =2)	2,232.5	41.4%
Alternator	2,800	51.9%
Mechanical Water Pump	185	3.4%
Hydraulic Power-Assisted Steering Pump	175	3.3%
Estimated Total Auxiliary Load @ 3000 RPM	5,392.5	

Almost all the auxiliary equipment listed in the study are belt-driven and thus, there's a significant dependency on engine speed and subsequently on vehicular speed as well. Therefore, when tested on a driving cycle, the said auxiliary equipment portrays a significant impact on the operating fuel economy of light duty vehicles.

When analyzing the belt-driven mechanical auxiliary loads of the A/C unit, alternator, water pump and steering pump, it's conspicuous that the major contributors towards the engine power demand are the A/C unit and the alternator accounting for a substantial portion of more than 93% of the total auxiliary power requirement. Also, it is lucid that the power requirement of the water pump and the steering pump lies quite low, i.e., around 7% of the total auxiliary power demand. When determining the said power requirements, an operating RPM of 3,000 has been considered whereas the other physical factors are considered w.r.t. the local Sri Lankan context. In a context where a standard LDV comprising a rated engine power of around 100 bhp, i.e., equivalent to around 74.7 kW, an estimated 5,392.5 W portion would be demanded by the engine auxiliaries accounting for around 7.2% of the total engine rated power. Therefore, it can be concluded that auxiliary engine loads must be taken into account when modelling the overall engine power demand since they claim for a substantial portion of engine power and should then be considered as a main factor in modelling the engine loads on par with the tractive loads and other engine inertial loads.

3.6 Methodology for determining the theoretical model for fuel consumption estimation

The development of a mathematical model for fuel consumption characterization is one of the major deliverables of the study. The main goal is to develop a functional relationship between fuel consumption and vehicular speed (instantaneous). When developing a functional relationship, understanding the power demand of an ICE is of paramount significance. The power demand of an ICE can be segregated into two main types, i.e., the tractive power demand and the auxiliary power demand. Tractive power demand comprises of four main types of tractive loads viz. the power required to overcome rolling resistance load, aerodynamic drag load, grade resistance load and inertial resistance load. Apart from the main tractive power requirement which needs the vehicle to traverse along, a vehicle demands power to energize the other engine auxiliaries viz. A/C, alternator, water pump and power steering pump. The functionality of the said engine auxiliary equipment is necessary for the functionality of a vehicle. Equation (63) portrays the relationship on the tractive load requirement.

$$F_{\mathrm{TR}} = \underbrace{(C_{\mathrm{r}}.M.g)}_{\text{Rolling Resistance}} + \underbrace{\left(\frac{C_{\mathrm{D}}.A_{\mathrm{F}}.\rho.v^2}{2}\right)}_{\text{Drag Resistance}} + \underbrace{(M.g.\sin\alpha)}_{\text{Grade Resistance}} + \underbrace{(M.\delta.a)}_{\text{Rotational and linear inertia}} \quad (63)$$

where,

F_{TR} — the total tractive force

C_{r} the coefficient of rolling resistance

M the mass of the vehicle

g the gravitational acceleration

C_{D} the drag coefficient

A_{F} the frontal area of the vehicle

ρ the density of air

v the instantaneous vehicular speed

α the gradient angle of the road profile

a the instantaneous acceleration and finally

δ the mass correction factor.

By multiplying Equation (1) by v concerning $P = F.v$:

$$F_{\mathrm{TR}}.v = \{(C_{\mathrm{r}}.M.g) + \left(\frac{C_{\mathrm{D}}.A_{\mathrm{F}}.\rho.v^2}{2}\right) + (M.g.\sin\alpha) + (M.\delta.a)\}.v \quad (64)$$

$$P_{\mathrm{TR}} = \{(C_{\mathrm{r}}.M.g) + \left(\frac{C_{\mathrm{D}}.A_{\mathrm{F}}.\rho.v^2}{2}\right) + (M.g.\sin\alpha) + (M.\delta.a)\}.v \quad (65)$$

In (65), P_{TR} denotes the tractive power at the wheels.

During the study, it's only considered LDVs with IC engines. Therefore, the brake power generated by the IC engine P_{b} can be determined using Equation (66). The brake power is the aggregation of the tractive power, P_{TR} and the auxiliary power, P_{Aux} as stated in (66). Then brake thermal efficiency is determined using Equation (67).

$$P_{\mathrm{b}} = P_{\mathrm{TR}} + P_{\mathrm{Aux}} \quad (66)$$

$$\eta_{\mathrm{BT}} = \frac{3.6*10^3}{q_c*BSFC} \quad (67)$$

The instantaneous $BSFC$ value can be determined using Equation (68). In Equation (68), n_{r} denotes the number of cycles for one power stroke, n_{c} denotes the number of cylinders of the IC engine, v_{d} denotes the cylinder capacity, p_{me} denotes the instantaneous mean effective pressure and ω denotes the angular speed of the engine.

$$BSFC = 3.6 * 10^9 \frac{2*pi*n_r*\dot{m_{f[n]}}}{n_c v_d p_{me} \omega} \quad (68)$$

Let's look at the tractive power requirement P_{TR} as determined in Equation (69) pertaining to the tractive load requirement:

$$P_{\mathrm{TR}} = M.C_{\mathrm{r}}.g.v + 0.5.\text{Þ}.C_{\mathrm{D}}.A_{\mathrm{F}}.v^3 + m.v.\dot{v} + m.g.\sin\alpha.v \quad (69)$$

In Equation (69), each of the tractive load term is multiplied by v, which is the linear instantaneous velocity of the vehicle in order to determine the tractive power

requirement. A test vehicle is assumed with the following technical and operational specifications to determine the tractive power requirement for a sample calculation.

Table 24: Initialization of parameters for tractive power calculation

Attribute	Value
Coefficient of Rolling Resistance (C_{r}.)	0.012
Frontal Area (A_{f})	1.868 m^2
Mass (m)	730 kg
Gravitational Acceleration (g)	9.81 m/s^2
Coefficient of Aerodynamic Drag (C_{D})	0.32
Density of Air (Þ)	1.225 kg/m^3
The Road Gradient (α)	30^0

$$P_{\mathrm{TR}} = (85.94v + 0.37v^3 + 3580.65v + 730\dot{v}v) \tag{70}$$

$$P_{\mathrm{TR}} = f(v) \tag{71}$$

The tractive power is expressed as a function of v. In order to test the algorithm, a Heaviside step function as well as a Unit ramp function are given as inputs.

Next, in determining the auxiliary power component i.e., P_{Aux} in Equation (72), air-conditioning power demand and alternator power demand which closely account for 97% of total auxiliary power demand. The other engine auxiliaries viz. mechanical water pump, and power steering pump are approximately accountable for 3% of the total engine auxiliary power demand. Therefore, the auxiliary power demand, P_{Aux} can be determined as stated in Equation (72).

$$P_{\mathrm{Aux}} = P_{\mathrm{AC}} + P_{\mathrm{Alternator}} + P_{\mathrm{Water\,pump}} + P_{\mathrm{Steering}} \tag{72}$$

The air-conditioning load can be determined as in Equation (73) as stated below:

$$P_{\mathrm{AC}} = P_{\mathrm{met}} + P_{\mathrm{rad}} + P_{\mathrm{amb}} + P_{\mathrm{eng}} + P_{\mathrm{exh}} + P_{\mathrm{ven}} \tag{73}$$

In Equation (73), P_{met} denotes the metabolic heat load, P_{rad} denotes the radiation heat load, P_{amb} denotes the ambient load, P_{eng} denotes the engine load, P_{exh} denotes the exhaust load and P_{ven} denotes the ventilation load. When determining P_{met}, the Equations from (15) to (23) are referred. Using Equations (24) and (25) the result for P_{met} can be determined as stated in Equation (74).

$$P_{\text{met}} = 447\ W \tag{74}$$

The radiation heat load, P_{rad} can be determined by using Equations from (35) to (41). The result for P_{rad} can be depicted as shown in Equation (75).

$$P_{\text{rad}} = 2430\ W \tag{75}$$

The ambient heat load, P_{amb} can be determined by using Equations from (26) to (33). The result for P_{amb} can be determined as stated in Equation (76).

$$P_{\text{amb}} = 500\ W \tag{76}$$

The engine heat load, P_{eng} can be determined by using Equations from (47) to (49). The result for P_{eng} can be determined as stated in Equation (77).

$$P_{\text{eng}} = 538\ W \tag{77}$$

The exhaust heat load, P_{exh} can be determined by using Equations from (43) to (45). The result for P_{exh} can be determined as stated in Equation (78).

$$P_{\text{exh}} = 430\ W \tag{78}$$

Finally, the ventilation heat load, P_{ven} can be determined using Equations from (51) to (57). The result can be shown as stated in Equation (79).

$$P_{\text{ven}} = 120\ W \tag{79}$$

Thus, the total air-conditioning heat load, P_{AC} can be determined using the summation of the above stated six types of heat loads. The result is shown in Equation (80).

$$P_{\mathrm{AC}} = 4{,}465\ W \tag{80}$$

Then the other engine auxiliary loads viz., the alternator, the coolant pump and the mechanical power steering pump are determined using Equations from (59) to (62). The alternator load is stated in Equation (81), whereas the coolant pump load and the mechanical power steering pump loads are stated in Equations (82) and (83) respectively.

$$P_{\mathrm{Alternator}} = 2{,}800\ W \tag{81}$$

$$P_{\mathrm{Water\ pump}} = 185\ W \tag{82}$$

$$P_{\mathrm{Steering}} = 175\ W \tag{83}$$

The total average auxiliary engine load, P_{Aux} can be determined as 7,625.10 W, which is utilized in calculating the mass fuel flow rate.

When determining the fuel consumption using the instantaneous mass fuel flow rate, the calculation is based on specific $BSFC$ maps.

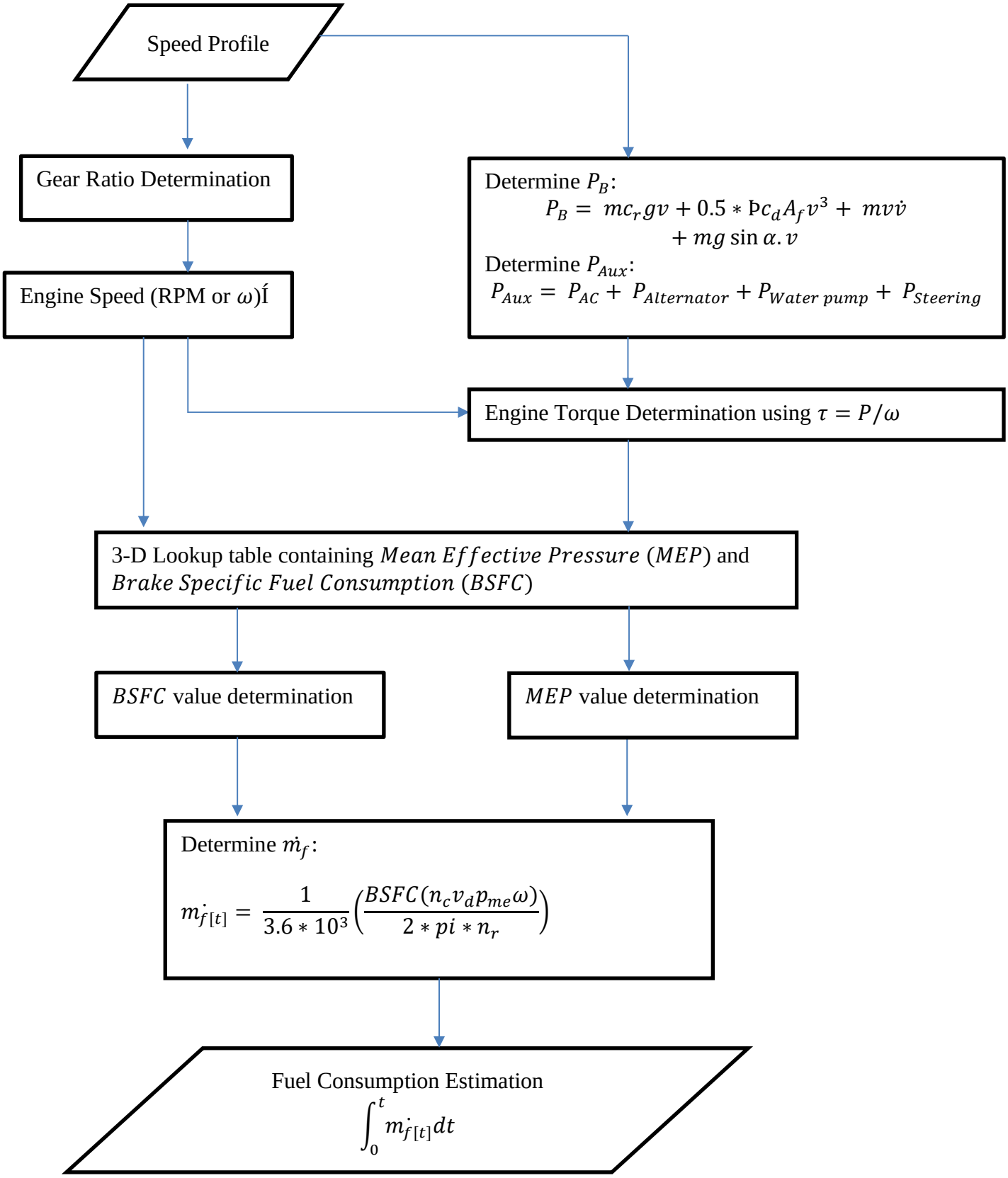
Speed Profile
Gear Ratio Determination
Engine Speed (RPM or ω)Í
Determine P_B:
$P_B = mc_r gv + 0.5 * Þc_d A_f v^3 + mv\dot{v} + mg \sin \alpha . v$
Determine P_{Aux}:
$P_{Aux} = P_{AC} + P_{Alternator} + P_{Water\ pump} + P_{Steering}$
Engine Torque Determination using $\tau = P/\omega$
3-D Lookup table containing $Mean\ Effective\ Pressure\ (MEP)$ and $Brake\ Specific\ Fuel\ Consumption\ (BSFC)$
$BSFC$ value determination
MEP value determination
Determine $\dot{m}_f$:
$\dot{m_{f[t]}} = \frac{1}{3.6 * 10^3}\left(\frac{BSFC(n_c v_d p_{me} \omega)}{2 * pi * n_r}\right)$
Fuel Consumption Estimation
$\int_0^t \dot{m_{f[t]}} dt$

Figure 34: Flow chart for the process of fuel economy estimation

- **Calculation for a Unit Ramp Function**

Assuming that, $v = \begin{cases} t; t > 0 \\ 0; else \end{cases}$ (86)

The gear ratios of a sample vehicle can be estimated as stated in (87).

$$e_n = \begin{cases} 2.79, & 0 < \mathrm{v} < 4.44 \\ 1.55, & 4.44 < \mathrm{v} < 6.66 \\ 1.43 & 6.66 < v < 15.55 \\ 1.00 & 15.55 < v < 24.44 \\ 0.50 & 24.44 < v < 28.88 \end{cases} \quad (87)$$

A three-dimensional lookup table is utilized to determine the instantaneous $BSFC$ values and subsequently the $\dot{m}_f$.

Table 25:BSFC Lookup Table

BSFC [B/kWh]	Engine torque [Nm]	15.6	31.2	46.8	62.4	78	93.6	109.2	124.8	140.4	156	171.6
	MEP [bar]	1.03	2.06	3.09	4.12	5.16	6.19	7.22	8.25	9.28	10.31	11.34
Engine speed [rpm]	500	612.2	442.7	370.8	331.2	306	313.2	302.4	324,0	288	288	288
	1000	612	403.2	336.6	307.8	284.4	286.2	282.6	284.4	288	288,0	288,0
	1500	612	406.8	345.6	306	280.8	262.8	254.5	246.6	252	288,0	288
	2000	594,0	396	334.8	300.6	275,4	259.2	244.8	244.8	248,4	262.8	288,0
	2500	558	381.6	320.4	284.4	266.4	246.6	244.8	244.8	244.8	255.6	288
	3000	522	365.4	311.4	279	262.8	255.6	248.4	244.8	244.8	259.2	288
	3500	468	340.2	288	280.8	277.2	267.5	259.2	248.4	248.4	262.8	288
	4000	522	356.4	317.5	304.2	282.6	275.4	262.8	253.8	262.8	266.4	288
	4500	540	392.4	351.4	316.8	293.4	279	271.8	270	272.9	275,4	288
	5000	684	460.8	378	333	306	284.4	283.3	279	283	284.4	288
	5500	756	511.2	421.2	365.4	327.6	295.2	298,8	295.2	291.6	289.8	288
	6000	756	529.2	432	374.4	334.8	313.2	298.8	295.2	291.6	288	288

The respective $\dot{m}_f$ values are determined using the instantaneous $BSFC$ values from Table 25. The $BSFC$ map which is portrayed in Table 25 is pertaining to a 4-stroke, 4-cylinder vehicle with a 1.9 litre engine capacity with a cylinder bore size of 82 mm and a piston stroke of 90 mm.

Assuming the insertion of a unit ramp speed function for the driving cycle test, the below tractive power formula can be determined as stated in Equation (88).

$$P_{TR} = (85.94t + 0.37t^3 + 3580.65t + 730t) \quad (88)$$

When $t = 1$ for the specific test vehicle, P_{TR} value can be determined as stated in Equation (89).

$$P_{TR} = 4396.96\ W \tag{89}$$

Using the fundamental formula of $P = \tau\omega$, the instantaneous τ value can be determined.

$$\tau_{(t)} = \frac{P_{b(t)}}{\omega_{(t)}}$$

The τ value for $t = 1$,

$$\tau_{(1)} = \frac{P_{b(1)}}{\omega_{(1)}}$$

$$N_{(1)} = 1440 \text{ RPM}$$

As of Equation (68),

$$P_{b(1)} = P_{TR(1)} + P_{Aux}$$

$$P_{b(1)} = 4396.96 + 7{,}625.10$$

$$P_{b(1)} = 12022.06\ W$$

The respective torque value, i.e., $\tau_{(1)}$ can be determined as stated in Equation (90).

$$\tau_{(1)} = \frac{(12022.06*60)}{(2*3.142*1440)}$$

$$\tau_{(1)} = 79.71\ Nm \tag{90}$$

When referring to the Table 25, approximated values for engine speed is taken as 1500 RPM and engine torque is taken as 78.00 Nm. Thus, the corresponding mean effective pressure value is obtained as 5.16 bar for the said engine operating point. Consequently, the respective BSFC value is obtained from the 3-D lookup table as 280.8 g/kWh.

Thus, the mass fuel flowrate, i.e., $\dot{m_f}$ can be determined using Equation (70).

$$BSFC = 3.6 * 10^9 \frac{2*pi*n_r*\dot{m_{f[n]}}}{n_c v_d p_{me} \omega}$$

When substituting to Equation (70), $n_r = 2, n_c = 4, v_d = 475\ cm^3$, $p_{me} = 5.16\ bar$ and $\omega = 2\pi N/60$, $N_{(1)}(engine\ speed) = 1500$, $BSFC = 280.8\ g/kWh$

$$\dot{m_{f[n]}} = \frac{(BSFC) n_c v_d p_{me} \omega}{3.6*10^9*2*pi*n_r} \tag{91}$$

$$\dot{m_{f[1]}} = 1.34 * 10^{-3} \frac{kg}{s} \; or \; 1.34 \frac{g}{s}$$

The brake thermal efficiency at $t = 1$, can be determined using Equation (69):

$$\eta_{BT} = \frac{3.6*10^3}{q_c * BSFC}$$

Substituting $BSFC = 280.8 \frac{g}{kWh}$, $q_c = 46.4 \frac{MJ}{kg}$ into (69):

$$\eta_{BT(1)} = \frac{3.6*10^3}{q_c * 280.8} * 100\%$$

$$\eta_{BT(1)} = 27.63\%$$

Thus, for the said engine operating point at $t = 1$, the mass fuel flowrate and the corresponding brake thermal efficiency values can be determined.

Using this approach, the fuel consumption of a given vehicle can be determined when the specific $BSFC$ map is provided. Similarly, the instantaneous fuel flowrate values are determined for the entire driving cycle.

4. RESULTS AND VALIDATION

4.1 Results and validation of the driving cycles developed for 2W and 3W

The scores of the highest two candidate driving cycles for both urban and extra-urban phases have been portrayed in Table 30. The opted candidate cycle for the urban phase has a CSI score of 4.5489 whereas that of the extra-urban phase lies at 4.8087. The representative driving cycles for urban and extra-urban phases spanning 641 s and 574 s, respectively, are shown graphically in Figure 35 and Figure 36.

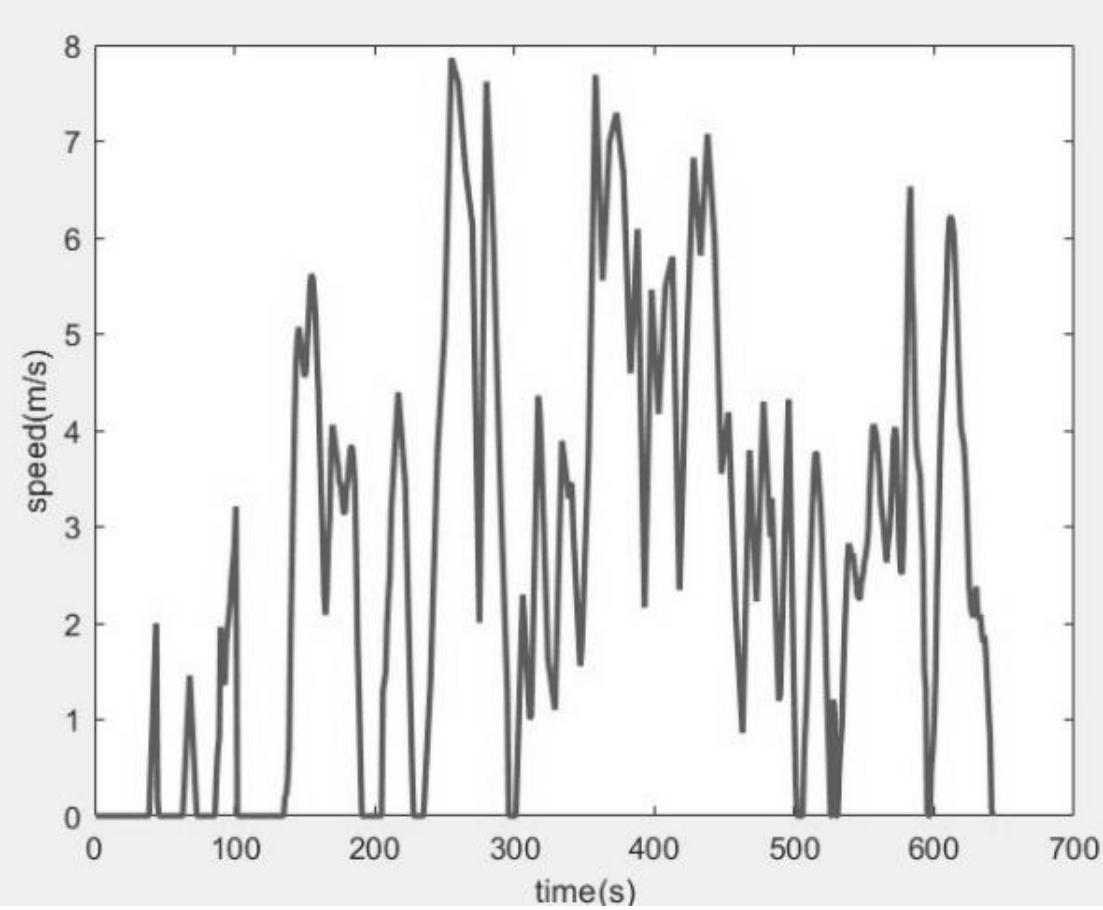

Figure 35: Representative Urban Driving Cycle.

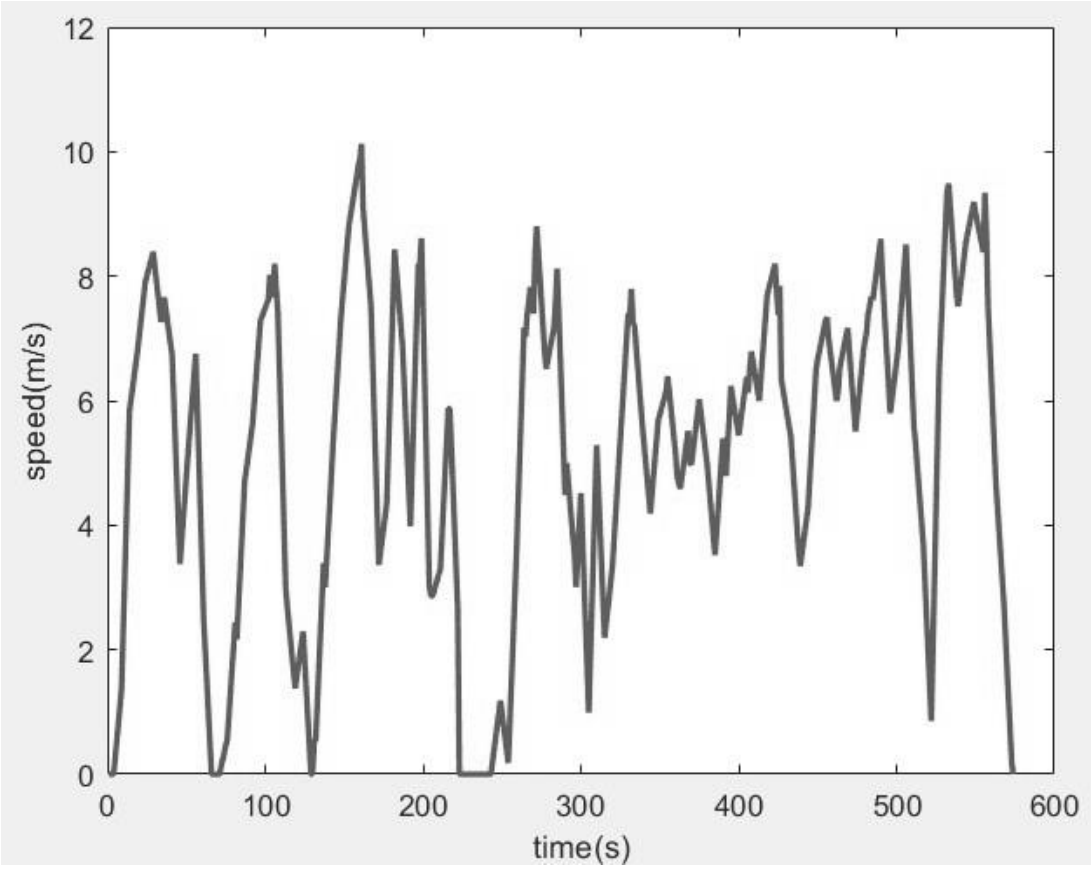

Figure 36 : Representative Extra-Urban Driving Cycle.

Figure 36 portrays the combined driving cycle which combines both the urban and extra-urban phases of the driving cycle. The total driving cycle spans for 1215 s. The properties of the representative driving cycle in terms of five selected CPs are depicted in Table 27. Finally, to evaluate the quality of fit of the representative driving cycle to the population data set, Speed Acceleration Frequency Distribution (SAFD) is determined for the representative driving cycle as well as for the population data set.

Table 26: Selection of Urban and Extra-Urban Representative Cycles using CSI scores of CPs.

Attribute	Average Speed (CP_1)	Average Running Speed (CP_2)	Average Acceleration (CP_3)	Average Deceleration (CP_4)	Percentage Idle Time (CP_5)	CSI Score (out of 5)
SI of the Representative Urban Cycle	0.8953	0.9379	0.8657	0.8766	0.9732	4.5489
SI of the Representative Extra-Urban Cycle	0.9864	0.9875	0.9296	0.9964	0.9086	4.8087

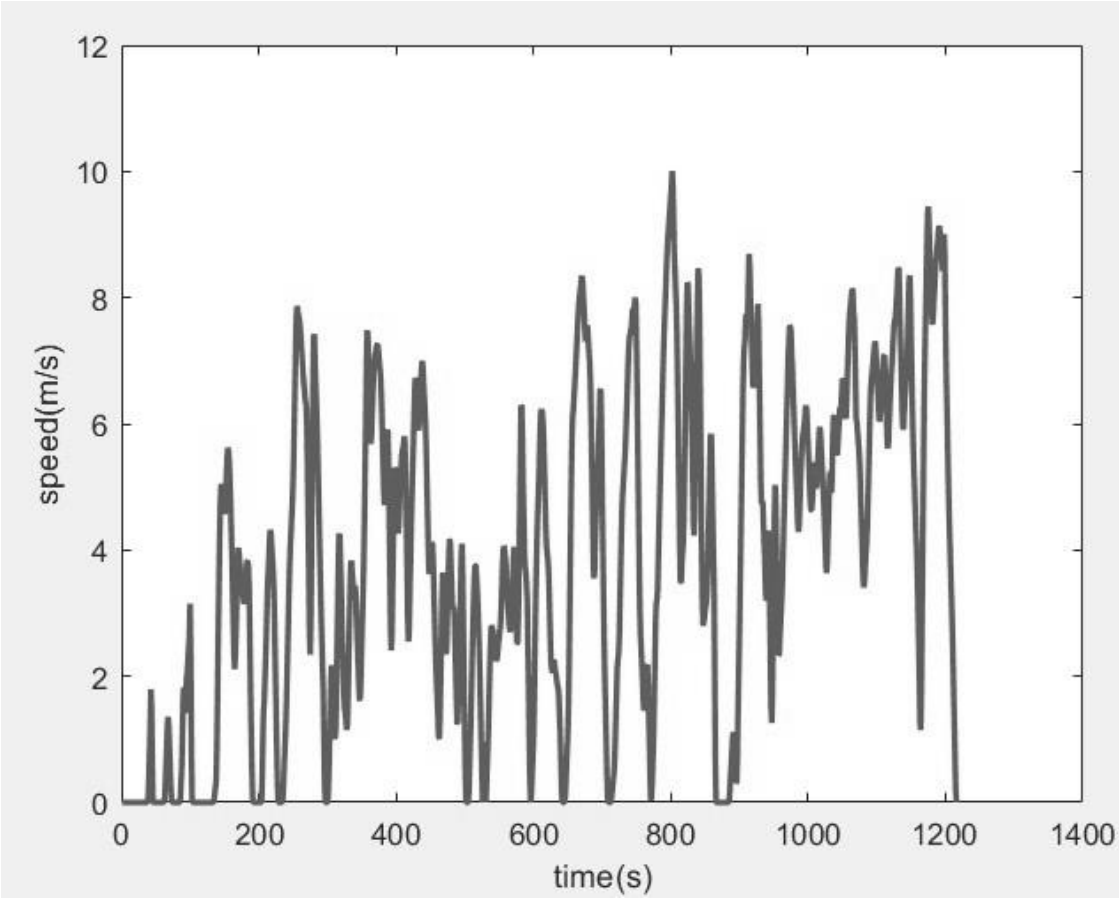

Figure 37 : Representative Driving Cycle.

Table 27: CP values of the Representative Driving Cycle

Characteristic Parameter	Value
Average Speed	3.87 m/s
Maximum Speed	10.01 m/s
Average Running Speed	4.44 m/s
Average Acceleration	0.33 m/s^2
Average Deceleration	-0.36 m/s^2
Idle Time Percentage	12.75%

Then a comparison between the SAFDs of the representative driving cycle and the population data set is performed. Three plots have been developed: one for the speed-frequency distribution of the population data set, which is depicted by Figure 38, then the speed-frequency distribution of the representative driving cycle which is depicted by Figure 39 and Figure 40 portrays the acceleration-frequency distributions of both the population data set and the representative driving cycle graphed together. As shown in Figure 38 and Figure 39, the trends of the representative driving cycle and the population data set for both speed-frequency distributions look similar. Moreover, the trends of the acceleration-frequency distribution of the population data set and the representative driving cycle remain quite similar. When analyzing the speed-frequency distributions, it can be noted that the highest number of speed-frequency is noted at zero speed, i.e., the idle speed. Similarly, when evaluating the acceleration-frequency distributions, the highest acceleration frequency is recorded at the origin, denoting the idle and cruising phases. Due to the similarities in SAFD trends, the developed representative driving cycle can be validated against the population data set. Therefore, the quality of fit of the representative driving cycle remains higher.

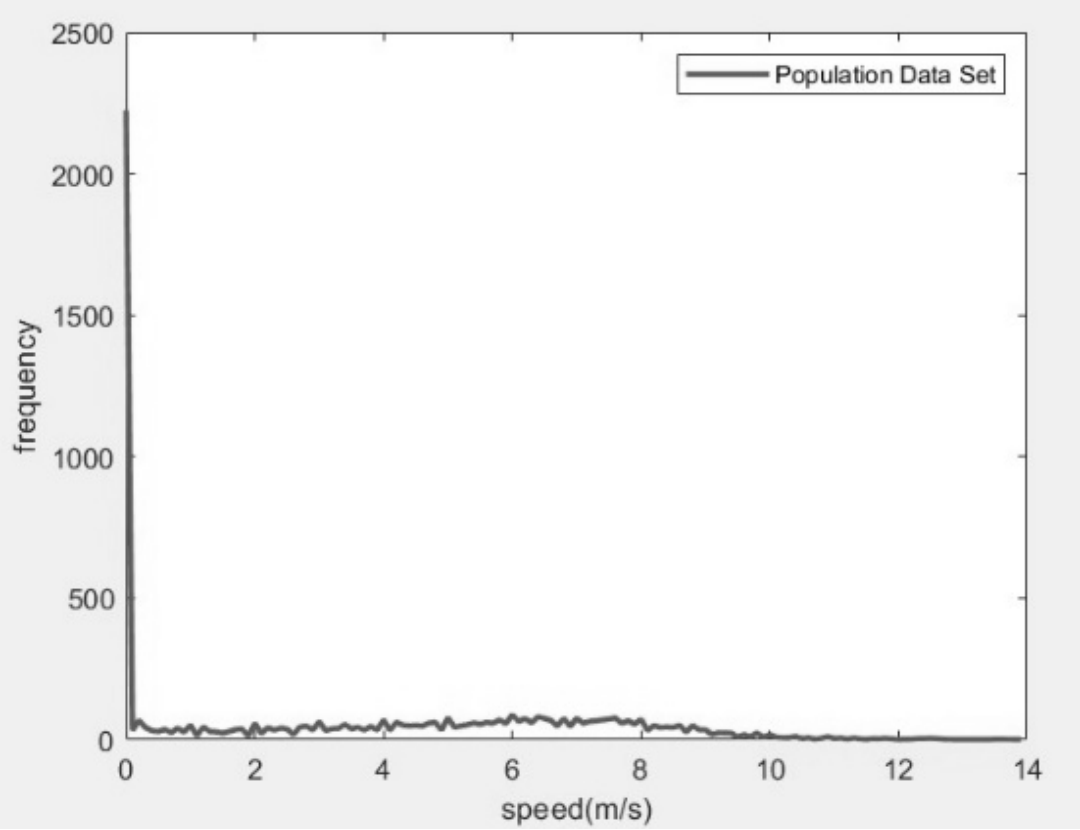

Figure 38 : Speed-Frequency Distribution of the Population data set.

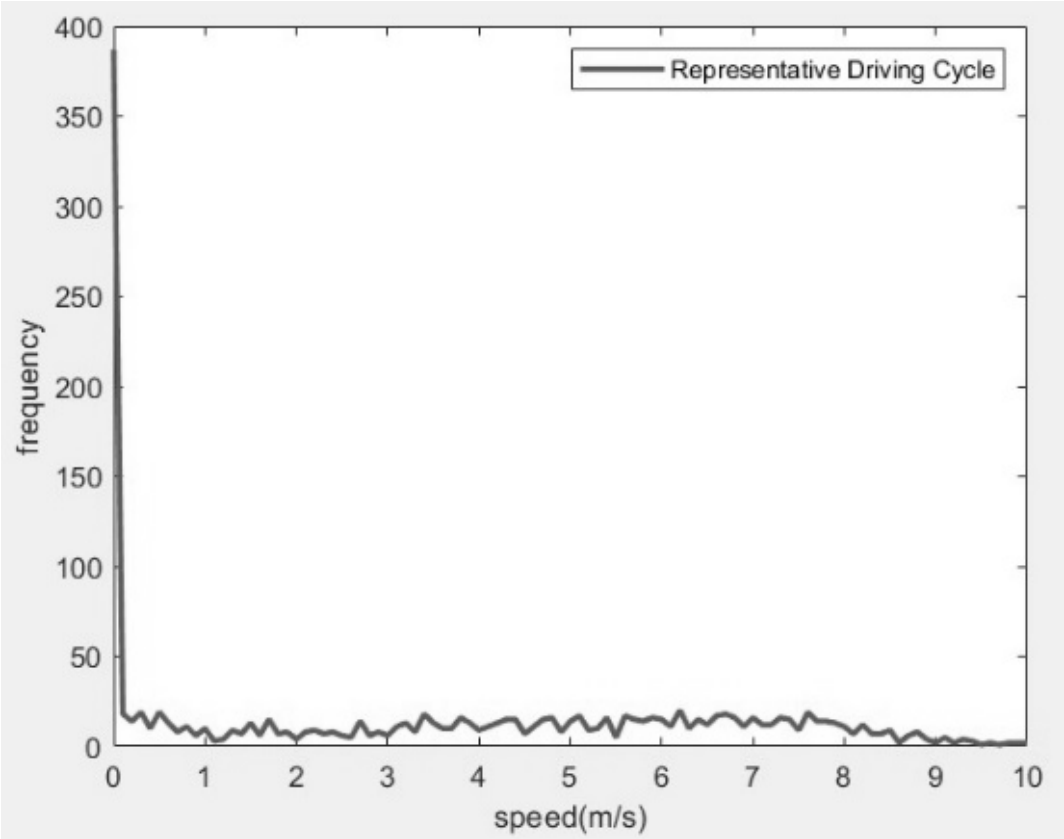

Figure 39 : Speed-Frequency Distribution of the Representative Driving Cycle.

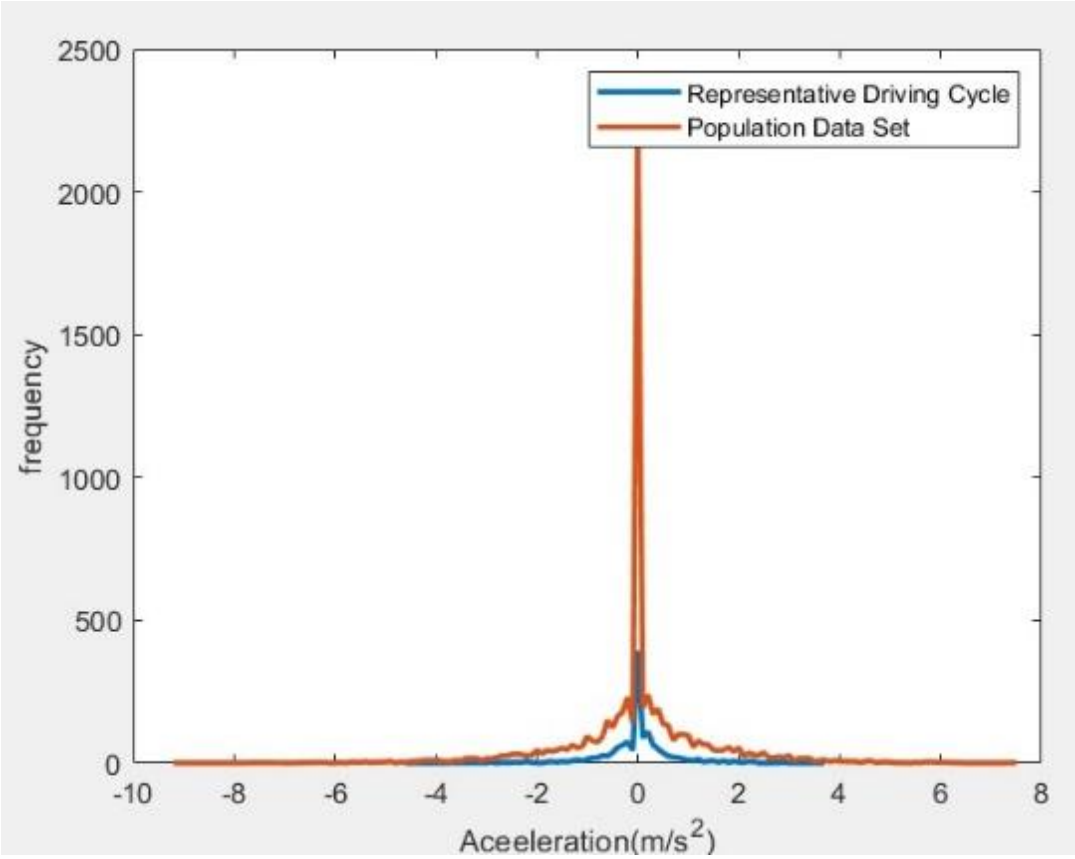

Figure 40 : Comparison of the Graphs for Acceleration-Frequency Distributions.

During the initial phase of the study, the necessity of a driving cycle construction, specifically for motorcycles, has been emphasized citing the literature. As a main deliverable of the study, a driving cycle is being developed for motorcycles comprising two-wheeled motorcycles and three-wheeled motor tricycles, in the geographic scope of the Colombo Metropolitan Area. The developed driving cycle comprises two phases, i.e., the urban phase and the extra-urban phase. Using five CPs, a representative driving cycle has opted from a pool of candidate driving cycles. The opted representative driving cycle portrays the characteristics, viz., an average speed of 3.87 m/s, an average running speed of 4.44 m/s, an average acceleration of 0.33 m/s^2, an average deceleration of -0.36 m/s^2, an idle time percentage of 12.75% and a time length of 1215 s. Having an average speed of 3.87 m/s depicts the fact that the level of congestion within the Colombo Metropolitan Area remains quite high. The

developed representative driving cycle can be utilized for research purposes on fuel consumption quantification as well as emission characterization.

4.2 Results and validation of the driving cycles developed for 4W.

The scores of the highest two candidate driving cycles for both urban and extra-urban phases have been portrayed in Table 28. The candidate cycle opted for the urban phase has a CSI score of 4.5947 whereas that of the extra-urban phase lies at 4.8846. The representative driving cycles for urban and extra-urban phases spanning 1004 s and 495 s respectively are shown graphically in Figure 41 and Figure 42. The combined representative driving cycle is shown in Figure 43.

Table 28: Selection of Urban and Extra-Urban Representative Cycles using CSI scores of CPs.

Attributes	Average Speed (CP_1)	Average Running Speed (CP_2)	Average Acceleration (CP_3)	Average Deceleration (CP_4)	Percentage Idle Time (CP_5)	CSI Score(out of 5)
SI of the Representative Urban Cycle	0.8979	0.9177	0.9499	0.9333	0.8958	4.5947
SI of the Representative Extra-Urban Cycle	0.9968	0.9719	0.9799	0.9981	0.9378	4.8846

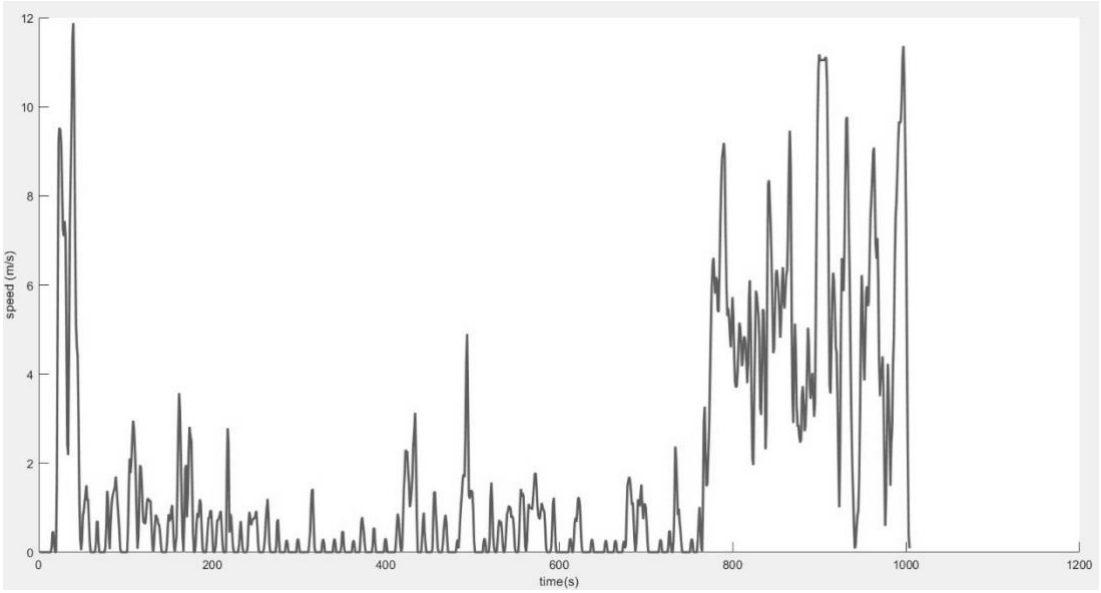

41

Figure 41 : Representative Urban Driving Cycle for 4W.

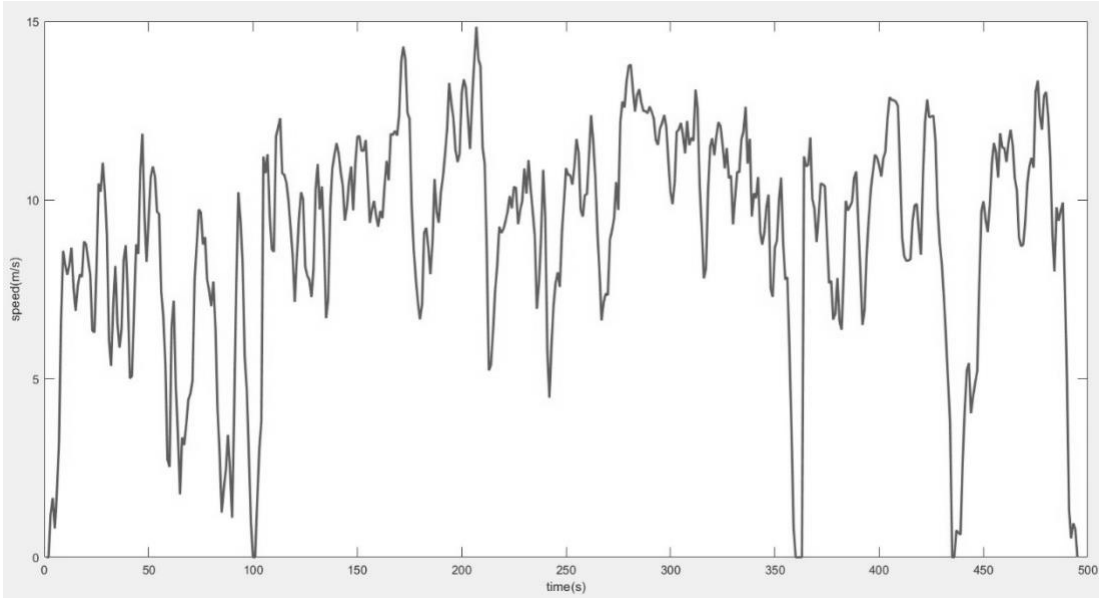

Figure 42 : Representative Extra Urban Driving Cycle for 4W.

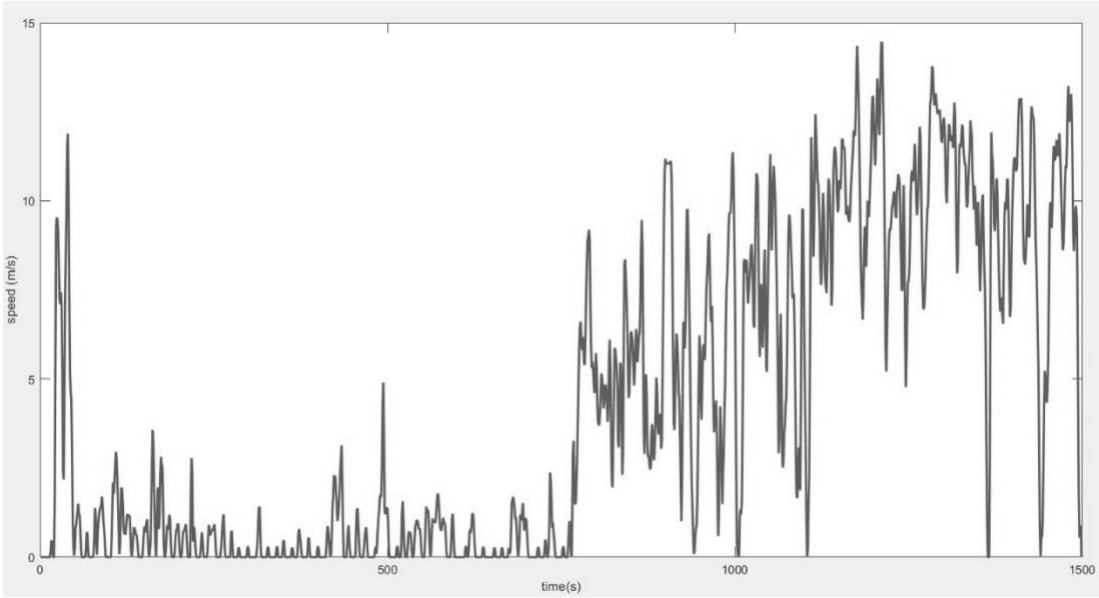

Figure 43 : Representative Driving Cycle for 4W.

Table 29: CP values of the representative driving cycle

Characteristic Parameter	Value
Average Speed	4.83 m/s
Maximum Speed	14.47 m/s
Average Running Speed	5.38 m/s
Average Acceleration	0.95 m/s^2
Average Deceleration	-0.97 m/s^2
Idle Time Percentage	22.35%

As performed in 2W and 3W driving cycle validation, in 4W driving cycle validation too, speed frequency distributions are determined for both representative driving cycle and for the population set. Both the plots in Figure 44 and Figure 45 depict a similar kind of trend which suggests that the speed frequency distribution of the representative driving cycle properly reflects that of the population set.

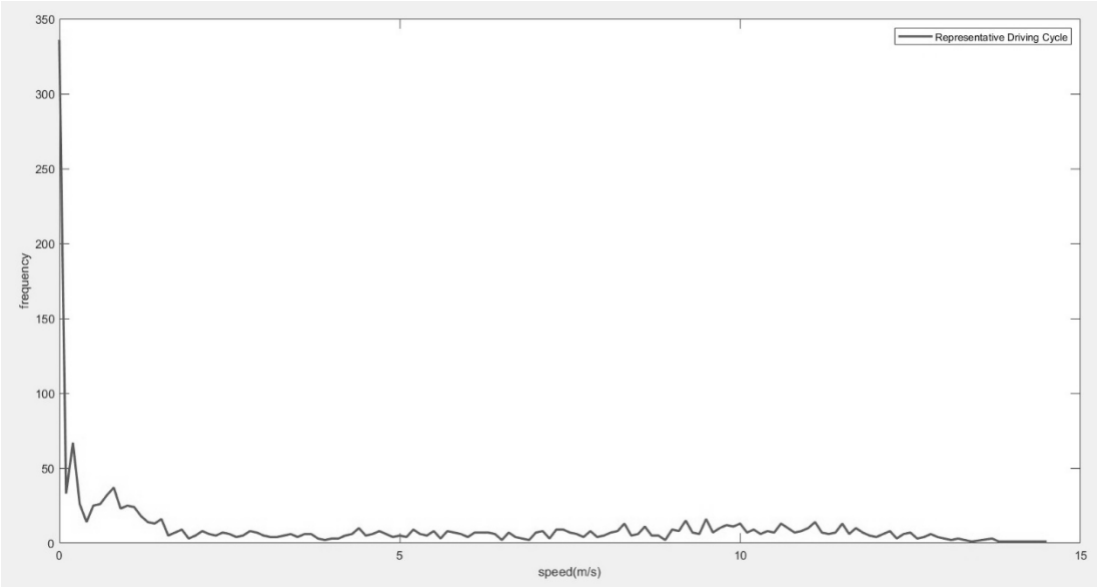

Figure 44 : Speed Frequency Distribution for the representative driving cycle.

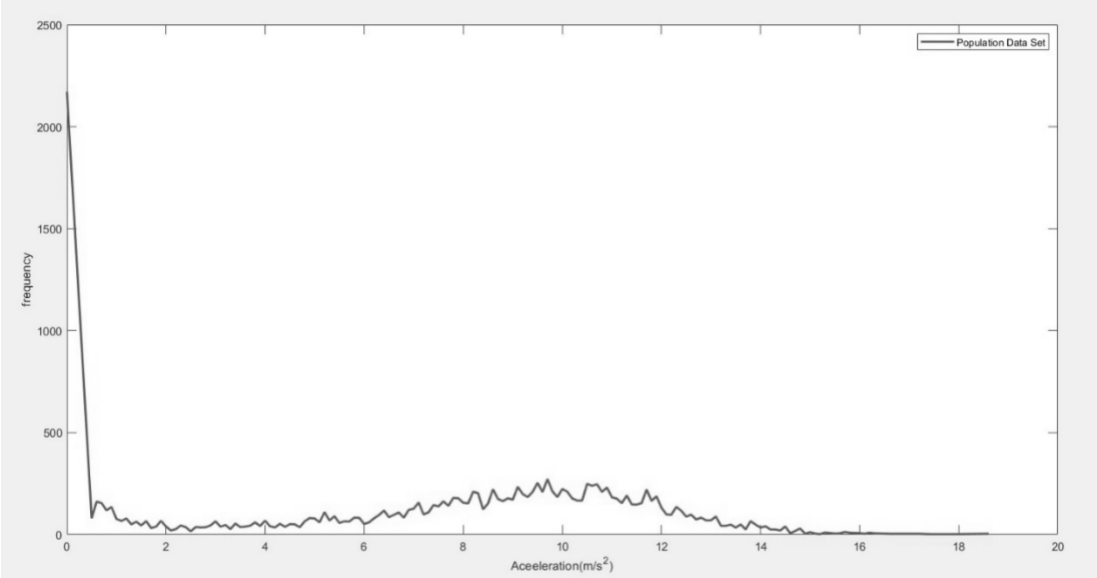

Figure 45 : Speed Frequency Distribution for the population data set.

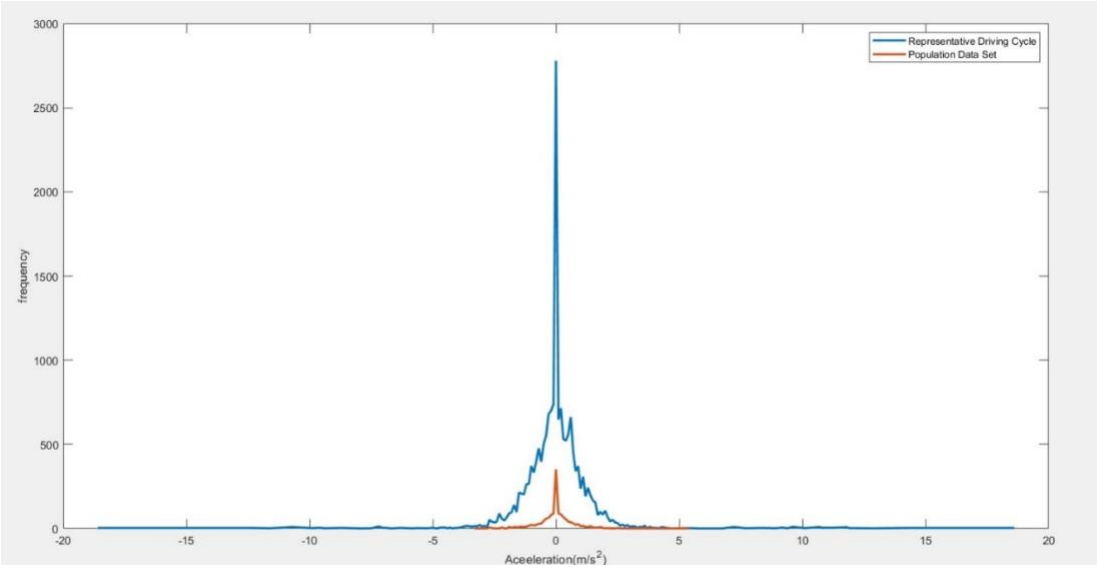

Figure 46: Speed vs Time (Step Input).

: Acceleration Frequency Distribution for the population data set and the representative driving cycle.

The acceleration frequency distributions for both the population set and the representative driving cycle are portrayed in Figure 46. It's lucid the fact that both the plots adhere to a similar trend which suggests that the representative driving cycle reflects the acceleration distribution that's visible in the population data set.

4.3 Representative driving cycles' validation against the regional driving cycles.

In this chapter, the developed representative DCs on the 2W/3W and 4W are benchmarked against the regional DCs and World Harmonized Light Vehicle Test Procedure (WLTP). The benchmarking happens to pertain to the characteristic parameters (CPs) of each DC. The regional DCs opted for the benchmarking of representative DCs for 4W are New European Driving Cycle (NEDC), United States Federal Test Procedure (US06 FTP) and Japanese JP 10-15 Driving Cycle. Moreover, WLTP is used to compare the representative cycles against the harmonized driving cycle. The statistics are shown in Table 30.

Table 30: Comparison of CPs of the representative DC against regional DCs for 4W.

CPs	Representative DC	NEDC	US06	JP 10-15	WLTP
Duration (s)	1499	1180	596	660	1800
Distance (m)	6,261	11017	12894	4165	23266
Average Speed (m/s)	4.83	9.33	21.64	6.31	12.92
Maximum Speed (m/s)	14.47	33.36	35.81	19.47	36.47
Average Running Speed (m/s)	5.38	11.73	22.12	8.54	14.86
Average Acceleration (m/s^2)	0.95	0.53	0.54	0.37	1.35
Average Deceleration (m/s^2)	-0.97	-0.72	0.57	-0.39	-1.70
Idle Time Percentage %	22.35	20.42%	2.18	26.06	13.40

When comparing against the other regional driving cycles, it's visible the fact that the average speed of the developed Colombo driving cycle is much lower than the other DCs. The main 3 DCs that are used for the comparison are from developed regions/countries such as Europe, the United States and Japan. The arterial route network of the most congested cities of those regions accountable for greater average speeds, which in return reflects the improved level of service (LoS) of those regions. One of the major reasons for a lowered average speed in the Colombo Metropolitan Area can be considered as the lower LoS due to lower standards of arterial road infrastructure and higher peak hour traffic volume. The quality of the route network, especially on the standard of the infrastructure in the metropolitan is reflected by the lower maximum speed of the representative cycle, i.e., 14.47 m/s which is comparatively lower than that of other cycles compared here. When considering the idle time percentage, the representative driving cycle seems to have quite the identical idle time percentage as NEDC. The CPs of US06 FTP are having major discrepancies

with those of the developed representative driving cycle and the other driving cycles compared here since the US06 driving cycle comprises a higher portion of expressway and freeway driving which eventually escalates the speed parameters of the US06 driving cycle.

The regional DC opted for the benchmarking of representative DCs for 2W/3W is World Harmonized Motorcycle Test Cycle (WMTC). The comparison is portrayed in Table 31.

Table 31: Comparison of CPs of the representative DC against WMTC for 2W/3W.

CPs	Representative DC	WMTC
Duration (s)	1215	1800
Distance (m)	4,707	28,920
Average Speed (m/s)	3.87	16.07
Maximum Speed (m/s)	10.01	34.81
Average Running Speed (m/s)	4.44	19.84
Average Acceleration (m/s^2)	0.33	0.58
Average Deceleration (m/s^2)	-0.36	-0.70
Idle Time Percentage %	12.75	8.93

When comparing the representative DC for 2W and 3W with the WMTC, it's conspicuous that major discrepancies on the speed parameters can be seen. The maximum speed of the representative DC lies as low as 10.01 m/s whereas that of WMTC lies at 34.81. The major reason for this is that when developing WMTC, more data has been acquired from the European and American regions where they do allow especially the 2W to travel on freeways. A similar discrepancy can be seen in acceleration parameters as well.

4.4 Results and validation of the theoretical model developed.

The equations from (63) to (87) are scripted in Python using the Google-Colab development environment. The developed algorithm is provided with different speed inputs in terms of arrays to determine the consistency of the output. As shown below, the Heaviside Step function and the Ramp function are provided as speed input arrays and the corresponding output fuel economy array is plotted against time. Moreover, the engine speed (RPM) is also plotted against the time to depict the changes owing to gear shifts.

<u>When provided with a Step Speed Input:</u>

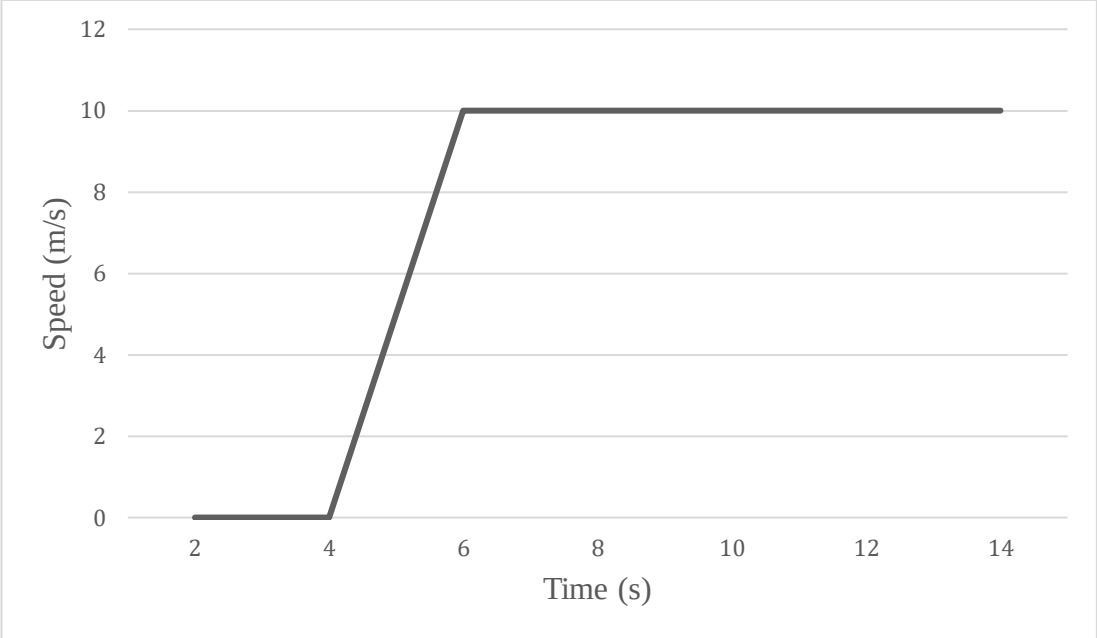

Figure 47 : Speed vs Time (Step Input).

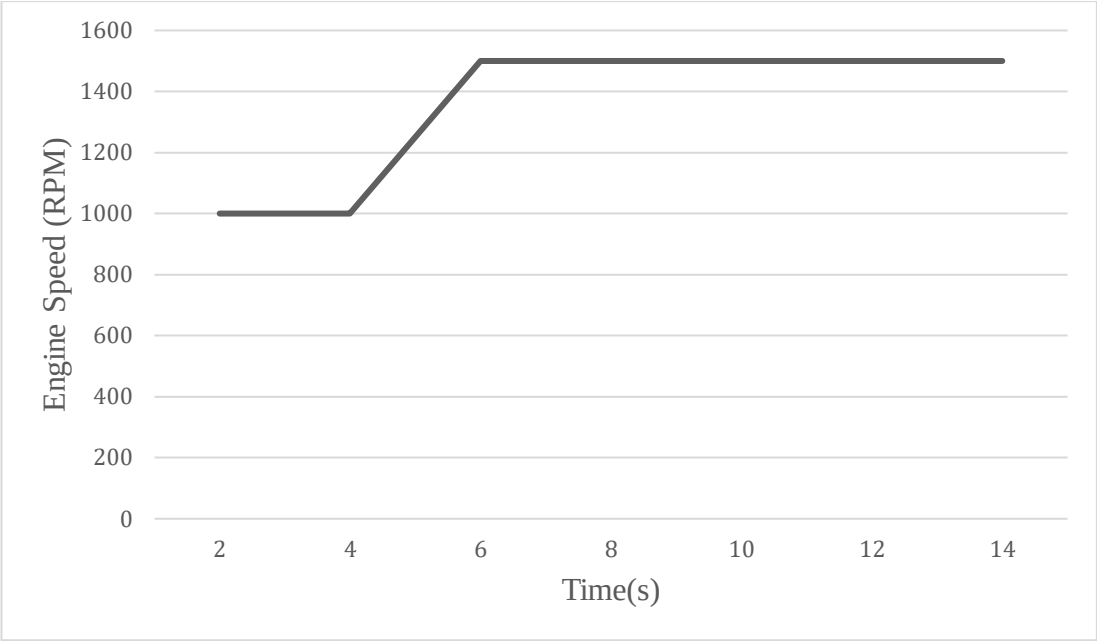

Figure 48 : Engine Speed vs time (when step input is provided).

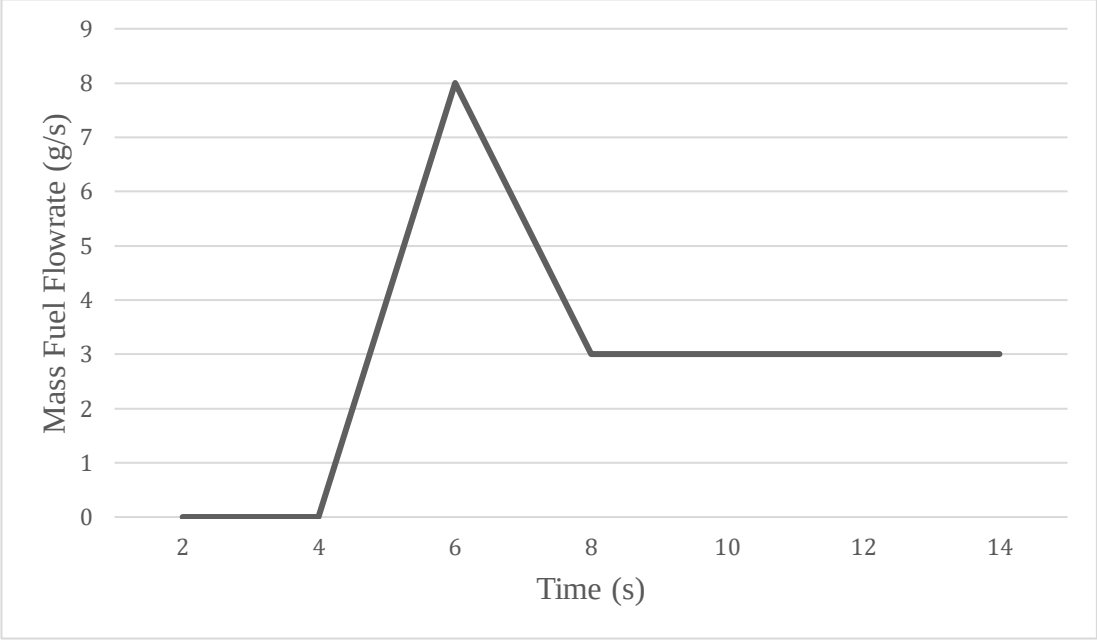

Figure 49: Mass fuel flowrate output (when step input is provided).

When provided with a Ramp Speed Input:

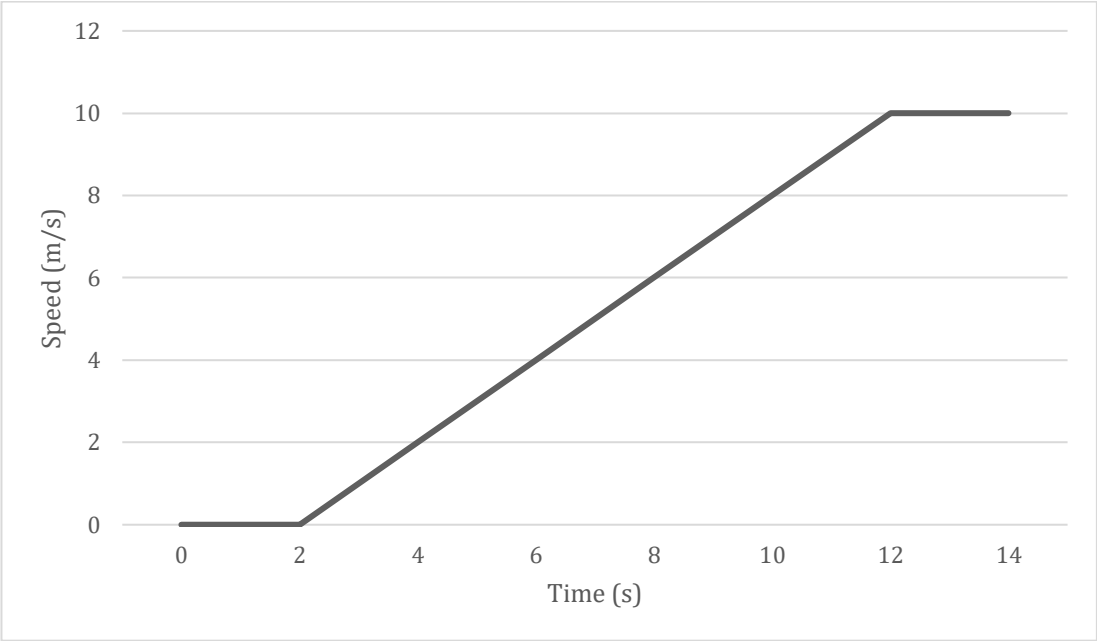

Figure 50: Speed vs Time (Ramp Input).

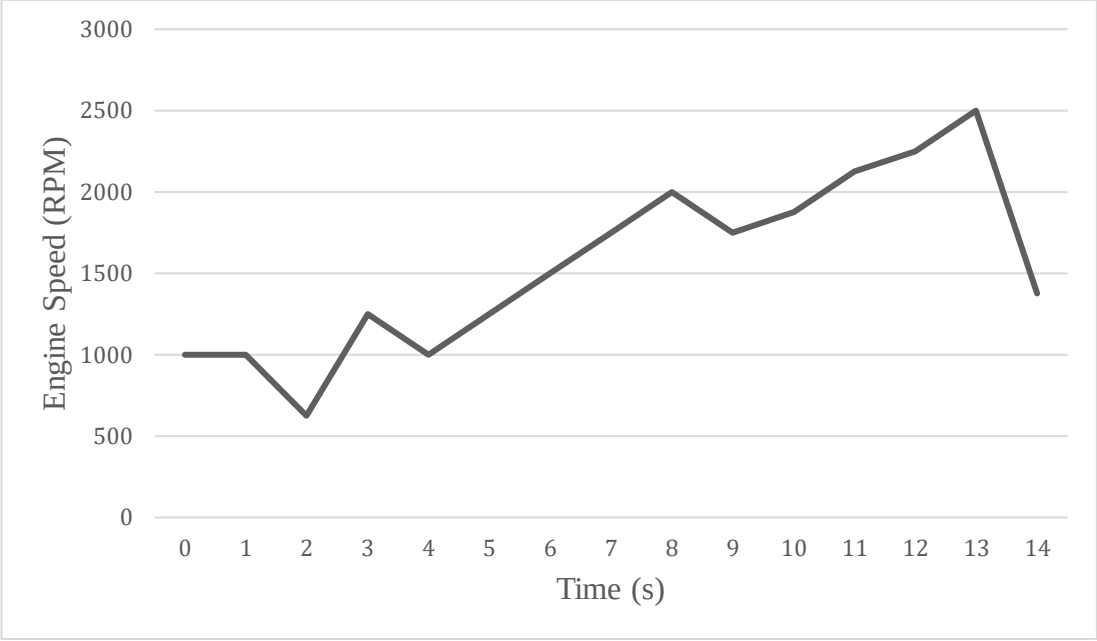

Figure 51: Engine Speed vs time (when ramp input is provided).

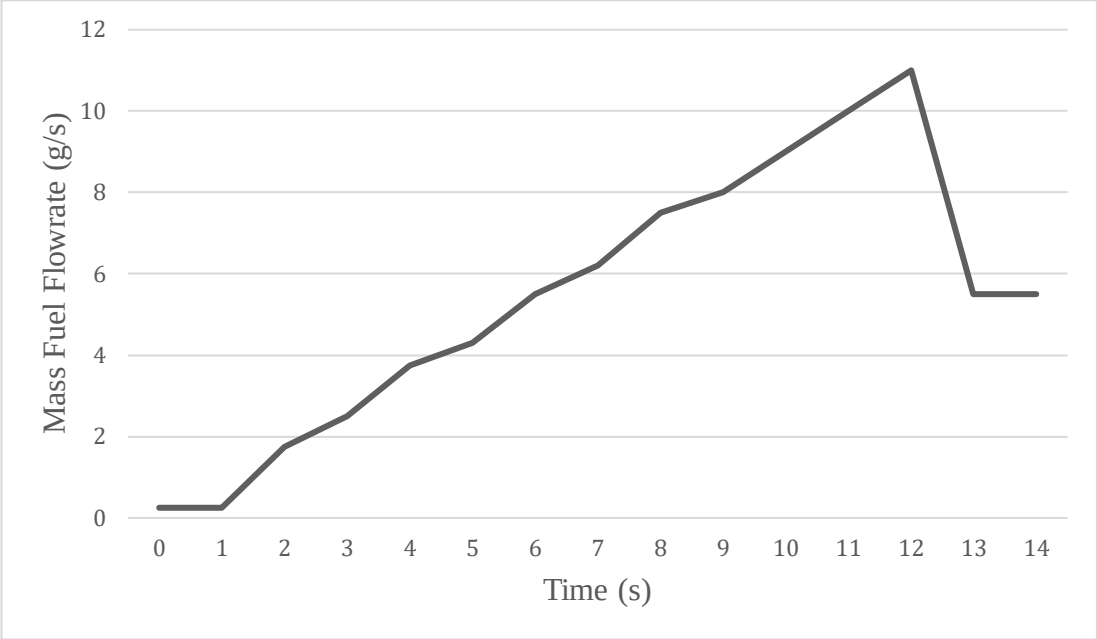

Figure 52 : Mass fuel flow rate output (when ramp input is provided).

When analyzing both the step function output and the ramp function output on fuel economy, a transient phase followed by a steady state phase can clearly be seen. The reason for such a transient phase may be the sudden gear shift which is apparent during the transient period as well as the increase in the speed profile. Subsequently, the determined fuel consumption will be validated against the chassis dynamometer-tested real values for the same driving cycle. Any discrepancies between the tested values and the theoretically estimated values will be used for the revisions of the model accordingly.

4.5 Results of simulation tests: Simulation-based validation

In order to further validate the model, a simulation study has been conducted using FASTSim™ simulation software. The simulation tool that was used during the study is "FASTSim" which stands for "**F**uture **A**utomotive **S**ystems **T**echnology **Sim**ulator" which is developed by NREL (National Renewable Energy Laboratory, US). The other possible alternative simulator can be cited as the "ADVISOR" - "**AD**vanced **V**eh**I**cle **S**imulat**OR**", which is also another development of NREL. FASTSim is considered to

be the successor of ADVISOR software and the latter was first developed in 1994 and the final version of it was released in 2004. ADVISOR comes in as a plug-in to the graphical, object-oriented programming language of Simulink/ MATLAB from MathWorks, Inc., whereas FASTSim comes in two major forms a Python-based software and an excel-based software tool. The one that was chosen for the study is the latter one, i.e. the Excel-based. Unlike the ADVISOR which requires quite a lot of data points to analyze the powertrain characteristics, the same analysis can be performed using the FASTSim which produces very rapid estimates of vehicle efficiency, performance, cost, and battery life in conventional and advanced powertrain technologies. The capability of FASTSim over its predecessor is that it requires only a few publicly available vehicle parameters, such as peak power output of the engine and hybrid/electric components, vehicle mass, frontal area, and rolling resistance in order to model the powertrain characteristics [34]. When analyzing the strengths of FASTSim tool, it can be noted that it is the fastest to calibrate, requires a small amount of public vehicle information and is also suitable for large-scale simulation/evaluation of thousands of vehicle designs. When eyeing the limitations, it captures the most important factors for high-level comparisons but lacks detail for focused studies, yet the analysis capability of FASTSim is quite adequate for the study, hence it has been utilized as a simulation tool to model the powertrain performance characteristics viz. fuel consumption and emissions.

Five LDVs have been utilized for the simulation study as depicted in Table 36.

Table 32: List of LDVs selected for the simulation study.

Test Vehicle	Model	Engine Capacity	No. Cylinders	Year of Manufacture
1	Audi A3	1400 CC	4	2016
2	BMW 328d	2000 CC	4	2016
3	Toyota Corolla	1500 CC	4	2016
4	Toyota Camry	2000 CC	4	2016
5	Hyundai Elantra	1500 CC	4	2016

Table 33: Model output versus the simulated output

Test Vehicle	JP10			JP15			LA92			US06		
	Model Output (ml)	Simulated (ml)	Accuracy	Model Output (ml)	Simulated (ml)	Accuracy	Model Output (ml)	Simulated (ml)	Accuracy	Model Output (ml)	Simulated (ml)	Accuracy
1	36.82	33.67	90.17%	154.89	144.45	92.71%	1331.98	1240.44	92.63%	1211.56	1110.54	90.90%
2	48.16	43.83	90.16%	177.98	164.75	91.99%	1481.21	1380.64	92.78%	1239.89	1146.35	91.84%
3	46.13	41.8	89.61%	168.11	155.54	91.93%	1423.71	1320.48	92.14%	1217.43	1125.15	91.79%
4	54.19	49.25	89.91%	195.67	182.36	92.71%	1628.76	1517.52	92.61%	1339.72	1232.65	91.31%
5	49.82	45.39	90.22%	181.55	168.45	92.24%	1517.39	1410.28	92.43%	1312.76	1195.67	90.20%

Table 36 depicts the output fuel consumption determined from the theoretical model versus the output fuel consumption from the simulation study using FASTSim software tool. All the quantities are in milliliters. When analyzing the data portrayed in Table 36, it can conspicuously be seen the fact that the percentage accuracy converged to a certain band throughout the study. The experienced accuracy band spanned from 89.61% to 92.78%.

4.6 Validation against the manufacturers' test data.

In order to complete a two-way validation, another step for validation is adopted: i.e., the validation of the model tested data against the manufacturers' test data which are available in catalogues. Three vehicles have been used to do the validation under WLTP driving cycle. WLTP has been opted as the desired driving cycle since it represents the global context pertaining to driving behaviour. Moreover, most of the manufacturers' data is available w.r.t. WLTP test results.

Table 34: Model tested performance against the manufacturers' data.

Car No	Model (Engine Capacity)	WLTP tested (km/l)	WLTP model (km/l)	Percentage Accuracy
1	Mercedez Benz E200 W213 (2.0l)	11.91	11.59	97.24%
2	Toyota Corolla 2018 (1.2l)	14.70	13.89	94.17%
3	BMW 520i (2.5l)	14.28	15.11	94.51%

As portrayed in Table 37, three different models of motor cars have been tested for the validation purpose. A percentage accuracy band between 94.17% – 97.24% has been stated. This reflects that the developed theoretical model is having a considerable level of accuracy.

4.7 Results of driving cycle data tested on the developed model and the development of driving cycle conversion factors.

The developed theoretical model for fuel economy estimation is tested with different driving cycle data. The speed data from four different regional driving cycles along with the World Harmonized Light Vehicle Test Procedure is used to test the model. The developed 4W driving cycle for the Colombo Metropolitan Area is also among the regional driving cycles which are used for the testing of the model. The speed arrays are used as input data for the theoretical model and the used input speed arrays are shown in Appendix-III.

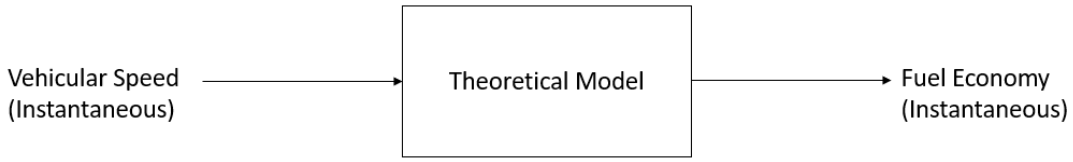

Figure 53 : Input – Output representation of the developed theoretical model.

As depicted in Figure 53, the theoretical model which is developed during the study can be provided with a specific driving cycle and the model outputs the corresponding instantaneous fuel consumption data along with the instantaneous engine speed (RPM) data (Refer Figure 34). Utilizing the output data streams of the model, average cycle

fuel economy can be determined. Four regional driving cycles viz., Japan's JP10 driving cycle which spans for 135 seconds, United States' SC03 driving cycle which spans for 596 seconds, United States' LA92 driving cycle which spans for 900 seconds and Sri Lanka's Colombo Metropolitan driving cycle which spans for 1499 seconds is also a deliverable of the study, are used in the study to test against the developed theoretical model and the determined output data streams are provided in the section below. Furthermore, world harmonized light vehicle test procedure (WLTP) is used as the fifth driving cycle to test against the model and the reason for opting WLTP is that it provides the generalized driving data throughout the world.

Five different driving cycle tests have been carried out using the aforementioned driving cycle data and the results are portrayed from Figure 53 – Figure 67. Similar testing conditions have been used, and only the respective driving cycle data is varied when the said five tests are carried out. The testing conditions are similar to which listed in Table 27 in Section 3.6.

- **Test 1 – Results when tested against JP10 driving cycle data.**

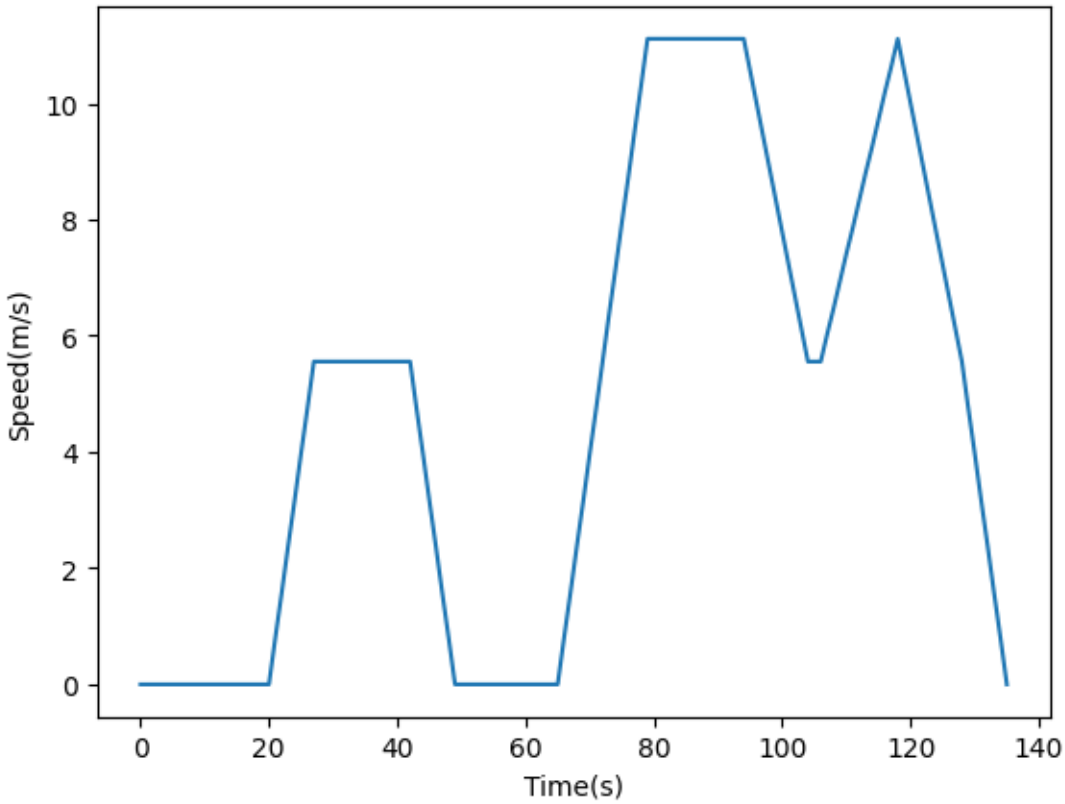

Figure 54: JP10 driving cycle data.

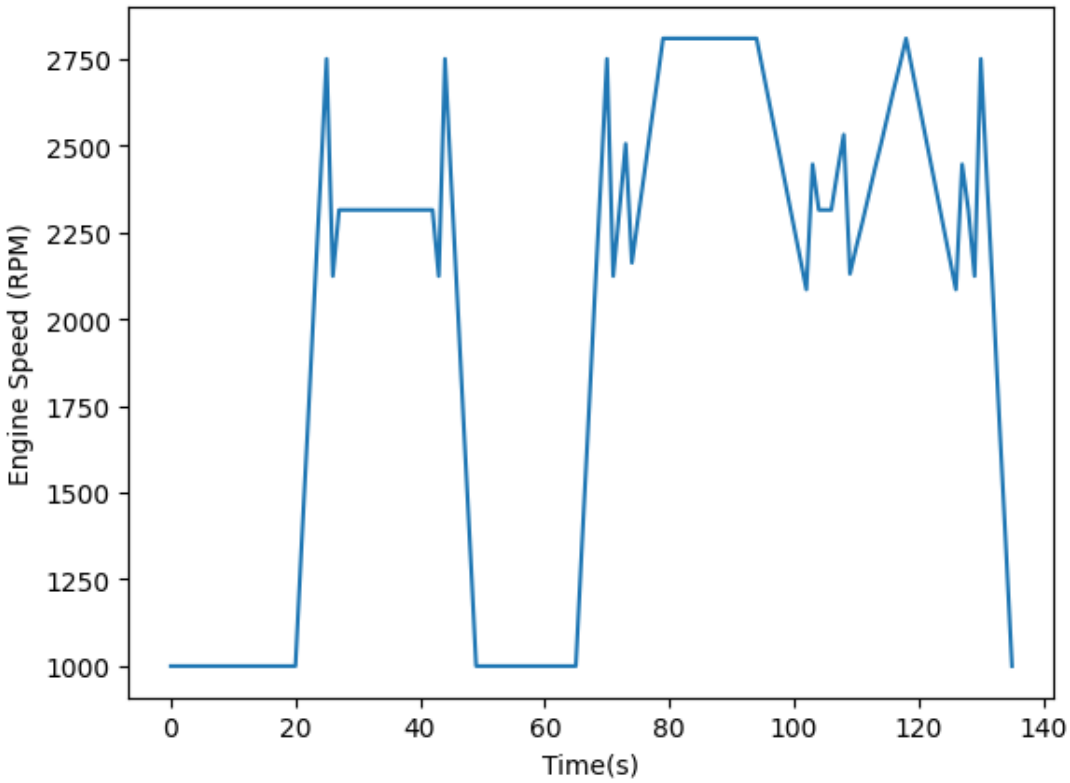

Figure 55: Engine speed profile when tested against JP10 driving cycle.

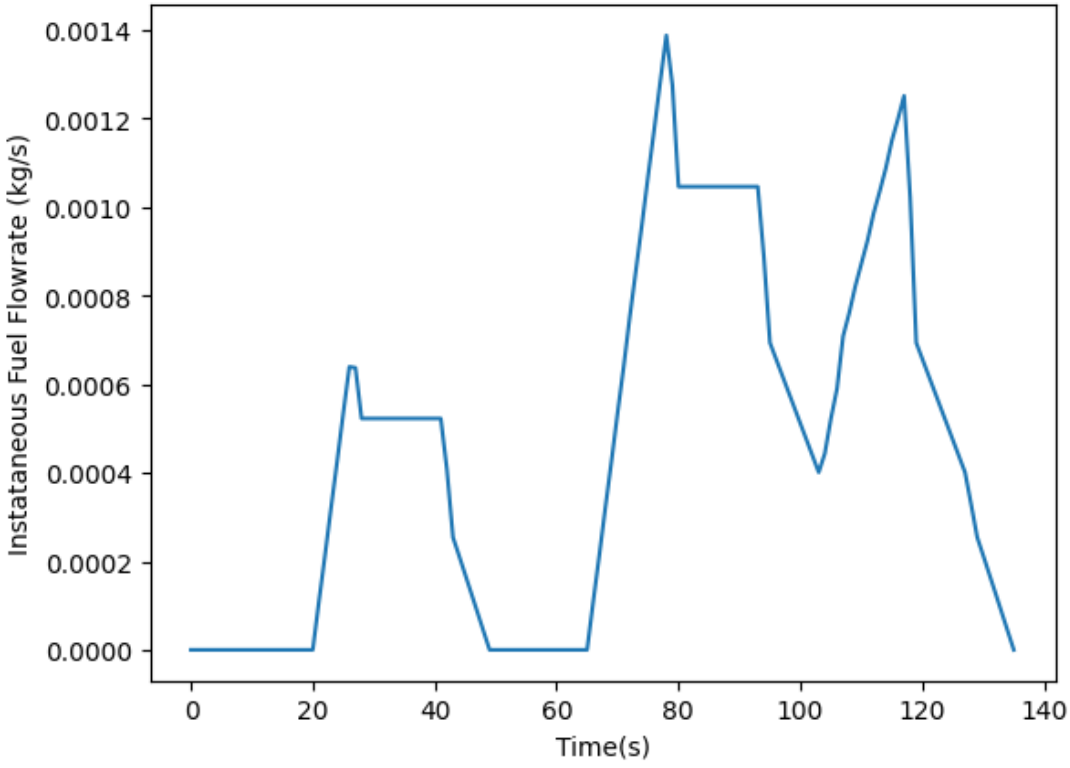

Figure 56 : Instantaneous Fuel Flowrate when tested against JP10 driving cycle.

Test 2 – Results when tested against SC03 driving cycle data.

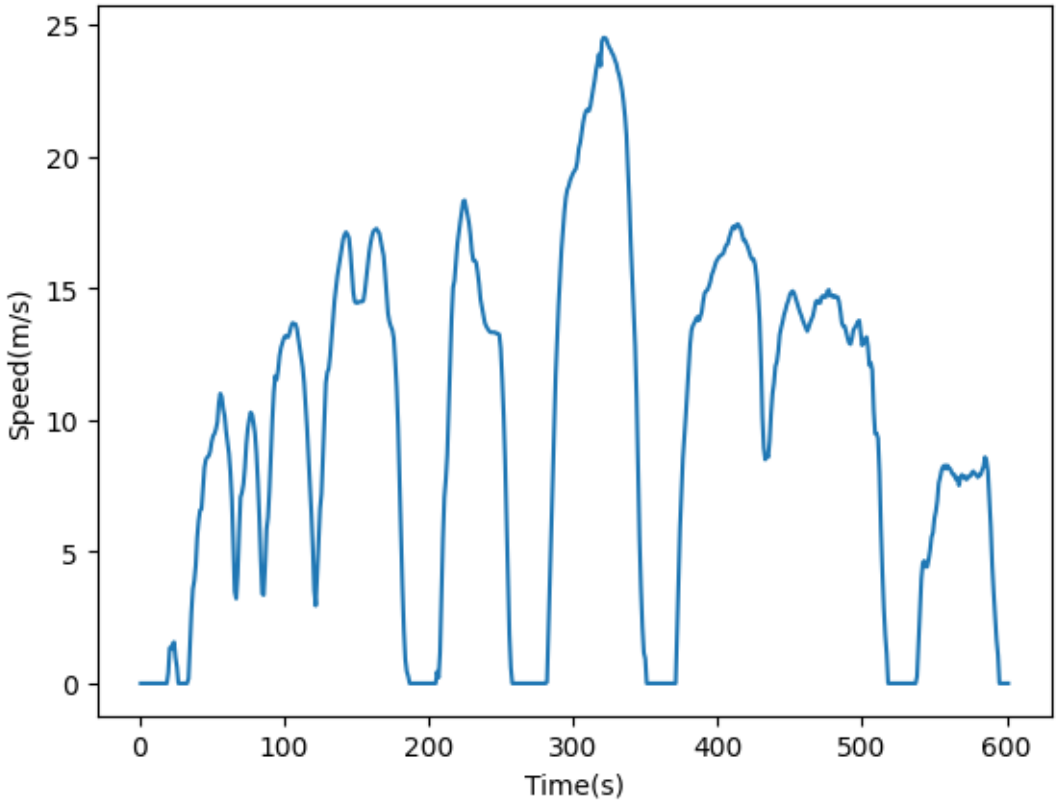

Figure 57 : SC03 driving cycle data.

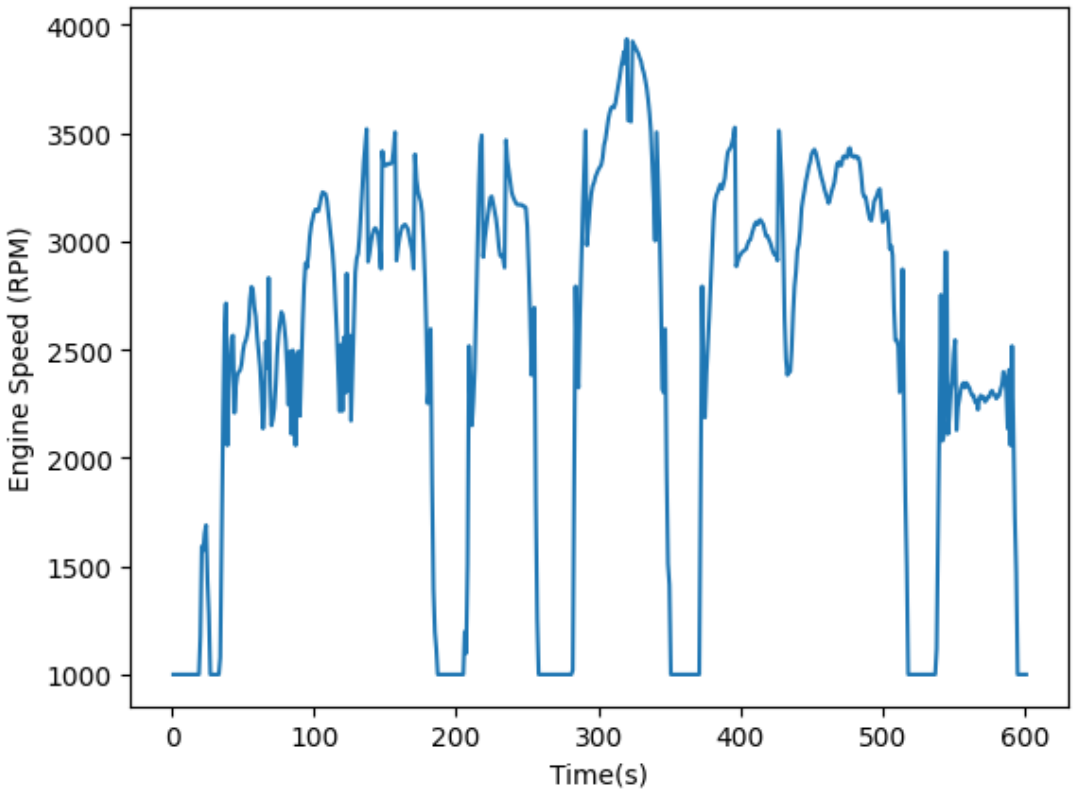

Figure 58: Engine speed profile when tested against SC03 driving cycle.

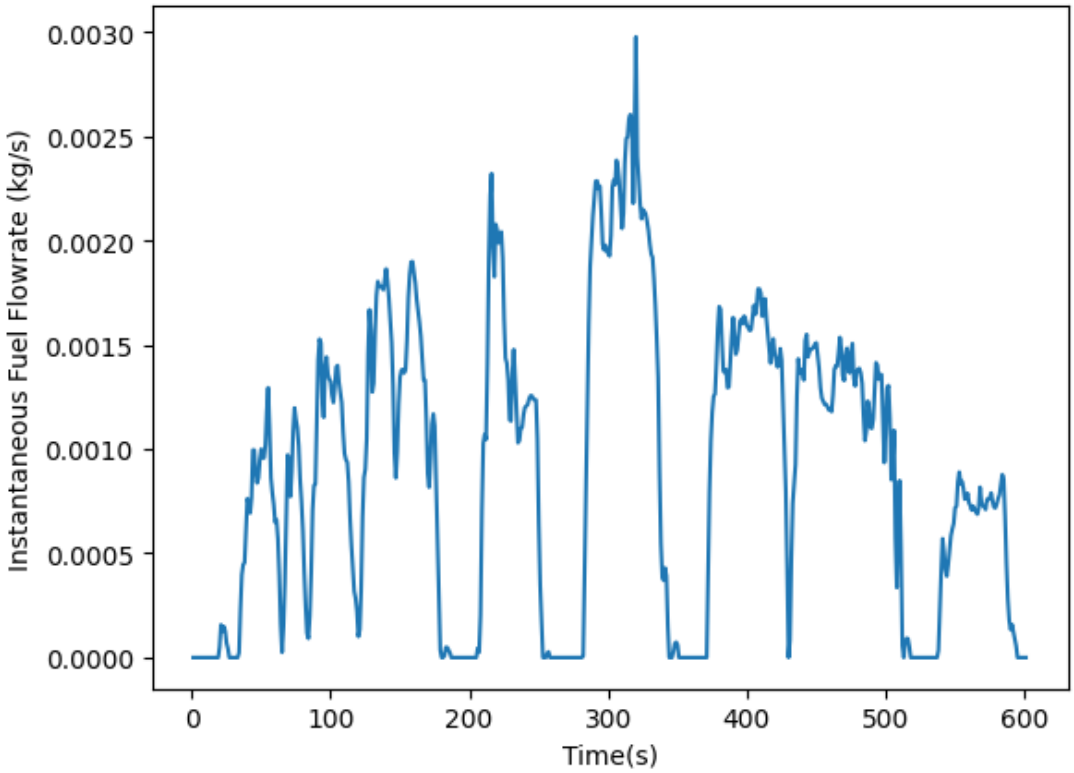

Figure 59 : Instantaneous Fuel Flowrate when tested against SC03 driving cycle.

Test 3 – Results when tested against LA92 driving cycle data.

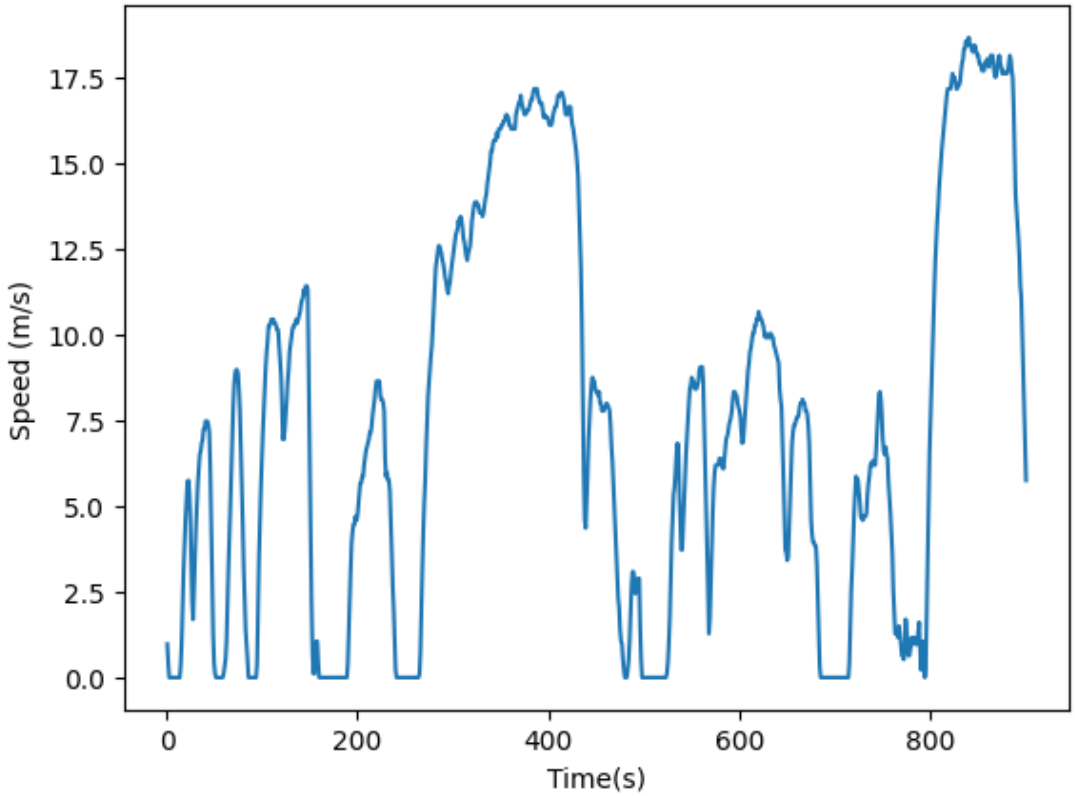

Figure 60 : LA92 driving cycle data.

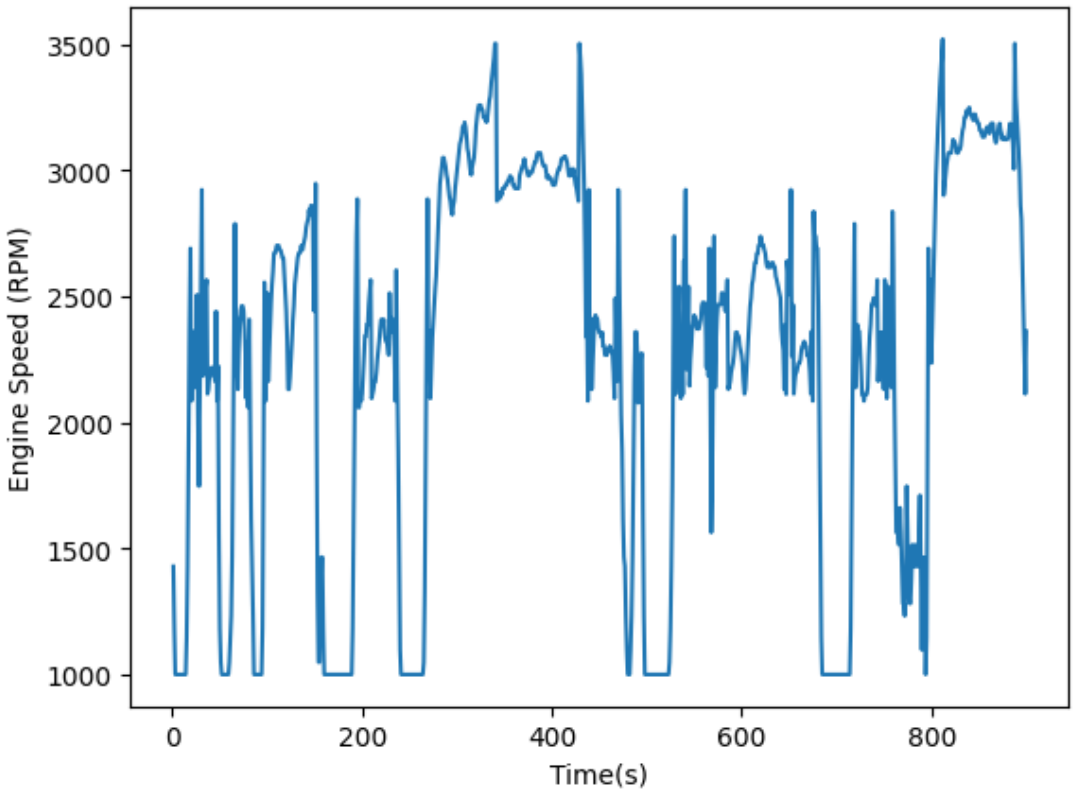

Figure 61 : Engine speed profile when tested against LA92 driving cycle.

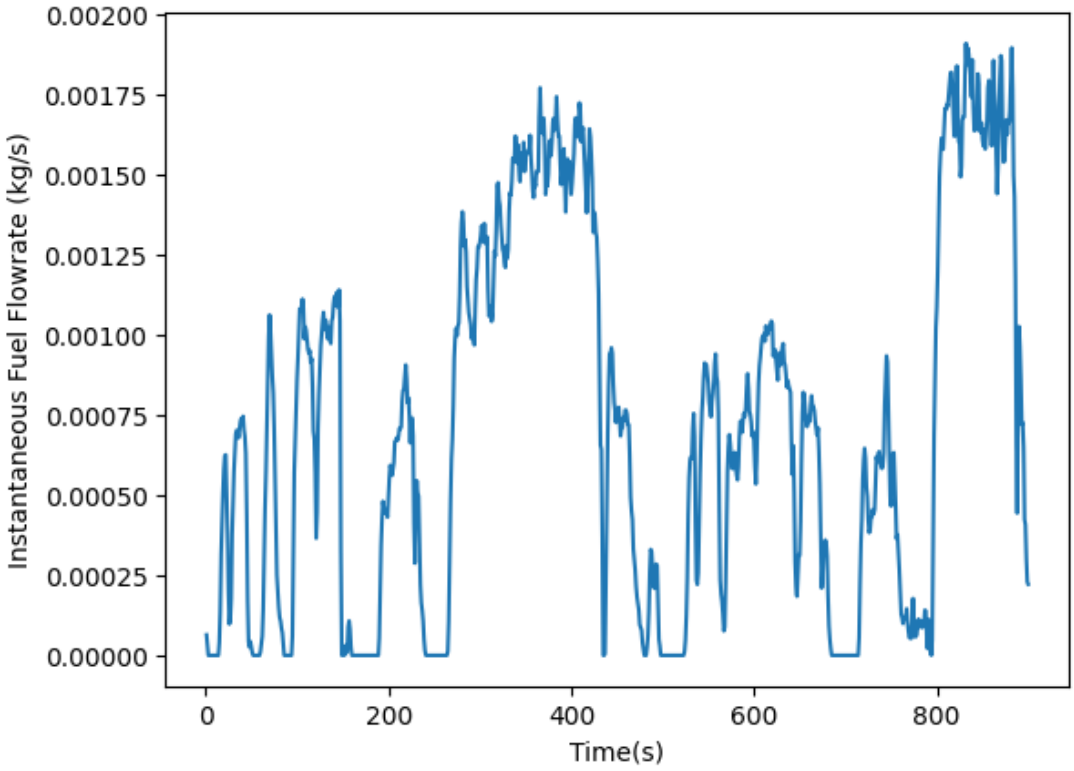

Figure 62: Instantaneous Fuel Flowrate when tested against LA92 driving cycle.

Test 4 – Results when tested against Colombo Metropolitan driving cycle data.

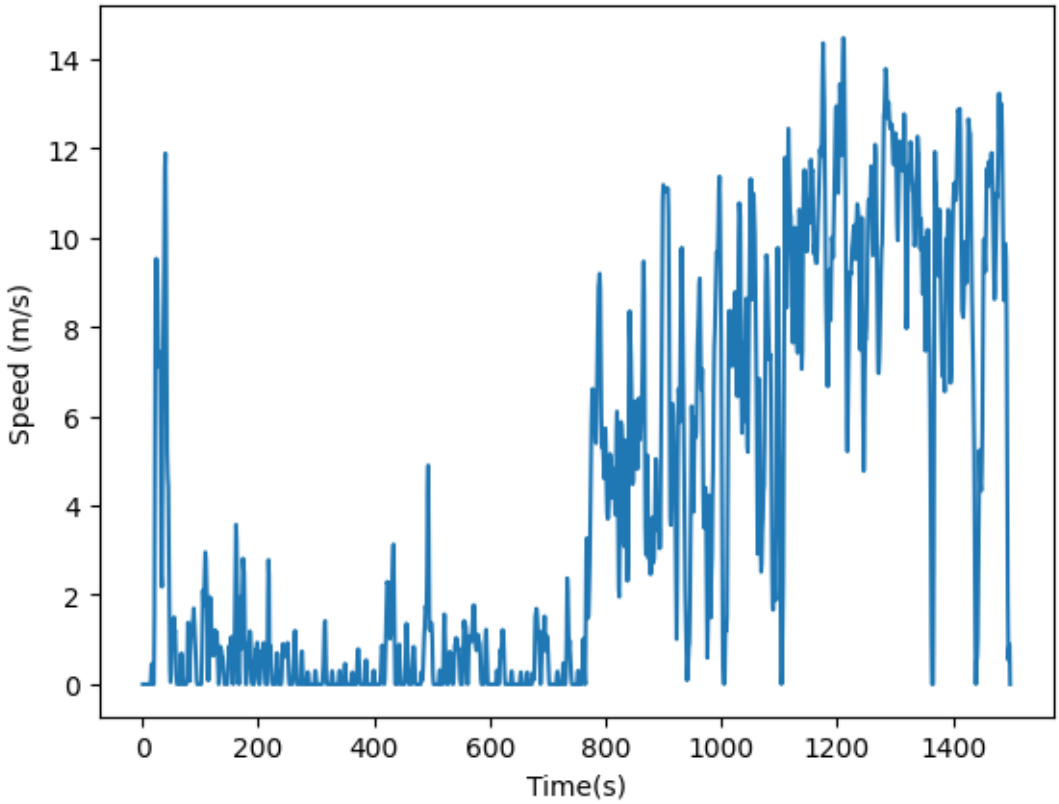

Figure 63: Colombo Metropolitan driving cycle data.

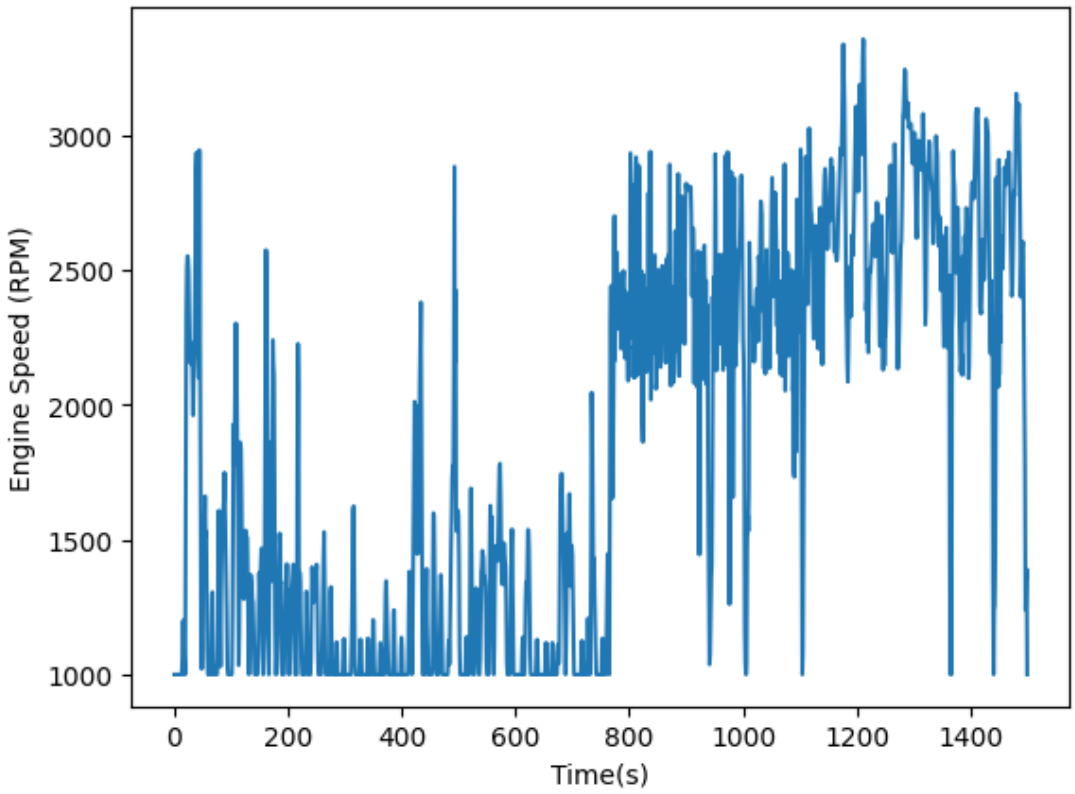

Figure 64: Engine speed profile when tested against Colombo Metropolitan driving cycle.

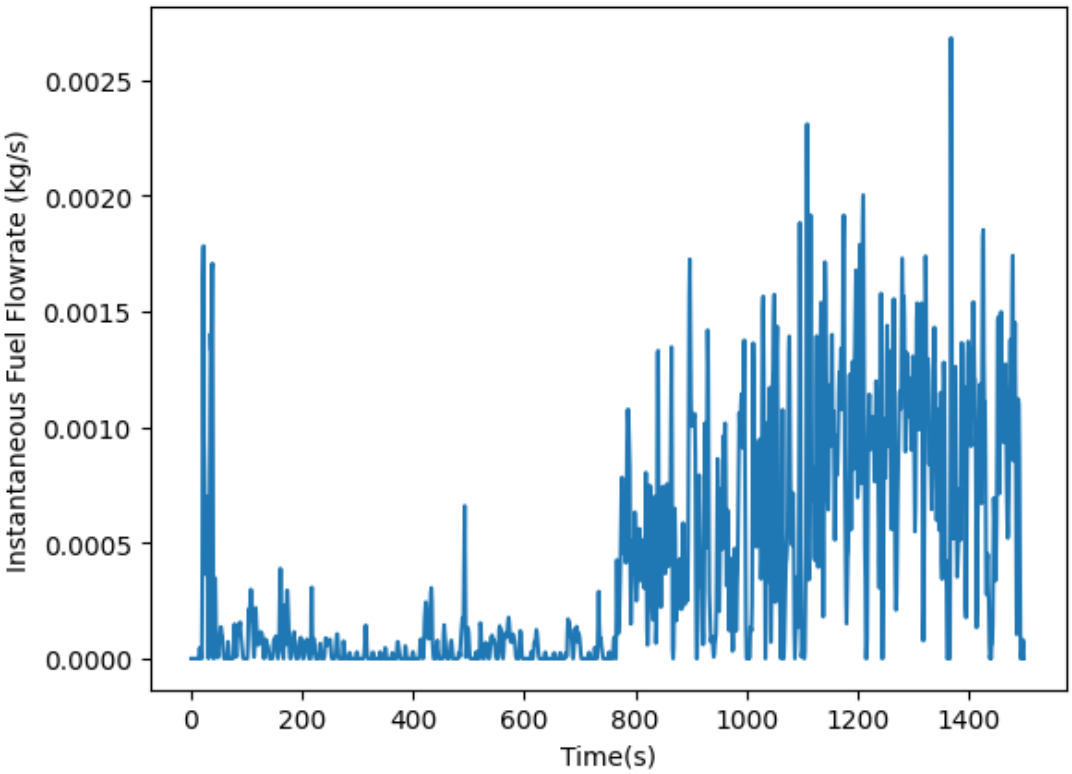

Figure 65: Instantaneous Fuel Flowrate when tested against Colombo Metropolitan driving cycle.

Test 5 – Results when tested against WLTP driving cycle data.

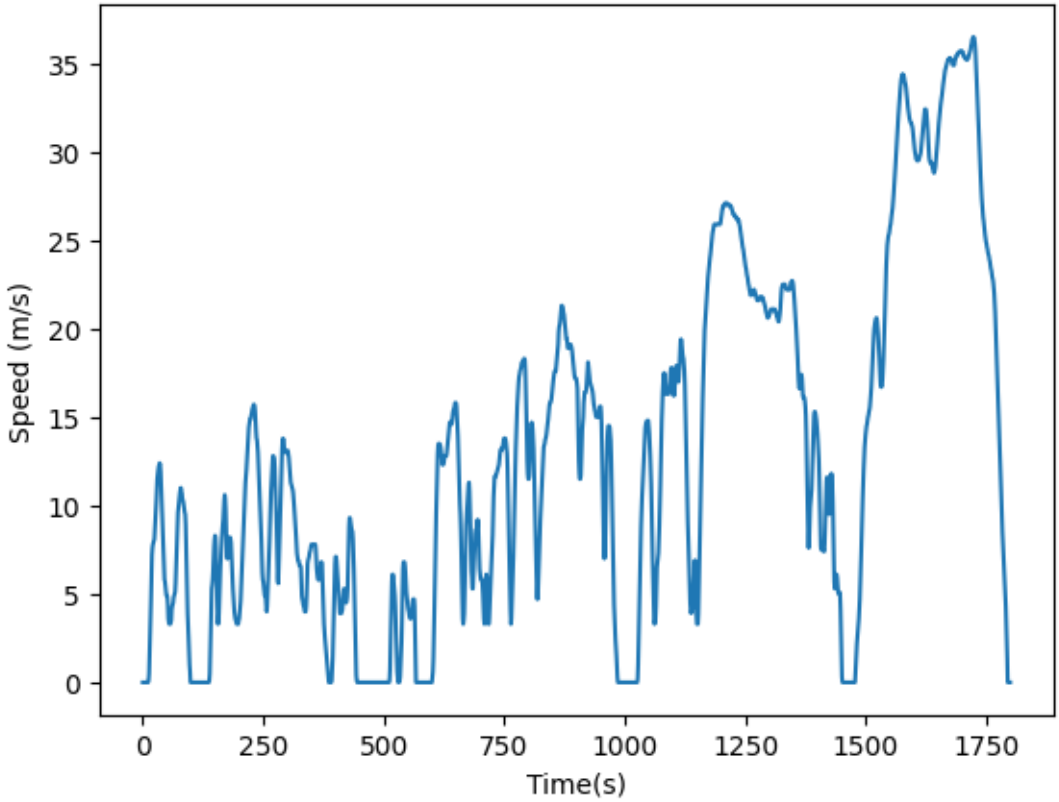

Figure 66 : WLTP driving cycle data.

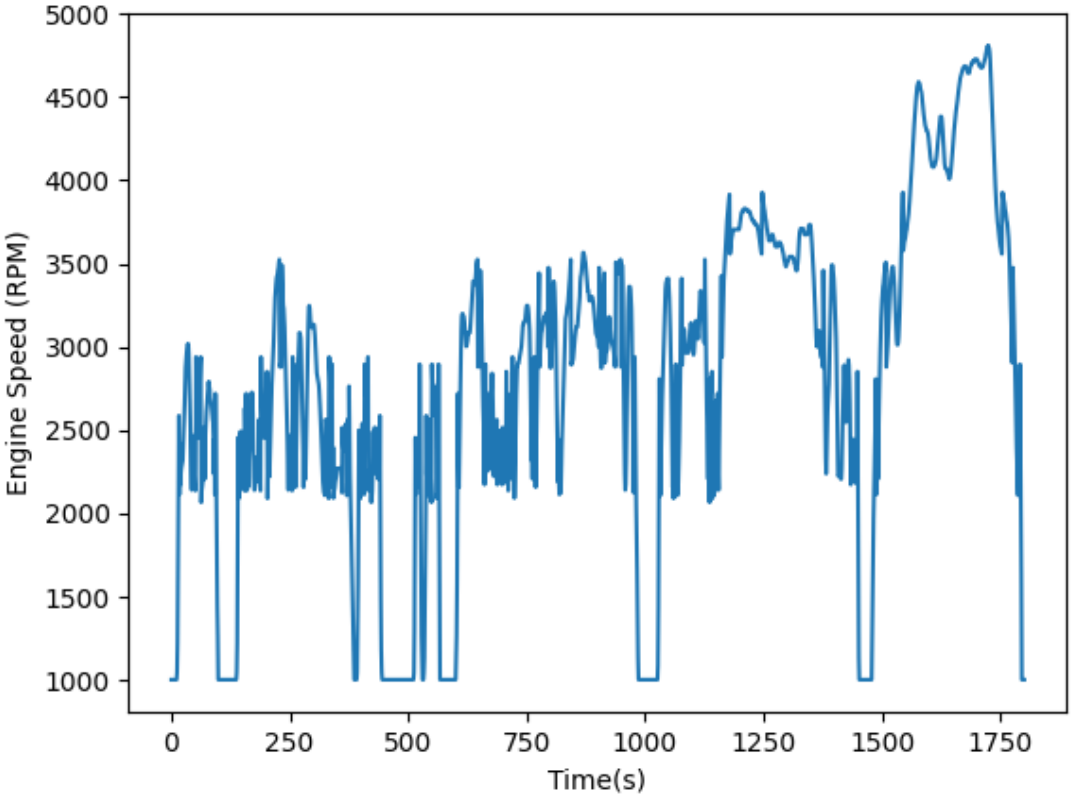

Figure 67: Engine speed profile when tested against WLTP driving cycle.

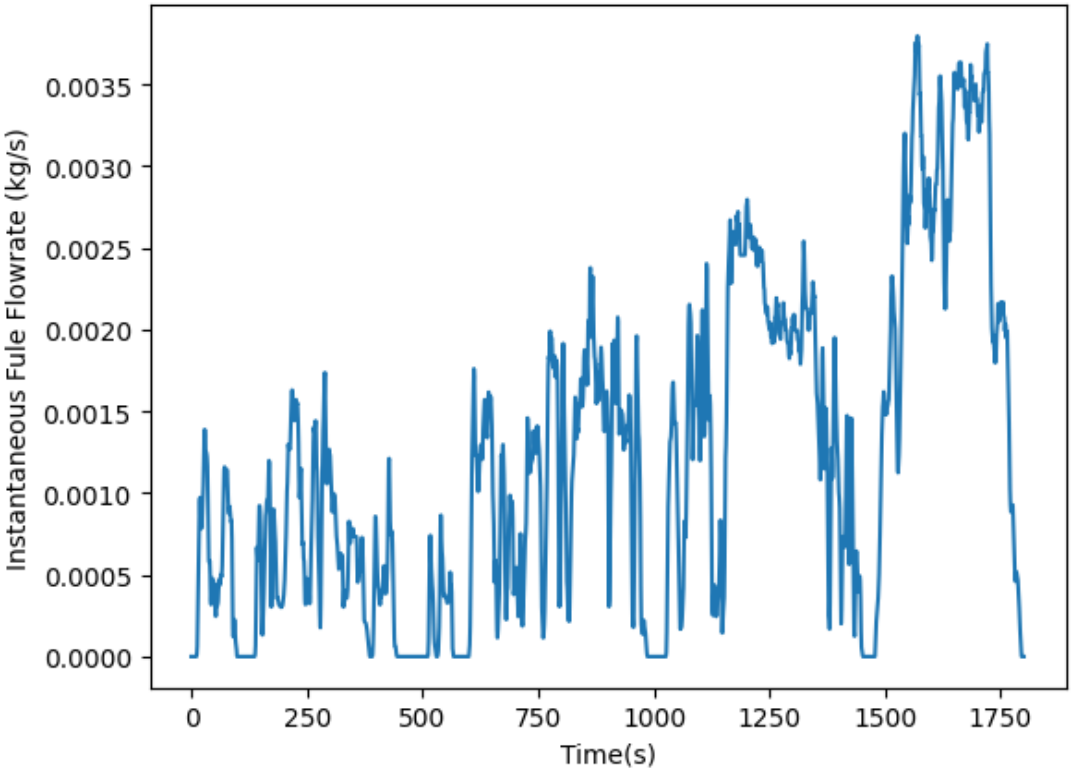

Figure 68 : Instantaneous Fuel Flowrate when tested against WLTP driving cycle.

When determining the average cycle fuel economy (FE_{Avg}), the formula stated in Equation (92) is used.

$$FE_{\text{Avg}} = \frac{\int_0^t v(t)dt * 10^{-3}}{\left(\int_0^t \dot{m}_f dt / \rho(T)\right) * 10^3} \tag{92}$$

Simplified version of (92) is portrayed in (93).

$$FE_{\text{Avg}} = = \frac{\rho(T) * \int_0^t v(t)dt * 10^{-6}}{\left(\int_0^t \dot{m}_f dt\right)} \tag{93}$$

When determining the density of the fuel, (during the study, it's considered as Gasoline), $\rho(T)$, which is a function of temperature is referred w.r.t. the volume correction factors [237]. Using the formula stated in Equation (93), FE_{Avg} of each driving cycle stated below is determined and listed in the Table 38.

Table 35 : Comparison of average fuel economy values of different driving cycles.

Driving Cycle	FE_{Avg} (km/l)
JP10	8.41
SC03	10.52
LA92	14.89
Colombo Metropolitan Driving Cycle	10.71
WLTP	8.89

When referring to the data listed in Table 38, it's conspicuous that though the similar vehicular test conditions exist, the FE_{Avg} value is varied under varying driving cycles.

The FE_{Avg} is obtained for WLTP driving cycle as well as for Colombo Metropolitan driving cycle under five varying operating conditions. The test results are depicted in Table 39. The test conditions are similar to those depicted in Table 24. The mass of the vehicle has been used as a variable.

Table 36 : Average fuel economy data for five different driving cycles.

WLTP FE_{Avg} (km/l)	Colombo Metropolitan DC FE_{Avg} (km/l)	SC03 FE_{Avg} (km/l)	LA92 FE_{Avg} (km/l)	JP10 FE_{Avg} (km/l)
6.45	7.78	7.63	10.80	6.10
7.40	8.92	8.76	12.39	7.01
8.18	9.86	9.69	13.70	7.75
8.89	10.71	10.52	14.89	8.42
9.52	11.48	11.27	15.94	9.01

The FE_{Avg} data shown in Table 39 are then graphed in the same plot as shown in the plot depicted in Figure 73.

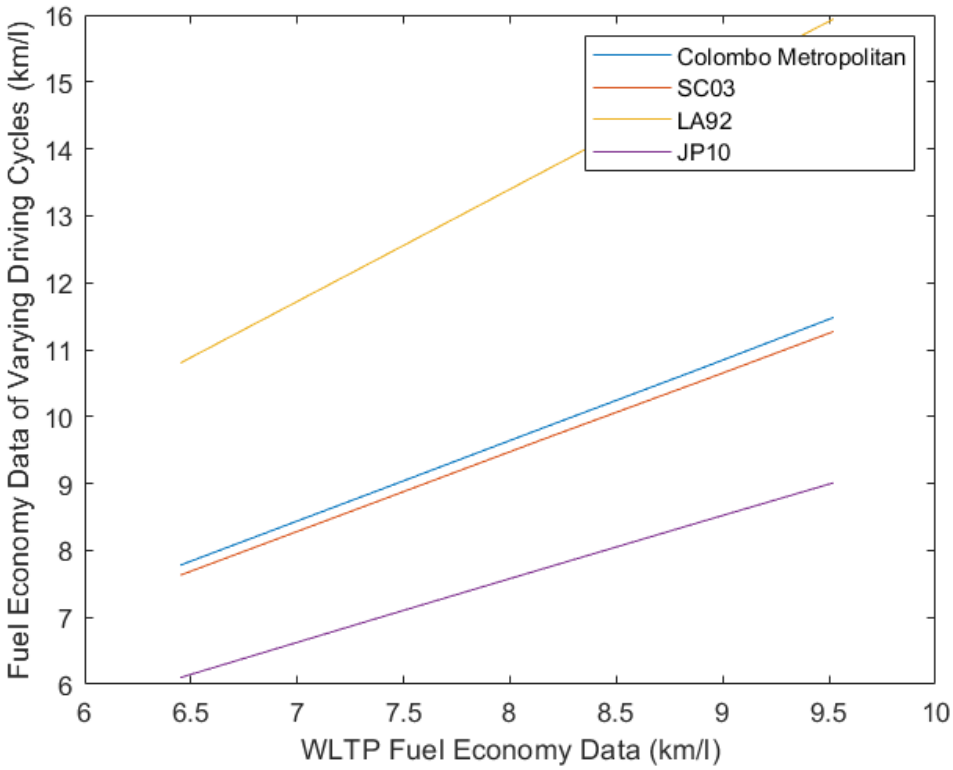

Figure 69 : The relationship for average fuel economy between varying driving cycles versus WLTP.

The portrayed relationships in Figure 69 can be determined using regression analysis. Once curve-fitted using linear regression, the following relationships can be determined: Colombo Metropolitan DC and WLTP as stated in Equation (94), SC03 DC and WLTP as stated in Equation (95), LA92 DC and WLTP as stated in Equation (96) and JP10 DC and WLTP as stated in Equation (97).

If FE_{Avg} data for WLTP is x, whereas the FE_{Avg} data for Colombo Metropolitan, SC03, LA92 and JP10 driving cycles is y, then the curve-fitted relationships can be determined as follow:

$$y = 1.204x + 0.0101 \quad (94)$$

$$y = 1.185x + 0.0100 \quad (95)$$

$$y = 1.675x + 0.0038 \quad (96)$$

$$y = 0.948x - 0.0087 \quad (97)$$

The determined relationships are linear with an intercept. The stated relationships can be used to translate average fuel economy values between two cycles, in this case, from WLTP to a specific cycle. The reason for opting WLTP as the independent cycle as it is the worldwide harmonized test cycle which represents the driving behavior in the global context. Thus, it’s fair to benchmark other regional driving cycles against WLTP.

5. CONCLUSIONS AND FUTURE DIRECTIONS

The work presented in the thesis advances the understanding of the reader on two main aspects viz., the development of localized driving cycles to suit local conditions of the Colombo Metropolitan Area and the development of a theoretical model to characterize the fuel consumption of light duty vehicles. The driving cycles developed during the study could be used as input speed-array data for the theoretical model developed and thus, the model shall be providing a fuel economy estimation. Furthermore, the standard driving cycles viz., WLTP, SC03, LA92 and JP10 driving cycles have been used as input data for the developed theoretical model and the correlations have been developed for the driving cycle conversion factors against the WLTP using regression analysis. The developed theoretical model for fuel economy characterization possesses a physical validation accuracy level between 88.79% and 91.76% whereas when validated against simulations, it gets converged to a band between 89.61% to 92.78%. Conclusively, it can be stated that the developed and validated theoretical model can be utilized as a tool to estimate the fuel consumption of different vehicle types under varying driving conditions. Furthermore, it is recommended to refer to the developed local driving cycles to mimic the local driving behavior when using the theoretical model for localized fuel consumption estimations. The following sections summarize the key findings and suggest important areas for future research.

5.1 Objective 1: Development of local driving cycles to mimic the local driving behaviour.

When developing local driving cycles aiming at 2W, 3W and 4W in Colombo Metropolitan Area, the standardized approach of route selection, data collection, cycle construction and cycle validation is adopted. Novelty is brought forward in each step of the cycle development. When opting for the routes for data collection, a novel approach of utilizing the travel time data as a base parameter to quantify the level of congestion is used. A dedicated application called MTRADA^{TM} is used to identify the routes respectively. In the data collection phase, a dedicated application called Geo-updater^{TM} is used to obtain the spatial and temporal data. When it comes to the third

phase of cycle development, i.e., cycle construction, a novel approach of Kriging spatial interpolation is used with the classification technique of Jenks Natural Breaks. It further improves the sensitivity of the driving cycles towards the spatial data. Finally, when it comes to the last step, i.e., cycle validation, a novel approach of determining the Similarity Indices (SIs) for the candidate cycles and the population data set and use the Cumulative Similarity Indices (CSIs) to opt for the best representative driving cycle out of the candidate cycles.

Two separate driving cycles are developed for the two main LDV classes, i.e., motorcycles (including 2W, 3W and four-wheeled quadricycles) and other four-wheeled LDVs. The representative local driving cycle for motorcycles is having a CSI score of 4.5489 and 4.8087 out of 5 for the urban and extra-urban driving cycles respectively and it depicts the representativeness of the developed driving cycle against the population parameters. The key highlights of the developed driving cycles for the motorcycles can be listed viz. the average speed of 3.87 m/s, the maximum speed of 10.01 m/s, average running speed of 4.44 m/s, average acceleration of 0.33 m/s^2, average deceleration of -0.36 m/s^2 and an idle time percentage of 12.75%. Secondarily, the developed driving cycle for the other four-wheeled LDVs is having a CSI score of 4.5947 and 4.8846 out of 5 for the urban and extra-urban driving cycles respectively and it too portrays the representativeness of the developed driving cycle data against the population data set. The key highlights of the developed driving cycles for the other four-wheeled LDVs can be listed viz. the average speed of 4.83 m/s, the maximum speed of 14.47 m/s, average running speed of 5.38 m/s, average acceleration of 0.95 m/s^2, average deceleration of -0.97 m/s^2 and an idle time percentage of 22.35%. It can lucidly be seen the fact that the kinematic parameters of four-wheeled LDVs are having comparatively higher values than those of motorcycles. A main reason can be claimed as the limitations of the power, engine capacity and top speed of motorcycles compared to the other four-wheeled LDVs. Furthermore, the idle time percentage is significantly less in the motorcycle driving cycle than that in the four-wheeled LDV driving cycle. A major reason for this can be claimed as the motorcycles tend to tweak in through the traffic in congested situations, thus resulting in less stoppage time durations.

As a future directive, it's recommended to develop localized driving cycles specifying the expressways which have been recently added to the national route network of Sri Lanka. Since the study is scoped to the development of driving cycles for arterial routes, it is recommended to develop driving cycles for expressways as well in order to reflect real world driving behaviour.

5.2 Objective 2: Development of the theoretical model for fuel consumption characterization.

The second major deliverable of the study is to develop a theoretical model to characterize fuel consumption and to utilize the developed model for fuel consumption estimation under different driving cycles. When developing the theoretical model, a kinetics and kinematics-related approach is adopted. The brake power of the engine is modelled using the two main components of tractive power and auxiliary power requirements. Tractive power requirement comprises four major components of power required to overcome rolling resistance, aerodynamic drag resistance, grade resistance and inertial resistance. The said four components have been theoretically modelled during the study. The remaining component of the auxiliary engine power requirement is developed under the schemes of air-conditioning, alternator power requirements and other minor engine auxiliary power requirements. During the study, it reveals the fact that 97% of the engine auxiliary power requirement is demanded by the air-conditioner and the alternator whereas the remaining 3% of the power requirement is demanded by the other minor engine auxiliaries viz., mechanical water pump, power steering pump, etc., and the latter component is considered as negligible. A comprehensive analysis of air-conditioning load is performed during the study. In that analysis, the air-conditioning load is segregated into six main types of loads, viz., metabolic load, engine load, exhaust load, ambient load, radiation load and ventilation load. The loads have analytically been modelled and the developed model is tuned to suit the local Sri Lanka context.

The developed theoretical model which comprises both tractive power components as well as the auxiliary power components, has been tested and performed with two-way validation: i.e., the physical validation using chassis dynamometer tests and

simulation-based validation using FASTSim^{TM} tool developed by the National Renewable Energy Laboratory, United States. The model reflects an accuracy band of 88.79% to 91.76% for physical validation and an accuracy band of 89.61% to 92.78%. for simulation-based validation.

Furthermore, using the developed model, driving cycle conversion factors have been critically evaluated. Five different driving cycles inclusive of the developed 4W driving cycle for Colombo Metropolitan area have been tested using the model and the output fuel economy data has been compared among the different driving cycles. Driving cycle fuel economy conversion factors have been determined using linear regression against the World Harmonized Light Vehicle Test Procedure.

The developed theoretical model is scoped to model the fuel consumption estimation of internal combustion engine vehicles which are either Diesel or Gasoline powered. As a future directive, it's recommended to develop a model to estimate the range of the electric vehicles inclusive of battery electric vehicles, plug-in hybrid electric vehicles, hybrid electric vehicles and fuel cell vehicles.

5.3 Discussion of limitations of the study

The current study aims to develop more comprehensive and representative driving cycles for the entire Colombo Metropolitan Area, using improved route selection, data acquisition, cycle construction and validation approaches. Separate driving cycles are developed for 2-wheelers/3-wheelers and 4-wheelers.

So, while this is not the first attempt at driving cycle development in Sri Lanka, the thesis does represent a novel effort to construct localized driving cycles with greater scientific rigor and representativeness.

Regarding emissions - the thesis focuses primarily on fuel economy characterization. However, it does mention that driving cycles are used for both fuel consumption and emission estimation purposes. The theoretical model developed aims to predict fuel consumption, but in principle, fuel use is directly related to CO_2 emissions. With some extensions, the modeling framework could likely be adapted for exhaust emission analysis as well.

- **Rationale for considering CO_2 emissions only**
    - Fuel economy is a critical sustainability metric in its own right, given concerns around oil dependence, energy security, and the costs of fuel imports for many countries. Developing an accurate understanding of real-world fuel consumption can inform important transportation and energy policy decisions.
    - While CO_2 is not directly toxic like other pollutants, it is the primary greenhouse gas driving climate change. Given the urgent need to mitigate climate risks, quantifying the CO_2 emissions associated with different vehicle fleets and driving behaviors is environmentally consequential.
    - From a methodological standpoint, fuel consumption is relatively straightforward to estimate from driving parameters like speed, acceleration, engine size, etc. Modeling other exhaust pollutants like carbon monoxide, nitrogen oxides or particulates would require more complex chemical analysis of engine and catalyst technologies.
    - Harmful tailpipe emissions are tightly regulated through vehicle emissions standards, whereas fuel economy policies often give manufacturers more

flexibility in meeting fleet-average targets. Localized fuel consumption data may be valuable for Sri Lanka in setting its own fuel economy rules.

- Strategically, leading with fuel economy characterization may lay the groundwork for later expanding the research to other emission types. Demonstrating the scientific rigor of the approach with CO_2 could build confidence in using locally-developed driving cycles for other pollutant regulations.

- **Consideration of alternative fuels**
  - Fuel economy is a critical sustainability metric in its own right, given concerns around oil dependence, energy security, and the costs of fuel imports for many countries. Developing an accurate understanding of real-world fuel consumption can inform important transportation and energy policy decisions.
  - While CO_2 is not directly toxic like other pollutants, it is the primary greenhouse gas driving climate change. Given the urgent need to mitigate climate risks, quantifying the CO_2 emissions associated with different vehicle fleets and driving behaviors is environmentally consequential.
  - From a methodological standpoint, fuel consumption is relatively straightforward to estimate from driving parameters like speed, acceleration, engine size, etc. Modeling other exhaust pollutants like carbon monoxide, nitrogen oxides or particulates would require more complex chemical analysis of engine and catalyst technologies.
  - Harmful tailpipe emissions are tightly regulated through vehicle emissions standards, whereas fuel economy policies often give manufacturers more flexibility in meeting fleet-average targets. Localized fuel consumption data may be valuable for Sri Lanka in setting its own fuel economy rules.
  - Strategically, leading with fuel economy characterization may lay the groundwork for later expanding the research to other emission types. Demonstrating the scientific rigor of the approach with CO_2 could build confidence in using locally-developed driving cycles for other pollutant regulations.

- **Representativeness of the developed driving cycles**
  - Colombo is the largest city and economic hub of Sri Lanka, with a significant share of the country's vehicle fleet and transportation activity. Accurately characterizing fuel consumption patterns in this high-traffic region can have outsized environmental and energy implications.
  - Many other regions of Sri Lanka, particularly urban areas, are likely to share some key traffic and driving characteristics with Colombo, such as congestion, frequent stop-and-go conditions, lower average speeds, etc. So the Colombo driving cycles could be a reasonable proxy for other cities, even if not a perfect match.
  - The thesis methodology for data collection, cycle construction, and validation is highly generalizable. The same approach could be applied to develop custom driving cycles for other specific regions of interest in Sri Lanka. The Colombo study provides a template.
  - In the absence of other localized driving data, the Colombo cycles are still likely to be more representative of Sri Lankan conditions than standard international cycles like the European NEDC or the US FTP. Using these cycles for national fuel economy estimates is an improvement over unadjusted foreign cycles.
  - The Colombo cycles can serve as a benchmark for comparing against other regions. Future studies could collect data in other cities or rural areas and assess how well the Colombo cycles match those conditions. This could guide decisions about whether the Colombo cycles are sufficient or if separate regional cycles are warranted.
  - Going forward, applying this methodology to a representative sample of other key regions could yield a powerful dataset for Sri Lanka to develop its own national driving cycle, akin to the US EPA's FTP or the EU's WLTP. This study is a crucial first step in that process.

- **Discussion on modern trends in internal combustion engines**

  The automotive industry has made significant strides in improving engine performance and reducing heat losses since the 1970s and 80s. Modern internal combustion engines have benefited from a range of design innovations and

technologies that have helped to boost thermal efficiency and reduce heat rejection.

Some key developments include,

- Direct fuel injection: Many modern engines use direct injection systems that spray fuel directly into the combustion chamber, allowing for more precise control over the air-fuel mixture and improved combustion efficiency.
- Variable valve timing and lift: Advanced valve control technologies like variable valve timing (VVT) and variable valve lift (VVL) enable engines to optimize valve opening and closing for different operating conditions, enhancing efficiency across a wider range of speeds and loads.
- Turbocharging and downsizing: The use of turbochargers to boost intake air pressure has allowed for engine downsizing, where smaller displacement engines can produce the same power as larger naturally aspirated engines, but with improved fuel efficiency and reduced heat losses.
- Cylinder deactivation: Some engines can selectively deactivate cylinders during low-load conditions, reducing pumping losses and improving efficiency.
- Cooled exhaust gas recirculation (EGR): Cooled EGR systems recirculate a portion of the exhaust gases back into the intake, lowering combustion temperatures and reducing heat losses.
- Improved materials and thermal management: The use of advanced materials and coatings, as well as sophisticated thermal management strategies, help to reduce heat transfer to the engine block and coolant, keeping more energy available for mechanical work.

As a result of these and other advancements, modern gasoline engines can achieve thermal efficiencies in the range of 35-40%, with some high-performance engines exceeding 40%. Diesel engines, which inherently have higher compression ratios and lean combustion, can reach efficiencies of 40-45% or higher.

Research has shown that the thermal efficiency of gasoline engines can be improved through various methods. Sok et al. [238] found that lean-boosted combustion and high knock resistant fuel can enhance efficiency, while Mu et al. [239] demonstrated that altering the engine's structural design and using cooled exhaust gas recirculation can also lead to efficiency gains. Kim et al. [240] proposed a hybrid system using spark-assisted ignition, which achieved a high indicated efficiency of 61.6%. Moreno et al. [241] further explored the use of hydrogen and methane blends, finding that a 30% hydrogen and 70% methane blend can achieve a good balance between thermal efficiency and pollutant emissions. These studies collectively suggest that a combination of advanced combustion processes, engine design modifications, and alternative fuel blends can contribute to improved thermal efficiency in gasoline engines.

- **The representativeness of the factors affecting fuel consumption**

Sensitivity Analysis and Parameter Representativeness: Throughout the study, various factors affecting fuel consumption were considered, including tractive loads and auxiliary engine loads. To assess the significance of these factors and validate their selection, a sensitivity analysis was conducted.

The sensitivity analysis involved varying the values of selected parameters within a reasonable range and observing their impact on the estimated fuel consumption. This analysis helps identify the parameters that have the greatest influence on fuel consumption and provides insights into the robustness of the developed model.

Based on the literature review and the findings of this study, it was found that tractive loads, such as rolling resistance, aerodynamic drag, and inertial forces, are among the most significant contributors to fuel consumption. These factors collectively account for a substantial portion of the energy required to propel the vehicle. The sensitivity analysis confirmed that variations in these parameters have a notable impact on the estimated fuel consumption, highlighting their importance in the overall fuel consumption model.

Auxiliary engine loads, including A/C, alternator, and other accessories, were also found to have a significant impact on fuel consumption. The literature suggests that these auxiliary loads can account for a considerable percentage of the total energy consumption, especially in urban driving conditions with frequent stops and idling. The sensitivity analysis demonstrated that variations in auxiliary load parameters have a noticeable effect on the estimated fuel consumption, confirming their relevance in the model.

The selected parameters, encompassing both tractive loads and auxiliary engine loads, were found to be representative of the major factors influencing fuel consumption. The literature review and the results of this study indicate that these parameters collectively account for a significant portion of the total fuel consumption, often in the range of 80% to 20%, with tractive loads being the dominant contributor.

However, it's important to acknowledge that the exact percentages may vary depending on the specific vehicle type, driving conditions, and other factors. The 80%-20% representation is a general approximation based on the available literature and the findings of this study. Future research could further refine these estimates and explore the influence of additional parameters on fuel consumption.

Despite the limitations and approximations, the sensitivity analysis and the representativeness assessment provide a strong justification for the selection of the key parameters considered in this study. The developed model, incorporating tractive loads and auxiliary engine loads, offers a comprehensive approach to estimating fuel consumption and provides valuable insights into the relative importance of different factors.

Further validation and refinement of the model can be achieved through additional experimental data, real-world driving tests, and collaboration with industry partners. This will help enhance the accuracy and applicability of the model in various driving scenarios and vehicle types.

- **Representatives of factors affecting the driving cycle development**

Representativeness of Factors and Values: In this study, various factors and values were used to develop driving cycles and estimate fuel consumption for different vehicle types, including motorcycles. While efforts were made to ensure the representativeness of these factors and values, it's important to acknowledge potential limitations and areas for future improvement.

For motorcycles, the study considered a sample of vehicles and collected data over a specific time period. However, the representativeness of this sample could be enhanced by considering additional factors such as the year of manufacture (YoM) and other relevant characteristics. The YoM can influence the fuel efficiency, emission levels, and overall performance of motorcycles due to advancements in engine technology and emission regulations over time. In future studies, it would be valuable to expand the dataset and include motorcycles from different YoMs to capture a more diverse and representative sample. This would allow for a more comprehensive analysis of the driving patterns and fuel consumption characteristics of motorcycles in the Colombo Metropolitan Area.

Additionally, other factors such as engine capacity, fuel type, and vehicle weight could be considered to further refine the representativeness of the motorcycle dataset. These factors can influence the driving dynamics and fuel consumption of motorcycles, and incorporating them into the analysis would provide a more accurate representation of the motorcycle fleet.

Similar considerations can be applied to other vehicle types, such as cars and 3W, to enhance the representativeness of the factors and values used in the study. Expanding the dataset to include vehicles from different YoM, engine capacities, fuel types, and other relevant characteristics would strengthen the overall representativeness of the study.

Future work could also involve collaborating with industry partners, government agencies, and transportation authorities to access more comprehensive vehicle data and ensure the representativeness of the sample. This collaboration could provide access to a larger and more diverse dataset,

enabling a more accurate representation of the vehicle fleet in the Colombo Metropolitan Area.

Furthermore, conducting sensitivity analyses on the selected factors and values would help identify the most influential parameters and their impact on the results. This analysis would provide insights into the robustness of the developed models and highlight areas where further refinement and data collection efforts should be focused.

In conclusion, while the current study provides valuable insights into the driving patterns and fuel consumption characteristics of vehicles in the Colombo Metropolitan Area, there is room for improvement in terms of the representativeness of the factors and values used. Future studies should aim to expand the dataset, consider additional relevant characteristics, and collaborate with stakeholders to enhance the representativeness of the sample. This will ultimately lead to more accurate and reliable results, enabling better decision-making and policy formulation in the context of sustainable transportation planning.

- **Discussion on GPS accuracy**

GPS Accuracy: The accuracy of GPS data depends on various factors, such as the quality of the GPS receiver, the number of visible satellites, atmospheric conditions, and the presence of obstructions (e.g., tall buildings, tunnels). In general, standard GPS receivers, like those used in smartphones or vehicle navigation systems, have an accuracy ranging from a few meters to about 20 meters under good conditions.

However, it's important to note that the vertical accuracy of GPS is typically lower than its horizontal accuracy. While horizontal accuracy can be within a few meters, vertical accuracy can be several times worse. This means that the altitude data provided by GPS, which is crucial for determining slope, may have a higher level of uncertainty compared to the latitude and longitude data.

Handling Slope Information: In the context of this study and the Geo-Updater application, the slope information is derived from the altitude data recorded by

the GPS receiver. The application captures the altitude along with the latitude, longitude, and other parameters for each data point.

The change in altitude is divided by the horizontal distance between the points to calculate the slope between two points,. However, given the lower vertical accuracy of GPS, the calculated slope values may have a certain level of error or noise.

To mitigate the impact of GPS vertical inaccuracy on slope calculations, several techniques can be employed:

- Data Filtering: Applying statistical filters or smoothing algorithms to the altitude data can help reduce the noise and outliers. Techniques such as moving averages, median filters, or Kalman filters can be used to obtain a more stable and reliable estimate of the altitude profile.
- Map Matching: Integrating the GPS data with digital elevation models (DEMs) or high-resolution topographic maps can help improve the accuracy of slope information. By matching the GPS points to the corresponding locations on the DEM or map, the altitude values can be corrected or refined based on the known terrain information.
- Sensor Fusion: Combining GPS data with other sensors, such as accelerometers or barometric pressure sensors, can provide additional information to estimate the vehicle's inclination and improve the accuracy of slope calculations.
- Post-Processing: After data collection, further post-processing techniques can be applied to analyze and correct the slope data. This may involve identifying and removing outliers, applying curve-fitting techniques, or using machine learning algorithms to learn the patterns and characteristics of the slope data.

- **Fleet level impact in using the developed model**

  - Vehicle segmentation: Segment the fleet into different categories based on vehicle size, engine type, fuel type, or other relevant characteristics. For example, you can group vehicles into small cars (e.g., Suzuki Alto), mid-size cars, large cars (e.g., Audi A8), SUVs, and so on. This segmentation allows

you to apply the fuel consumption model to each category separately, considering the specific attributes and performance parameters of each segment.

- Representative vehicle selection: Within each vehicle segment, select representative vehicle models that capture the average or typical characteristics of that segment. These representative vehicles should be chosen based on factors such as market share, popularity, and data availability. The fuel consumption model can then be applied to these representative vehicles to estimate the fuel consumption for each segment.
- Fleet composition analysis: Obtain data on the composition of the vehicle fleet in the region of interest, including the number of vehicles in each segment and their respective market shares. This information is crucial for weighting the fuel consumption estimates of each segment to derive overall fleet-wide results.
- Weighted averaging: Calculate the fleet-wide fuel consumption by taking a weighted average of the fuel consumption estimates for each vehicle segment. The weights should be based on the proportion of vehicles in each segment within the fleet. This approach ensures that the contributions of different vehicle types are appropriately accounted for in the overall fleet results.
- Sensitivity analysis: Conduct sensitivity analyses to assess the impact of variations in vehicle characteristics and operating conditions on the fleet-wide fuel consumption estimates. This can help identify the most influential factors and quantify the range of uncertainty in the fleet-level results. For example, you can explore how changes in the proportion of small cars versus large cars in the fleet affect the overall fuel consumption.
- Model validation and calibration: Validate the fleet-wide fuel consumption estimates against real-world data, such as fuel sales data or fleet-level fuel economy reports. If discrepancies are observed, calibrate the model by adjusting the parameters or assumptions to better match the observed data. This validation and calibration process helps improve the accuracy and reliability of the fleet-wide estimates.

- Scenario analysis: Use the fleet-wide model to analyze different scenarios and policy interventions. For example, you can explore the impact of shifting the fleet composition towards more fuel-efficient vehicles or the potential benefits of implementing fuel economy standards. By running scenarios with different fleet compositions and characteristics, you can assess the sensitivity of the fleet-wide fuel consumption to various factors.

- **The representativeness of data collection period and sample size**

  - Vehicle segmentation: Segment the fleet into different categories based on vehicle size, engine type, fuel type, or other relevant characteristics. For example, you can group vehicles into small cars (e.g., Suzuki Alto), mid-size cars, large cars (e.g., Audi A8), SUVs, and so on. This segmentation allows you to apply the fuel consumption model to each category separately, considering the specific attributes and performance parameters of each segment.
  - Representative vehicle selection: Within each vehicle segment, select representative vehicle models that capture the average or typical characteristics of that segment. These representative vehicles should be chosen based on factors such as market share, popularity, and data availability. The fuel consumption model can then be applied to these representative vehicles to estimate the fuel consumption for each segment.
  - Fleet composition analysis: Obtain data on the composition of the vehicle fleet in the region of interest, including the number of vehicles in each segment and their respective market shares. This information is crucial for weighting the fuel consumption estimates of each segment to derive overall fleet-wide results.
  - Weighted averaging: Calculate the fleet-wide fuel consumption by taking a weighted average of the fuel consumption estimates for each vehicle segment. The weights should be based on the proportion of vehicles in each segment within the fleet. This approach ensures that the contributions of different vehicle types are appropriately accounted for in the overall fleet results.

- Sensitivity analysis: Conduct sensitivity analyses to assess the impact of variations in vehicle characteristics and operating conditions on the fleet-wide fuel consumption estimates. This can help identify the most influential factors and quantify the range of uncertainty in the fleet-level results. For example, you can explore how changes in the proportion of small cars versus large cars in the fleet affect the overall fuel consumption.
- Model validation and calibration: Validate the fleet-wide fuel consumption estimates against real-world data, such as fuel sales data or fleet-level fuel economy reports. If discrepancies are observed, calibrate the model by adjusting the parameters or assumptions to better match the observed data. This validation and calibration process helps improve the accuracy and reliability of the fleet-wide estimates.
- Scenario analysis: Use the fleet-wide model to analyze different scenarios and policy interventions. For example, you can explore the impact of shifting the fleet composition towards more fuel-efficient vehicles or the potential benefits of implementing fuel economy standards. By running scenarios with different fleet compositions and characteristics, you can assess the sensitivity of the fleet-wide fuel consumption to various factors.

- **Infrastructure limitations**

  Infrastructure Limitations and Vehicle Selection: It's important to note that all the vehicles used in the simulation study, as presented in Table 35, have the same year of manufacture (YoM) of 2016. This consistency in YoM was not intentional but rather a result of the limitations in the available infrastructure and data.

  The simulation study relied on the FASTSim software, which requires specific vehicle parameters and performance data as inputs. The availability of comprehensive and reliable data for vehicles across different YoMs was limited. Consequently, the vehicles selected for the simulation were based on the availability of complete and accurate data required by the FASTSim software.

Furthermore, the infrastructure limitations, such as access to a diverse range of vehicle models and years, restricted the ability to include vehicles with varying YoMs in the simulation study. The focus was on ensuring the accuracy and reliability of the simulation results, given the available data and resources.

While the consistency in YoM does not significantly impact the validity of the simulation results, it's important to acknowledge this limitation. Future studies could aim to expand the vehicle dataset and include vehicles with different YoMs, subject to the availability of comprehensive and reliable data. This would provide a more diverse representation of the vehicle fleet and enhance the generalizability of the simulation results.

Despite this limitation, the simulation study using vehicles with the same YoM still provides valuable insights into the performance of the developed fuel consumption model and its ability to estimate fuel economy under different driving conditions. The results demonstrate the model's accuracy and reliability, even with the constraints in vehicle data availability.

5.4 Concluding remarks.

The study portrays a comprehensive work carried out in order to mimic the local driving behaviour pertaining to Colombo Metropolitan Area of Sri Lanka and to develop a comprehensive mathematical model for fuel economy characterization of internal combustion engine powered light duty vehicles. The results presented in the thesis emphasizes the significance of the adoption of a validated mathematical model for fuel economy characterization of ICE-powered LDVs which shall be providing a clear scientific basis for fuel economy estimations. Furthermore, the results also portray the importance of the development of localized driving cycles to reflect the local driving behaviour. Finally, as a recommendation, it’s strongly recommended to utilize the developed mathematical model along with the developed local driving cycles for fuel economy estimations of ICE-powered LDVs in varying driving conditions.

This research makes several key contributions that advance the state of knowledge in modeling real-world fuel economy of vehicles. The study puts forward a novel physics-based modeling approach to characterize fuel consumption, incorporating analytical formulations of tractive loads and engine auxiliaries. Unlike predominantly empirical methods in literature, the theoretical foundation provides a generalized capability to estimate fuel use across vehicle segments and driving patterns. The formulation of A/C load is particularly innovative, capturing factors like metabolic, radiation and ventilation loads specific to the local context. The research further makes a pioneering effort in spatial interpolation and analytics to construct driving cycles reflecting indigenous traffic conditions. The work also encompasses extensive field data gathering and rigorous multi-stage validation to demonstrate accuracy. Altogether, these efforts represent the first scientifically grounded characterization of on-road fuel economy tailored to Sri Lankan vehicles and driving habits. The frameworks for localized modeling and benchmark testing can be continually refined as new vehicle technologies emerge. Thus, the mission-oriented research makes important strides to enable data-driven transportation policy aimed at efficiency and emissions mitigation.

While the study makes important contributions, there are certain limitations that provide avenues for further work. The scope is currently constrained only to spark ignition and compression ignition internal combustion engine vehicles running on gasoline and diesel respectively. Emerging propulsion technologies like electric and hybrid electric vehicles still need to be incorporated into the modeling frameworks. Additionally, the field data gathering and spatial interpolation rely heavily on instruments like OBD devices and GPS that have accuracy limitations in terms of captured parameters. The subjectivity of route and sample selection for driving cycle development also leads to inherent biases. From an analytical perspective, simplifying assumptions are made in quantifying tractive loads and lumping minor auxiliaries. Validating the fuel consumption models against a wider range of vehicle categories can also reveal discrepancies. There is potential for machine learning techniques to enhance the model based on continuous real-world training data. On the whole, the accuracy range achieved in the high 80s to low 90s percentage indicates scope to advance the precision of the theoretical formulations. Addressing such research gaps

can further boost the utility of the predictive models in policymaking and consumer awareness around sustainable transportation.

6. Reference List

[1] International Energy Agency, "International Energy Agency (IEA) World Energy Outlook 2022," 2022. [Online]. Available: https://www.iea.org/reports/world-energy-outlook-2022/executive-summary. [Accessed: July 08, 2019].

[2] GFEI Global Fuel Economy Initiative, "About GFEI," [Online]. Available: https://www.globalfueleconomy.org/about-gfei. [Accessed: Oct. 12, 2019].

[3] Global Fuel Economy Initiative (GFEI), *Global Fuel Economy Initiative Handbook*, 2015.

[4] T. Sugathapala, "Fuel Economy of Light Duty Vehicles in Sri Lanka," Clean Air Sri Lanka, 2015.

[5] A. Bandivadekar, "On the road in 2035: reducing transportation's petroleum consumption and GHG emissions," Cambridge, MA: Massachusetts Institute Of Technology, 2008.

[6] J. Kuhlwein, G. John, and A. Bandivadekar, "Development Of Test Cycle Conversion Factors Among Worldwide Light Duty Vehicle CO2 Emission Standards," The International Council on Clean Transportation, 2014.

[7] J. I. Huertas et al., "Driving Cycles Based on Fuel Consumption," Energies, vol. 11, no. 11, 2018.

[8] E. Silvas, K. Hereijgers, H. Peng, T. Hofman, and M. Steinburch, "Synthesis of Realistic Driving Cycles With High Accuracy and Computational Speed, Including Slope Information," IEEE Transactions on Vehicular Technology, vol. 65, no. 6, pp. 4118–4128, 2016.

[9] "Vehicle Weight Classifications for the Emission Standards Reference Guide," 2017. [Online]. Available: https://www.epa.gov/emission-standards-reference-guide/vehicle-weight-classifications-emission-standards-reference-guide. [Accessed: 3rd November 2019].

[10] Open Government Licence v3.0. [Online]. Available: https://www.gov.uk/vehicle-weights-explained. [Accessed: Nov. 3, 2019].

[11] "Code of Federal Regulations (Vol. 5)," Department of Transportation, 2004.

[12] "Towing a Trailer," National Highway Traffic Safety Administration, 2002.

[13] Sri Lanka Parliament, "The Motor Traffic Act 2009 (Section 122)."

[14] "INDIA: LIGHT DUTY: EMISSIONS," 2018. [Online]. Available: https://www.transportpolicy.net/standard/india-light-duty-emissions/. [Accessed: Nov. 5, 2019].

[15] "Australia: Light Duty: Emissions," 2018. [Online]. Available: https://www.transportpolicy.net/standard/australia-light-duty-emissions/. [Accessed: Nov. 5, 2019].

[16] "China: Light Duty: Emissions," 2018. [Online]. Available: https://www.transportpolicy.net/standard/china-light-duty-emissions/. [Accessed: Nov. 5, 2019].

[17] "Japan: Light Duty: Emissions," 2018. [Online]. Available: https://www.transportpolicy.net/standard/japan-light-duty-fuel-economy/. [Accessed: Nov. 5, 2019].

[18] "European Union: Light Duty: Emissions," 2018. [Online]. Available: https://www.transportpolicy.net/standard/eu-vehicle-definitions/?title=eu:_vehicle_definitions. [Accessed: Nov. 5, 2019].

[19] Department of Census and Statistics - Sri Lanka, "Statistical Abstract 2018 (Chapter – 7)," 2018.

[20] Central Bank of Sri Lanka, "Economic and Social Statistics of Sri Lanka (Vol. XL)," 2018.

[21] E. Ericsson, "Driving pattern in urban areas-descriptive analysis and initial prediction model," Bulletin 185/3000 of Lunds University, 2000.

[22] O. Badran and M. Al-Momani, "Experimental investigation of factors affecting vehicle fuel consumption," 2007.

[23] D. Slavin, M. A. Abou-Nasr, D. P. Filev, and I. V. Kolmanovsky, "Empirical modeling of vehicle fuel economy based on historical data," in Proceedings of the International Joint Conference on Neural Networks, 2013, pp. 313.

[24] S. Gautam, "What Factors Affect Average Fuel Economy of US Passenger Vehicles?" 2010.

[25] J. Hilliard and S. Springer, "Fuel Economy in Road Vehicles powered by Spark Ignition Engines," 1984.

[26] F. Ament, D. E. Cole, and D. J. Patterson, "Heat Balance and Comparison at Part Load of a 1975 Chevrolet 350-Cubic-Inch V-8 and an Experimental 222-Cubic-Inch V-6 Engine, Final Report Project 320445," Dept. of Mech. Eng., University of Michigan, Dec. 1974.

[27] J. Y. Wong, "Theory of ground vehicles," 3rd ed., John Willey & Sons, Inc., 2001, pp. 255–260.

[28] J. G. Giles, "Gears and Transmissions," Automotive Technology Series, vol. 4, London: Butterworths, 1969.

[29] C. W. Coon and C. D. Wood, "Improvement of Automobile Fuel Economy," SAE paper 740969, 1974.

[30] D. J. Gasser and G. J. Huebner, "Energy and the Automobile--General Factors Affecting Vehicle Fuel Consumption," SAE paper 730518, 1973.

[31] F. An and F. Stodolsky, "Modeling the effect of engine assembly mass on engine friction and vehicle fuel economy," SAE paper 950988, 1995.

[32] R. B. Farrington and V. H. Johnson, "The impact of vehicle air-conditioning fuel use and what can be done to reduce it," in 13th annual earth technologies forum, Washington, DC, USA, Mar. 25–27, 2002, Washington, DC, Earth Technology Forum.

[33] J. Beouali and D. Clodic, "Fuel consumption of mobile air conditioning: method of testing and result," in 14th annual earth technologies forum, Washington, DC, USA, Apr. 22–24, 2003, Washington, DC, Earth Technology Forum.

[34] J. Lee et al., "Effect of the air-conditioning system on the fuel economy in a gasoline engine vehicle," Proceedings of the Institution of Mechanical Engineers, Part D: Journal of Automobile Engineering, vol. 227, no. 1, pp. 66–77, 2013.

[35] M. Kluger and J. Harris, "Fuel economy benefits of electric and hydraulic off engine accessories," SAE paper 2007-01- 0268, 2007.

[36] B. Murty et al., "Magnetorheological coupling based hydraulic power steering: low-cost solution for fuel economy improvement," SAE 2009-01-0046, 2009.

[37] M. Wellenzohn, "Improved fuel consumption through steering assist with power on demand," SAE paper 2008- 21-0046, 2008.

[38] T. Kiatsiriroat and T. Euakit, "Performance analyses of an automobile air-conditioning system with R22/R124/R152A refrigerant," Appl Thermal Engng, vol. 17, no. 11, pp. 1085–1097, 2008.

[39] H. K. David et al., "Air conditioning system of an intelligent vehicle cabin," Appl Energy, vol. 83, no. 6, pp. 545–557, 2006.

[40] S. Tsereqounis, M. McMillan, and R. Olree, "Engine oil effects on fuel economy in gm vehicles-separation of viscosity and friction modifier effects," SAE paper 982502, 1998.

[41] J. S. Welstand et al., "Evaluation of air conditioning operation and associated environmental conditions on vehicle emissions and fuel economy," SAE paper 2003-01-2247, 2003.

[42] T. Malik and C. Bullard, "Air conditioning HEV while stopped in traffic," SAE paper 2004-01-1513, 2004.

[43] T. H. Bradley and A. A. Frank, "Design, demonstrations and sustainability impact assessments for plug-in hybrid electric vehicles," Renewable Sustainable Energy Rev, vol. 13, no. 1, pp. 115–128, 2009.

[44] E. B. Ratts and J. S. Brown, "An experimental analysis of cycling in an automotive air conditioning system," Appl Thermal Engng, vol. 20, no. 11, pp. 1039–1058, 2000.

[45] O. Kaynakli and I. Horus, "An experimental analysis of automotive air conditioning system," Int Commun Heat Mass Transfer, vol. 30, no. 2, pp. 273–284, 2003.

[46] H. Nadamoto and A. Kubota, "Power saving with the use of variable displacement compressor," SAE paper 1999- 01-0875, 1999.

[47] T. C. Austin and K. H. Hellman, "Passenger Car Fuel Economy Trends and Influencing Factors," SAE paper 730790, 1973.

[48] D. Hahne, "A Continuously Variable Automatic Transmission for Small Front Wheel Drive Cars in Driveline '84," in Institution of Mechanical Engineers, 1984.

[49] B. Chen, S. A. Evangelou, and R. Lot, "Impact of Optimally Controlled Continuously Variable Transmission on Fuel Economy of a Series Hybrid Electric Vehicle," 2018 European Control Conference, ECC.

[50] D. Robinette et al., "Torque Converter Clutch Optimization: Improving Fuel Economy and Reducing Noise and Vibration," SAE Int. J. Engines, vol. 4, no. 1, pp. 94-105, 2011.

[51] J. Eckert et al., "Fuzzy gear shifting control optimization to improve vehicle performance, fuel consumption and engine emissions," Control Theory and Applications, The Institution of Engineering and Technology, [13], pp. 2658-2669, 2019.

[52] C. Marks and G. Niepoth, "Car Design for Economy and Emissions," SAE paper 750954, 1975.

[53] S. Zoepf, "Automotive Features; Mass Impact and Deployment Characterization," M.S. Thesis, Massachusetts Institute of Technology, 2011.

[54] U.S. Department of Energy Vehicle Technologies Program, "FY 2009 Progress Report for Lightweighting Materials," Washington, DC: Department of Energy.

[55] W. J. Joost, "The Journal of The Minerals, Metals & Materials Society," vol. 64, pp. 1032 - 1038, 2012.

[56] L. Cheah, "Cars on a Diet: The Material and Energy Impacts of Passenger Vehicle Weight Reduction in the U.S.," Ph.D. Thesis, Massachusetts Institute of Technology, 2010.

[57] Y. Kan, R. Shida, J. Takahashi, and K. Uzawa, "(Paper presented at the 10th Japan International SAMPE Symposium & Exhibition (JISSE-10), Tokyo, Japan)," 2007.

[58] D. Cole, "Automotive Fuel Economy, Fuel Economy in Road Vehicles Powered by Spark Ignition Engines," New York: Plenum Press, 1984.

[59] J. S. Priyadarshini et al., "Use of Aerodynamic Lift in Increasing the Fuel Efficiency of Heavy Vehicles," IOSR Journal of Mechanical and Civil Engineering, vol. 12, no. 4, pp. 2278–1684, 2015.

[60] W. H. Hucho and G. Sovran, "Aerodynamics of road vehicles," Annual Review of Fluid Mechanics, vol. 25, no. 1, pp. 485-537, 1993.

[61] W. Mayer and G. Wickern, "The new audi A6/A7 family-aerodynamic development of different body types on one platform," SAE International Journal of Passenger Cars-Mechanical Systems, vol. 4, no. 1, pp. 197-206, 2011.

[62] A. Chainani and N. Perera, "CFD Investigation of airflow on a model radio control race car," WCE 2008, 2-4 July, London, 2008.

[63] M. N. Sudin et al., "Review of research on vehicles aerodynamic drag reduction methods," International Journal of Mechanical and Mechatronics Engineering, vol. 14, no. 2, pp. 35–47, 2014.

[64] R. M. Wood, "Impact of advanced aerodynamic technology on transportation energy consumption," SAE Technical Paper 2004-01-1306, 2004.

[65] M. Bellman et al., "Reducing energy consumption of ground vehicles by active flow control," in ASME 2010 4th International Conference on Energy Sustainability, pp. 785- 793, American Society of Mechanical Engineers, 2010.

[66] Engineering ToolBox, "Drag Coefficient," [Online]. Available: https://www.engineeringtoolbox.com/drag-coefficient-d_627.html. [Accessed: 10-Nov-2019].

[67] The Physics HyperText Book, "Aerodynamic Drag," [Online]. Available: https://physics.info/drag. [Accessed: 11-Nov-2019].

[68] K. B. Kelly and H. J. Holcombe, "Aerodynamics for Body Engineers," in Automotive Aerodynamics, Progress in Technology Series, 16, Society of Automotive Engineers, 1978.

[69] C. W. Can, "Potential for Aerodynamic Drag Reduction in Car Design," in Impact of Aerodynamics on Vehicle Design, Technological Advances in Vehicle Design Series, SP3, Inderscience Enterprises Limited, 1983.

[70] G. Rousillon, J. Marzin, and J. Bourhis, "Contribution to the Accurate Measurement of Aerodynamic Drag by the Deceleration Method," in Advances in Road Vehicle Aerodynamics, BHRA Fluid Engineering, Cranfield, England, 1973.

[71] R. A. White and H. H. Korst, "The Determination of Vehicle Drag Contributions from Coastdown Tests," SAE Transactions, vol. 81, paper 720099, 1972.

[72] G. W. Eaker, "Wind Tunnel-to-Road Aerodynamic Drag Correlation," in Research in Automotive Aerodynamics, Society of Automotive Engineers, Special Publication SP-747, 1988.

[73] G. A. Necati, "Measurement and Test Techniques," in Aerodynamics of Road Vehicles, London: Butterworths-Heinemann, 1990.

[74] W. H. Hucho, L. J. Janssen, and H. J. Emmelmann, "The Optimization of Body Details - A Method for Reducing the Aerodynamic Drag of Road Vehicles," Society of Automotive Engineers, paper 760185, 1976.

[75] C. Marks and G. Niepoth, "Car Design for Economy and Emissions," SAE paper 750954, 1975.

[76] T. C. Austin and K. H. Hellman, "Passenger Car Fuel Economy-Trends and Influencing Factors," SAE paper 730790, 1973.

[77] T. French, "Tyre Technology," Bristol and New York: Adam Hilger, 1989.

[78] V. E. Gough, "Structure of the Tyre," in Mechanics of Pneumatic Tyres, Monograph 122, Washington, DC: the National Bureau of Standards, 1971.

[79] D. F. Moore, "The Friction of Pneumatic Tyres," Amsterdam: Elsevier, 1975.

[80] "Vehicle Dynamics Terminology," SAE J670e, Society of Automotive Engineers, 1978.

[81] T. French, "Construction and Behaviour Characteristics of Tyres," in Proc. of the Institution of Mechanical Engineers. Automobile Division, AD 14/59.

[82] H. C. A. Van Eldik and H. B. Pacejka, "The Tyre as a Vehicle Component," in Mechanics of Pneumatic Tyres, Monograph 122, Washington, DC: the National Bureau of Standards, 1971.

[83] M. Djordjevic, "Improvement fuel consumption used low rolling resistance tyres," in Scientific Conference PNEUMATICI, Kikinda, Serbia, 2006.

[84] R. Rajesh, "Vehicle Dynamics and Control," University of Minnesota, Minneapolis, MN, 2006.

[85] G. Paterlini, "Rolling Resistance Validation," [Online]. Available: mndot.gov/research/TS/2015/201539.pdf. [Accessed: 13-Nov-2019].

[86] L. R. Evans et al., "Tyre Fuel Efficiency Consumer Information Program Development," National Technical Information Services, Springfield, Virginia, 2009.

[87] K. A. Grosch and A. Schallamach, "Tyre Wear at Controlled Slip," Wear, vol. 4, pp. 356 – 371, 1961.

[88] NHTSA, "Tyre Pressure Maintenance – A Statistical Investigation, April," 2009, DOT HS 811 086, Washington, DC: National Highway Traffic Safety Administration.

[89] C. Schernus et al., "Turbocharging of downsized gasoline DI engines with 2 and 3 cylinders," SAE paper 2011-24-0138, 2011.

[90] N. Fraser et al., "Challenges for increased efficiency through gasoline engine downsizing," SAE paper 2009-01-1053, 2009.

[91] K. J. Douglas, N. Milovanovic, and D. Blundell, "Fuel economy improvement using combined CAI and cylinder deactivation (CDA) – an initial study," SAE paper 2005- 01-0110, 2005.

[92] T. Barlow et al., "A reference book of driving cycles for use in the measurement of road vehicle emissions," London: Department for Transport, HMSO, 2009.

[93] C. J. Oglieve, M. Mohammadpour, and H. Rahnejat, "Optimization of vehicle transmission and gear-shifting strategy for the minimum fuel consumption and the minimum nitrogen oxide emissions," 2017.

[94] O. Dingel et al., "Model-Based Assessment of Hybrid Powertrain Solutions," SAE Technical Papers, no. June, pp. 2016–2018, 2018.

[95] E. J. Lees, "Fuel consumption measurement from driving cycles," Measurement Science and Technology, vol. 1, no. 6, pp. 586– 593, 1990.

[96] B. Heywood, "Internal combustion engine fundamentals," New York: McGraw-Hill, 1988.

[97] P. Thiruvengadam et al., "Comparison of energy usage of three passenger cars in real-world driving: Hybrid electric vehicle, plug-in hybrid electric vehicle, and internal combustion engine," Energy Policy, vol. 39, no. 9, pp. 6007–6016, 2011.

[98] Y. Wang, L. Lu, and X. Han, "Real-world fuel economy and CO2 emissions of plug-in hybrid electric vehicles," Applied Energy, vol. 88, no. 5, pp. 2001–2013, 2011.

[99] G. Meyer, "Compliance and emissions testing of a light-duty vehicle on a chassis dynamometer," in 2004 IEEE Vehicle Power and Propulsion Conference, pp. 391–396, IEEE, 2004.

[100] W. H. Hucho, "Aerodynamics of road vehicles: From fluid mechanics to vehicle engineering," Berlin: Springer-Verlag, 1987.

[101] W. H. Hucho, "Aerodynamics of road vehicles," Annual Review of Fluid Mechanics, vol. 25, pp. 485–537, 1993.

[102] T. Gillespie, "Fundamentals of vehicle dynamics," Warrendale, PA: Society of Automotive Engineers, 1992.

[103] P. A. Lakshminarayanan, "Fundamentals of vehicle dynamics," 1st ed., SAE International, 2017.

[104] J. R. Davis, "Vehicle Propulsion Systems," CRC Press, 2013.

[105] H. G. Koelman and E. B. Leusden, "Aerodynamic Drag Reduction and Noise Control," SAE International, Warrendale, PA, 1999.

[106] P. A. Tipler, "Physics for Scientists and Engineers: Volume 1," New York: W. H. Freeman, 1999.

[107] J. D. Anderson, "Fundamentals of aerodynamics," McGraw-Hill, 2010.

[108] E. Gutierrez-Miravete, "Vehicle aerodynamics: Recent progress and new problems," Progress in Aerospace Sciences, vol. 55, pp. 1–17, 2012.

[109] S. T. Ho, K. C. Lee, and S. Abdullah, "The role of aerodynamics in automotive," International Journal of Engineering and Technology, vol. 5, no. 1, pp. 30–38, 2008.

[110] H. El-Katatny, "Aerodynamics simulation in automotive industry," Master's thesis, Ain Shams University, Cairo, 2003.

[111] G. Paterlini, "Rolling Resistance Validation," Tech. Rep., Minnesota Department of Transportation, 2015.

[112] P. Y. Papalambros and D. J. Wilde, "Principles of Optimal Design: Modeling and Computation," Cambridge University Press, 2000.

[113] W. J. Palm, "System dynamics," 2nd ed., McGraw-Hill Higher Education, 2006.

[114] C. Y. Hsu, "Finite element analysis concepts: Via solidworks," World Scientific Publishing Co. Inc., 2009.

[115] D. D. DeCarlo and J. M. Rubin, "Applied optimal estimation," 1st ed., MIT Press, 1979.

[116] J. J. Duderstadt and L. J. Hamilton, "Nuclear reactor analysis," Wiley, 1976.

[117] S. E. Schwarz, "Aerospace engineering: From the ground up," in IEEE Potentials, vol. 18, no. 4, pp. 22–27, 1999.

[118] W. E. Deming, "Quality, productivity, and competitive position," MIT Center for Advanced Engineering Study, 1982.

[119] J. E. Shigley and C. R. Mischke, "Mechanical Engineering Design," 7th ed., McGraw-Hill Higher Education, 2003.

[120] G. P. Walsh and G. H. Allen, "Automobile engineering," 3rd ed., CBS Publishers and Distributors Pvt Ltd, 2003.

[121] D. V. Rosato and M. M. Rosato, "Plastics engineering, manufacturing, & data handbook," 1st ed., Springer Science & Business Media, 2001.

[122] E. Wever, "Introduction to Automotive Engineering," 2nd ed., Routledge, 2017.

[123] J. K. Lefebvre, "Gas Turbine Combustion: Alternative Fuels and Emissions," 3rd ed., CRC Press, 2010.

[124] M. G. Say and F. A. Engin, "Internal combustion engine in theory and practice," 2nd ed., The M.I.T. Press, 1972.

[125] M. P. Walsh and A. A. Khalid, "Vehicle aerodynamics: Past, present and future perspectives," Progress in Aerospace Sciences, vol. 78, pp. 16–26, 2015.

[126] S. H. Frankel, "Understanding smart sensors," Artech House, 2000.

[127] R. G. Budynas and K. J. Nisbett, "Shigley's Mechanical Engineering Design," 10th ed., McGraw-Hill Education, 2015.

[128] E. A. Stinson and E. J. Finn, "Aerodynamics of high-speed ground transportation vehicles," SAE International, 2000.

[129] D. H. K. Tsang, "Dynamics of railway bridges," Taylor & Francis, 2017.

[130] R. M. Schmidt and S. M. Boggs, "Encyclopedia of automotive engineering," Wiley, 2015.

[131] J. Heisler, "Advanced Engine Technology," 4th ed., SAE International, 2012.

[132] K. F. Kuhne and R. A. Johnson, "Engineering mechanics: An introduction to dynamics," Prentice Hall, 1995.

[133] S. C. Yadav, "Elements of Mechanical Engineering," S. Chand Publishing, 2008.

[134] J. C. Lin, "Fluid mechanics for engineers," 3rd ed., CRC Press, 2012.

[135] E. A. Spalding and J. R. Woolley, "Applied gas dynamics," Taylor & Francis, 1975.

[136] D. J. Peckham, "Aerodynamics for engineering students," Elsevier, 2012.

[137] W. A. Wood, "Fundamentals of fluid dynamics," CRC Press, 2012.

[138] M. J. Moran and H. N. Shapiro, "Fundamentals of Engineering Thermodynamics," 8th ed., Wiley, 2014.

[139] J. T. C. Liu and J. J. Liu, "Analysis of engineering cycles," 2nd ed., Cambridge University Press, 2009.

[140] C. J. Mifsud, "Automotive aerodynamics handbook," Taylor & Francis, 1999.

[141] W. Bolton, "Mechatronics: Electronic control systems in mechanical and electrical engineering," Pearson Education, 2019.

[142] R. L. M. Asnani, "Automobile Engineering," Prentice Hall of India, 2007.

[143] A. K. Agarwal, "Automobile Engineering," Khanna Publishers, 2007.

[144] S. Mahapatra, "Automobile engineering," Tata McGraw-Hill Education, 2008.

[145] J. C. Mahapatra, "Automobile Engineering," Jain Brothers, 2007.

[146] G. B. Nagaraju, "Automobile Engineering," Pearson Education India, 2006.

[147] K. M. Gupta, "Automobile Engineering," Satya Prakashan, 2005.

[148] V. K. Jain, "Automobile Engineering," Metropolitan Book Co., 2008.

[149] K. C. Arora, "Automobile Engineering," Tata McGraw-Hill Education, 2001.

[150] V. D. Prasad and A. M. Ambekar, "Automobile Engineering," Tata McGraw-Hill Education, 2005.

[151] M. N. Srinivasan, "Automobile Engineering," Laxmi Publications, 2008.

[152] R. K. Rajput, "Automobile Engineering," S. Chand & Company Ltd., 2008.

[153] H. K. Patel and H. D. Patel, "Automobile Engineering," Charotar Publishing House Pvt. Ltd., 2008.

[154] V. R. Goswami and A. M. Chitale, "Automobile Engineering," Tata McGraw-Hill Education, 2008.

[155] M. Heisler, "Vehicle and engine technology," 2nd ed., Elsevier, 2000.

[156] J. Denton, "Aftertreatment control strategies for ultra-low NOx emissions from diesel engines," SAE International, 2005.

[157] E. Z. Nadkarni, "Vehicle Dynamics and Control," CRC Press, 2011.

[158] J. Y. Wong, "Theory of ground vehicles," 4th ed., Wiley, 2008.

[159] R. H. Stone, "Introduction to internal combustion engines," 4th ed., Palgrave Macmillan, 2012.

[160] H. Rupasinghe and T. M. Rengarasu, "Development of driving cycles for Galle," in MERCon 2018 - 4th International Multidisciplinary Moratuwa Engineering Research Conference, 2018, pp. 108–113.

[161] U. Galgamuwa, L. Perera, and S. Bandara, "A Representative Driving Cycle for the Southern Expressway Compared to Existing Driving Cycles," Transportation in Developing Economies, vol. 2, no. 22, Springer International Publishing, 2016.

[162] M. Tutuiana et al., "Development of a Worldwide harmonized Light Duty driving Test Cycle - Draft Technical Report," 2013.

[163] P. Mock et al., "The WLTP: How a new test procedure for cars will affect fuel consumption values in the EU," International Council on Clean Transportation, 2014.

[164] E. Milkiins and H. Watson, "Comparison of Urban Driving Patterns," SAE Technical Paper Series 830939, 1983.

[165] T. J. Barlows et al., "A Reference Book of Driving Cycles to Use in Measurement of Road Vehicle Emission," 3rd ed., TRL, 2009.

[166] S. Pandian, S. Gokhale, and A. K. Goshal, "Evaluating Effects of Traffic and Vehicle Characteristics on Vehicular Emissions near Traffic Intersections," Transportation Research Part D, vol. 14, pp. 180-196, 2009.

[167] X. Zhang, D.-J. Zhao, and J.-M. Shen, "A Synthesis of Methodologies and Practices for Developing Driving Cycles," Energy Procedia, vol. 16, pp. 1863-1873, 2012.

[168] H. Y. Tong and W. T. Hung, "A Framework for Developing Driving Cycles with on Road Driving Data," Transport Review, vol. 30, pp. 589-615, 2010.

[169] M. M. Davari, J. Jerrelind, and A. Stensson Trigell, "Energy efficiency analyses of a vehicle in modal and transient driving cycles including longitudinal

and vertical dynamics," Transportation Research Part D: Transport and Environment, vol. 53, pp. 263–275, 2017.

[170] "OJ L 60, 2.3.2013, p. 52–128, Special edition in Croatian: Chapter 13 Volume 063 P. 166 – 242.

[171] H. Steven, "Worldwide Harmonized Motorcycle Emissions Certification Procedure," Tech. Rep. 9, pp. 1–131, 2002.

[172] N. Unies, "Global registry Addendum 2: Global technical regulation No. 2 Proposal to amend global technical regulation No. 2 (Worldwide harmonized motorcycle emission test cycle) I. Objective of the proposal," vol. 2, no. 2, pp. 1–11, 2011.

[173] "Regulation (EC) No 715/2007 of the European Parliament and of the Council of 20 June 2007 on type approval of motor vehicles with respect to emissions from light passenger and commercial vehicles (Euro 5 and Euro 6) and on access to vehicle repair and maintenance information". Eur-lex.europa.eu. [Online]. Available: http://eur-lex.europa.eu. [Accessed: 02-Feb-2011].

[174] [4] G. Notifications, "The Gazette of the Democratic Socialist Republic of Sri Lanka," vol. 507, no. 26, pp. 8–9, 2008.

[175] [5] "Statistical Pocket Book 2021," [Online]. Available: http://www.statistics.gov.lk/pocket%20book/. [Accessed: 12-May-2022].

[176] [6] "Commission Regulation (EU) No 459/2012 of 29 May 2012 amending Regulation (EC) No 715/2007 of the European Parliament and of the Council and Commission Regulation (EC) No 692/2008 as regards emissions from light passenger and commercial vehicles (Euro 6)". Eur-lex.europa.eu. [Online]. Available: http://eur-lex.europa.eu. [Accessed: 01-Jun-2012].

[177] G. Gibson et al., "Two- and three-wheeled vehicles and quadricycles," IEA ETSAP - Technology Brief, January, pp. 1–11, 2013.

[178] F. Report, "Two-and-Three-Wheelers in India. Final Report," Innovative Transport Solutions Pvt. Ltd., 2009.

[179] E. G. Giakoumis, *Driving and Engine Cycles*, pp. 1–408, 2016. [Online]. Available: https://doi.org/10.1007/978-3-319-49034-2

[180] S. Gota, "Two-and-Three-Wheelers: A Policy Guide to Sustainable Mobility Solutions for Motorcycles," pp. 40. [Online]. Available: https://www.sutp.org/files/contents/documents/resources/A_Sourcebook/SB4_Vehicles and Fuels/GIZ_SUTP_TUMI_SB4c_Two- and Three-Wheelers_EN.pdf

[181] R. Sithananthan, Masilamani, and R. Kumar, "Development of Indian Motorcycle Driving Cycles, Evaluation for Fuel Economy and Emission," SSRN Electronic Journal, 2022. [Online]. Available: https://doi.org/10.2139/ssrn.4013438

[182] A. Fotouhi and M. Montazeri-Gh, "Tehran Driving Cycle Development Using the K-Means Clustering Method," *Scientia Iranica*, vol. 20, no. 2, pp. 286–93, 2013. [Online]. Available: https://doi.org/10.1016/j.scient.2013.04.001

[183] Y. Peng, Z. Yuan, and Y. Yang, "A Driving Cycle Construction Methodology Combining K-Means Clustering and Markov Model for Urban Mixed Roads," *Proceedings of the Institution of Mechanical Engineers, Part D: Journal of Automobile Engineering*, vol. 234, no. 2–3, pp. 714–24, 2020. [Online]. Available: https://doi.org/10.1177/0954407019848873

[184] OJ L 60, 2.3.2013, p. 52–128, Special edition in Croatian: Chapter 13 Volume 063 P. 166 – 242.

[185] H. Steven, "Worldwide Harmonized Motorcycle Emissions Certification Procedure," Tech. Rep. 9, pp. 1–131, 2002.

[186] G. Notifications, "The Gazette of the Democratic Socialist Republic of Sri Lanka," vol. 507, no. 26, pp. 8–9, 2008.

[187] N. Unies, "Global registry Addendum 2: Global technical regulation No. 2 Proposal to amend global technical regulation No. 2 (Worldwide harmonized motorcycle emission test cycle) I. Objective of the proposal," vol. 2, no. 2, pp. 1–11, 2011.

[188] "Regulation (EC) No 715/2007 of the European Parliament and of the Council of 20 June 2007 on type approval of motor vehicles with respect to emissions from light passenger and commercial vehicles (Euro 5 and Euro 6) and on access to vehicle repair and maintenance information". Eur-lex.europa.eu. Retrieved 2011-02-02

[189] "Commission Regulation (EU) No 459/2012 of 29 May 2012 amending Regulation (EC) No 715/2007 of the European Parliament and of the Council and Commission Regulation (EC) No 692/2008 as regards emissions from light passenger and commercial vehicles (Euro 6)". Eur-lex.europa.eu. Retrieved 2012-06-01

[190] G. Gibson et al., "Two- and three-wheeled vehicles and quadricycles," *IEA ETSAP - Technology Brief*, January, pp. 1–11, 2013.

[191] F. Report, "Two-and-Three-Wheelers in India. Final Report," Innovative Transport Solutions Pvt. Ltd., 2009.

[192] "ECE TRANS 180a2app1e | Download Free PDF | Emission Standard | Motorcycle," *Scribd*. https://www.scribd.com/document/456421516/ECE-TRANS-180a2app1e (accessed Jun. 10, 2021).

[193] E. G. Giakoumis, "Driving and engine cycles," *Driving and Engine Cycles*, pp. 1–408, 2016. [Online]. Available: https://doi.org/10.1007/978-3-319-49034-2

[194] "WLTP-GS-TF-41 GTR 15 annex 1 and annex 2 08," (n.d.).

[195] G. Medeiros, S. De Andrade, F. Wesley, and C. De Ara, "Energy and Kinematics," 2020.

[196] W. Informal, G. T. R. No, I. After, G. Registry, G. T. R. No, C. Parties, G. T. R. No, and C. Parties, "Transmitted by the informal group on WMTC Informal document No. 11(June)," pp. 3–6, 2008.

[197] F. An, D. Gordon, H. He, D. Kodjak, and D. Rutherford, "Passenger vehicle greenhouse gas and fuel economy standards: A global update," Washington DC: The International Council on Clean Transportation, July 2007.

[198] J. Kasab and S. Velliyiur, "Analysis of greenhouse gas emission reduction potential of light duty vehicle technologies in the European Union for 2020-2025," Washington DC: Project report of Ricardo Inc. on behalf of the International Council on Clean Transportation, 13 April 2012. Addendum: 17 May 2012.

[199] J. Kuhlwein, J. German, and A. Bandivadekar, "Development of Test Cycle Conversion Factors Among Worldwide Light Duty Vehicle CO2 Emission Standards," *The International Council on Clean Transportation - ICCT*, September, p. 64, 2014.

[200] J. Welstand, H. Haskew, R. Gunst, and O. Bevilacqua, "Evaluation of the Effects of Air Conditioning Operation and Associated Environmental Conditions on Vehicle Emissions and Fuel Economy," *SAE Technical Paper 2003-01-2247*, 2003.

[201] H. Nadamoto and A. Kubota, "Power saving with the use of variable displacement compressor," *SAE paper 1999- 01-0875*, 1999.

[202] Q. Zhaogang, "Advances on air conditioning and heat pump system in electric vehicles – A review," *Renewable and Sustainable Energy Reviews*, vol. 38, pp. 754-764, 2014.

[203] Z. Zhang, J. Wang, X. Feng, L. Chang, Y. Chen, and X. Wang, "The solutions to electric vehicle air conditioning systems: A review," *Renewable and Sustainable Energy Reviews*, vol. 91, pp. 443–463, 2018. https://doi.org/10.1016/J.RSER.2018.04.005

[204] M. L. M. Tasuni, Z. A. Latiff, H. Nasution, M. R. M. Perang, H. M. Jamil, and M. N. Misseri, "Performance of a water pump in an automotive engine cooling system," *Jurnal Teknologi*, vol. 78, no. 10–2, pp. 47–53, 2016.

[205] B. M. Patel, A. J. Modi, and P. P. Rathod, "Analysis on Engine Cooling Water Pump of Car and Significance of its Geometry," *Intl. Journal of Mechanical Engineering and Technology*, vol. 4, no. 3, pp. 100-107, 2013.

[206] X. Wang, X. Liang, Z. Hao, and R. Chen, "Comparison of Electrical and Mechanical Water Pump Performance in Internal Combustion Engine," *International Journal of Vehicle Systems Modelling and Testing*, vol. 10, no. 3, pp. 205–223, 2015. https://doi.org/10.1504/IJVSMT.2015.070155

[207] G. Cho, H. Wi, J. Lee, J. Park, and K. Park, "Effect of Alternator Control on Vehicle Fuel Economy," *Transactions of KSAE*, vol. 17, no. 2, pp. 20-25, 2008.

[208] M. Bradfield, "Improving Alternator Efficiency Measurably Reduces Fuel Costs," *Remy, Inc*, pp. 1–31, 2008.

[209] A. P. Roskilly, R. Palacin, and J. Yan, "Novel technologies and strategies for clean transport systems," *Appl Energy*, vol. 157, pp. 563–6, 2015.

[210] P. Weldon, P. Morrissey, and M. O'Mahony, "Environmental impacts of varying electric vehicle user behaviours and comparisons to internal combustion

engine vehicle usage–An Irish case study," *J Power Sources*, vol. 319, pp. 27–38, 2016.

[211] X. K. Wu, D. Freese, A. Cabrera, and W. A. Kitch, "Electric vehicles' energy consumption measurement and estimation," *Transp Res D Transp Environ*, vol. 34, pp. 52–67, 2015.

[212] M. U. Cuma and T. Koroglu, "A comprehensive review on estimation strategies used in hybrid and battery electric vehicles," *Renew Sustain Energy Rev*, vol. 42, pp. 517–31, 2015.

[213] ISO 8996, "Ergonomics of Thermal Environments – Determination of Metabolic Heat Production. ISO", Geneva,1989.

[214] "Non-Communicable Disease Risk Factor Survey Sri Lanka" (PDF). World Health Organization. 2015. p. 81.

[215] R. Martinez et al., "Height and body-mass index trajectories of school-aged children and adolescents from 1985 to 2019 in 200 countries and territories: a pooled analysis of 2181 population-based studies with 65 million participants," *The Lancet*, vol. 396, no. 10261, pp. 1511–1524, Nov. 2020. doi:10.1016/S0140-6736(20)31859-6

[216] G. Havenith, I. Holmér, and K. Parsons, "Personal factors in thermal comfort assessment: Clothing properties and metabolic heat production," *Energy and Buildings*, vol. 34, pp. 581-591, 2002.

[217] M. A. Fayazbakhsh and M. Bahrami, "Comprehensive modeling of vehicle air conditioning loads using heat balance method," *SAE Technical Papers*, vol. 2(x), 2013. https://doi.org/10.4271/2013-01-1507

[218] Department of Meteorology. (2017). Retrieved July 25, 2021, from https://www.meteo.gov.lk

[219] D. Hara and G. O. Özgen, "Investigation of Weight Reduction of Automotive Body Structures with the Use of Sandwich Materials," *Transportation Research Procedia*, vol. 14, pp. 1013–1020, 2016. https://doi.org/10.1016/j.trpro.2016.05.081

[220] "Square Footage Help," 2015. Retrieved July 29, 2021, from https://www.secondskinaudio.com/square-footage-help/

[221] O. Abdulsalam, B. Santoso, and D. Aries, "Cooling Load Calculation and Thermal Modeling for Vehicle by MATLAB," *International Journal of Innovative Research in Science, Engineering and Technology*, vol. 3297(5), pp. 3052–3060, 2015. https://doi.org/10.15680/IJIRSET.2015.0405076

[222] "Solar elevation angle (for a day) Calculator," 2014. Retrieved October 2, 2021, from https://keisan.casio.com/exec/system/1224682277

[223] ASHRAE. (2017). Hvac System Design Software. Ashrae, 2nd. http://www.carrier.com/commercial/en/us/software/hvac-system-design/

[224] ITU-R. (1990). Report P.1008-1: Reflection from the surface of the Earth

[225] "Surface Absoptivity," 2016. Retrieved August 2, 2021, from https://www.engineeringtoolbox.com/radiation-surface-absorptivity-d_1805.html

[226] "Body dimensions," 2018. Retrieved June 20, 2021, from https://www.automobiledimension.com/

[227] S. Gota, "Two-and-Three-Wheelers: A Policy Guide to Sustainable Mobility Solutions for Motorcycles," 2018. Retrieved from https://www.sutp.org/files/contents/documents/resources/A_Sourcebook/SB4_Vehicles-and-Fuels/GIZ_SUTP_TUMI_SB4c_Two- and Three-Wheelers_EN.pdf.

[228] H. Khayyam, A. Z. Kouzani, and E. J. Hu, "Reducing Energy Consumption of Vehicle Air Conditioning System by an Energy Management System," Presented in *IEEE The 4th International Green Energy Conference*, China, 2009.

[229] D. J. Allen and M. P. Lasecki, "Thermal Management Evolution and Controlled Coolant Flow," *SAE Technical Paper Series 2001-01-1732*, 2001.

[230] SAE International, *Automotive Handbook*, 8th Edition, Robert Bosch, Plochigen, pp. 952-968, 2011.

[231] X. Wang, X. Liang, Z. Hao, and R. Chen, "Comparison of electrical and mechanical water pump performance in internal combustion engine," *International Journal of Vehicle Systems Modelling and Testing*, vol. 10, no. 3, pp. 205–223, 2015. https://doi.org/10.1504/IJVSMT.2015.070155

[232] R. Herkommer, “Ways toward energy saving in hydraulic steering system,” in *3rd International Fluid Power Conference, IFK02*, vol. 1, pp. 465–474, Aachen, Germany, March 2002, ISBN 3–8265–9900–4.

[233] C. Breitfeld et al., “Actuator principles for integrated chassis control system - a comparison,” in *3rd International Fluid Power Conference*, vol. 1, pp. 399–418, Aachen, Germany, March 2002, ISBN 3–8265–9900–4.

[234] C. R. Ferguson and A. T. Kirkpatrick, *Internal Combustion Engines*, 3rd ed. Wiley, 2020, pp. 15.

[235] A. Irimescu, l. Mihon, and g. Pãdure, “Automotive Transmission Efficiency Measurement Using a Chassis Dynamometer,” *International Journal of Automotive Technology*, vol. 12, no. 4, pp. 555–559, 2011.

[236] “Brake Specific Fuel Consumption (BSFC),” https://x-engineer.org/brake-specific-fuel-consumption-bsfc/. [Online]. Available: https://x-engineer.org/brake-specific-fuel-consumption-bsfc/. [Accessed: 31-Dec-2022].

[237] "Volume Correction Factors - Gasoline," July 2018.

[238] R. Sok et al., "Thermal Efficiency Improvement of a Lean-Boosted Spark Ignition Engine by Multidimensional Simulation with Detailed Chemical Kinetics," *International journal of automotive engineering*, vol. 6, pp. 97-104, 2015.

[239] H. Mu et al., "Technical research on improving engine thermal efficiency," *Advances in Mechanical Engineering*, vol. 14, 2022.

[240] J. Kim et al., "Analysis on the operating performance of 5-kW class solid oxide fuel cell-internal combustion engine hybrid system using spark-assisted ignition," *Applied Energy*, vol. 260, p. 114231, 2020.

[241] F. Moreno et al., "Efficiency and emissions in a vehicle spark ignition engine fueled with hydrogen and methane blends," *International Journal of Hydrogen Energy*, vol. 37, pp. 11495-11503, 2012

7. Annexture I – The Driving Cycle Development Programs

Barlow et al. [159] have classified all 256 driving cycles into 28 driving cycle development programs as listed below:

1. EU Legislative Cycles - European test cycles used for type approval purposes – cars, HGVs & buses;

2. US Cycles - A variety of test cycles from the USA including their type approval cycles– cars, HGVs & buses;

3. Japanese Legislative Cycles - Test cycles used for type approval purposes in Japan – cars;

4. Legislative motorcycle cycles - Harmonized worldwide type approval test cycles for motorcycles;

5. WSL (Warren Spring Laboratory) cycles - Car test cycles developed by TRL over the Stevenage and Hitchin routes, used by the former Warren Spring Laboratory for road tests;

6. TRAMAQ UG 214 - Test cycles developed within the DfT TRAMAQ programme, project UG214 – cars, vans, HGVs & buses;

7. Millbrook - Test cycles developed by Millbrook Proving Ground – HGVs & buses;

8. OSCAR - Test cycles developed within the European 5th Framework project: OSCAR – cars;

9. ARTEMIS driving cycle - Test cycles developed within the European 5th Framework project: ARTEMIS - cars;

10. EMPA driving cycles - Swiss test cycles developed by EMPA for the UBA;

11. Handbook driving cycles - The German/Austrian/Swiss (DACH) Handbook of emission factors;

12. MODEM-IM driving cycles - Short test cycles developed for inspection & maintenance purposes within the JCS project;

13. INRETS driving cycles - Test cycles developed by INRETS from data logged around Lyon, France;

14. INRETS short cycles (cold starts) - Short versions of the INRETS driving cycles;

15. MODEM driving cycles - Realistic driving cycle developed within the MODEM project, based on data from 60 cars in normal use in 6 towns in the UK, France and Germany;

16. ARTEMIS WP3141 - Additional test cycles for cars derived within the ARTEMIS project, based on data collected in Naples;

17. MODEM-Hyzem for passenger cars - Test cycles developed for evaluating hybrid vehicles;

18. Driving cycles for passenger cars with professional use - Test cycles developed by INRETS from data collected from cars used for business purposes;

19. Driving cycles for light vans (1.3 - 1.7 tonnes) - Test cycles developed by INRETS for small vans;

20. Driving cycles for 2.5 tonnes vans - Test cycles developed by INRETS for medium vans;

21. Driving cycles for 3.5 tonnes vans - Test cycles developed by INRETS for large vans;

22. MTC cycles - Test cycles developed by MTC for cars;

23. TUG cycles - Test cycle developed by TUG, Graz, to evaluate the effects of gradient;

24. TRRL cycles - Stylised test cycles developed by TRRL, based on logged data;

25. TRL M25 - High-speed car test cycle developed by TRL, based on data collected on the M25 motorway;

26. BP bus cycle - Bus test cycle developed by BP;

27. TNO bus - Bus test cycle developed by TNO, The Netherlands;

28. FHB motorcycle cycles - Motorcycle test cycles developed by Biel University of applied science, Switzerland.

8. Annexture II - The Comparison among the Performance Values of the Most Commonly Used Driving Cycles

The comparison among the performance values of the most used driving cycles is discussed here.

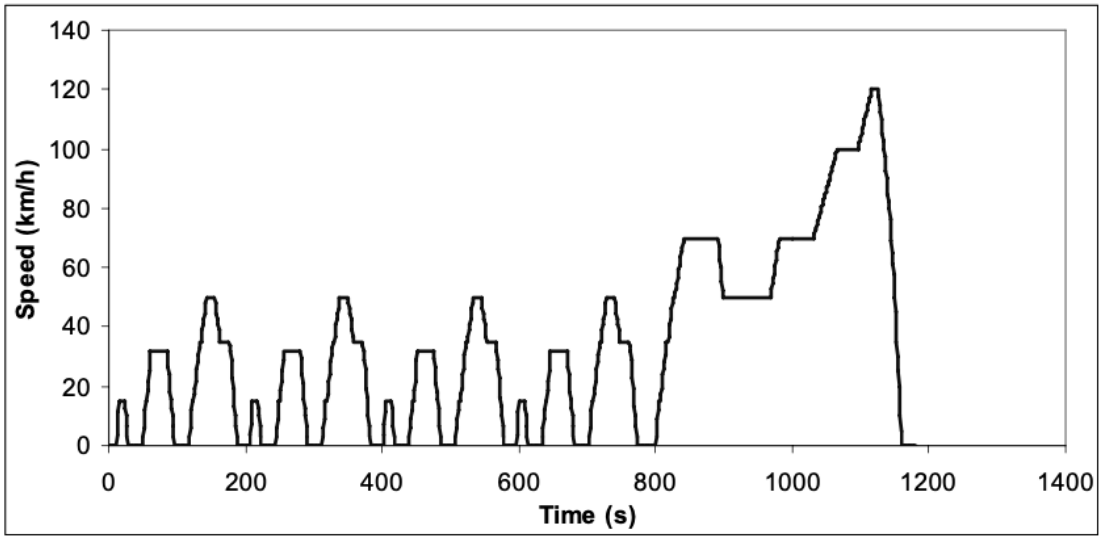

Figure 70 : New European Driving Cycle (NEDC) - Adopted from reference [159].

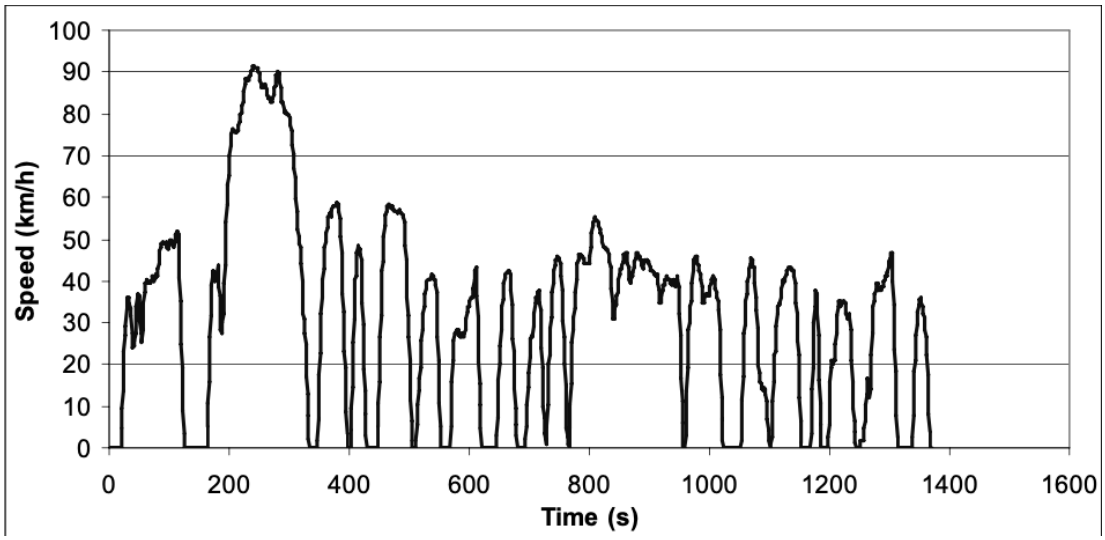

Figure 71: Federal Test Procedure (FTP)-72 driving cycle - Adopted from reference [159].

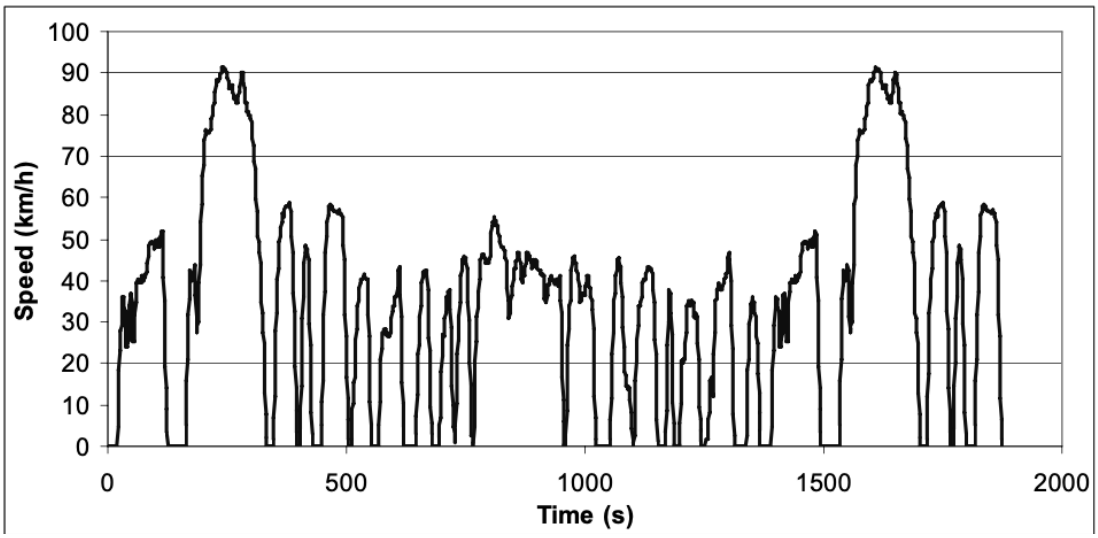

Figure 72: FTP-75 driving cycle - Adopted from reference [159].

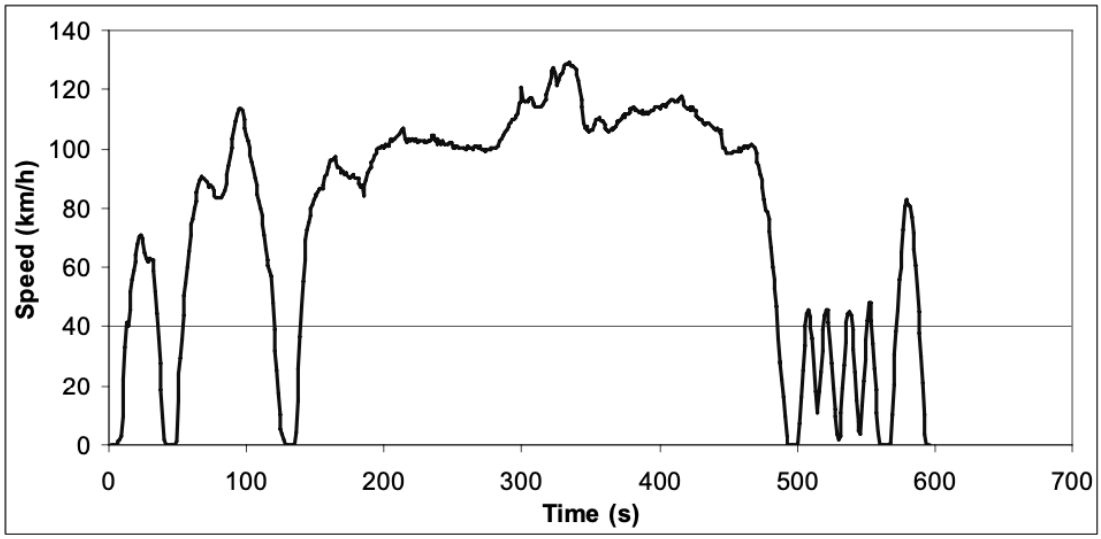

Figure 73: US06 Supplemental Federal Test Procedure (SFTP) driving cycle - Adopted from reference [159].

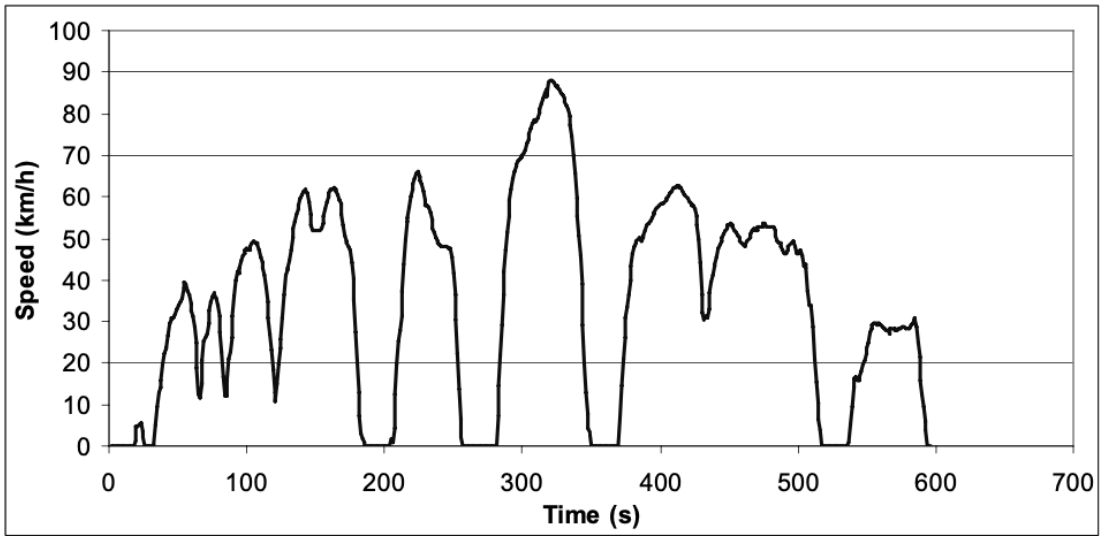

Figure 74: SC03 SFTP driving cycle - Adopted from reference [159].

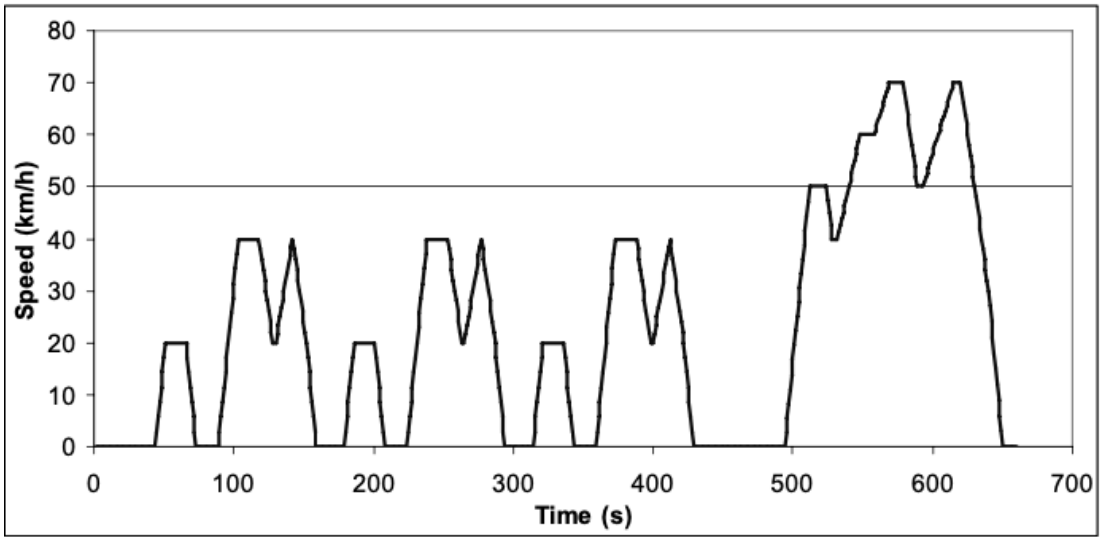

Figure 75: Japanese (JP) 10-15 Mode driving cycle - Adopted from reference [159].

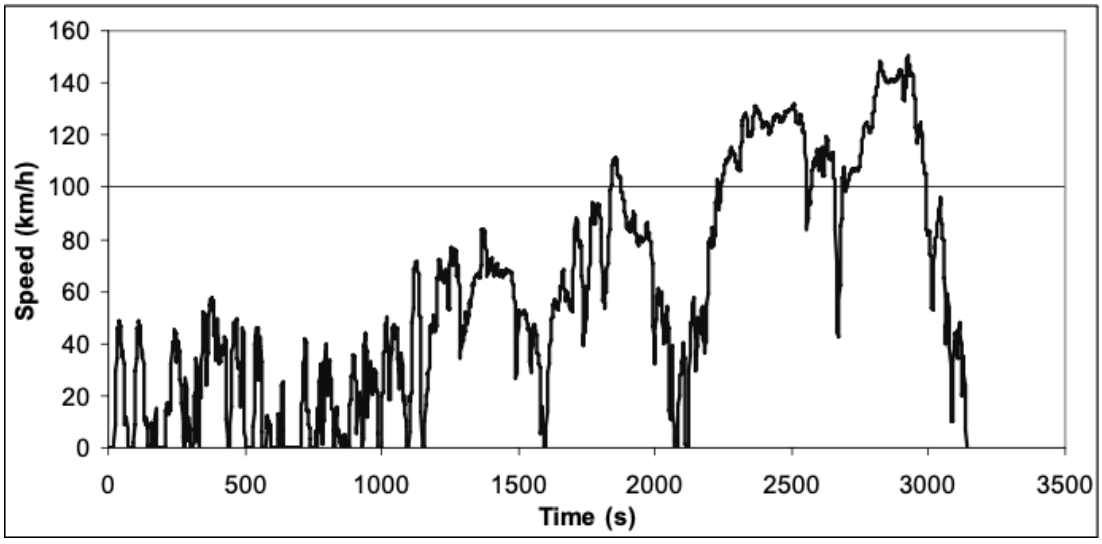

Figure 76: Common Artemis Driving Cycle (CADC) - Adopted from reference [159].

Table 37 : Comparison of the Performance Values of different driving cycles [159].

Characteristic Parameters	NEDC	FTP-72	FTP-75	US06	SC03	JP 10-15
Total Distance(m)	11,016.63	11,996.85	17,786.59	12,893.77	5765.65	4165

Total Time(s)	1180	1369	1874	596	596	660
Driving Time(s)	939	1180	1633	583	514	488
Drive Time(s)	458	247	376	153	81	120
Drive time spent accelerating(s)	278	506	683	216	236	195
Drive time spent decelerating(s)	204	427	574	214	197	173
Time spent braking(s)	200	271	383	128	128	149
Standing time(s)	241	189	241	13	82	172
% of time driving	79.58%	86.19%	87.14%	97.82%	86.24 %	73.94 %
% of time cruising	38.81%	18.04%	20.06%	25.67%	13.59 %	18.18 %
% of time accelerating	23.56%	36.96%	36.45%	36.24%	39.60 %	29.55 %
% of time decelerating	17.29%	31.19%	30.63%	35.91%	33.05 %	26.21 %
% of time braking	16.95%	19.80%	20.44%	21.48%	21.48 %	22.58 %
% of time standing	20.42%	13.81%	12.86%	2.18%	13.76 %	26.06 %
Average Speed(km/h)	33.6	31.6	34.2	77.9	34.8	22.7

Average driving speed(km/h)	42.24	36.6	39.21	79.62	40.38	30.73
The standard deviation of speed	28.91	21.46	23.51	37.53	21.75	19.68
Speed: 75^{th} – 25^{th} percentile(km/h)	46.7	34.92	37.49	62.25	40.18	39.82
Maximum speed(km/h)	120.09	91.15	91.09	128.91	88.07	70.09
Average acceleration(m/s^2)	0.00	0.00	0.00	0.00	0.00	0.00
Average positive acceleration (m/s^2)	0.528	0.429	0.420	0.541	0.424	0.370
Average negative acceleration (m/s^2)	-0.719	-0.464	-0.457	-0.570	-0.516	-0.389
The standard deviation of acceleration (m/s^2)	0.476	0.637	0.629	0.896	0.678	0.474
The standard deviation of	0.243	0.421	0.423	0.716	0.439	0.285

positive acceleration (m/s^2)						
Acceleration: $75^{th} – 25^{th}$ percentile(m/s^2)	0.00	0.363	0.358	0.380	0.398	0.373
Number of accelerations	31	48	61	20	18	13
Accelerations per km	2.814	4.001	3.430	1.551	3.122	3.121
Number of stops	14	14	16	5	6	8
Stops per km	1.27	1.17	0.9	0.39	1.04	1.92
Average stop duration(s)	17.21	13.5	15.06	2.6	13.67	21.5
Average distance between stops(m)	786.9	856.92	1111.66	2578.75	960.94	520.66
Relative positive acceleration(m/s^2)	0.1113	0.1652	0.1613	0.1715	0.1933	0.1605
Positive Kinetic Energy(m/s^2)	0.224	4.307	4.197	4.474	5.028	4.171
Relative positive speed (km/h)	0.286	0.505	0.505	0.524	0.552	0.534

Relative real speed(km/h)	0.840	0.823	0.816	0.847	0.782	0.722
Relative square speed(m/s)	17.223	13.660	14.804	27.023	14.466	12.030
Relative positive square speed(m/s)	5.284	6.658	7.195	14.311	7.902	6.681
Relative real square speed(m/s)	14.771	11.677	12.575	23.690	11.600	8.971
Relative cubic speed(m^2/s^2)	361.85	218..99	255.41	768.68	232.59	167.51
Relative positive cubic speed(m^2/s^2)	120.96	103.54	119.95	409.86	26.02	96.02
Relative real cubic speed(m^2/s^2)	311.37	192.32	222.94	685.80	190.09	127.66
Root mean square (RMS) acceleration(m^2/s^2)	0.139	0.200	0.190	0.190	0.202	0.162

9. Annexture III – Data Arrays of Colombo Metropolitan Driving Cycle for 2W, 3W and 4W.

Appendix-III includes the driving cycle data which has been utilized during the study. Two major driving cycles have been developed targeting 2W, 3W and 4W in Colombo Metropolitan area. The numerical data of those two driving cycles are stated in this section.

i.) Data array of Colombo Metropolitan Driving Cycle for 4W.

[0, 0, 0, 0, 0, 0, 0, 0, 0, 0, 0, 0, 0, 0, 0, 0.122966598, 0.444683332, 0.455865862, 0.156514187, 0, 0, 1.559731374, 5.665542834, 9.241007287, 9.52630949, 9.480510575, 9.192587294, 8.177527305, 7.254789421, 7.098034968, 7.435271985, 7.076982267, 5.191959804, 2.423459748, 2.180548177, 4.666147777, 7.321729006, 8.484565749, 9.772667136, 11.52539158, 11.88340276, 10.25954459, 7.313337162, 5.162392834, 4.643478135, 4.411813992, 2.976970629, 1.115581659, 0.309258935, 0.046277138, 0.243908424, 0.826177754, 0.908105736, 1.102576235, 1.313382913, 1.499876032, 1.160002163, 1.200154124, 0.691918039, 0.211955462, 0, 0, 0, 0, 0, 0, 0.191179623, 0.678277985, 0.692644467, 0.234279069, 0, 0, 0, 0, 0, 0, 0, 0.112126115, 0.601870641, 1.377704631, 1.154357299, 0.370149013, 0.067427332, 0.680110669, 1.029266446, 1.220243028, 1.327446702, 1.390262478, 1.47208799, 1.698906245, 1.416936221, 1.075541437, 0.817262217, 0.524763794, 0.08999973, 0, 0, 0, 0, 0, 0, 0, 0, 0.50630768, 1.448766644, 2.101520062, 1.774724289, 2.064216348, 2.55799564, 2.954124972, 2.768592289, 2.309432169, 1.692787191, 0.83733527, 0.078214227, 0.342105521, 1.180921789, 1.951431318, 1.897045287, 1.515757852, 0.924628212, 0.673830054, 0.660506664, 0.634409572, 0.880580001, 1.123815744, 1.212665062, 1.147183258, 1.16359763, 1.140836478, 0.708153216, 0.194303625, 0, 0.19813174, 0.573707615, 0.839434724, 0.784108108, 0.740308129, 0.625169974, 0.614486522, 0.427389085, 0.168470861, 0, 0, 0, 0, 0, 0, 0.202336647, 0.581986191, 0.852048665, 0.694005229, 0.751290143, 0.949936275, 1.059702802, 0.626122308, 0.150034363, 0, 0.189264965, 0.355892137, 1.471761036, 2.632136791, 3.570680278, 3.19246641, 2.134022404, 1.050925944, 0.337162547, 0, 0.792144743, 1.860107291, 1.95471316, 0.783684654, 1.273854596, 2.204963723, 2.813990637,

2.613500084, 2.497297614, 1.528427819, 0.45805989, 0, 0, 0.211174505, 0.612565121, 0.879989658, 0.770142233, 0.964908524, 1.186510166, 1.086959754, 0.514439143, 0.085441753, 0, 0, 0, 0, 0.210384423, 0.55786613, 0.780219218, 0.766677008, 0.92870996, 0.926066603, 0.533279354, 0.116419469, 0, 0, 0.122741711, 0.447985564, 0.720945922, 0.719335655, 0.775320921, 0.850374932, 0.925452503, 0.58612228, 0.193796381, 0, 0, 0, 0, 1.791457558, 2.782511776, 2.433619252, 0.437751724, 0.860650921, 0.76960604, 0.473507077, 0.136873979, 0, 0, 0, 0, 0, 0, 0.150830151, 0.471236569, 0.698479235, 0.421003478, 0.120690296, 0, 0, 0, 0, 0, 0.146888443, 0.619102875, 0.904077629, 0.785724955, 0.604499156, 0.694600563, 0.736989245, 0.760093645, 0.754452085, 0.844119741, 0.924998212, 0.622344133, 0.203531308, 0, 0, 0, 0, 0, 0, 0.129624847, 0.360936092, 0.726393369, 0.985961108, 1.198744681, 0.761381183, 0.223575558, 0, 0, 0, 0, 0, 0, 0, 0.149569631, 0.688518167, 0.736188531, 0.292580724, 0, 0, 0, 0, 0, 0, 0, 0.192428255, 0.272606695, 0.192428255, 0, 0, 0, 0, 0, 0, 0, 0, 0, 0, 0.212924439, 0.301642956, 0.212924439, 0, 0, 0, 0, 0, 0, 0, 0, 0, 0, 0.192861021, 0.438522858, 1.000051511, 1.375739212, 1.416486207, 0.673080005, 0.108845748, 0, 0, 0, 0, 0, 0, 0, 0, 0.208662946, 0.29560584, 0.208662946, 0, 0, 0, 0, 0, 0, 0, 0, 0, 0, 0.214493731, 0.303866119, 0.214493731, 0, 0, 0, 0, 0, 0, 0.151062819, 0.459346216, 0.453020426, 0.132085449, 0, 0, 0, 0, 0, 0, 0, 0, 0, 0, 0.187954412, 0.266268751, 0.187954412, 0, 0, 0, 0, 0, 0, 0.307947099, 0.679293735, 0.786076568, 0.59035524, 0.430871816, 0.171323347, 0, 0, 0, 0, 0, 0, 0, 0, 0.1356311, 0.522497507, 0.542219961, 0.194798459, 0, 0, 0, 0, 0, 0, 0, 0, 0, 0, 0.2193748, 0.310780966, 0.2193748, 0, 0, 0, 0, 0, 0, 0, 0, 0, 0, 0, 0.232105923, 0.632438897, 0.865973328, 0.726677477, 0.450369111, 0.138820108, 0, 0.113410265, 0.700685678, 1.406956935, 1.773167215, 2.295141142, 2.249136723, 2.262871674, 1.802995351, 1.516723295, 1.013262606, 1.135248144, 1.41047347, 1.774869142, 2.420030992, 2.723116102, 3.131142896, 2.12526145, 0.818165261, 0, 0, 0, 0, 0, 0.309064058, 0.667115831, 0.889233068, 0.443718304, 0.175025541, 0, 0, 0, 0, 0, 0, 0, 0.067390885, 0.830782013, 1.35708597, 1.339913608, 0.847140121, 0.493145238, 0.099287265, 0, 0, 0, 0, 0, 0.193567632, 0.490216267, 0.689022665, 0.838244512, 0.689213373, 0.290535849, 0, 0, 0, 0, 0, 0, 0, 0, 0, 0, 0.199796717, 0.28304535, 0.085584855, 0.349759539, 0.759689927, 1.078589574, 1.316681818, 1.656106246, 1.753859343, 1.685766418, 2.536298936, 4.272193759, 4.898023711, 3.230195706, 1.292125852, 1.205234388, 1.373800789, 1.380754042, 1.337602687, 0.964947428, 0.24632114, 0, 0, 0, 0, 0, 0, 0, 0, 0, 0, 0.222897414, 0.315771336, 0.222897414, 0, 0, 0, 0, 0.337001242, 1.225876825, 1.565380791, 1.032141444, 0.361536667, 0.105411438, 0, 0, 0, 0.221030596, 0.560961085, 0.727020887, 0.595969719, 0.693324521, 0.505399232, 0.176314882, 0, 0, 0.126046678, 0.503403376, 0.860885687, 0.908445387, 1.040388368, 1.016686043, 0.984959917, 0.772255483, 0.819003641, 0.752763017, 0.509981416, 0.119329369, 0, 0, 0, 0, 0.382729953, 1.047654469, 1.419877468, 1.242334758, 1.327340427, 1.254326238, 0.703646804, 0.145998737, 0, 0.230069845, 0.783172395, 1.081062235, 1.016657037, 0.988101821, 1.001194496, 0.957078997, 1.202773288, 1.482674652, 1.752283723, 1.773478024, 1.497670793, 1.055339467, 0.837297271, 0.759549579, 0.756994457, 0.946146981, 1.105156822, 1.006859657, 0.951841952, 0.905935069, 0.57276855, 0.115776566, 0, 0, 0, 0, 0, 0.113527659, 0.538892382, 1.078669219, 1.2218864, 0.761881983, 0.182593806, 0, 0, 0, 0, 0, 0, 0, 0, 0, 0, 0, 0, 0, 0, 0.220213304, 0.311968848, 0.220213304, 0, 0, 0.241012726, 0.636132504, 0.776142926, 0.677458738, 0.895464841, 1.216919752, 1.213732791, 1.051202823, 0.574557146, 0.170477572, 0, 0, 0, 0, 0, 0, 0, 0, 0, 0, 0.206710563, 0.292839965, 0.206710563, 0, 0, 0, 0, 0, 0, 0, 0, 0, 0, 0, 0, 0.189301688, 0.268177392, 0.189301688, 0, 0, 0, 0, 0, 0, 0, 0, 0.18861396, 0.26720311, 0.18861396, 0, 0, 0, 0, 0, 0, 0, 0, 0.178988416, 0.253566922, 0.090212028, 0.177054385, 0.90036555, 1.51637233, 1.615891269, 1.690264007, 1.566534417, 1.35087464, 1.059805533, 1.120559303, 0.73089381, 0.273329886, 0, 0.212712795, 0.549578353, 1.187724294, 1.078550638, 1.035882418, 1.298228103, 1.518685145, 1.046056816, 0.742497555, 1.07216364, 1.08471099, 1.002899558, 0.648636823, 0.248481611, 0, 0, 0, 0, 0, 0, 0, 0, 0, 0, 0, 0, 0, 0, 0.201242863, 0.285094055, 0.201242863, 0, 0, 0, 0, 0, 0, 0, 0.128933292, 0.462917156, 0.473870719, 0.16179398, 0, 0, 0.241329564, 1.005241087, 2.371781928, 2.104484432, 1.533036744, 0.830042139, 0.977876435, 0.695760286, 0.487786906, 0.197066285, 0, 0, 0, 0, 0, 0, 0, 0, 0, 0, 0.214477668,

0.303843363, 0.214477668, 0, 0, 0, 0, 0, 0.277020376, 0.70665823, 1.013500353, 0.573471141, 0.11290483, 0, 1.256828299, 2.928970521, 3.2696046, 2.226984971, 1.481530786, 1.54868756, 2.118436748, 2.731925658, 3.857023842, 4.923161002, 5.894172546, 6.437255274, 6.610903903, 6.205306039, 5.808845479, 6.174351093, 6.096911553, 5.434225491, 5.393061611, 6.273466451, 7.41572376, 8.218565409, 8.861911514, 9.03213738, 9.189576939, 8.861075224, 7.207092027, 5.997190462, 5.303791087, 5.483177212, 5.266714886, 4.875881699, 4.601763085, 5.149841499, 5.727250521, 5.281705202, 4.385933031, 3.831815896, 3.698738493, 3.737047059, 4.121460792, 4.65916462, 5.153169946, 5.0215421, 4.651256057, 4.177500997, 4.351795292, 4.834972423, 4.817624106, 4.69541265, 4.285967786, 3.795061275, 4.25448964, 5.683595875, 6.104703849, 5.119826065, 3.390317276, 2.125581162, 1.955657796, 3.358017656, 4.725104509, 5.870908192, 5.78012882, 5.542016602, 5.277013288, 4.742930535, 3.24186321, 3.079669299, 4.051201629, 5.457162094, 5.390835633, 4.398989024, 2.311159072, 2.938691221, 5.73483732, 8.259524086, 8.352438804, 7.827141258, 7.337897546, 6.571099731, 5.501029955, 4.471792889, 4.578139346, 5.423509053, 6.25701952, 6.3349373, 6.142295987, 5.8241348, 5.382879067, 4.814495114, 5.212141309, 6.062685912, 6.400133814, 5.651634543, 5.471498994, 5.85896274, 6.233575412, 6.330247893, 7.093350315, 8.697651332, 9.465481036, 8.679840476, 5.962750258, 3.526835843, 2.900040286, 4.290470212, 5.129794523, 4.523019117, 3.263102804, 2.81770388, 2.859350279, 2.599914544, 2.460169451, 2.541102287, 3.462359967, 3.73108154, 3.428950106, 2.719144085, 2.815582357, 3.277938761, 4.211374923, 5.041507571, 4.674857412, 3.736999219, 3.444286994, 3.69293683, 4.023442848, 3.622215898, 3.038601324, 3.339455393, 5.226699475, 7.521075903, 9.643641376, 10.83464212, 11.17778083, 11.05000019, 11.05000019, 11.05000019, 11.05000019, 11.05000019, 11.04535503, 11.11256896, 11.0862778, 10.53086722, 8.618387262, 5.943474804, 3.757021945, 3.563014678, 4.564158304, 5.751570709, 6.275250163, 6.070732471, 5.531713479, 4.587321172, 4.495267476, 3.560578428, 2.110740113, 1.008701515, 2.390493083, 5.033051437, 6.6055311, 6.38064736, 5.85965399, 6.725009809, 8.316821534, 9.717101698, 9.77097337, 8.801374872, 7.375798838, 6.167333065, 4.548217283, 3.11040334, 2.014727809, 1.291275828, 0.59568106, 0.08445869, 0.171462485, 0.567095304, 0.822955818, 0.918199488, 1.643646749, 3.178423662, 5.018748692, 6.22403918, 5.712655776, 4.378326716, 3.857039628, 4.75880676, 5.841147818, 5.971963269, 5.526609298, 5.63401116, 6.575217983, 7.526073633, 7.894837952, 8.330552415, 8.968368898, 9.084145914, 8.079648154, 6.930592769, 6.589336354, 7.053362376, 6.096432849, 4.360847888, 3.503781468, 3.972188997, 4.093567821, 4.396064759, 3.631578468, 2.007191689, 0.590835171, 1.272392481, 2.787299771, 4.229515924, 3.507761335, 2.799963541, 1.490307597, 2.433087429, 2.833090067, 4.174401922, 4.826269627, 6.499778796, 7.536727183, 7.88834313, 8.505939769, 9.229677976, 9.6681427, 9.632566616, 9.685041617, 10.18891855, 11.071735, 11.36565026, 10.69729324, 9.264052542, 7.616111306, 4.937773112, 2.244351946, 0.379473394, 0.089720978, 0, 0.079107121, 1.083029873, 1.338063506, 1.205105158, 1.538095985, 3.633145571, 6.390785612, 8.290789904, 8.360595689, 7.976142011, 8.309491008, 8.329053988, 7.647124113, 7.115526581, 7.44558382, 7.787807492, 8.153862299, 8.592397417, 8.782113988, 8.451753126, 7.581344387, 6.548224695, 6.440190724, 8.261792592, 9.882242788, 10.77151225, 10.70674795, 10.43873843, 8.552870272, 6.393400642, 5.622408635, 6.962489619, 7.660325663, 6.847064059, 5.882015773, 6.653726864, 8.089061819, 8.631611661, 7.131216853, 5.34614394, 5.195892484, 6.974491773, 8.191651412, 9.236127144, 10.68209635, 11.31169496, 9.785728429, 8.608501925, 9.339807645, 10.55130683, 10.97724797, 10.51218235, 10.07502503, 9.038651399, 7.929349572, 6.632814033, 5.03141173, 2.916757972, 3.309000792, 5.837857839, 6.832167156, 5.257206365, 3.015557221, 2.514033222, 2.693849257, 3.420834841, 3.713440609, 4.293821901, 4.445364523, 5.509146309, 7.22536211, 8.981308732, 9.607054383, 9.514064353, 9.135119302, 8.55801205, 8.052822508, 7.265063613, 7.396002279, 7.363061401, 6.332239349, 4.441655496, 2.547053364, 1.698862624, 1.662071514, 2.708562984, 3.081582121, 2.167333794, 1.876186484, 3.996919066, 7.796972074, 9.760360882,

9.771133628, 7.901108592, 6.12521694, 4.418478838, 2.869428894, 1.061211792, 0, 0.193401876, 1.45982899, 2.340058544, 5.672668717, 9.215552004, 11.78827097, 10.75288345, 9.824789975, 8.428267752, 9.294982964, 10.98198198, 12.43680199, 11.84850758, 11.1729624, 10.56742758, 10.47334235, 9.960710962, 9.281810569, 8.135657065, 7.642169789, 8.169151469, 9.501909557, 10.22202541, 9.67097043, 8.549460099, 7.798684161, 7.581254292, 7.414333875, 8.338636822, 10.07787365, 10.6257382, 10.41635105, 9.921102008, 8.733208971, 7.0545678, 7.452664824, 9.414693751, 10.88684152, 11.36535969, 11.51321441, 11.3171787, 10.89013743, 10.17412575, 9.680936514, 9.766214697, 10.57382769, 10.46014497, 10.322813, 10.75348391, 11.71737644, 11.74246911, 11.46038813, 11.52346192, 11.40525712, 10.51228709, 9.631457411, 9.634290041, 9.858236885, 9.564267322, 9.422352246, 9.428739602, 9.74425425, 10.35779509, 10.72962862, 11.08931111, 11.45270857, 11.98051063, 11.82093405, 11.85684308, 12.54957204, 13.66070222, 14.34836802, 13.69363343, 12.95623714, 11.6694637, 10.209868, 8.569193009, 7.772865486, 7.082404069, 6.664145279, 7.434000792, 8.686210524, 9.279841192, 8.555389486, 8.144733905, 9.054098539, 9.998005991, 9.908058712, 9.544117628, 10.0239326, 10.70411889, 11.22148822, 12.23658311, 12.90051488, 12.9393716, 12.15990263, 11.49422692, 10.99187584, 11.60608055, 12.69015849, 13.43360059, 13.08624775, 12.1408156, 11.84408114, 12.57967568, 14.05227119, 14.46743772, 14.40141008, 13.167386, 12.13300541, 10.59868315, 8.290301185, 5.8390681, 5.208970901, 6.325491483, 7.332744721, 8.375013597, 8.984548719, 9.22518455, 9.179658862, 9.398190635, 9.773889541, 9.88502753, 10.04880006, 10.26228646, 10.10111387, 9.65624406, 9.515546144, 10.23681712, 10.41448566, 10.74728086, 10.66935604, 10.50351658, 9.785998003, 8.536687361, 7.505013044, 7.475303813, 9.276509927, 10.44271194, 9.19933356, 6.193941088, 4.772403213, 5.672562981, 7.032233838, 7.736426381, 7.719425705, 8.011300931, 8.803114169, 10.12024242, 10.68256882, 10.85297457, 10.56785379, 10.56442762, 11.02009307, 11.59711996, 11.09599318, 10.0059633, 9.597190093, 9.87902554, 10.39859984, 11.33426721, 12.07755364, 11.79529634, 10.55189114, 9.263462067, 7.7603902, 6.987987859, 6.958499609, 7.218828624, 7.747187832, 8.524977534, 9.216573524, 9.751342556, 9.858078713, 10.59861287, 11.65259481, 12.71889057, 12.83615859, 13.23293547, 13.77583389, 13.68738891, 13.0774377, 12.6761337, 12.83215117, 13.02143563, 12.78433317, 12.53037319, 12.43667409, 12.50253538, 12.54003814, 12.52890998, 12.17523717, 11.74337654, 11.6300666, 11.89385455, 12.24102516, 12.33412413, 11.97966093, 11.11784998, 10.23004576, 9.934008844, 10.65876119, 11.59203333, 12.15644474, 12.07028778, 11.70643539, 11.69338234, 11.74281752, 11.84711917, 11.48584017, 12.10902993, 12.76228185, 12.36258692, 10.73596095, 8.965180726, 7.962235219, 8.324224337, 9.992575036, 11.44560484, 11.60428325, 11.50313585, 11.72325946, 12.1414899, 12.04424005, 11.44503381, 11.22608182, 11.03005355, 11.01109818, 10.17234592, 9.810123229, 9.953103639, 10.59434033, 11.05917762, 11.46178722, 12.25894484, 11.98373247, 11.84748366, 10.77982813, 10.33355315, 9.748536982, 10.42586512, 10.11237586, 9.428535624, 8.736346272, 9.134027154, 9.972680636, 9.469137736, 8.04717042, 7.459046501, 8.244268199, 9.157249178, 10.02937164, 10.17575454, 9.05977722, 8.068210329, 7.431500932, 6.029085987, 3.356695386, 1.115031144, 0, 0, 0, 2.908038139, 8.260067286, 11.91953414, 11.29321319, 11.13292326, 10.54467828, 9.375473485, 9.145645578, 9.513647486, 10.28457925, 10.62796922, 10.14057183, 8.989934392, 7.997672598, 7.316808524, 6.89294529, 7.043351773, 7.288791656, 6.814673669, 6.550509766, 8.050179563, 9.500334971, 9.970609106, 9.741327395, 10.07881581, 10.62167176, 10.56238206, 9.531105329, 7.808973271, 6.742136015, 7.005360535, 8.2918943, 9.511521312, 10.24401659, 10.85929938, 11.17921925, 11.21696061, 10.89003765, 10.83069273, 10.97787568, 11.54016217, 12.22245644, 12.78733692, 12.87178252, 12.78931969, 12.88134115, 12.37171271, 10.86775219, 9.174705806, 8.36769431, 8.287738119, 8.213387516, 8.570304108, 9.245945822, 9.899003465, 9.784267153, 8.979023552, 9.024452101, 10.38999451, 12.19203813, 12.64755287, 12.50068457, 12.3566309, 12.3303026, 11.41612081, 9.98116774, 8.817992374, 8.155622605, 7.301868453, 6.170423842, 5.1787467, 2.991001926, 0.799446855, 0, 0.544897931, 0.579711633, 1.042972572,

2.41521485, 4.178652722, 5.231941305, 5.073877157, 4.502484199, 4.330407701, 4.695292813, 5.62185094, 7.571209826, 9.50118073, 9.963783686, 9.455136272, 9.236076791, 9.871389663, 10.9466516, 11.54013664, 11.16131524, 11.14011511, 11.39111601, 11.70833972, 11.27410101, 11.27623602, 11.5731772, 11.89391591, 11.46514156, 10.83327533, 9.958779471, 9.197836577, 8.615679523, 8.789598983, 9.460178864, 10.34128857, 10.9921978, 10.90470071, 11.51552265, 12.62573484, 13.22463915, 12.45505202, 12.22047926, 12.72892181, 12.9959486, 12.39864513, 10.96837801, 9.092110935, 8.59404929, 9.121662739, 9.720421274, 9.856586579, 9.492315156, 7.82121954, 4.55931282, 1.809899713, 0.545486719, 0.797219667, 0.884659348, 0].

ii.) Data array of Colombo Metropolitan Driving Cycle for 2W and 3W.

[0, 0, 0, 0, 0, 0, 0, 0, 0, 0, 0, 0, 0, 0, 0, 0, 0, 0, 0, 0, 0, 0, 0, 0, 0, 0, 0, 0, 0, 0, 0, 0, 0, 0, 0, 0, 0.068571429, 0.365714286, 0.8, 1.2, 1.793474633, 1.466101467, 0.617929459, 0, 0, 0, 0, 0, 0, 0, 0, 0, 0, 0, 0, 0, 0, 0, 0, 0.04992005, 0.266240266, 0.582400582, 0.873600874, 1.214721215, 1.356161356, 1.214721215, 0.873600874, 0.582400582, 0.266240266, 0.04992005, 0, 0, 0, 0, 0, 0, 0, 0, 0, 0, 0, 0, 0.077034477, 0.350284921, 0.570620875, 1.110805609, 1.664871524, 1.826605538, 1.431834262, 1.429750613, 1.704828964, 1.964787156, 2.08104837, 2.258042935, 2.459431362, 2.625252281, 3.148805929, 2.301849357, 0.873917826, 0, 0, 0, 0, 0, 0, 0, 0, 0, 0, 0, 0, 0, 0, 0, 0, 0, 0, 0, 0, 0, 0, 0, 0, 0, 0, 0, 0, 0, 0, 0, 0.042397972, 0.135561324, 0.241982929, 0.33786761, 0.843438899, 1.67530699, 2.599925195, 3.378853257, 4.130113247, 4.691524901, 4.990638188, 5.046332183, 4.963282735, 4.818195956, 4.672630092, 4.567760821, 4.643529333, 4.882540988, 5.202698558, 5.466062151, 5.620867729, 5.563142191, 5.393360002, 5.10007425, 4.778106301, 4.346869925, 3.878933941, 3.358223309, 2.832101059, 2.335160337, 2.111999654, 2.353274454, 2.736856331, 3.237402453, 3.715785115, 4.036013045, 3.987046235, 3.845822716, 3.738576331, 3.608677026, 3.500024836, 3.396252387, 3.282472454, 3.147289487, 3.185963651, 3.335381658, 3.523129014, 3.677200685, 3.816644757, 3.828439747, 3.725849683, 3.395199173, 2.688713489, 1.869980705, 1.17649686, 0.563648389, 0.099782589, 0, 0, 0, 0, 0, 0, 0, 0, 0, 0, 0, 0, 0.325415577, 0.978648257, 1.459129862, 1.578574677, 1.934857143, 2.251344479, 2.62030236, 3.062057212, 3.46215002, 3.66647918, 3.90922823, 4.18890711, 4.320866666, 4.24355718, 4.01852837, 3.830429392, 3.67750547, 3.38388132, 2.890931846, 2.257282144, 1.6588075, 1.048622875, 0.445690324, 0.067465713, 0, 0, 0, 0, 0, 0, 0.047512731, 0.25340123, 0.55431519, 0.831472784, 1.091164769, 1.420719194, 1.849245409, 2.347634064, 2.828557109, 3.330051813, 3.749259881, 4.051895217, 4.272243917, 4.513164277, 4.725538595, 5.052097077, 5.540416456, 6.142919998, 6.7168775, 7.344565533, 7.757331441, 7.865624339, 7.758995113, 7.706096418, 7.663728893, 7.579236688, 7.435067854, 7.24877434, 7.073011996, 6.892283898, 6.731418815, 6.598693003, 6.485830206, 6.368001654, 6.310787528, 6.011115701, 5.367962131, 4.48235086, 3.657354013, 2.665435822, 2.34120301, 2.962857819, 4.252198006, 5.374616848, 6.620953643, 7.371618627, 7.420081879, 6.97287332, 6.649582714, 6.343309093, 5.96896753, 5.498196385, 4.959357299, 4.437535198, 3.907125661, 3.411065869, 2.963668218, 2.550620312, 2.12898497, 1.781413537, 1.027382385, 0.294472073, 0, 0, 0, 0, 0.078668339, 0.419564474, 0.917797286, 1.37669593, 1.897052936, 2.17157649, 2.09783599, 1.778262038, 1.520146448, 1.236390939, 1.00186226, 1.125957858, 1.654832613, 2.371398846, 3.03463223, 3.768666617, 4.232769507, 4.253950957, 3.871220192, 3.441745899, 2.980046858, 2.529722132, 2.049871733, 1.68812403, 1.49368848, 1.417355627, 1.311497099, 1.148684956, 1.213687276, 1.601426753, 2.216980695, 2.77558102, 3.39232303, 3.776498302, 3.831204031, 3.653343021, 3.533623697, 3.390997099, 3.35230206, 3.432656338, 3.367796484, 3.066224734, 2.698652884, 2.422828347, 2.13367981, 1.806525446, 1.609252483, 1.71591349, 2.100068599, 2.534785503, 2.947360502, 3.328124596, 3.836132307, 4.524401809, 5.339914927, 6.12361714, 7.011059472, 7.483541333, 7.36816253, 6.837823256, 6.411224101, 5.923444653, 5.680386372, 5.784016411, 6.132367615, 6.419538529, 6.726142543, 6.955014152, 7.073764853, 7.114783149, 7.175234545, 7.251772588, 7.263964048, 7.184997849, 7.041685067, 6.914458932, 6.811783786,

6.610904679, 6.270903294, 5.832697947, 5.41904359, 4.944233017, 4.714047311, 4.830413503, 5.191404563, 5.491239405, 5.884127407, 5.904802773, 5.398176906, 4.519338403, 3.73355306, 2.823851588, 2.409814628, 2.69796906, 3.481788003, 4.141690819, 4.880246511, 5.304190697, 5.282435248, 4.946068292, 4.688354214, 4.385828795, 4.262548736, 4.393199604, 4.703095832, 4.968180719, 5.250742119, 5.463397472, 5.577019262, 5.620735007, 5.681927262, 5.807666051, 5.675218708, 5.177007677, 4.420610515, 3.728759885, 2.9352789, 2.548319337, 2.737265124, 3.332732332, 3.826569186, 4.328141453, 4.798772063, 5.225568655, 5.621423589, 6.025013937, 6.480587038, 6.728229129, 6.681302289, 6.42644444, 6.223569343, 5.98171734, 5.895772961, 6.030697716, 6.321530094, 6.573385567, 6.865318871, 6.996940849, 6.901455116, 6.645658057, 6.42993883, 6.237658242, 5.951623096, 5.532768995, 5.020160336, 4.530990316, 3.988982448, 3.658325975, 3.627083981, 3.807193383, 3.934464937, 4.107437588, 4.097605847, 3.82880122, 3.377192201, 2.971284281, 2.552863507, 2.184494144, 1.887030944, 1.639619155, 1.379694512, 1.04715304, 1.005078889, 1.374500111, 2.034388655, 2.621660369, 3.286239496, 3.641588968, 3.558863093, 3.166907562, 2.852259444, 2.475049884, 2.348086097, 2.575637159, 3.053433995, 3.468669387, 3.943590776, 4.179768179, 4.077724935, 3.736937705, 3.455836472, 3.11602453, 3.081710687, 3.097469802, 2.94769192, 2.456582273, 2.03612789, 1.575046092, 1.234732722, 1.29447202, 1.741791738, 2.299209876, 2.803423894, 3.310503635, 3.929459653, 4.100910558, 3.638395884, 2.728376096, 1.930232586, 1.092300682, 0.384898451, 0.017459416, 0, 0, 0, 0.139657642, 0.529642475, 0.964925414, 1.324331633, 1.848426834, 2.385014404, 2.826837363, 3.213903557, 3.560066428, 3.75570849, 3.751861572, 3.595368692, 3.392349788, 3.162343638, 2.845209033, 2.492120716, 2.034278085, 1.517282447, 0.985815067, 0.473187986, 0, 0.276456187, 0.954329681, 0.934984228, 0.224861103, 0.002324765, 0.396117267, 0.699995743, 0.994615843, 1.436185421, 1.931699362, 2.326008599, 2.646420009, 2.807134901, 2.765228585, 2.716217988, 2.660572986, 2.589804486, 2.433939805, 2.326200335, 2.237457609, 2.296105957, 2.391904865, 2.522754839, 2.606298705, 2.706086213, 2.78723321, 3.023774324, 3.357527787, 3.745634086, 3.984804276, 4.067513057, 4.001068, 3.891105843, 3.750747163, 3.520862804, 3.289385605, 3.1035707, 2.968847084, 2.771158614, 2.703093611, 2.777411624, 2.972616189, 3.183162151, 3.543028552, 3.879500662, 4.050336388, 3.861104761, 3.385696132, 2.852287899, 2.523794916, 2.530063711, 2.955980321, 3.661542872, 4.565596608, 5.468395498, 6.294361482, 6.270669392, 5.779118715, 5.049332169, 4.498586784, 3.945584951, 3.703451347, 3.64489928, 3.455664158, 3.204748668, 2.488946308, 1.855669768, 0.942215957, 0.350195902, 0, 0.111763848, 0.395378331, 0.711947593, 0.949685328, 1.520791001, 2.250056447, 3.005694253, 3.610460485, 4.093702446, 4.474026203, 4.78978499, 5.152260603, 5.554463005, 5.962554591, 6.192382595, 6.227420739, 6.173264463, 5.999183287, 5.69737384, 5.254215567, 4.79700286, 4.364271355, 4.082502134, 3.943739306, 3.85901428, 3.667573677, 3.322272982, 2.851150969, 2.424225119, 2.175387396, 2.087525647, 2.066250746, 2.207616704, 2.262706586, 2.173511267, 2.058325001, 2.032134628, 1.925602664, 1.847503502, 1.817725587, 1.678655202, 1.378836802, 1.119211225, 0.667180314, 0.220318233, 0, 0, 0, 0, 0.047136965, 0.251397147, 0.549931258, 0.824896888, 1.047016146, 1.480520888, 2.2134884, 3.157841397, 4.049348022, 5.001039685, 5.711991197, 6.081894162, 6.211056975, 6.400404827, 6.586826982, 6.784951921, 6.999655803, 7.226062468, 7.449543437, 7.683692438, 7.875169313, 8.006194011, 8.094546582, 8.193567186, 8.320312733, 8.336158503, 8.194896256, 7.942734231, 7.718297151, 7.467253188, 7.303836845, 7.408511102, 7.557671159, 7.5167517, 7.28855779, 7.102482517, 6.957934485, 6.647277485, 6.101299447, 5.389212441, 4.718652678, 3.960802324, 3.552114329, 3.638073008, 4.073194044, 4.421024492, 4.770611412, 5.11317244, 5.44578012, 5.771361907, 6.098700167, 6.527075211, 6.551303121, 6.002989257, 5.05052826, 4.199104045, 3.317493566, 2.556628147, 1.966818229, 1.49775337, 0.998502247, 0.45645817, 0.085585907, 0, 0, 0, 0, 0.019524894, 0.104132769, 0.227790433, 0.341685649, 0.433305907, 0.614025998, 0.920970853, 1.31701554, 1.690785269, 2.119908327, 2.260851267, 2.355192549, 2.606465728, 3.180159445, 3.687086359, 4.221635179, 4.645696378, 4.913233448,

5.070282898, 5.254954253, 5.427008816, 5.649530546, 5.943547428, 6.288031477, 6.619898734, 6.974299342, 7.238566546, 7.375144759, 7.421589567, 7.490567727, 7.53172659, 7.747918305, 7.832356888, 7.767633921, 7.838270621, 8.0038086, 7.920373877, 7.342308885, 6.600479154, 5.663082488, 4.77289456, 3.832685064, 3.088692386, 2.643633065, 2.420586906, 2.162996987, 1.901537617, 1.602002024, 1.454771319, 1.523305871, 1.744145311, 1.926908529, 2.164636051, 2.182506357, 1.888912276, 1.375460979, 0.916973986, 0.419188108, 0.034018763, 0.091366328, 0.346950817, 0.688521758, 1.077568653, 1.690299519, 2.257486191, 2.907005332, 3.153917901, 3.227386618, 3.386760097, 3.921572844, 4.38310889, 4.849286144, 5.296898571, 5.718210827, 6.120958257, 6.528346893, 6.945510848, 7.323573529, 7.646242737, 7.92981067, 8.223153922, 8.528128196, 8.786578381, 8.97911944, 9.125136409, 9.282784401, 9.439353488, 9.607123786, 9.738228305, 10.00694343, 9.826408377, 9.328700747, 8.718881135, 8.466485019, 8.152574171, 7.883139069, 7.435800982, 6.736433666, 5.859163365, 5.026368811, 4.105333338, 3.537261537, 3.469221606, 3.754145348, 3.950828171, 4.09432038, 4.450575047, 5.108243197, 5.978673806, 6.7959138, 7.709751622, 8.237198131, 8.217256945, 7.810924445, 7.501189773, 7.21458053, 6.835469573, 6.325314521, 5.722657756, 5.143126419, 4.442006424, 4.227241061, 4.701478093, 5.662069758, 6.501072764, 7.410739764, 8.003264337, 8.46501761, 8.312689419, 7.622602007, 6.371179418, 5.251469009, 4.048481636, 3.165903911, 2.798540221, 2.866167399, 2.943706292, 3.03847344, 3.125758971, 3.176436184, 3.373546669, 3.77810429, 4.329095184, 4.843477759, 5.402154187, 5.838492396, 5.804483338, 5.282554779, 4.585571305, 3.943425022, 3.47416327, 2.08543776, 0.628735808, 0, 0, 0, 0, 0, 0, 0, 0, 0, 0, 0, 0, 0, 0, 0, 0, 0, 0, 0, 0, 0, 0, 0, 0, 0, 0, 0, 0, 0, 0.033521426, 0.178780938, 0.391083301, 0.586624951, 0.781393792, 1.013929403, 1.112142136, 1.016951422, 0.782285768, 0.582295648, 0.310073068, 0.326780323, 0.752804844, 1.4677592, 2.110481096, 2.743523474, 3.415283928, 4.141894988, 4.907224125, 5.662873742, 6.496071901, 6.974669165, 7.206930719, 7.313997218, 7.645921065, 7.745583595, 7.556817743, 7.639478679, 8.229801685, 8.692371816, 8.473550367, 7.998912435, 7.598368653, 7.187764018, 6.781595045, 6.575668555, 6.61289604, 6.783293662, 6.917883537, 7.028615111, 7.225316562, 7.702284203, 7.899447145, 7.503048589, 6.668323298, 5.94081386, 5.107128742, 4.767491652, 4.752135499, 4.768525302, 4.401358183, 4.103536375, 3.823339073, 3.386339568, 3.194684579, 3.42158858, 4.114898818, 4.307644818, 3.9135224, 3.105139923, 2.400322461, 1.56146366, 1.258770215, 1.715644356, 2.708683854, 3.567682012, 4.553333721, 5.032371228, 4.793705283, 4.048425136, 3.429798539, 2.738523696, 2.33784184, 2.348833383, 2.650417914, 2.879354197, 3.092865441, 3.368076846, 3.730696814, 4.155016944, 4.563912033, 4.97316702, 5.380982417, 5.786758393, 6.191094779, 6.595791062, 7.040179698, 7.282350225, 7.557956726, 7.541779717, 7.446226172, 7.111208473, 6.897266122, 6.552463794, 6.230135116, 5.904144666, 5.592801301, 5.302207973, 5.02626173, 4.746653715, 4.417445069, 4.286638952, 4.436903086, 4.785569749, 5.08463578, 5.401358457, 5.64745455, 5.793496313, 5.868911492, 5.961983316, 6.042210535, 6.215922505, 6.293995266, 6.184843928, 5.894422676, 5.64610775, 5.407121171, 5.110579661, 4.83890994, 4.634510044, 4.630945143, 4.750712795, 4.959462469, 5.145158195, 5.39083199, 5.354818186, 5.125773758, 4.974568779, 5.165228401, 5.395137559, 5.604790502, 5.850323271, 5.952336732, 5.851031171, 5.606206302, 5.397261261, 5.195415239, 4.965173137, 4.694703254, 4.395837291, 4.104070349, 3.755130945, 3.634881384, 3.838609099, 4.271026655, 4.646271751, 5.088202548, 5.246155127, 5.034159015, 4.905658151, 5.214581204, 5.799054022, 6.10933952, 6.13560286, 5.918296321, 5.759459946, 5.570942745, 5.50114885, 5.599546305, 5.816667065, 6.004106999, 6.228903863, 6.250970721, 6.282018095, 6.473984906, 6.721667082, 6.670058274, 6.473336369, 6.3147579, 6.113490756, 6.082978307, 6.294368341, 6.676513068, 7.015969123, 7.375862231, 7.654007122, 7.816342039, 7.896928739, 7.997952492, 8.142722463, 8.112549784, 7.759611772, 7.698215419, 7.316675455, 6.742942521, 6.075377194, 6.036510768, 5.88245983, 5.727301337, 5.596222278, 5.392822495, 5.08250737, 4.692487825, 4.322117497, 3.94016256, 3.568141301, 3.407385185, 3.499261124, 3.72517148, 3.914677079, 4.082622097, 4.33680944,

4.713173411, 5.175779706, 5.616825419, 6.08222277, 6.452904029, 6.674830852, 6.784105208, 6.906969376, 7.032524, 7.164265999, 7.30579688, 7.261137438, 7.047911037, 6.776243535, 6.591014447, 6.392810351, 6.165041685, 6.035653711, 6.174705988, 6.459066872, 6.672121972, 6.779710145, 6.908695652, 7.077182607, 7.087663773, 6.874303405, 6.50293725, 6.171072541, 5.78878867, 5.608181449, 5.713282813, 6.020060826, 6.276419678, 6.539643038, 6.77927554, 6.950038695, 7.144586581, 7.349844528, 7.55726383, 7.613094437, 7.68022698, 7.795630676, 8.012025781, 8.207443968, 8.46961762, 8.452753418, 8.105672247, 7.559659877, 7.128466964, 6.685258054, 6.186462148, 5.910014223, 5.948559271, 6.2094523, 6.414758333, 6.608759546, 6.847980043, 7.151261193, 7.499761627, 7.836957239, 8.253040903, 8.353572364, 8.007071539, 7.345018511, 6.761853535, 6.151861125, 5.65433935, 5.288196074, 5.000117403, 4.664567683, 4.334178868, 4.023739222, 3.633502895, 3.130221267, 2.547142958, 1.984013818, 1.276280916, 1.146963066, 1.837066538, 3.105585063, 4.229499824, 5.400228101, 6.383702315, 7.10189994, 7.632843502, 8.21060058, 8.827623412, 9.328377642, 9.443448264, 9.170287508, 8.773214839, 8.416936587, 8.04624261, 7.699186221, 7.569920184, 7.691127145, 7.934019628, 8.1428868, 8.358847352, 8.546434382, 8.693825589, 8.812843274, 8.93895434, 9.090328075, 9.137100409, 9.054920506, 8.891810684, 8.768166423, 8.640971438, 8.420923066, 8.713788908, 9.005236693, 8.663411277, 7.641794889, 6.886750021, 6.366872862, 5.797807625, 5.212683039, 4.691795849, 4.261911634, 3.896264815, 3.514558647, 3.144440173, 2.727970923, 2.245838076, 1.717354453, 1.200458525, 0.653542945, 0.186679768, 0, 0].